

Microbial dynamics in high latitude ecosystems

Responses to mixing, runoff and seasonal variation a rapidly changing environment

Maria Lund Paulsen



Avhandling for graden philosophiae doctor (ph.d.)
ved Universitetet i Bergen

2017

Dato for disputas: 8 November

© Copyright Maria Lund Paulsen

The material in this publication is protected by copyright law.

Year: 2017

Title: Microbial dynamics in high latitude ecosystems. Subtitle: Responses to mixing, runoff and seasonal changes in a rapidly changing environment

Author: Maria Lund Paulsen

Print: AiT Bjerch AS / University of Bergen



"I knew the woodpeckers were a mistake."

I want to dedicate this dissertation to the person I admire the most and who I feel so lucky to share all my life-stages with, my little sister Vibe

Scientific environment

This Ph.D. was carried out at the Faculty of Mathematics and Natural Sciences of the University of Bergen, at the Department of Biology in the Marine Microbiology group. The work was mainly part of the project “MicroPolar [μ P]: Processes and Players in Arctic Marine Pelagic Food Webs” (RCN 225956), funded by the Research Council of Norway, in close collaboration with the project CarbonBridge (RCN 226415). The thesis was supervised by Aud Larsen (Uni Research), Gunnar Bratbak (UiB) and Colin Stedmon (DTU-Aqua). Research in the Subarctic Atlantic was funded by the European Union Seventh Framework Programme project EUROBASIN (ENV.2010.2.2.1-1) under grant agreement n°264933 and ERC grant Microbial Network Organisation (MINOS 250254). Research in NE Greenland was additionally supported by the Danish Research Council for Independent Research (DFR 1323–00336). The Arctic Science Partnership and the Greenland Ecosystem Monitoring program facilitated the work.



UNIVERSITY OF BERGEN

MicroPolar [μ P]

Processes and Players in Arctic
Marine Pelagic Food Webs

DTU Aqua
National Institute of Aquatic Resources



CAMPING

Changes in Arctic Marine Production due
to melting Ice in Greenland

Acknowledgements

First of all I want to thank Torkel Gissel Nielsen and Karen Riisgaard for making my first encounters with the microbial world and paper writing a great experience. Torkel thank you for always looking out for your students and giving me many possibilities for fieldwork and traveling. I value your honesty and advice regarding career choices. I am grateful for all the help and support I have received during my time as a Ph.D. student, and I especially thank my three **Ph.D. supervisors** for support and allowing me the freedom to pursue my interests. To Gunnar for always keeping an eye on me and organising a great project. To Aud Larsen for doing a really great job helping me structure my time (I know I haven't been easy!!). To Colin Stedmon for always having inspiring ideas and for spending a great deal of hours with me in the lab. and with MATLAB. I really admire your sharp mind and efficiency!

Thank you to all my colleagues in our **Marine Microbiology group** for a very relaxed working environment and especially to Ela, the Hilde's and Evy for keeping superb order in the lab. To Tanya, Antonio, Bryan, Chris, Birte, Petra, Selina and the new energy boost: Dorinde, Jeroen, Hannah for making breaks and beer o'clock fun. To the one person I spend most time with the last years, my officemate Julia; I love our messy office and how we spice up everyday life with small gifts, beer and good playlists! To Eliana for many daily hugs and warmth, to Pia always being so wonderfully chilled, to Berna for her energy and support through rough times! To Oli for having been a great part of my life! I could not have done this thesis without you, thank you for patiently sharing your molecular skills!

To my **CarbonBridge** colleague Lena Seuthe, thank you so much for great collaboration on experiments and ever encouraging meetings and emails, you have made a big difference a to my PhD! Du er en knupp! Achim Randelhoff and Marina Sanz Martín my co-phd's for making the cruises and project meetings lots of fun. Marina, I'm gonna make my yearly visits to you in Spain a tradition in the future☺!

Thank you to the **Young Sound** team; Mathias Middelboe, Eva F Møller, Mikael Sejr, Tage Dalsgaard, Stiig Markager, Thomas J Pedersen for great effort, originality and teamwork in Daneborg and efforts writing papers afterwards! Specially thank you to Mathias for excellent collaboration on writing papers. To Sophia and Ane for making the Young Sound field work it the most fun summer of my life!

Til mine dejlige danske venner Sharangka, Julie, Zina, Peter, Cecillie, Maiken og Milo tak for at det altid har været så hyggeligt at komme til KBH! Til min bedste rejsekammerat, glimraveninde og læsemakker de sidste +10 år, Anne Marie, tak for at Tagensvej 96 har været mit andet hjem. Jeg beundre din arbejdsmoral, energi og arrangement. Glæder mig til at nørde videre med dig i fremtiden! Tak til min kære familie i KBH som har passet så godt på mig; mine skønne kusiner Sofie, Katrine og Rikke og kære fastre Karen og Dorte! Den aller-ALLER største tak til verdens sejeste forældre Vivian og Mikkel og mine dejlige søstre Vibe og Cian, for altid at være der for mig, også når jeg er tudefjæs og teenager sur. Jeg elsker jer overalt på jorden! Og til hundene Isa og Ylle og kattene Per og Per for altid at være så glade og nuttede☺ Og til Noah, Jeppe og Anker for at bringe liv og glade dage ind i vores familie. Til min kæreste Håkon for altid at minde mig om hvad der er vigtigt her i livet, jeg glæder mig så meget til vores fremtid sammen!

Abstract

The pronounced warming at high latitude alters a range of physical conditions i.e. the magnitude of runoff, sea-ice extent and strength of stratification and thus affect the biological systems. As microorganisms form the living base of the pelagic food web and are the major drivers of biogeochemical processing it is critical to understand their response to these changes. This Ph.D. project focuses on the smallest ($<2\mu\text{m}$) and most abundant microorganisms, heterotrophic bacterioplankton (bacteria and Archaea) and autotrophic picophytoplankton, and the factors regulating their abundance, diversity and activity in the Arctic-Subarctic Atlantic Ocean. The study covers hydrographic regimes off and around Iceland, Norway (including Svalbard) and East Greenland (60-83°N), and combines field observations and experiments during different seasons. The main aim is to elucidate the three following topics: **1)** Challenges phytoplankton face related to high seasonality and low light conditions **2)** Bioavailability of dissolved organic matter (DOM) to bacterial communities and their response to an increase in terrestrial loading **3)** Importance of top-down control by heterotrophic nanoflagellates (HNF) on both pico-sized phytoplankton and bacteria.

My study underpins that picophytoplankton are important contributors to primary production, especially during the winter-spring transition (**Paper I and III**) and autumn (**Paper V**). They boosted the growth of heterotrophic microorganisms before the onset of the diatom spring bloom in the Subarctic Atlantic (**Paper I**) and dominated the phytoplankton biomass in the high turbid parts of a NE Greenland fjord influenced by glacial meltwater (**Paper V**). Picophytoplankton were better adapted to low light conditions and demonstrated higher growth rates, than larger phytoplankton (**Paper I, II, III, V**). In the Polar-influenced water near Greenland, *Synechococcus* were negligible, while in the Atlantic influenced waters picoeukaryotes and *Synechococcus* were often equally abundant and the latter dominated on several occasions during autumn and winter (**Paper I and III**). Unexpectedly, abundances of *Synechococcus* were as high at 65°N as at 79°N, and molecular analysis suggests the presence of new clades specially adapted to Arctic conditions.

Bacteria were generally rather carbon- than nutrient limited, and their abundance increased rapidly in response to the pre-bloom picophytoplankton production of labile carbon in both the Arctic and Subarctic (**Paper I and V**). In NE Greenland the terrestrial DOM supplied from the Greenland ice sheet proved to be highly bioavailable compared to the

autochthonous fjord DOM (**Paper IV**). The *in situ* changes in DOM, which were examined via fluorescence signal of different DOM components (FDOM), surprisingly demonstrated that the highest net-growth of bacteria was not coupled to the labile glacial runoff in the surface, but rather to sub-surface the humic-DOM, commonly considered to be refractory. This may be explained by the presence of specific dominating taxa of bacteria that had the ability to degrade humic-DOM (**Paper V**).

Across regions, HNF exerted strong control of picophytoplankton and bacteria (**Paper I, II, III, V**). HNF grew significantly faster than microzooplankton and were therefore less affected by mixing and relatively more important grazers than their micro-sized counterparts in well-mixed water columns (**Paper I and II**). HNF larger than 5 μ m controlled picophytoplankton particularly in the early productive season, while small HNF (3-5 μ m) mainly kept bacteria in check in autumn (**Paper III, V**). In conclusion, the studies underline that pico-sized plankton play a fundamental part in the carbon transfer in high latitude ecosystems both as primary producers and via the microbial loop. Picophytoplankton appeared better adapted than larger phytoplankton to low light conditions, and bacteria were capable of degrading terrestrial derived DOM, however, these abilities are highly community specific. The data suggest that a change in mixing patterns will affect the microbial food structure and that shifts in coastal microbial community composition should be anticipated with increased runoff.

List of publications

The thesis is based on preliminary data and the following five papers referred to in the text by their Roman numerals:

Paper I: Paulsen ML, Riisgaard K, Thingstad TF, John MS and Nielsen TG. (2015). Winter–spring transition in the subarctic Atlantic: microbial response to deep mixing and pre-bloom production. *Aquat. Microb. Ecol.* 76, 49–69. doi:10.3354/ame01767.

Paper II: Paulsen ML, Riisgaard K, John MS, Thingstad TF and Nielsen TG. (2017). Heterotrophic nanoflagellate grazing facilitates subarctic Atlantic spring bloom development. *Aquat. Microb. Ecol.* 78, 161–176. doi:10.3354/ame01807.

Paper III: Paulsen ML, Doré H, Garczarek L, Seuthe L, Müller O, Sandaa R-A, Bratbak G and Larsen A. (2016). *Synechococcus* in the Atlantic Gateway to the Arctic Ocean. *Front. Mar. Sci.* doi:10.3389/fmars.2016.00191.

Paper IV: Paulsen ML, Nielsen SEB, Müller O, Møller EF, Stedmon CA, Juul-Pedersen T, Markager S, Sejr MK, Huertas AD, Larsen A and Middelboe M. (2017). Carbon bioavailability in a high Arctic fjord influenced by glacial meltwater, NE Greenland. *Front. Mar. Sci.* doi:10.3389/fmars.2017.00176.

Paper V: Paulsen ML, Müller O, Larsen A, Møller EF, Sejr MK, Middelboe, M, Wunsch U and Stedmon CA. Microbial transformation of humic-like dissolved organic matter in a high Arctic fjord, NE Greenland. (*Manuscript*)

The published papers are reprinted with permission from Inter-Research and Frontiers in Marine Science. All rights reserved.

Contents

SCIENTIFIC ENVIRONMENT	4
ABSTRACT.....	6
LIST OF PUBLICATIONS.....	8
CONTENTS.....	9
LIST OF ABBREVIATIONS.....	9
1. INTRODUCTION.....	11
<i>Box 1 Plankton.....</i>	<i>12</i>
2. AIMS AND RESEARCH QUESTIONS.....	15
3. THE STUDY AREA.....	16
3.1. DESCRIPTION THE REGIONS AND DATA COLLECTION	17
<i>Box 2 Water masses.....</i>	<i>18</i>
4. SUBARCTIC AND ARCTIC PHYTOPLANKTON COMMUNITIES.....	19
4.1 PICOPHYTOPLANKTON TYPES	19
4.2 ADAPTATIONS TO LOW LIGHT CONDITIONS.....	21
5. HETEROTROPHIC BACTERIA IN SUBARCTIC-ARCTIC WATERS.....	25
5.1. SPATIOTEMPORAL VARIATIONS IN BACTERIAL ABUNDANCE AND ACTIVITY	25
5.2. BACTERIAL RESPONSE TO TERRESTRIAL CARBON INPUT	27
<i>Box 3 The Bottle Effect.....</i>	<i>30</i>
6. TOP DOWN CONTROL OF PICO-SIZED PLANKTON.....	31
6.1. HNF, THE KEY GRAZER IN HIGH LATITUDE SYSTEMS.....	31
6.2. VIRUS CONTROL ON BACTERIA	33
<i>Box 4 Methodological considerations.....</i>	<i>35</i>
7. CONCLUSION AND FUTURE PERSPECTIVES	36
REFERENCES.....	38

OPPONENT'S REPORT OF THESIS

PAPER I-V

List of abbreviations

FDOM	Fluorescent organic matter (measured as intensity, Raman Units R.U.)
TDOM	Terrestrial derived DOM
DOC	Dissolved organic matter (measured as concentration μM)
BDOC	Bioavailable carbon
POM	Particulate organic matter
DON	Dissolved organic nitrogen DOP
C:N	Carbon to Nitrogen ratio

MZP	Microzooplankton (ciliates and heterotrophic dinoflagellates)
HNF	Heterotrophic nanoflagellates

NB. The term "protozooplankton" includes all heterotrophic protists, i.e. both MZP and HNF

VBR	Virus to bacteria ratio
HNA	High nucleic acid
LNA	Low nucleic acid
BCD	Bacterial carbon demand
BGE	Bacterial growth efficiency

MLD	Mixed layer depth
DCM	Deep chl <i>a</i> max
WSC	West Spitsbergen Current
EGC	East Greenland Current
AW	Atlantic Water
PW	Polar Water
AIW	Arctic Intermediate Water
DW	Deep Water

1. Introduction

The Arctic-Subarctic Atlantic Ocean has been exploited for centuries and are today recognised as some of the most productive waters in the Ocean (Field, 1998). There are pieces of evidence that current climate changes already affect the ecosystem (Brierley and Kingsford, 2009; Wassmann et al., 2011), but the lack of historical datasets and fragmented knowledge about the systems, makes it challenging to assess changes. The Ocean is dominated by microorganisms (Gasol et al., 1997), which form the link between its chemistry and biology by their ability to both fix inorganic- and remineralise organic matter in the pelagic. The physical environment determines the structure of marine microbial ecosystems, directly by their influence on the growth of phytoplankton (irradiance and mixing) and indirectly by affecting food web interactions (mixing and temperature) (Cullen et al., 2002; Margalef, 1978). Microbial communities however undergo succession even when water mass and the environment is kept stable due to the continuous trophic interactions (Calbet et al., 2015). The smallest living organisms capable of independent growth are pico-sized (0.2-2 μm , **Box 1**). Despite their small size, they comprise by far the largest biomass in the pelagic Ocean. They consist of the two major functional groups, picophytoplankton and bacteria, which both have sinking rates close to zero (Kiørboe, 1993), osmotrophic feeding modes (Chakraborty et al., 2017), and heterotrophic nanoflagellates (HNF) as their main predators (Azam et al., 1983; Christaki et al., 2001, 2005; Pernthaler, 2005) (**Box 1**). At high latitude systems, the majority of picophytoplankton are eukaryotes and/or prokaryotic cyanobacteria belonging to the genus *Synechococcus*. The role of picophytoplankton in northern systems has received more attention in recent years (Irigoien et al., 2005; van De Poll et al., 2016; Seuthe et al., 2011; Sherr et al., 2003; Tremblay et al., 2009), although traditionally the focus has been on larger, spring-blooming phytoplankton (Leblanc, 2005; Rees et al., 1999; Velasco et al., 2013). During bloom periods the relative abundance of picophytoplankton is low (Li et al. 1993), but a bloom is a short-term feature and smaller phytoplankton and associated grazers dominate the rest of the year. Although there has been a great effort to estimate protozooplankton herbivory and bacterivory in marine and freshwater systems (**Box 4**) since the microbial-loop concept was introduced (Azam et al., 1983; Pomeroy and Deibel, 1986), food web models predicting net-primary production in the Arctic-Subarctic marine waters still greatly needs to improve when it comes to including the impact of protozooplankton grazing.

Box 1 | Plankton

1. Size. Grouping according to size is a simple and widely used way to organise plankton. The logarithmic size classes (Sieburth et al. 1978) based on equivalent spherical diameter (ESD) are:

- **Mesoplankton** (200-2000 μm) primarily include multicellular metazooplankton such as copepods, but also protozooplankton and phytoplankton can be found within this size range.
- **Microplankton** (20-200 μm): large phytoplankton species (e.g. diatoms), dinoflagellates, ciliates, small metazoans (e.g. small copepod species, metazoan larvae and metazoan eggs).
- **Nanoplankton** (2-20 μm): heterotrophic and autotrophic flagellates.
- **Picoplankton** (0.2-2 μm): heterotrophic prokaryotes (incl Bacteria and Archaea) for simplicity termed bacteria. Photoautotrophic bacteria (cyanobacteria), eukaryotic picophytoplankton.
- **Femtoplankton** (0.02-0.2 μm): viruses.

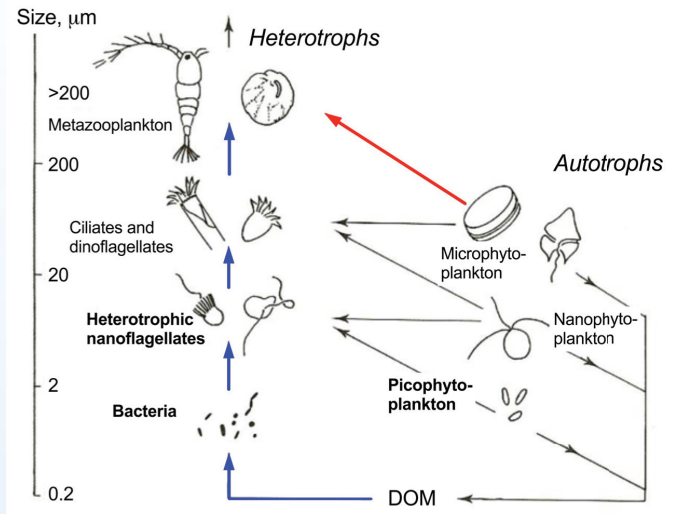


Figure 1: Schematic diagram of the planktonic food web grouped after organism's function and size. Arrows indicate trophic interactions. Autotrophic organisms are to the right and serve as food for proto- and metazooplankton. All groups excrete dissolved organic matter (DOM), which serves as substrate for the heterotrophic bacteria. Note the two major trophic pathways: "the microbial-loop" (DOM → bacteria → protozooplankton) and the "linear classical food chain" (micro-sized phytoplankton → metazoans). After Fenchel (1987)

- 2. Trophic strategies.** The suffix "-troph" comes from ancient Greek trophikós (τροφικός) and means nourishment. The trophic strategy is approach an organism applies to gain energy and nutrients. The strategy depends largely on the organism size (Andersen et al., 2016).
- **Autotrophy:** the process of synthesizing organic carbon from an inorganic source by utilising energy from sunlight (photo-autotrophy) or gaining energy by oxidising inorganic compounds (chemo-autotrophy).
 - **Heterotrophy:** the process of gaining energy by taking up organic matter either in dissolved form (DOM) by osmotrophy (as bacteria) or by engulfment termed phagotrophy as protists).
 - **Mixotrophy:** a mix of the above strategies i.e. protozoa may delay the digestion of chloroplasts and utilise the continuous primary production (kleptoplastidy). Another widespread mixotrophic strategy is the ingestion of bacteria (bacterivory) by eukaryotic pico- and nanophytoplankton (Hartmann et al., 2012) to acquire nutrients and to gain extra energy. In similar manner prokaryotic picophytoplankton may ingest DOM.

Single celled organisms can ingest particle-sized food items (>0.2 μm) by engulfing a food cell or particle and ingesting it in a phagocytic vacuole. This is called **phagotrophy** and is the main feeding mode for heterotrophic protists (Jacobson and Anderson, 1996). The uptake of dissolved organic compounds (DOM, <0.2 μm) and nutrients, on the other hand, can pass over the cell membrane or ion-pumps by actively regulated osmosis. This is termed **osmotrophy** and is the way bacteria and phytoplankton take up nutrients (Jumars et al., 1993). Bacteria must often produce exoenzymes to break down DOM into molecules that are sufficiently small to enable uptake via osmosis. Based on the size and trophic mode organisms can be grouped into *functional groups*, e.g. picoplankton can be considered to be in the same functional group serving as prey for HNF, while they are in different functional groups in terms of trophic mode.

Variations in DOM quantity and quality, as well as bacterial uptake rates, are also in need of a better parameterization (Slagstad and Mcclimans, 2005; Vernet et al., 2017).

The Ocean's biological pump strips nutrients out of the surface waters and exports them into deep waters. Mixing of surface waters with nutrient rich deep water is therefore essential for continuous primary production and well-mixed waters are therefore essentially more productive. Nitrogen is the limiting nutrient in the Arctic (Tremblay et al., 2015). It has been argued that increased temperatures via increased ice melt and runoff will lead to increased thermal and haline stratification of the upper Arctic Ocean and thermal stratification will lead to more shallow mixing in the Subarctic, hence lower nutrient supply (Carmack and McLaughlin, 2011; Martínez-garcía et al., 2009; Schmittner, 2005). Further, the Arctic sea ice changing may lead to an increased inflow of Atlantic water into the Arctic Ocean (Itkin et al., 2014; Schauer et al., 2004; Zhang et al., 1998). Increased stratification and inflow, in turn, lead to increased importance of picophytoplankton as these have a higher affinity for nutrients (Thingstad, 1998) and their relative importance is observed increase with higher temperatures (Agawin et al. 2000, Daufresne et al. 2009, Morán et al. 2010). The co-variation between picophytoplankton abundance, temperature and other environmental factors remains controversial. Due to their small size, and small sized predators, their biomass production may largely be recycled within the microbial food web and be of minor contribution to higher trophic levels (Fig. 1), hence a shift towards smaller sized organisms, which it is often considered a threat to the existing food webs and to cause a weakening of the biological pump (Daufresne et al., 2009; Edwards and Richardson, 2004; Li et al., 2009). Mesozooplankton is regarded the most important phytoplankton grazer in high latitude systems and received far more attention than protist grazers of which ciliates are more extensively studied (Arendt et al., 2016; Calbet et al., 2011; Levinsen and Nielsen, 2002; Riisgaard et al., 2015). Top-down control of picophytoplankton by HNF is however rarely considered.

Aquatic microorganisms excrete, transform and consume dissolved organic matter (DOM), this result in a complex mixture of organic molecules. Oceanic DOM is one of largest active pools of organic carbon in the world (>20%) (Hansell et al., 2009; Hedges et al., 1997), and is especially high in the Arctic Ocean due to high terrestrial input (Stedmon et al., 2011). Even a small increase of 1% in bacterial respiration on a global scale would result in a larger CO₂ release than the anthropogenic sources combined (Hedges 2002). It remains controversial whether increasing temperature has a positive (Middelboe and Lundsgaard,

2003; Kritzberg et al., 2010) or insignificant effect (Kirchman et al., 2005, 2009) on bacterial respiration and growth efficiency (BGE), but it is largely agreed upon that DOM quality and quantity are the main factors determining the bioavailability. With the increased runoff and melting of permafrost and glaciers in high latitude marine ecosystem (Fichot et al., 2013; Lawson et al., 2014) an improved knowledge of DOM dynamics and the bioavailability is essential to understand how climate warming may impact carbon cycling. The composition of the bacterial community determines the range of enzymes and thus the ability to break down different DOM types. Links between community composition and DOM types have been considered only in few environmental studies (Baña et al., 2014; Kirchman et al., 2007; Osterholz et al., 2016; Sipler et al., 2017).

The increasing focus on Arctic environments has improved our understanding of microbial processes herein but also stresses that there are many understudied organism groups and processes, and that regional differences make it impossible to discuss Arctic ecosystems as one general system (Tremblay et al., 2015; Wassmann et al., 2015).

2. Aims and research questions

This Ph.D. project aims to improve understanding of the activity, diversity and distribution of the smallest plankton; picophytoplankton and heterotrophic bacteria, in high latitude ecosystems by combining observations with experimental studies from contrasting regions. I focus not only on the short productive season but also on the prevailing low productive seasons, as these are particularly understudied. Heterotrophic nanoflagellates (HNF) are the main predators of bacteria and picophytoplankton and the magnitude of HNF grazing as well as the effect this grazing has on the DOM composition is therefore considered. Climate warming poses numerous unknown impacts on high latitude systems, but the focus is here narrowed to study the microbial responses to three interrelated hydrographic features; freshwater run-off from land, mixing and advection via currents. The main objectives to address the impact of these on the bottom-up and top-control mechanisms are:

1. To assess the response of pico-sized phytoplankton and bacteria and their grazers to changes in stratification/mixing in the Subarctic Atlantic (**Paper I and II**) and in a glacier-influenced fjord system (**Paper IV and V**), and to sea ice distribution NW Svalbard Ocean (**Paper III**).
2. To describe how the two major currents (North Atlantic and East Greenland current) transport pico-sized plankton in the area and how microbial communities differ between the dominating water masses (**Paper I, III and V**).
3. To study how the picophytoplankton community adapt to low light conditions and freshwater input from both land and sea-ice (**Paper I, III, IV and V**).
4. To characterise dissolved organic carbon sources in Subarctic and Arctic environments and relate them to bacterial growth, diversity and protist grazing activities (**Paper I, IV and V**).

3. The Study Area

The study includes studies from four regions (Fig. 2) within the North Atlantic. “Subarctic” and “Arctic” are defined as provinces by Longhurst (1995). The northward Atlantic current and the southward East Greenland Current are the main forces in the study area. They create a sharp contrast between the relatively warm and saline Atlantic waters dominating in Eastern region, and the cold, fresh Arctic waters that dominate to the West.

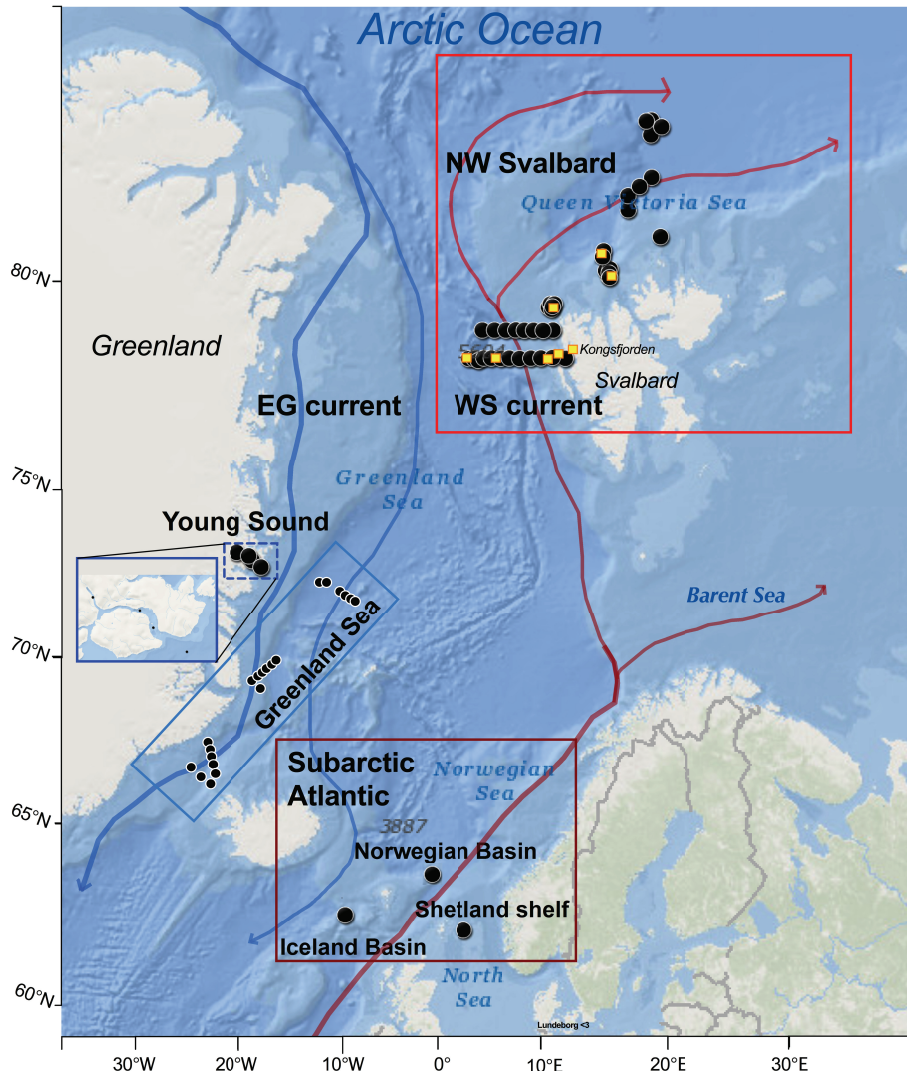


Figure 2: The study area. The major currents illustrate the warm saline Norwegian Atlantic Current of which a branch becomes the West Spitsbergen Current (WSC) (Red) and the cold, fresh Arctic water of which the major branch is the East Greenland Current (EGC) (blue). Currents are drawn after Blindheim and Østerhus, (2005). Black dots mark the sampling stations and yellow squares mark stations where tDOM experiment were performed.

3.1. Description the regions and data collection

Subarctic Atlantic: Three stations were sampled the Iceland and Norwegian Basin (1300m) and on the Shetland Shelf (160m) from March to May 2012 by repeated visits. The Iceland Basin and Shetland Shelf consisted of Atlantic Water (AW) and were well mixed by winter convection. In the Norwegian Basin the AW was constrained to the upper 100m, while the remaining water column consisted of cold Deep Water (Box 2) and the water column therefore remained stratified. **Paper I** includes data from all three sampling stations. In **Paper II** the microbial interactions of the surface community at the Iceland Basin station were studied experimentally via three fractionation experiments (Box 4) (using the size fractions <0.8, <10 and <50 μm) and a 10% dilution every second day.

NW Svalbard: Samples were collected in January, March, May, August and November 2014. The sampling concentrated on the core of the northwards drifting warm AW, which enters the Arctic Ocean north of Svalbard. The choice of sampling area and stations was dictated by the extension of the sea ice, which extended further south in summer than in winter (**Paper III**). Fractionation experiments were performed on each cruise (<0.8, <3, <5, <10 and <90 μm). In August and November terrestrial DOM addition experiments were executed (Fig. 7).

Greenland Sea: Data was collected from the Denmark Strait region, Iceland Sea and along a number of sections across the East Greenland Current (EGC) in September 2012. I counted the organisms from this study, however the data are not included in any of the publications, but are used to support the discussions in the thesis and included in figure 4 and 5.

Young Sound: The fjord system is ice-free for less than 4 months a year and during this time it receives freshwater runoff from land-terminating glaciers. The run-off is highly turbid due to silt particles. A mixture of EGC and coastal water form an estuarine compensation current that enters the fjord over a sill. The fjord was sampled throughout the ice-free period (July-October) at four stations located along a longitudinal section of the fjord (Fig. 2). In addition, the three major rivers discharging freshwater into the fjord system were sampled.

In order to describe how the microbial communities differ between regions and water masses I have compiled data from the four study areas (collected in within the period 2012 to 2014) and included overview of these as surface plots and TS diagrams (Box 2) in the following chapters (Fig. 4, 6 and 10).

Box 2 | Water masses

The Norwegian Atlantic Current feeds warm and saline water into the Subarctic and Arctic Atlantic (Fig. 2). The Atlantic water gradually cooled down and freshened due to repeated annual melting and large terrestrial freshwater input (Schauer et al., 2004). The Arctic-Subarctic Atlantic mainly consists of four water masses; **Atlantic Water** (AW: $T > 3^{\circ}\text{C}$, $S > 34.7\text{-}34.9$), Norwegian Sea **Deep Water** (DW: $T < 0^{\circ}\text{C}$, $S = 34.88\text{-}34.96$), **Arctic Surface Water** (ASW: $T > 2^{\circ}\text{C}$, $S < 34.9$) and 4) and **Polar Water** (PW: $T < 0^{\circ}\text{C}$, $S < 34.4$) as in Gonçalves-Araujo et al. (2016). There are intermediate forms of Arctic Water i.e. **Arctic Intermediate Water** (AIW), here upper and lower AIW are included. The water masses studied in the 4 regions are all mapped in the temperature-salinity (T-S) diagram (Fig. 3), illustrating the stiletto heel shape, which is characteristic for water masses in the Fram Strait. N.B. this is a broader Water mass definition than the one applied in **Paper III**, as this study covers a larger area. The gradual freshening can be observed, e.g. measurements at $T = 7$ and $S < 35$ (“upper strap” of the stiletto) from the NW Svalbard region; these represent surface samples from an area where sea ice had recently retreated in August.

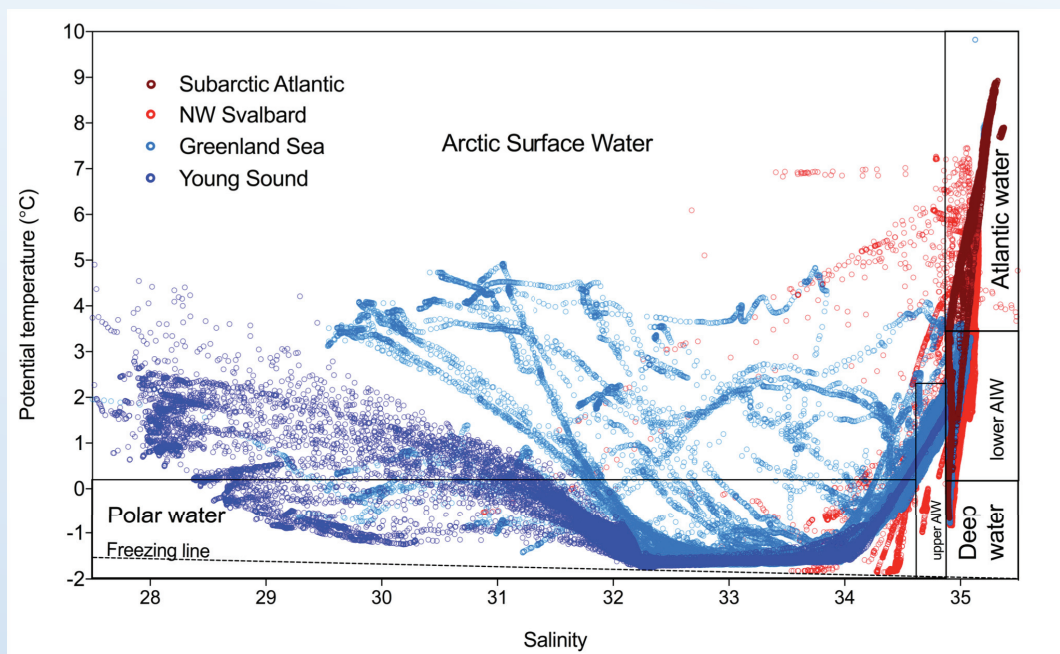


Figure 3: Temperature-salinity (T-S) compiled from CTD data from all the studied regions (following the color code in Fig. 2). Boxes mark the 6 dominant water masses in the study area. More detail on intermediate water masses in the region are given in (Blindheim and Østerhus, 2005; Gonçalves-Araujo et al., 2016).

4. Subarctic and Arctic Phytoplankton Communities

4.1 Picophytoplankton types

Picoeukaryotes in the Arctic are often reported to be comprised mainly by the genus *Micromonas* (Sherr et al., 2003; Tremblay et al., 2009). A *Micromonas* strain (isolated from 76°N, 75°W) showed relatively fast growth at low temperatures (0°C) and under low light conditions, suggesting they could have a selective advantage in both the Arctic and Subarctic (Lovejoy et al., 2007; Not et al., 2004). In the NW Svalbard region as well as other high latitude systems, picoeukaryotes are not necessarily dominated by prasinophytes, however, but rather comprise a quite diverse group (Elianne D. Egge pers. comm, (Sørensen et al., 2017; Vaultot et al., 2008). Also in Young Sound (**Paper V**), the picoeukaryotes were taxonomically diverse but dominated by pico-sized silicoflagellates (*Florenciellales*) and prasinophytes including *Micromonas*-like forms (**Paper V** and **own unpublished data**).

Picoeukaryotes were evidently more abundant than *Synechococcus* in the Greenland Sea (Fig. 4 A, D) and within the Arctic Surface Water (ASW) and Polar Water (PW). The highest abundances of both groups were, however, recorded within the Atlantic Water (AW) (Fig. 4 B, E). Chl *a* values were higher within the Arctic water masses (AIW, ASW, PW) than in the AW, as the Arctic waters include most surface samples. Maximum chl *a* concentrations of up to 17 µg L⁻¹ in the NW Svalbard region during a *Phaeocystis* dominated spring bloom in May (Fig. 4 C). Inorganic nitrogen was generally depleted within the ASW (Fig. 4 F).

The high abundances of *Synechococcus* (>20.000 mL⁻¹) observed at high latitude 79°N (**Paper III**), challenge former observations in the area (Gradinger and Lenz, 1995) and the general understanding that *Synechococcus* is almost absent in polar oceans due to low temperatures. We found that *Synechococcus* even exceeded the number of picoeukaryotes at several occasions during autumn and winter, during which the *Synechococcus* community consisted mainly of two specific novel operational taxonomic units (OTUs). This suggests that these may be particularly adapted to the cold and darkness (**Paper III**). *Synechococcus* were absent in Young Sound, but found in moderate concentrations (up to 2.000 mL⁻¹) along the east Greenland coast due to advection of AW around Iceland (Fig. 4 D). Freshwater cyanobacteria, entering the fjord via rivers, persisted within the freshwater lens in Young Sound (**Paper IV**). A reason for their persistence in the fjord environment may be their

ability to fix nitrogen, as the surface water was strongly N-limited (**Paper IV and V**). While cyanobacteria are a major part of Arctic freshwater ecosystems, it remains a paradox why there are no nitrogen fixators in Arctic marine waters, since the entire Arctic is largely N-limited (Tremblay et al., 2015).

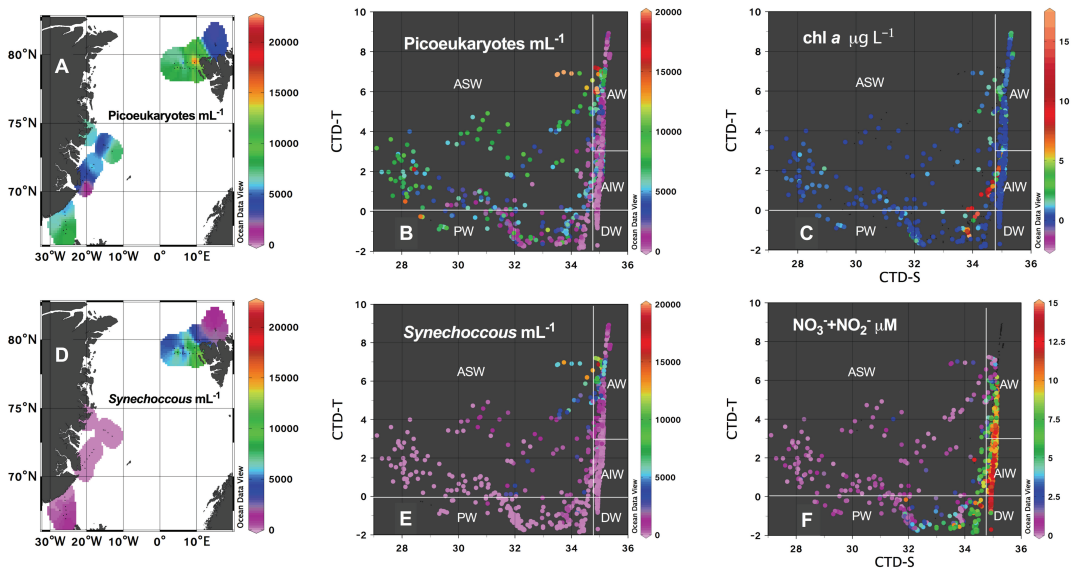


Figure 4: A, E) Picophytoplankton abundance in surface samples collected in NW Svalbard in August 2014, NE Greenland (Sept 2012) and Young Sound (Aug+Sept 2014). B, C, E, F) T-S plots (as explained in Box 2), with an additional z-axis illustrating the abundance of picophytoplankton, chl *a* and nitrate and nitrite concentration measured from discrete water samples including all regions and seasons.

4.2 Adaptations to low light conditions

One of the most intriguing questions in high latitude systems is how phytoplankton survive the many months of darkness and are able re-inhabit the surface of the deep ocean when the light returns. This is especially challenging for larger sized phytoplankton that may sink to large depths. In shallow seas, phytoplankton resting spores or sediment dwelling overwintering phytoplankton can be re-suspended from the sediment and triggered to germinate in spring (Eilertsen and Wyatt, 2000; Wetz et al., 2004). This mechanism is proposed as a reason for diatom blooms starting earlier in coastal areas than off shore (Smetacek, 1985) and illustrated in **Paper I** where diatoms at the shallow Shetland Shelf recolonised the water column earlier during the winter-spring transition than what was the case at the deep basins stations. Oceanic diatom blooms are not likely seeded from the sediment, as the depths (>1000 m) are far too great for remixing and rather reach the open ocean by progressing from the coast due to advection (Smetacek, 1985). Alternatively, diatoms may sustain growth during winter by occasionally resurfacing to acquire light energy via the circular movement of the deep convection (Backhaus et al. 2003), an option probable in the case of the Iceland Basin spring bloom. Although large diatoms comprised a limited fraction of the total phytoplankton biomass (1.3 cells mL⁻¹) in late March, they increased in numbers during April to 249 cells mL⁻¹. In the Norwegian Basin large diatoms were virtually absent (max 0.5 cells mL⁻¹) and remained at low concentrations during spring and summer, while the community was dominated by small (<5µm) diatoms and cryptophytes (Daniels et al., 2015, **Paper I**). The lack of diatoms in the Norwegian Basin has also been observed other years (Dale et al., 1999). The reason for the contrasting development at the deep stations is likely due to the distinctive degrees of mixing, which alters the development of grazing pressure differently (**Paper II**, Daniels et al., 2015; Morison and Menden-Deuer, 2015).

Both at the Subarctic Deep Basin Stations (**Paper I**) and north of Svalbard (own unpublished data) small phytoplankton communities comprise the far majority (90-98%) of phytoplankton biomass during the winter-spring transition (based on <10µm chl *a* fraction), these can therefore be considered the best winter survivors. Similar observations are reported from the Amundsen Gulf (Terrado et al., 2011). The success of small cells can partly be explained by their greater affinity for light due to the absence of a cell wall and efficient packaging of photosynthetic pigments inside the cell (Raven, 1998). Additionally their low sinking rates (−0.2 m d⁻¹ according to Kiørboe (1993)), potentially gives these small cells a

opportunity to utilise the first seasonal increase in irradiance. Another recognised survival strategy for small phytoplankton is mixotrophic bacterivory (Box 1). Bacterivory by pico and nano-sized phytoplankton is widely distributed, also in the Subarctic and Arctic (Hartmann et al., 2012; Sanders and Gast, 2012; Zubkov and Tarran, 2008). It does not increase with depth (i.e. decreasing light availability) and is therefore not likely an active low-light adaption that can be regulated with depth, but rather a passive and constant energy/nutrient supplement that may benefit picophytoplankton during winter (Hartmann et al., 2012). *Synechococcus* has another mixotrophic strategy in that it is able to utilise dissolved organic matter (DOM) (Cottrell and Kirchman, 2009; Yelton et al., 2016). I found evidence for such mixotrophic strategies as positive growth of the winter community of *Synechococcus* when incubated in darkness (**Paper III**). Picoeukaryotes did not grow under these conditions, suggesting that in this case the overwintering mixotrophic strategy of *Synechococcus* was more successful.

The relative contribution of picophytoplankton to the phytoplankton community usually correlates negatively to total chl *a* (Agawin et al., 2000). However, in Young Sound, and recently also seen in turbid lakes (Somogyi et al., 2017), the highest chl *a* concentrations were measured in periods when picophytoplankton dominated the biomass (**Paper V** and **own unpublished results**). Picophytoplankton dominated the murky inner part of Young Sound (>89% biomass) (**Paper V** and **own unpublished results**), likely because picophytoplankton had a relatively more efficient adjustment of chl *a* content per cell (Fig. 5A-B) than larger nanophytoplankton (>10 μ m) (Fig. 5 E-H). Also in the Subarctic Atlantic picophytoplankton adapted well to decreasing light within the photic zone when the mixed layer was not below 100m (**Paper I**). These observations decouple chl *a* measurements (Fig. 5M-P) from the actual phytoplankton biomass, especially when picophytoplankton dominate the biomass (Fig. 5 I-L), and as a consequence at surface phytoplankton biomass is underestimated relative to deep biomass. It is well-known that carbon to chl *a* ratio (weight:weight) can vary from 20 to almost 200 in marine systems (Goldman, 1980; Jakobsen and Markager, 2016), but my observations are novel in that they show that the change may depend on the size of phytoplankton. Agawin et al. (2000) similarly suggest that chl *a* to an especially poor indicator for biomass in the picoplankton size class. The explanation for their fast adjustment of chl *a* content may be their low sinking rates which give them longer time to adapt to the given light conditions when waters are not well mixed. This is supported by observations in **Paper I**, where picophytoplankton could only adjust chl

a per cell at the stratified station (Norwegian Basin) and not at the well-mixed locations. Picophytoplankton expressed higher growth rates than nanophytoplankton in the studied areas (**Paper II, III, IV**), and this may have facilitated a faster adaption. An additional explanation for the change in fluorescence may be subscribed to a different picophytoplankton species composition at different depths i.e. light regimes, as recently indicated in Cabello et al., (2016). In Young Sound, there was considerable difference between the surface and the DCM phytoplankton community composition (**own unpublished results**). As a consequence of the fast light adaption an autumn picophytoplankton bloom ($>10.000 \text{ mL}^{-1}$) (**Paper IV**) occurred in Young Sound when the runoff from land ceases in September, as this led to a deepening of the photic zone in the inner fjord (Fig. 5).

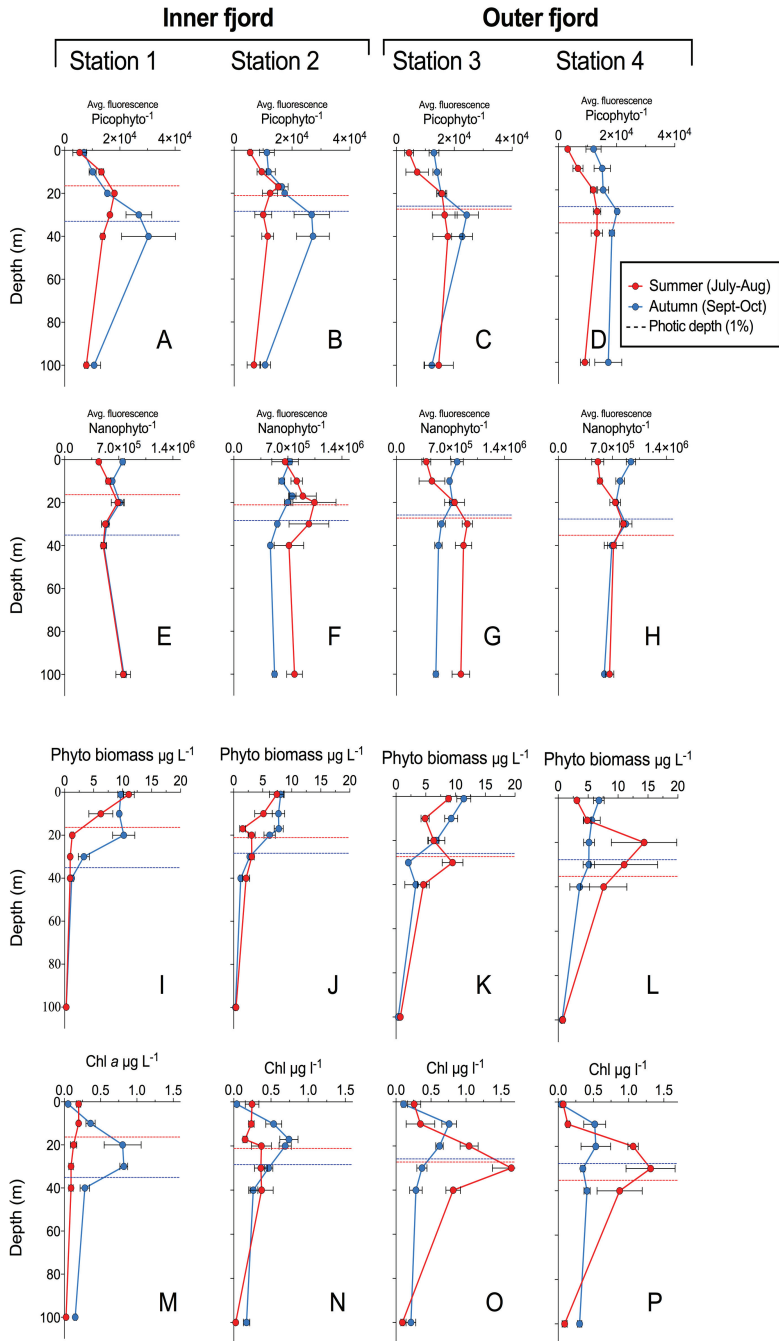


Figure 5: Distribution of fluorescence per pico-phytoplankton cell (A-D) and per large (>10µm) Nanophytoplankton cell (E-H) measured by flow cytometry as in Li, (1993). The total biomass of pico and nanophytoplankton ($\mu\text{g L}^{-1}$) (I-L) by converting cell counts to biomass using conversion factors given in **Paper I**, and total chlorophyll *a* ($\mu\text{g L}^{-1}$) (M-P) in the upper 100m in summer (red) and autumn (blue). Profiles are shown as average \pm SE of 3-4 profiles sampled at each of the four stations within each period (as in **Paper V**). The averaged photic zone (1% surface PAR) is illustrated by the dashed line (red= summer, blue= autumn).

5. Heterotrophic bacteria in Subarctic-Arctic waters

5.1. Spatiotemporal variations in bacterial abundance and activity

Bacteria exhibited large seasonal changes in both abundance (**Paper I and IV**) and in diversity (Wilson et al., 2017, **Paper V and IV**). During winter/early spring bacteria appeared to be carbon rather than nutrient limited as they increased fast in abundance in response to the pre-bloom picophytoplankton production of labile carbon in both the Arctic and Subarctic (**Paper I and III**). This was supported by fractionation experiments conducted in March 2012 (**Paper I**) and in January and March in NW Svalbard waters 2014 (**own unpublished data**) showing that the bacterial growth was boosted rather when larger organisms were present than when bacteria were alone (i.e. estimated grazing rates were negative; Table 1). This suggests that the bacteria were resource limited rather than top-down controlled, and that the presence of protists stimulated labile carbon production. The C:N ratio of the dissolved organic matter (DOM) produced tend to display a seasonal change, with elevated C:N during late winter (up to 18) and decreasing to 14.5 during the early pre-bloom production (**Paper I**), similar trends were observed in the NW Svalbard region (Seuthe et al., in prep). Low C:N ratios is in this study found to be a good indicator of bacterial bioavailability (**Paper I and IV**), and thus the high C:N ratios in winter supports the apparent low quality of DOM.

While bacteria were in general most abundant in the ASW and AW and low in the cold Polar Water (Fig. 6 A, B), the activity of bacteria (indicated by the HNA:LNA ratio¹) was higher the Polar Water than in any other water mass (Fig. 6 D). The maximum HNA:LNA ratios were found in the Greenland Sea in September and NW Svalbard during the spring bloom in May in the cold surface water. This distribution results in an weak, yet significant negative correlation between HNA:LNA and temperature ($r^2=0.12$, $p<0.0001$, $n=770$) in North Atlantic region. This is somewhat counterintuitive as high bacterial activity is usually positively correlated with higher temperatures, however the cold surface waters inevitably provides a favourable environment in other ways.

¹ I found HNA:LNA correlated significantly to bacterial production in summer months in both Young Sound ($r^2=0.10$, $p<0.005$) and NW Svalbard ($r^2=0.15$, $p=0.004$)

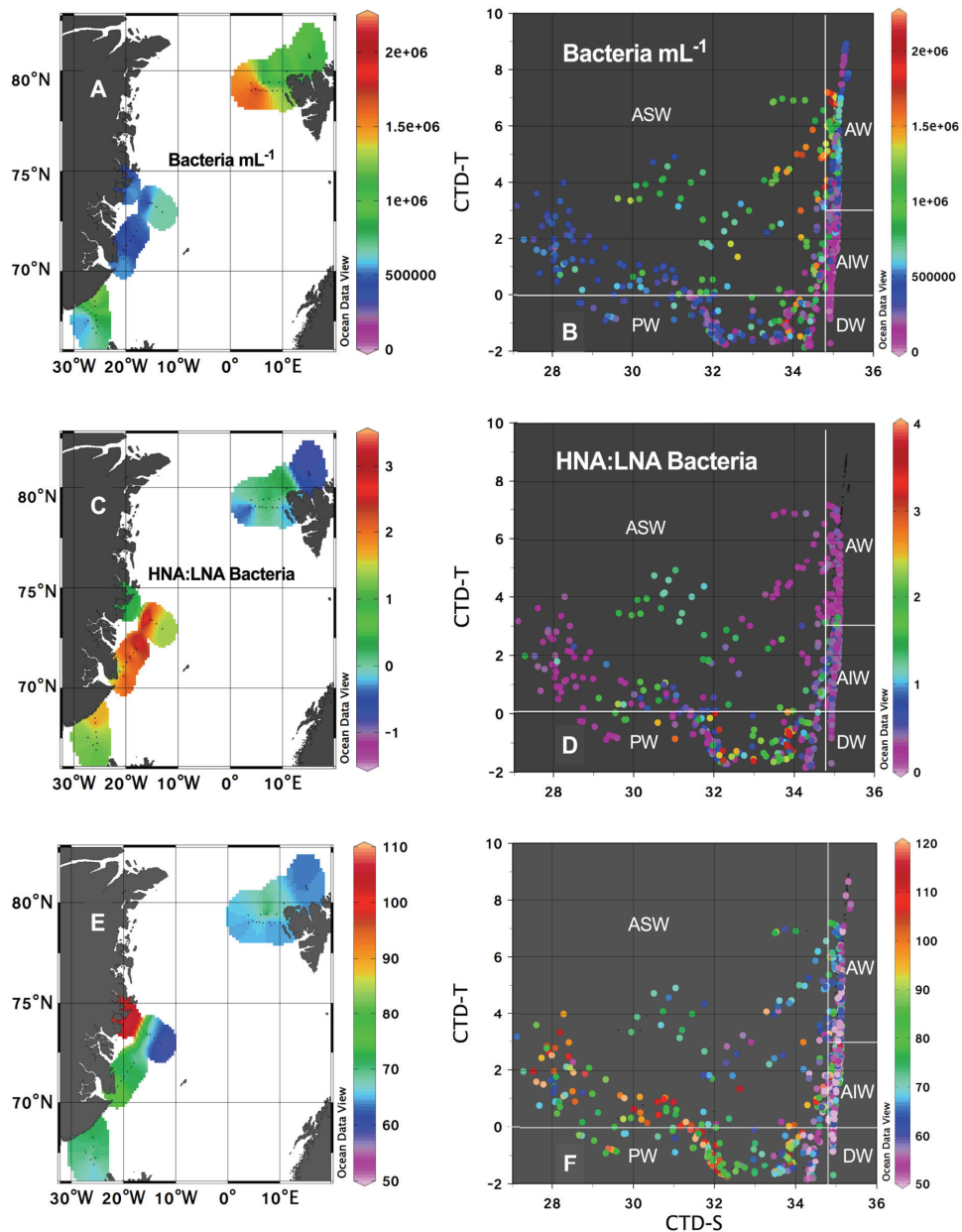


Figure 6: A, C, E) Bacterial abundance, HNA:LNA ratio and TOC concentration in surface samples collected in NE Greenland (Sept 2012) and Young Sound (Aug+Sept 2014). B, D, F) T-S plots (as explained in Box 2), with an additional z-axis illustrating the abundance of bacteria HNA:LNA ratio and TOC concentration measured from discrete water samples including all regions and seasons.

During an annual cycle in the surface waters of the NW Svalbard region the bacterial abundance and the community structure followed the seasonality of phytoplankton production (Wilson et al. 2017), as also found in the western Arctic Ocean (Pedrós-Alió et al. 2015). While the correlation between total bacterial abundance and chl *a* was poor ($r^2=0.02$, $p<0.02$) the correlation between chl *a* and the more active ‘HNA-bacteria’ was stronger ($r^2=0.11$, $p<0.0001$). There are several reasons not to expect a strong straight linear correlation between bacteria and chl *a*. Firstly, because the abundance of bacteria is regulated by top-down control from both grazers and viruses. Secondly, because chl *a* is not a good measure for phytoplankton biomass or activity across different environments (as discussed in the previous chapter). Further the fact that bacteria and phytoplankton may be competing for nutrients in nutrient deplete conditions e.g. in the stratified surface waters (Thingstad et al., 2008) complicate the relationship. In the to the ‘atlantified’ region bacterial abundance and activity (HNA:LNA ratio) correlated positively to chl *a*, while in the Arctic surface- and Polar waters around Greenland, the bacterial activity did not correlate to chl *a* but rather to TOC ($r^2=0.06$, $p<0.001$), as also illustrated by the surface water patterns in Figure 6 C, E. This suggests that other non chl-*a*-related organic carbon sources inputs are relatively more important in the Polar waters i.e. the input from terrestrial runoff.

5.2. Bacterial response to terrestrial carbon input

The Arctic Ocean resembles an estuary (McClelland et al., 2012) receiving far more freshwater than the global oceans. The catchment area of the Arctic Ocean contains more than half of the organic carbon stored globally in soils (Dittmar and Kattner, 2003) the concentration of dissolved organic matter (DOM) in the Arctic Ocean is therefore higher than in other Oceans (as evident as elevated TOC concentrations in Fig. 6 E, F) and the DOM is characterised by having elevated humic-content (Gonçalves-Araujo et al., 2016). As the Arctic is warming the land to ocean transport of carbon from thawing permafrost soils and melting ice sheets will increase. Only few studies have addressed the degradation potential of the terrigenous DOM (tDOM) by bacteria by adding river water (Herlemann et al., 2014; Sipler et al., 2017). In NE Greenland the terrestrial DOM supplied mainly from the Greenland Ice Sheet proved to be highly bioavailable (30-40%) compared to the autochthonous fjord DOM (9%) (**Paper IV**), indicating that glacial DOM will be subjected to rapid turn-over in Greenland coastal waters.

While long term (months) bioavailability measurements appears to be a good quantitative measure of the bioavailable DOM pool, they do not take *in situ* conditions nor bacterial community composition at the time of sampling into account (as the bottle effect alters the bacterial community, Box 3). To evaluate biological transformation of the various DOM sources in Young Sound the fluorescence characteristics of DOM (FDOM) was followed (**Paper V**). The development in the fjord as well as fractionation experiments demonstrated that the highest net-growth of bacteria was not coupled to the labile glacial runoff in the surface, but rather to the humic-DOM, though this is commonly considered to be refractory (**Paper V**). This highlights one of the most debated questions in the DOM-field, whether quantity or quality of specific DOM types is more important for the bacterial utilisation (Arrieta et al., 2015a, 2015b). The findings in **Paper IV** and **V** suggest that in Young Sound the quantity of DOM is more important as bacteria were able to utilize humic-DOM only when it was elevated in concentration. This is likely explained by an adaption of the bacterial community; when humic-DOM is sufficiently high bacterial strains with the right range of enzymes will be favoured. In Young Sound the relative abundance of certain bacterial taxa (e.g. SAR92 clade and *Glaciecola*) showed positive correlations to humic-DOM (**Paper V**). These taxa were also recently found to be river-DOM degraders in the Canadian Arctic (Sipler et al. 2017).

In order to test the effect of permafrost DOM on coastal and marine bacterial communities, permafrost from the active layer was collected from svalbard and aged for 1 month in seawater. Hereafter the seawater was filtered through 0.2 μ m filters and added to bacterial communities (3 μ m pre-filtered) in the ratio 1:2.5 to a final concentration of ca. 112 μ M TOC, while controles were added 0.2 μ m filtered sea water in the same ratio (amounting to a final TOC concentration of ca. 60 μ M) (Fig. 7). The aged permafrost DOM (tDOM) had a strong humic signal and when this was added to the sufrage community in Kongsfjorden (Fig. 2) the taxa *Marinomonas* and *Glaciecola* were favoured (**own unpublished results**, not shown). Thus there may be some general responses, like the positive response of the genus *Glaciecola* to humic-DOM/permafrost DOM (**Paper V** and **own unpublished results**), but also regional differences in which taxa are favoured. This was further explored by adding tDOM to off-coast bacterial communities at different depth and measuring the short-term response (up to 8 days) in net-growth (Fig. 7) (**own unpublished results**). Generally communities in high chl *a* waters did not increase growth with the addition of tDOM, while mesopelagic communities increased significantly in net-growth, especially in

Arctic Intermediate Water and Polar Water (Fig. 7). This suggests either that only carbon limited mesopelagic bacterial communities respond to tDOM addition or that the communities in Arctic Intermediate Water and Polar Water are better humic-DOM degraders than the Atlantic Water communities. In case of the first option, these observations are important as run-off maximum in summer coincides with phytoplankton blooms and the coastal bacteria would thus be less likely to consume tDOM.

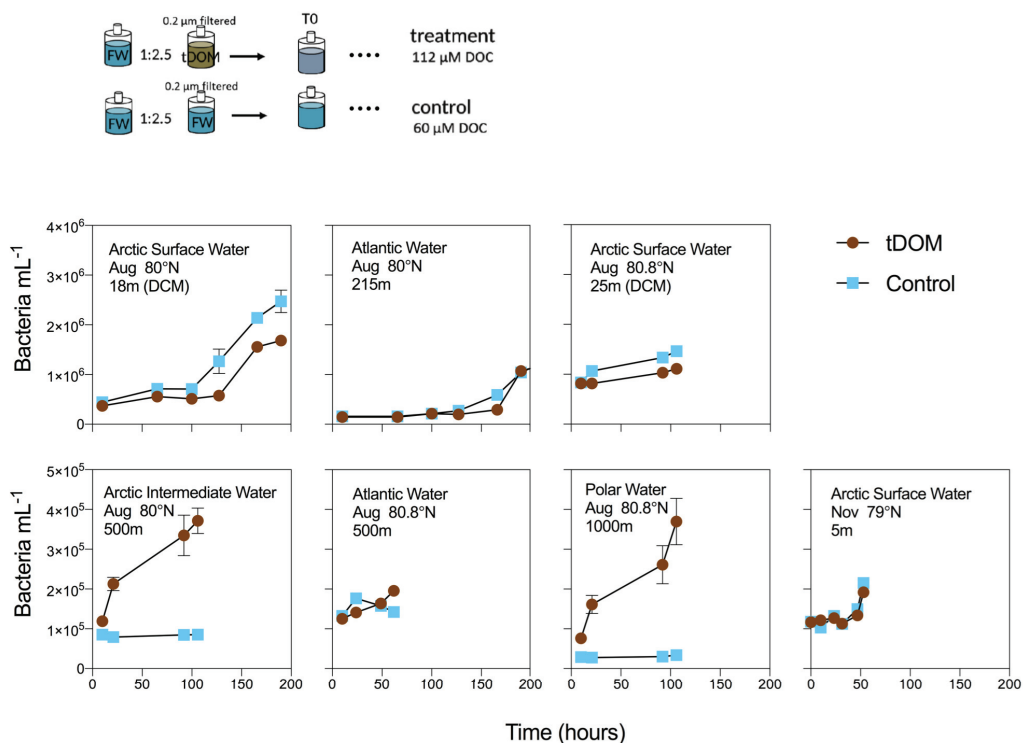


Figure 7: Illustration of the experimental set-up where 0.2 μm filtered permafrost solution (tDOM) or 0.2 μm filtered SW (control) were added to 3 μm pre-filtered water sampled from each location in the ratio 1: 2.5. The response in bacterial net-growth to tDOM addition (brown) compared the control (blue). Water mass of origin (Box 2), month, latitude and sampling depth is given for each experiment. Sample locations are shown in Figure 2.

In addition to terrestrial inputs and bacterial transformation of DOM, I found indications that protist grazing produce humic-DOM and that mesozooplankton grazers enriched the water with amino-like DOM. This study provides evidence that biological processes can play a key role in spatiotemporal FDOM dynamics in an Arctic fjord suggesting the need to consider biological processes when interpreting large-scale FDOM variations (**Paper V**).

Box 3 | The Bottle Effect

The major challenge with incubation experiments is the so-called “bottle effect”, where microorganisms grow ‘unnaturally’ fast and into peculiar high concentrations. This may be due to biofilm forming on the sides of the bottle, changes in substrate availability due to adsorption of cells, carbon or nutrients on glass surfaces, or unintended changes in turbulence patterns, chemistry, or trophic dynamics (Amy and Hiatt, 1989; Calvo-Diaz et al., 2011; Fogg and Calvario-Martinez, 1989). Bottle effects are likely enhanced in smaller volume, but I was not able to document dampened bottle effects when increasing the volume from 2.5L to 3.9L (**Paper II, Paper III, Paper V**) as previously documented (Hammes et al., (2010). This may not come as a surprise given that bottle effects are evident even in large scale (>1000 L) mesocosm incubations (Calvo-Diaz et al., 2011; Hosia et al., 2014; Rahav et al., 2016). Thus the causes of bottle effects remain ambiguous and the problem inevitable. In the present studies the bottle effect occurred after ca. 4 days in low productive communities (January and March) indicated by >10 fold increase in bacterial production. Identification of the bottle effect was more challenging in high activity communities (May and August) (Fig. 8). The best possible incubation time in order to find representative growth and grazing rates is thus a major challenge (as discussed in **Paper II**). I chose a conservative approach and used data from the first 4-5 days in all experiment (**Paper II, III, V**), while the remaining 6-10 days served to qualitatively observe possible further interactions. It seems like the bottle effect can be avoided somewhat by periodically diluting the community (as in **Paper II** where a 10% dilution every second day was applied).

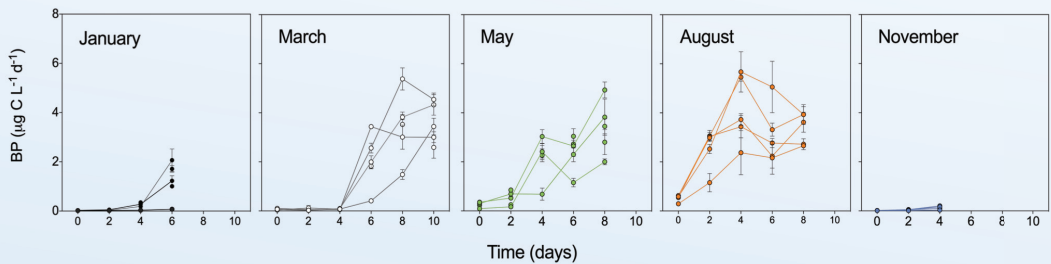


Figure 8: Bacterial production in experiments performed in NW Svalbard (**Paper III**) shown as avg. \pm SD for different size fractions.

When following the change in relative abundance within the bacterial community during a 9 day incubation the community becomes dominated by genus *Cobwellia* at day 4 (Fig. 9), which has also been documented by Stewart et al., (2012). However in incubations in Young Sound the *Cobwellia* genus did not become dominant to the same degree (**Paper V**), thus different communities respond differently to incubation.

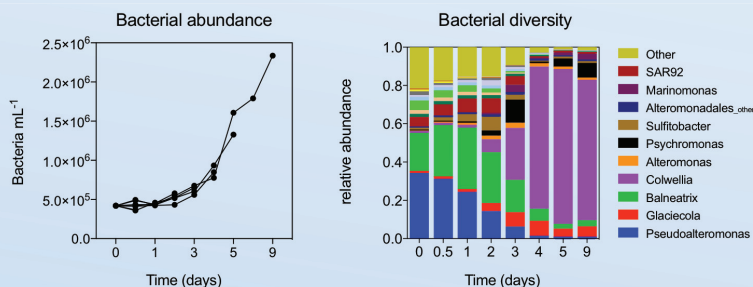


Figure 9: Bacterial abundance and diversity during a 9-day incubation using water from DCM in Kongsfjorden, Svalbard (Fig 2).

6. Top Down Control of Pico-Sized Plankton

6.1. HNF, the key grazer in high latitude systems

Growth and grazing in the microbial food web was in this study estimated by following the net-growth of size-fractionated communities (biases and benefits of the method are assessed in Box 3 and 4). I argue however that this method is more applicable than the dilution method (Box 4), because this technique provides a possibility to distinguish between HNF and MZP grazing. HNF had substantial top-down control on both picophytoplankton and bacteria in all the study regions, and more so than MZP, as the reduction of pico-sized prey growth was as strong or stronger in the treatments where MZP abundance was reduced (**Paper II, III and V**). The grazing pressure on picophytoplankton was highest in the spring period (Table 1) where also picophytoplankton growth and abundance was peaked. Only in March in the Iceland Basin was picophytoplankton grazing not measurable. As discussed in Chapter 5 bacterial grazing was not measurable in winter when bacteria were resources limited rather than top down controlled. Also during spring bloom (in NW Svalbard in May), grazing was not measurable with the fractionation method as the high phytoplankton production in larger size fractions stimulated bacterial growth more than what the advantage of reduced grazing. The grazing of MZP on HNF was only substantial during late winter in the Iceland Basin, possibly remnants of an active microbial loop during winter (**Paper I and II**). The data also suggest that MZP grazing to be more important in AW (dominant at the Iceland Basin) than in polar influenced water masses.

Table 1: Experimentally estimated grazing mortality rates (g, d^{-1}) of microorganisms calculated as the difference in growth rates (μ) between different size fractions (Box 4) in Region 1, 2 and 4. Values are given as mean \pm SD estimated from day 0 to 4-5. Estimates with negative grazing rates (i.e. where the net-growth higher in the grazing reduced treatment) are grey toned. Light green mark the more productive months.

Month	HNF grazing on bacteria			HNF grazing on picophytoplankton			MZP grazing on HNF		
	$\mu_{<0.8\mu m} - \mu_{<10\mu m}$ Iceland Basin	$\mu_{<0.8\mu m} - \mu_{<10\mu m}$ NW Svalbard	$\mu_{<0.8\mu m} - \mu_{<10\mu m}$ Young Sound	$\mu_{<0.8\mu m} - \mu_{<10\mu m}$ Iceland Basin	$\mu_{<3\mu m} - \mu_{<10\mu m}$ NW Svalbard	$\mu_{<3\mu m} - \mu_{<10\mu m}$ Young Sound	$\mu_{<3\mu m} - \mu_{<50\mu m}$ Iceland Basin	$\mu_{<3\mu m} - \mu_{<90\mu m}$ NW Svalbard	$\mu_{<3\mu m} - \mu_{<90\mu m}$ Young Sound
January		-0.022 \pm 0.01			0.05 \pm 0.01			-0.113 \pm 0.01	
March	-0.07 \pm 0.25	-0.017 \pm 0.01		-0.08 \pm 0.29	0.06 \pm 0.01		0.13 \pm 0.29	-0.007 \pm 0.00	
April	0.19 \pm 0.09			0.20 \pm 0.28			0.41 \pm 0.16		
May	0.03 \pm 0.05	-0.20 \pm 0.02		0.02 \pm 0.13	0.19 \pm 0.02		-0.03 \pm 0.29	-0.168 \pm 0.05	
July			0.20 \pm 0.10			0.11 \pm 0.08			0.06 \pm 0.02
August		0.07 \pm 0.02	0.03 \pm 0.06		0.012 \pm 0.00	0.12 \pm 0.04		0.013 \pm 0.01	0.06 \pm 0.04
September			0.03 \pm 0.03			0.02 \pm 0.06			0.03 \pm 0.09
November		0.01 \pm 0.00			0.011 \pm 0.05			-0.007 \pm 0.001	

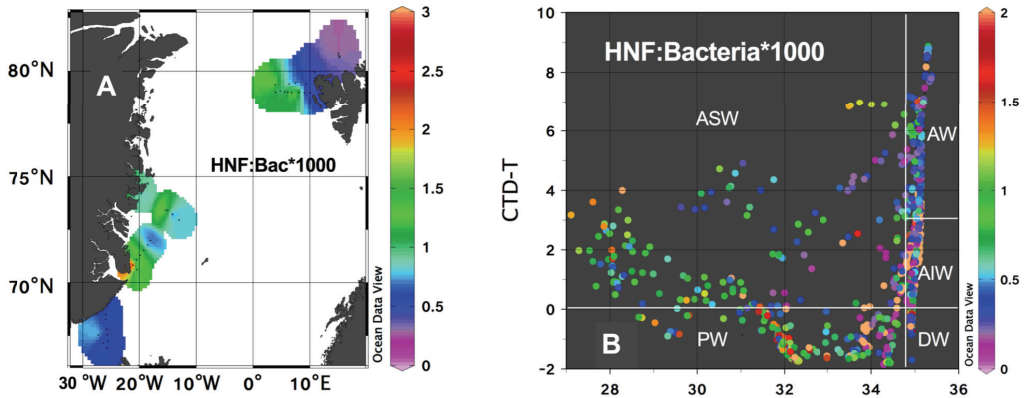


Figure 10: **A)** HNF:Bacteria*1000 in surface samples collected in NE Greenland (Sept 2012) and Young Sound (Aug+Sept 2014). **B)** T-S plots (as explained in Box 2), with an additional z-axis illustrating the HNF:Bact measured from discrete water samples including all regions and seasons.

The ratio of predator to prey proved to be applicable as a rough estimate of grazing pressure (**Paper V**; Sanders et al., 1992). HNF abundance (data not shown) followed a pattern similar to that of bacterial abundance (the two generally correlate positively) and therefore the grazing pressure from HNF (indicated by the ratio HNF:Bac) appeared rather uniform in all water masses even the DW. The highest HNF:Bac (500 bacteria per HNF) was recorded within the PW during spring bloom in the NW Svalbard region and in the Young Sound and NE Greenland dataset (Fig. 10 B). However in the surface water of Young Sound, which is directly influenced by freshwater runoff ($S < 25$) the HNF:Bac was significantly reduced (5000 bacteria per HNF) (data not shown). It has been suggested that small heterotrophic flagellates $< 5\mu\text{m}$ are the main grazers on bacteria, while flagellates $> 5\mu\text{m}$ may also feed on picoeukaryotes (Sherr and Sherr, 2002; Vaqué et al., 2008). This hypothesis was tested in Young Sound. The two size groups of HNF showed different distribution patterns and developed differently in incubations (**Paper V**), suggesting that they have different predators. *In situ* we found a significant positive correlation between large HNF and picophytoplankton abundance in the first period, while small HNF correlated to bacterial abundance (**Paper V**).

HNF have an impressive clearance rate of $\sim 10^6$ body volumes h^{-1} (**Paper II**) as well as the highest growth rate (up to 0.8 d^{-1}) of all microorganisms included in this study, emphasising a high ability to adapt to changing prey densities. Thus pico-sized prey is not necessarily 'grazer relieved' during mixing events (**Paper I and II**) as discussed in Chapter 4. The only environment in which I found HNF grazing to be permanently reduced was within the freshwater lens ($\text{Sal} < 25$) in Young Sound formed by glacial run-off and melting sea ice and icebergs. As a consequence there was extensive growth of both bacteria and picophytoplankton within this layer, and freshwater bacteria and cyanobacteria remained active herein throughout the fjord (**Paper IV and V**).

6.2. Virus control on bacteria

Viruses are major regulators of both picophytoplankton and bacterial abundance (Suttle, 2005). Viral activity was not successfully measured in this study but viruses were counted and the virus to bacteria ratio (VBR) may be used as an indicator of viral activity (Bratbak et al., 2011; Maranger et al., 2015; Weinbauer, 2004). While the HNF:Bac was reduced in surface water of the coastal area and north of Svalbard HNF:Bac (Fig. 10 A), the VBR was elevated (Fig. 11 A), indicating the top-down control from virus and HNF on bacteria may be disconnected. The VBR between different water masses suggest that the AW may generally have higher VBR (around 10) than the water masses with polar influence (around 5) (Fig. 11 B). This overall proposes that pico-sized plankton in Arctic waters are rather HNF controlled, while Atlantic waters to a higher degree are virus controlled.

There were large seasonal differences in the VBR. During pre-bloom in the Subarctic Atlantic the VBR decreased, mirroring an increase in bacteria while viral abundance remained stable (**Paper I and II**), this was observed as well in spring (March and May) in the NW Svalbard region (Fig. 12 B). In the NW Svalbard region VBR followed a annual pattern with a minimum in the most productive summer months (< 10) and a maximum in winter (up to 40), indicating that virus control may be more important in late autumn/winter than in summer. This was supported by incubation experiments where VBR only showed an increase in August and November. The reason that it did not increase in January was most likely that VBR already was extraordinarily high (> 30) in the initial conditions (Fig. 12 B). In conclusion in most seasons there was no strong indications of virus control in the studied Subarctic and Arctic systems.

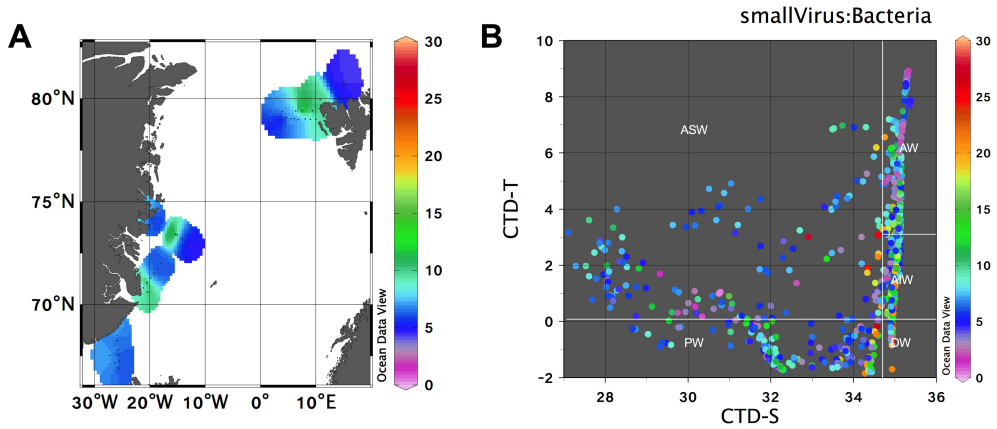


Figure 11: **A)** Virus to bacteria ratio (VBR) in surface samples collected in NE Greenland (Sept 2012) and Young Sound (Aug+Sept 2014). **B)** T-S plots (as explained in Box 2), with an additional z-axis illustrating the HNF:Bact measured from discrete water samples including all regions and seasons.

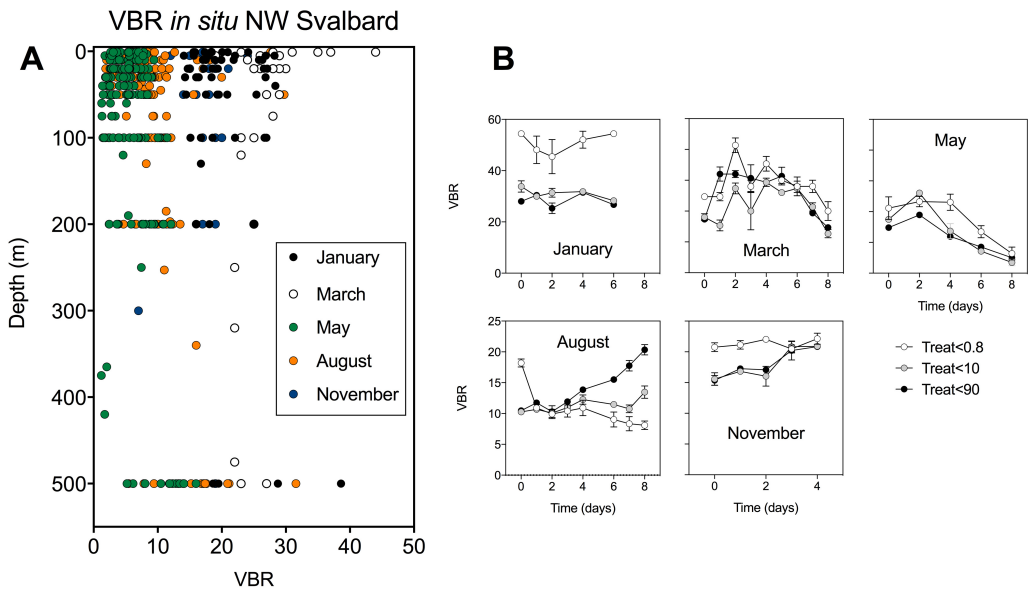


Figure 12: **A)** Seasonal changes in the virus to bacteria ratio (VBR) in the upper 500 m NW Svalbard. **B)** Development in VBR in fractionation experiments (treatments <0.8, 10 and 90 μ m), conducted in NW Svalbard region.

Box 4 | Methodological considerations

Quantification of protozooplankton grazing losses is critical for understanding nutrient and carbon pathways in aquatic systems. The **dilution technique** has been highly valuable (Landry and Calbet, 2004; Landry and Hassett, 1982). With more than 1500 dilution experiments conducted it is the most applied method (Schmoker et al., 2013). The technique relies on several assumptions (Landry and Hassett, 1982) that may not always be valid (reviewed by Calbet and Saiz, 2013; Pree et al., 2015). Further, as the method relies on dilution, it may not work well in environments that are already dilute i.e. the deep mixed station in Iceland Basin (**Paper II**) or winter communities (the method was tested in NW Svalbard during winter, but did not produce measurable results).

Here I obtained grazing estimates using the alternative **size-fractionation technique** (Christaki et al., 2001; Jürgens et al., 2000; Sato et al., 2007; Simek and Chrzanowski, 1992). The technique assumes that predators and prey can be separated by size and that the community essentially can be predator-free by size-screening. Grazing rates of the prey are estimated by the difference in prey growth rates in samples with predators (non-screened) and in samples without predators (screened). This technique also has implications when the presence of larger organisms stimulate prey growth (e.g. bacteria that are carbon limited may grow better when larger phytoplankton are present) or when prey and predator have similar size e.g. chain-forming diatoms can be of the same size as their major protist grazers (dinoflagellates). The advantage of the fractionation method is that it enables a higher degree of detail i.e. the effect of nano- and micro-sized grazers can be distinguished, which is particularly useful when understanding grazing on pico-sized plankton. In **Paper II, III and IV** the growth of pico-sized plankton was generally equal to or even higher in fractions that included MZP compared to those that had only HNF-grazers. Thus the presence of MZP did further increase the grazing pressure on pico-plankton, but could even lower it due to trophic cascading effects (**Paper II**).

A third method to estimate picoplankton grazing is the uptake of or **disappearance of fluorescently labelled bacteria** (FLB) (Vaqué et al., 2008). I attempted to use this technique both in Region 2 and 4 in addition to the fractionation method, by measuring disappearance of FLB using flow cytometry. The experiments, however, failed as the control (0.2µm filtered SW) showed a disappearance in the same order of magnitude as incubations that included protist grazers.

In conclusion, there is no all-around ideal method for estimating growth or grazing impact by protozooplankton. It is therefore important to be confident with the system you are working with before manipulating it or before applying a model. Combinations of several methods would give the more robust result as in Christaki et al., (2001). Further, when aiming to measure grazing on one specific prey type it is worth considering the abundance of other prey types within the same size-class (when grazing is merely size specific). The grazing pressure of less abundant prey types is likely relaxed when other prey are more abundant. This is here illustrated by *Synechococcus*, which expressed highest growth rates in the months where the total pico-sized prey to HNF ratio was high (**Paper III**) i.e. grazing was relaxed (Fig. 13).

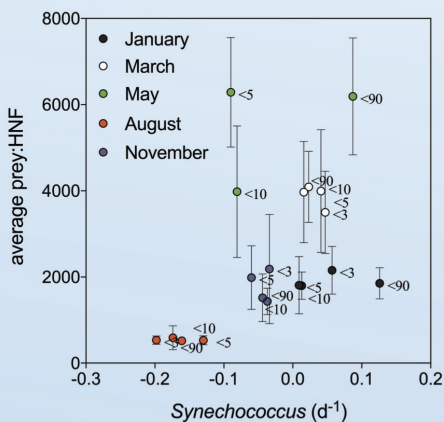


Figure 13: Growth rates of *Synechococcus* plotted against the ratio of pico-sized prey to HNF grazers, the latter is shown as average \pm SD within the same time period as the growth was estimated. Prey is here the sum of bacteria, picoeukaryotes and *Synechococcus*. Data was collected from the 5 fractionation-experiment performed at the NW Svalbard region. Colours indicate month and labels specify the given size-fraction.

7. Conclusion and future perspectives

My studies underline that pico-sized plankton play a fundamental role in the carbon transfer in high latitude ecosystems both as primary producers (picophytoplankton) and via the microbial loop (bacteria). HNF grazing is often not considered in high latitude systems, however as HNF grazing is substantial throughout the entire year, both in the epipelagic and mesopelagic Ocean, the carbon flow in the pelagic food web cannot be assessed without addressing HNF grazing.

In high latitude systems microorganisms experience different challenges over a large spatial and seasonal scale. My studies suggest that pico-sized plankton are well adapted to these challenges. Picophytoplankton were better adapted to low light conditions than larger phytoplankton thus coping better with the seasonal darkness (**Paper I, III**) and with darkening of coastal water due to silty runoff (Fig. 5, **own unpublished results**). Bacteria proved to be highly capable of degrading terrestrial organic carbon sources, but these abilities were highly community specific (**Paper V**). In both the Greenland and the Svalbard fjord systems studied the genus *Glaciecola* responded positively to humic-/permafrost DOM, while in the mesopelagic marine environments off the coast of NE Svalbard it was *Marinomonas* and *Oleispira* that benefited. In conclusion, this suggests a picophytoplankton are likely to become more prominent in the phytoplankton community under the predicted climate changes and that the bacterial community will adapt to new carbon sources and degrade these when present in sufficient concentrations, thus leading to an increased CO₂ production. Shifts in coastal microbial community composition may thus be anticipated, but the ecological consequences of such changes remain unresolved.

Increased dominance of pico-sized plankton is often considered a threat to the existing Subarctic and Arctic food webs where the linear classical food chain based on large phytoplankton species (Fig. 1). This view has been opposed by Barber & Hiscock (2006) and Barber (2007), who suggest that picophytoplankton contribute greatly to both the classical food web and the pelagic-benthic coupling, both indirectly and directly by forming aggregates. Further Barber emphasises the importance of an active microbial food web in regard to retaining nutrients in the surface waters and thus prolonging the productive period, while the classic linear food web empties the surface water via the biological pump.

Marine microbial science is growing and a strong emphasis is put on improving the molecular data of microbial communities, with ‘omics and modelling proposed to be the way forward to understand the system better (Brussaard et al., 2016). However, I would stress that there is also a need to develop methods of simple enumeration and activity measurements. Even the counts of bacteria and HNF performed on flow cytometer today have inherent challenges and uncertainties. The standard methods of quantifying bacterial production are not applicable in low active systems (Hill et al., 2013), and all incubation experiments are biased due to the bottle effect (Box 3) and there is no ideal way to measure grazing across different systems (Box 4). Thus I would argue that there is a strong need to advance also in the more traditional methods used to measure microbial activities such as grazing, production and uptake rates, especially to understand low productive systems, as many standard methods are not accurate enough. These measures are paramount in helping enlighten metabolic pathways and test hypotheses on metabolic interactions, competition and responses to environmental changes. I would suggest increasing the use of radio-isotope labelled cells and organic matter to trace flows of carbon in the food web and e.g. measure HNF grazing (Zubkov and Tarran, 2008). To avoid the bottle effect I suggest to use only short-term incubations of a few days, no matter the volume, and to experiment with keeping bottles in motion or using silicone-coating bottles for incubations to reduce biofilm formation. There is still much space for both methodological development and improved sampling coverage of the high latitude systems in order to better understand the microbial systems herein.

References

- Agawin, N. N. S. R., Duarte, C. M., and Agustí, S. (2000). Nutrient and temperature control of the contribution of picoplankton to phytoplankton biomass and production. *Limnol. Oceanogr.* 45, 591–600.
- Amy, P. S., and Hiatt, H. D. (1989). Survival and Detection of Bacteria in. *Appl. Environmental Microbiol.* 55, 788–793.
- Andersen, K. H., Berge, T., Gonçalves, R. J., Hartvig, M., Heuschele, J., Hylander, S., et al. (2016). Characteristic Sizes of Life in the Oceans, from Bacteria to Whales. *Ann. Rev. Mar. Sci.* 8, 150710224004001. doi:10.1146/annurev-marine-122414-034144.
- Arendt, K. E., Agersted, M. D., Sejr, M. K., and Juul-pedersen, T. (2016). Glacial meltwater influences on plankton community structure and the importance of top-down control (of primary production) in a NE Greenland fjord. *Estuarine, Coast. Shelf Sci. Shelf Sci.* 183, 123–135. doi:10.1016/j.ecss.2016.08.026.
- Arrieta, J. M., Mayol, E., Hansman, R. L., Gerhard, J., Dittmar, T., Duarte, C. M., et al. (2015a). Comment on “Dilution limits dissolved organic carbon utilization in the deep ocean.” *Science (80-.).* 350, 1483–a. doi:10.1126/science.1258955.
- Arrieta, J. M., Mayol, E., Hansman, R. L., Gerhard, J., Dittmar, T., and Duarte, C. M. (2015b). Dilution limits dissolved organic carbon utilization in the deep ocean. *Scienceexpress*, 1–7.
- Azam, F., Fenchel, T., Field, J. G., Gray, J. S., and Thingstad, F. (1983). The Ecological Role of Water-Column Microbes in the Sea *. *Mar. Ecol. Prog. Ser.* 10, 257–263.
- Backhaus, J. O., Hegseth, E. N., Wehde, H., Irigoien, X., Hatten, K., and Logemann, K. (2003). Convection and primary production in winter. *Mar. Ecol. Prog. Ser.* 251, 1–14.
- Baña, Z., Ayo, B., Marrasé, C., Gasol, J. M., and Iriberry, J. (2014). Changes in bacterial metabolism as a response to dissolved organic matter modification during protozoan grazing in coastal Cantabrian and Mediterranean waters. *Environ. Microbiol.* 16, 498–511. doi:10.1111/1462-2920.12274.
- Blindheim, J., and Østerhus, S. (2005). The Nordic Seas, Main Oceanographic Features. *Geophys. Monogr. Ser.* 158, 11–37.
- Bratbak, G., Jacquet, S., Larsen, A., Pettersson, L. H., Sazhin, A. F., and Thyrraug, R. (2011). The plankton community in Norwegian coastal waters—abundance, composition, spatial distribution and diel variation. *Cont. Shelf Res.* 31, 1500–1514. doi:10.1016/j.csr.2011.06.014.
- Brierley, A. S., and Kingsford, M. J. (2009). Impacts of Climate Change on Marine Organisms and Ecosystems. *Curr. Biol.* 19, R602–R614. doi:10.1016/j.cub.2009.05.046.

-
- Brussaard, C. P. D., Bidle, K. D., Pedrós-alió, C., and Legrand, C. (2016). The interactive microbial ocean. *Nat. Publ. Gr.* 2, 1–2. doi:10.1038/nmicrobiol.2016.255.
- Cabello, A. M., Latasa, M., Forn, I., Morán, X. A. G., and Massana, R. (2016). Vertical distribution of major photosynthetic picoeukaryotic groups in stratified marine waters. *Environ. Microbiol.* 18, 1578–1590. doi:10.1111/1462-2920.13285.
- Calbet, A., Agersted, M. D., Kaartvedt, S., Møhl, M., Møller, E. F., Enghoff-Poulsen, S., et al. (2015). Heterogeneous distribution of plankton within the mixed layer and its implications for bloom formation in tropical seas. *Sci. Rep.* 5. doi:10.1038/srep11240.
- Calbet, A., and Saiz, E. (2013). Effects of trophic cascades in dilution grazing experiments: from artificial saturated feeding responses to positive slopes. *J. Plankton Res.* 35, 1183–1191. doi:10.1093/plankt/fbt067.
- Calbet, A., Riisgaard, K., Saiz, E., Zamora, S., Stedmon, C., and Nielsen, T. (2011). Phytoplankton growth and microzooplankton grazing along a sub-Arctic fjord (Godthåbsfjord, west Greenland). *Mar. Ecol. Prog. Ser.* 442, 11–22. doi:10.3354/meps09343.
- Calvo-Díaz, A., Díaz-Pérez, L., Suárez, L. Á., Morán, X. A. G., Teira, E., Marañón, E., et al. (2011). Decrease in the autotrophic-to-heterotrophic biomass ratio of picoplankton in oligotrophic marine waters due to bottle enclosure. *Appl. Environ. Microbiol.* 77, 5739–5746. doi:10.1128/AEM.00066-11.
- Carmack, E., and McLaughlin, F. (2011). Towards recognition of physical and geochemical change in Subarctic and Arctic Seas. *Prog. Oceanogr.* 90, 90–104. doi:10.1016/j.pocean.2011.02.007.
- Chakraborty, S., Nielsen, L. T., and Andersen, K. H. (2017). Trophic Strategies of Unicellular Plankton. *Am. Nat.* 189, E77–E90. doi:10.1086/690764.
- Christaki, U., Giannakourou, A., Wambeke, F. V. A. N. W., and Grégori, G. (2001). Nanoflagellate predation on auto- and heterotrophic picoplankton in the oligotrophic Mediterranean Sea. *J. Plankton Res.* 23, 1297–1310. doi:10.1093/plankt/23.11.1297.
- Christaki, U., Vázquez-Domínguez, E., Courties, C., and Lebaron, P. (2005). Grazing impact of different heterotrophic nanoflagellates on eukaryotic (*Ostreococcus tauri*) and prokaryotic picoautotrophs (*Prochlorococcus* and *Synechococcus*). *Environ. Microbiol.* 7, 1200–10. doi:10.1111/j.1462-2920.2005.00800.x.
- Cottrell, M. T., and Kirchman, D. L. (2009). Photoheterotrophic microbes in the Arctic Ocean in summer and winter. *Appl. Environ. Microbiol.* 75, 4958–4966. doi:10.1128/AEM.00117-09.
- Cullen, J. J., Franks, P. J. S., Karl, D. M., and Longhurst, A. (2002). *Chapter 8 . PHYSICAL INFLUENCES ON MARINE ECOSYSTEM DYNAMICS.*

-
- Dale, T., Rey, F., and Heimdal, B. R. (1999). Seasonal development of phytoplankton at a high latitude oceanic site. *Sarsia* 84, 419–435. doi:10.1080/00364827.1999.10807347.
- Daniels, C. J., Poulton, A. J., Esposito, M., Paulsen, M. L., Bellerby, R., St John, M., et al. (2015). Phytoplankton dynamics in contrasting early stage North Atlantic spring blooms: composition, succession, and potential drivers. *Biogeosciences* 12, 93–133. doi:10.5194/bg-12-2395-2015.
- Daufresne, M., Lengfellner, K., and Sommer, U. (2009). Global warming benefits the small in aquatic ecosystems. *Proc. Natl. Acad. Sci.* 106, 12788–12793. doi:10.1073/pnas.0902080106.
- Dittmar, T., and Kattner, G. (2003). The biogeochemistry of the river and shelf ecosystem of the Arctic Ocean: a review. *Mar. Chem.* 83, 103–120. doi:10.1016/S0304-4203(03)00105-1.
- Edwards, M., and Richardson, A. J. (2004). Impact of climate change on marine pelagic phenology and trophic mismatch. *Nature* 430, 881–884. doi:10.1038/nature02808.
- Eilertsen, H. C., and Wyatt, T. (2000). Phytoplankton models and life history strategies. *South African J. Mar. Sci.* 22, 323–338. doi:10.2989/025776100784125717.
- Fenchel, T. (1987). “Ecological Physiology: Feeding,” in *Ecology of Protozoa: The Biology of Free-living Phagotrophic Protists* (Berlin, Heidelberg: Springer Berlin Heidelberg), 32–52. doi:10.1007/978-3-662-06817-5_3.
- Fichot, C. G., Kaiser, K., Hooker, S. B., Amon, R. M. W., Babin, M., Bélanger, S., et al. (2013). Pan-Arctic distributions of continental runoff in the Arctic Ocean. *Sci. Rep.* 3, 1053. doi:10.1038/srep01053.
- Field, C. B. (1998). Primary Production of the Biosphere: Integrating Terrestrial and Oceanic Components. *Science (80-)*. 281, 237–240. doi:10.1126/science.281.5374.237.
- Fogg, G. E., and Calvario-Martinez, O. (1989). Effects of bottle size in determinations of primary productivity by phytoplankton. *Hydrobiologia* 173, 89–94. doi:10.1007/BF00015518.
- Gasol, J. M., del Giorgio, P. A., and Duarte, C. M. (1997). Biomass distribution in marine planktonic communities. *Limnol. Oceanogr.* 42, 1353–1363.
- Goldman, J. C. (1980). “Physiological processes, nutrient availability, and the concept of relative growth rate in marine phytoplankton ecology,” in *Primary productivity in the sea*, ed. P. G. FALKOWSK (New York: Plenum Press), 179–194.
- Gonçalves-Araujo, R., Granskog, M. A., Bracher, A., Azetsu-scott, K., Dodd, P. A., and Stedmon, Colin, A. (2016). Using fluorescent dissolved organic matter to trace and distinguish the origin of Arctic surface waters. *Sci. Rep.*, 1–12. doi:10.1038/srep33978.
- Gradinger, R., and Lenz, J. (1995). Seasonal occurrence of picocyanobacteria in the Greenland Sea and central

-
- Arctic Ocean. *Polar Biol.* 15, 447–452. doi:10.1007/BF00239722.
- Hammes, F., Vital, M., and Egli, T. (2010). Critical evaluation of the volumetric “bottle effect” on microbial batch growth. *Appl. Environ. Microbiol.* 76, 1278–81. doi:10.1128/AEM.01914-09.
- Hansell, D. A., Carlson, C. A., Repeta, D. J., and Schlitzer, R. (2009). Dissolved organic matter in the ocean - a controversy stimulates new insights. *Oceanography* 22, 202–211.
- Hartmann, M., Grob, C., Tarran, G. A., Martin, A. P., Burkill, P. H., Scanlan, D. J., et al. (2012). Mixotrophic basis of Atlantic oligotrophic ecosystems. *Proc. Natl. Acad. Sci.* 109, 5756–5760. doi:10.1073/pnas.1118179109.
- Hedges, J. I., Keil, R. G., and Benner, R. (1997). What happens to terrestrial organic matter in the ocean? *Org. Geochem.* 27, 195–212. doi:10.1016/S0146-6380(97)00066-1.
- Herlemann, D. P. R., Manecki, M., Meeske, C., Pollehne, F., Labrenz, M., Schulz-Bull, D., et al. (2014). Uncoupling of bacterial and terrigenous dissolved organic matter dynamics in decomposition experiments. *PLoS One* 9, 1–12. doi:10.1371/journal.pone.0093945.
- Hill, P. G., Warwick, P. E., and Zubkov, M. V. (2013). Low microbial respiration of leucine at ambient oceanic concentration in the mixed layer of the central Atlantic Ocean. *Limnol. Oceanogr.* 58, 1597–1604. doi:10.4319/lo.2013.58.5.1597.
- Hosia, A., Augustin, C. B., Dinasquet, J., Granhag, L., Paulsen, M. L., Riemann, L., et al. (2014). Autumnal bottom-up and top-down impacts of *Cyanea capillata*: A mesocosm study. *J. Plankton Res.* 37. doi:10.1093/plankt/fbv046.
- Irigoien, X., Flynn, K. J., and Harris, R. P. (2005). Phytoplankton blooms : a “ loophole ” in microzooplankton grazing impact ? *J. Plankton Res.* 27, 313–321. doi:10.1093/plankt/fbi011.
- Itkin, P., Karcher, M., and Gerdes, R. (2014). Is weaker Arctic sea ice changing the Atlantic water circulation? *J. Geophys. Res. Ocean.*, 5992–6009. doi:10.1002/2013JC009633. Received.
- Jacobson, D. M., and Anderson, D. M. (1996). Widespread Phagocytosis of Ciliates and Other Protists By Marine Mixotrophic and Heterotrophic Thecate Dinoflagellates1. *J. Phycol.* 32, 279–285. doi:10.1111/j.0022-3646.1996.00279.x.
- Jakobsen, H. H., and Markager, S. (2016). Carbon-to-chlorophyll ratio for phytoplankton in temperate coastal waters: Seasonal patterns and relationship to nutrients. *Limnol. Oceanogr.* 61, 1853–1868. doi:10.1002/lno.10338.
- Jumars, P. A., Deming, J. W., Hill, P. S., Karp-boss, L., Yager, P. L., and Dade, W. B. (1993). Physical Constraints on Marine Osmotrophy in an Optimal Foraging Context. *Mar. Microb. Food Web* 7, 121–159.

-
- Jürgens, K., Gasol, J. M., and Vaqué, D. (2000). Bacteria-flagellate coupling in microcosm experiments in the Central Atlantic Ocean. *J. Exp. Mar. Bio. Ecol.* 245, 127–147. doi:10.1016/S0022-0981(99)00156-2.
- Kjørboe, T. (1993). Turbulence, Phytoplankton Cell Size and the Structure of Pelagic Food Webs. *Adv. Mar. Biol.* 29, 2–61.
- Kirchman, D. L., Elifantz, H., Dittel, A. I., Malmstrom, R. R., and Cottrell, M. T. (2007). Standing stocks and activity of Archaea and Bacteria in the western Arctic Ocean. *Limnol. Oceanogr.* 52, 495–507. doi:10.4319/lo.2007.52.2.0495.
- Kirchman, D. L., Malmstrom, R. R., and Cottrell, M. T. (2005). Control of bacterial growth by temperature and organic matter in the Western Arctic. *Deep Sea Res. Part II Top. Stud. Oceanogr.* 52, 3386–3395. doi:10.1016/j.dsr2.2005.09.005.
- Kirchman, D. L., Morán, X. A. G., and Ducklow, H. (2009). Microbial growth in the polar oceans - role of temperature and potential impact of climate change. *Nat. Rev. Microbiol.* 7, 451–459. doi:10.1038/nrmicro2115.
- Landry, M. R., and Calbet, A. (2004). Microzooplankton production in the oceans. *ICES J. Mar. Sci.* 61, 501–507. doi:10.1016/j.icesjms.2004.03.011.
- Landry, M. R., and Hassett, R. P. (1982). Estimating the grazing impact of marine micro-zooplankton. *Mar. Biol.* 67, 283–288. doi:10.1007/BF00397668.
- Lawson, E. C., Wadham, J. L., Tranter, M., Stibal, M., Lis, G. P., Butler, C. E. H., et al. (2014). Greenland Ice Sheet exports labile organic carbon to the Arctic oceans. *Biogeosciences* 11, 4015–4028. doi:10.5194/bg-11-4015-2014.
- Leblanc, K. (2005). A seasonal study of diatom dynamics in the North Atlantic during the POMME experiment (2001): Evidence for Si limitation of the spring bloom. *J. Geophys. Res.* 110, C07S14. doi:10.1029/2004JC002621.
- Levinsen, H., and Nielsen, T. G. (2002). The trophic role of marine pelagic ciliates and heterotrophic dinoflagellates in arctic and temperate coastal ecosystems: A cross-latitude comparison. *Limnol. Oceanogr.* 47, 427–439. doi:10.4319/lo.2002.47.2.0427.
- Li, W. K. W. (1993). Composition of ultraphytoplankton in the central North Atlantic. 1992.
- Li, W. K. W., McLaughlin, F. a, Lovejoy, C., and Carmack, E. C. (2009). Smallest algae thrive as the Arctic Ocean freshens. *Science* 326, 539. doi:10.1126/science.1179798.
- Longhurst, A. (1995). Seasonal cycles of pelagic production and consumption. *Prog. Oceanogr.* 36, 77–167. doi:10.1016/0079-6611(95)00015-1.

-
- Lovejoy, C., Vincent, W. F., Bonilla, S., Roy, S., Martineau, M.-J., Terrado, R., et al. (2007). Distribution, phylogeny, and growth of cold-adapted picoprasinophytes in Arctic seas. *J. Phycol.* 43, 78–89. doi:10.1111/j.1529-8817.2006.00310.x.
- Maranger, R., Vaqué, D., Nguyen, D., Hébert, M. P., and Lara, E. (2015). Pan-Arctic patterns of planktonic heterotrophic microbial abundance and processes: Controlling factors and potential impacts of warming. *Prog. Oceanogr.* 139, 221–232. doi:10.1016/j.pocean.2015.07.006.
- Margalef, R. (1978). Life-forms of phytoplankton as survival alternatives in an unstable environment. *Oceanol. Acta* 1, 493–509.
- Martínez-garcía, S., Fernández, E., Aranguren-gassis, M., and Teira, E. (2009). LIMNOLOGY OCEANOGRAPHY: METHODS In vivo electron transport system activity: a method to estimate respiration in natural marine microbial planktonic communities. 459–469.
- McClelland, J. W., Holmes, R. M., Dunton, K. H., and Macdonald, R. W. (2012). The Arctic Ocean Estuary. *Estuaries and Coasts* 35, 353–368. doi:10.1007/s12237-010-9357-3.
- Middelboe, M., and Lundsgaard, C. (2003). Microbial activity in the Greenland Sea: role of DOC lability, mineral nutrients and temperature. *Aquat. Microb. Ecol.* 32, 151–163.
- Morán, X. A. G., López-Urrutia, À., Calvo-Díaz, a, and Li, W. K. W. (2010). Increasing importance of small phytoplankton in a warmer ocean. *Glob. Chang. Biol.* 16, 1137–1144. doi:10.1111/j.1365-2486.2009.01960.x.
- Morison, F., and Menden-Deuer, S. (2015). Early spring phytoplankton dynamics in the subpolar north atlantic: The influence of protistan herbivory. *Limnol. Oceanogr.* 60, 1298–1313. doi:10.1002/lno.10099.
- Not, F., Latasa, M., Marie, D., Cariou, T., Vaulot, D., Simon, N., et al. (2004). A Single Species, *Micromonas pusilla* (Prasinophyceae), Dominates the Eukaryotic Picoplankton in the Western English Channel. *Appl. Environ. Microbiol.* 70, 4064–4072. doi:10.1128/AEM.70.7.4064.
- Osterholz, H., Singer, G., Wemheuer, B., Daniel, R., Simon, M., Niggemann, J., et al. (2016). Deciphering associations between dissolved organic molecules and bacterial communities in a pelagic marine system. *ISME J.* 10. doi:10.1038/ismej.2015.231.
- Pedrós-Alió, C., Potvin, M., and Lovejoy, C. (2015). Diversity of planktonic microorganisms in the Arctic Ocean. *Prog. Oceanogr.* 139, 233–243. doi:10.1016/j.pocean.2015.07.009.
- Pernthaler, J. (2005). Predation on prokaryotes in the water column and its ecological implications. *Nat. Rev. Microbiol.* 3, 537–46. doi:10.1038/nrmicro1180.
- van De Poll, W. H., Maat, D. S., Fischer, P., Rozema, P. D., Daly, O. B., Koppelle, S., et al. (2016). Atlantic Advection Driven Changes in Glacial Meltwater: Effects on Phytoplankton Chlorophyll-a and

- Taxonomic Composition in Kongsfjorden, Spitsbergen. *Front. Mar. Sci.* 3, 1–11. doi:10.3389/fmars.2016.00200.
- Pomeroy, L. R., and Deibel, D. (1986). Temperature Regulation of Bacterial Activity During the Spring Bloom in Newfoundland Coastal Waters. *Science* (80-). 233, 359–361. Available at: <http://science.sciencemag.org/content/233/4761/359.abstract>.
- Pree, B., Kuhlisch, C., Pohnert, G., Sazhin, A. F., Jakobsen, H. H., Lund Paulsen, M., et al. (2015). A simple adjustment to test reliability of bacterivory rates derived from the dilution method. *Limnol. Oceanogr. Methods* 14, 114–123. doi:10.1002/lom3.10076.
- Rahav, E., Shun-Yan, C., Cui, G., Liu, H., Tsagaraki, T. M., Giannakourou, A., et al. (2016). Evaluating the Impact of Atmospheric Depositions on Springtime Dinitrogen Fixation in the Cretan Sea (Eastern Mediterranean)—A Mesocosm Approach. *Front. Mar. Sci.* 3, 1–13. doi:10.3389/fmars.2016.00180.
- Raven, J. A. (1998). Small is beautiful : the picophytoplankton. *Funct. Ecol.* 12, 503–513.
- Rees, A. P., Joint, I., and Donald, K. M. (1999). Early spring bloom phytoplankton-nutrient dynamics at the Celtic Sea shelf edge. *Deep. Res. Part I Oceanogr. Res. Pap.* 46, 483–510. doi:10.1016/S0967-0637(98)00073-9.
- Riisgaard, K., Nielsen, T., and Hansen, P. (2015). Impact of elevated pH on succession in the Arctic spring bloom. *Mar. Ecol. Prog. Ser.* 530, 63–75. doi:10.3354/meps11296.
- Sanders, R. W., Caron, David, A., and Berninger, U.-G. (1992). Relationships between bacteria and heterotrophic nanoplankton in marine and fresh waters: an inter-ecosystem comparison. *Mar. Ecol. Prog. Ser.* 86, 1–14.
- Sanders, R. W., and Gast, R. J. (2012). Bacterivory by phototrophic picoplankton and nanoplankton in Arctic waters. *FEMS Microbiol. Ecol.* 82, 242–53. doi:10.1111/j.1574-6941.2011.01253.x.
- Sato, M., Yoshikawa, T., Takeda, S., and Furuya, K. (2007). Application of the size-fractionation method to simultaneous estimation of clearance rates by heterotrophic flagellates and ciliates of pico- and nanophytoplankton. *J. Exp. Mar. Bio. Ecol.* 349, 334–343. doi:10.1016/j.jembe.2007.05.027.
- Schauer, U., Fahrbach, E., Osterhus, S., and Rohardt, G. (2004). Arctic warming through the Fram Strait: Oceanic heat transport from 3 years of measurements. *J. Geophys. Res. C Ocean.* 109, 1–14. doi:10.1029/2003JC001823.
- Schmittner, A. (2005). Decline of the marine ecosystem caused by a reduction in the Atlantic overturning circulation. *Nature* 434, 628–633. doi:10.1038/nature03476.
- Schmoker, C., Hernandez-Leon, S., and Calbet, A. (2013). Microzooplankton grazing in the oceans: impacts, data variability, knowledge gaps and future directions. *J. Plankton Res.* 35, 691–706.

doi:10.1093/plankt/fbt023.

- Seuthe, L., Iversen, K. R., and Narcy, F. (2011). Microbial processes in a high-latitude fjord (Kongsfjorden, Svalbard): II. Ciliates and dinoflagellates. *Polar Biol.* 34, 751–766. doi:10.1007/s00300-010-0930-9.
- Sherr, E. B., and Sherr, B. F. (2002). Significance of predation by protists in aquatic microbial food webs. *Antonie Van Leeuwenhoek* 81, 293–308.
- Sherr, E. B., Sherr, B. F., Wheeler, P. a., and Thompson, K. (2003). Temporal and spatial variation in stocks of autotrophic and heterotrophic microbes in the upper water column of the central Arctic Ocean. *Deep Sea Res. Part I* 50, 557–571. doi:10.1016/S0967-0637(03)00031-1.
- Simek, K., and Chrzanowski, T. H. (1992). Direct and Indirect Evidence of Size-Selective Nanoflagellates Grazing Pelagic Bacteria by Freshwater Nanoflagellates. *Appl. Environmantal Microbiol.* 58, 3715–3720.
- Sipler, R. E., Kellogg, C. T. E., Connelly, T. L., Roberts, Q. N., Yager, P. L., and Bronk, D. A. (2017). Microbial Community Response to Terrestrially Derived Dissolved Organic Matter in the Coastal Arctic. *Front. Microbiol.* 8, 1–19. doi:10.3389/fmicb.2017.01018.
- Slagstad, D., and Mcclimans, T. A. (2005). Modeling the ecosystem dynamics of the Barents sea including the marginal ice zone: I . Physical and chemical oceanography. 58, 1–18. doi:10.1016/j.jmarsys.2005.05.005.
- Smetacek, V. S. (1985). Role of sinking in diatom life-history cycles: ecological, evolutionary and geological significance. *Mar. Biol.* 84, 239–251. doi:10.1007/BF00392493.
- Somogyi, B., Pálffy, K., Balogh, K. V, Botta-Dukát, Z., and Vörös (2017). Unusual behaviour of phototrophic picoplankton in turbid waters. *PLoS One*, 1–15. doi:10.1371/journal.pone.0174316.
- Sørensen, N., Daugbjerg, N., and Richardson, K. (2017). Succession of picophytoplankton during the spring bloom 2012 in Disko Bay (West Greenland)— an unexpectedly low abundance of green algae. *Polar Biol.* 40, 463–469. doi:10.1007/s00300-016-1952-8.
- Stedmon, C. A., Amon, R. M. W., Rinehart, a. J., and Walker, S. a. (2011). The supply and characteristics of colored dissolved organic matter (CDOM) in the Arctic Ocean: Pan Arctic trends and differences. *Mar. Chem.* 124, 108–118. doi:10.1016/j.marchem.2010.12.007.
- Stewart, F. J., Dalsgaard, T., Young, C. R., Thamdrup, B., Revsbech, N. P., Ulloa, O., et al. (2012). Experimental Incubations Elicit Profound Changes in Community Transcription in OMZ Bacterioplankton. *PLoS One* 7. doi:10.1371/journal.pone.0037118.
- Suttle, C. A (2005). Viruses in the sea. *Nature* 437, 356–61. doi:10.1038/nature04160.
- Terrado, R., Medrinal, E., Dasilva, C., Thaler, M., Vincent, W. F., and Lovejoy, C. (2011). Protist community

- composition during spring in an Arctic flaw lead polynya. *Polar Biol.* 34, 1901–1914. doi:10.1007/s00300-011-1039-5.
- Thingstad, T. F. (1998). A theoretical approach to structuring mechanisms in the pelagic food web. *Hydrobiologia* 363, 59–72. doi:10.1007/978-94-017-1493-8.
- Thingstad, T. F., Bellerby, R. G. J., Bratbak, G., Børsheim, K. Y., Egge, J. K., Heldal, M., et al. (2008). Counterintuitive carbon-to-nutrient coupling in an Arctic pelagic ecosystem. *Nature* 455, 387–90. doi:10.1038/nature07235.
- Tremblay, G., Belzile, C., Gosselin, M., Poulin, M., Roy, S., and Tremblay, J. (2009). Late summer phytoplankton distribution along a 3500 km transect in Canadian Arctic waters: strong numerical dominance by picoeukaryotes. *Aquat. Microb. Ecol.* 54, 55–70. doi:10.3354/ame01257.
- Tremblay, J. É., Anderson, L. G., Matrai, P., Coupel, P., Bélanger, S., Michel, C., et al. (2015). Global and regional drivers of nutrient supply, primary production and CO₂ drawdown in the changing Arctic Ocean. *Prog. Oceanogr.* 139, 171–196. doi:10.1016/j.pocean.2015.08.009.
- Vaqué, D., Guadayol, Ò., Peters, F., Felipe, J., Angel-Ripoll, L., Terrado, R., et al. (2008). Seasonal changes in planktonic bacterivory rates under the ice-covered coastal Arctic Ocean. *Limnol. Oceanogr.* 53, 2427–2438.
- Vaulot, D., Eikrem, W., Viprey, M., and Moreau, H. (2008). The diversity of small eukaryotic phytoplankton ($\leq 3 \mu\text{m}$) in marine ecosystems. *FEMS Microbiol. Rev.* 32, 795–820. doi:10.1111/j.1574-6976.2008.00121.x.
- Velasco, E. M., Almeda, R., Saiz, E., Calbet, A., Isari, S., Anto, M., et al. (2013). Deep-Sea Research I Zooplankton distribution and feeding in the Arctic Ocean during a *Phaeocystis pouchetii* bloom. *Deep Sea Res. I* 72, 17–33. doi:10.1016/j.dsr.2012.10.003.
- Vernet, M., Richardson, T. L., Metfies, K., Nöthig, E., and Peeken, I. (2017). Models of Plankton Community Changes during a Warm Water Anomaly in Arctic Waters Show Altered Trophic Pathways with Minimal Changes in Carbon Export. *Front. Mar. Sci.* 4, 1–19. doi:10.3389/fmars.2017.00160.
- Wassmann, P., Duarte, C. M., Agustí, S., and Sejr, M. K. (2011). Footprints of climate change in the Arctic marine ecosystem. *Glob. Chang. Biol.* 17, 1235–1249. doi:10.1111/j.1365-2486.2010.02311.x.
- Wassmann, P., Kosobokova, K. N., Slagstad, D., Drinkwater, K. F., Hopcroft, R. R., Moore, S. E., et al. (2015). The contiguous domains of Arctic Ocean advection: Trails of life and death. *Prog. Oceanogr.* 139, 42–65. doi:10.1016/j.pocean.2015.06.011.
- Weinbauer, M. G. (2004). Ecology of prokaryotic viruses. *FEMS Microbiol. Rev.* 28, 127–181. doi:10.1016/j.femsre.2003.08.001.

-
- Wetz, M., Wheeler, P., and Letelier, R. (2004). Light-induced growth of phytoplankton collected during the winter from the benthic boundary layer off Oregon, USA. *Mar. Ecol. Prog. Ser.* 280, 95–104. doi:10.3354/meps280095.
- Wilson, B., Müller, O., Nordmann, E.-L., Seuthe, L., Bratbak, G., and Øvreås, L. (2017). Changes in Marine Prokaryote Composition with Season and Depth Over an Arctic Polar Year. *Front. Mar. Sci.* 4, 1–17. doi:10.3389/fmars.2017.00095.
- Yelton, A. P., Acinas, S. G., Sunagawa, S., Bork, P., Pedros-Alio, C., and Chisholm, S. W. (2016). Global genetic capacity for mixotrophy in marine picocyanobacteria. *ISME J.* Available at: <http://dx.doi.org/10.1038/ismej.2016.64>.
- Zhang, J., Rothrock, A., and Steele, M. (1998). Warming of the Arctic Ocean by a strengthened Atlantic inflow: Model results. *Geophys. Res. Lett.* 25, 1745–1748.
- Zubkov, M. V., and Tarran, G. A. (2008). High bacterivory by the smallest phytoplankton in the North Atlantic Ocean. *Nature* 455, 224–227. doi:10.1038/nature07236.

Report of doctoral Thesis 'Microbial dynamics in high latitude ecosystems' by
Maria Lund Paulsen

General comments

This dissertation examined crucial properties of dissolved organic material (DOM) and lower trophic levels in Arctic coastal waters and explored general issues about the carbon cycle and food web dynamics in the Arctic Ocean. The main focus is microbial dynamics in high latitude ecosystems, which is timely because high latitude ecosystems are already showing signs of being affected by global warming and other climate change impacts. DOM and lower trophic level processes are well known to be important in other oceans, and some work has been done in the Arctic, but these processes are still poorly understood in high latitude systems. The results from this Ph.D. dissertation add to the growing awareness of the importance of DOM and microbes in the carbon cycle and food web dynamics of the Arctic Ocean.

This is an impressive dissertation, immediately evident from the four publications in high profile journals, plus the fifth manuscript that should soon be another high quality publication. Another impressive aspect of the dissertation is its breadth. Virtually all aspects of modern microbial oceanography are covered, ranging from work on DOM quality to grazing and viral processes. The dissertation also shows that Paulsen clearly understands the physical oceanography of her study area and effectively used that information to interpret her results. It is not surprising that the thesis is well presented, clearly written, and illustrated, since almost everything in this thesis has already been peer-reviewed and published in high-rated, international, scientific journals.

The work presented here was undertaken during several oceanographic cruises in a remote and extremely important area of the subarctic section of the Atlantic Ocean. The present study is particularly significant since it investigates several understudied 'players' of the microbial planktonic community, such as small autotrophs, small heterotrophs, and also the bioavailability of organic matter. Besides the tremendous volume of work presented, the academic standards and the quality of the work are of a high level. We would like to underline here that in the introductory section Paulsen discusses the limits of the methods used for several estimations, which demonstrates her thoroughness and her perfect command of the methods she employed. Her contribution is undoubtedly pivotal, as she participated in all of the oceanographic cruises, undertook the experiments, and she is the first author of all five scientific papers presented here.

Our overall assessment is that this is a very good thesis, which undoubtedly has involved very strong technical and conceptual challenges, much work and dedication, and which has yielded results that contribute to our better understanding of the functioning of marine microbial communities. The thesis certainly deserves to be defended by the candidate, who should be complimented for her efforts.

Since almost all of this work has been published, the comments below are offered only to highlight the major original findings of this study.

Introduction: This 40 page chapter introduces marine microbial food webs and summarizes in a synthetic way the major objectives, results, and future perspectives of this work. This synthetic chapter demonstrates a good knowledge and experience of different aspects of the subject, which Paulsen has quite clearly gained during her thesis.

The overall study of the pico-phytoplankton community is timely and original. The vast majority of previous studies in the Arctic have been conducted on large phytoplanktonic cells (>10µm) because of their higher putative sedimentation capacities to the deep ocean. However, small phytoplanktonic cells (<10µm) can be the main contributors to CO₂ fixation because of their high cellular activities and abundances. The temperature increase of the surface ocean is leading to a higher stratification of the water column and thus to lower nutrient concentrations in the photic zone. Because of their better competition capacities in the acquisition of nutrients, small phytoplankton are becoming more abundant. Additionally, while most of previous studies have focused on the short productive period, here the prevailing 'low productive' seasons have been investigated. The data of contrasting regions explored here, has allowed the highlighting of the importance of pico-phytoplankton to primary production, in particular during the pre-bloom period, and its superior capacity to adapt to low light condition more than larger phytoplankton. The results presented here are a new contribution to our understanding of the functioning of high latitude plankton ecosystems, and highlight the necessity to carry on the study of the smallest compartments of the food webs.

Since the 1980s intensive research has been carried out on small heterotrophic nanoflagellates (HNF). HNF, through their grazing activity, play a crucial role in heterotrophic bacterial C transfer toward higher trophic levels. HNF also graze on autotrophic cells, both prokaryotic and eukaryotic. Given that pico-phytoplankton dominate the vast majority of the open oceans, the additional trophic role of HNF as herbivores, makes them even more important in marine waters. Although most of the HNF studies have focused on their role as heterotrophic bacteria consumers, relatively little attention has been paid to the role of heterotrophic flagellates as grazers of <5 µm phytoplankton, in particular, in high latitude systems where this role was considered as negligible. Paulsen took up the challenge, and also looked into the role of HNF as phytoplankton consumers in high latitude systems. She showed that they were the major consumers of pico-phytoplankton and that their grazing pressure adjusted to pico-phytoplankton production.

Synechococcus in Arctic waters. A general theme running through the dissertation is that microbes are important in Arctic waters than previous appreciated. Paper 3, published in *Frontiers in Marine Science*, examined a coccoid cyanobacterial genus, *Synechococcus*, in coastal waters of Svalbard. This cyanobacterium is well known to be abundant and important in primary production in low latitude oceans, but is generally not thought to be common in high latitude oceans. As with the other studies discussed in the dissertation, Paulsen and colleagues were comprehensive and looked at several aspects of the ecology of *Synechococcus* and other small phytoplankton in these waters. In this study, *Synechococcus* was found to be usually more abundant than small eukaryotic phytoplankton in Svalbard coastal waters, an important addition to previous studies that also found the cyanobacterium in other Arctic waters. Paulsen et al. also report some of the few growth rate and grazing rate

estimates for *Synechococcus* in high latitude waters. Unexpectedly, they observed net growth in January and March but negative growth in August and November (estimates from May were both positive and negative), the opposite from expectations based on light availability. The data suggest that *Synechococcus* grows heterotrophically in the absence of light in the winter. Although many questions remain to be answered, the work helps to explain the success of an important cyanobacterial genus in high latitude oceans under light limitation.

Another interesting aspect of the work was the use of sequences of an electron transport chain gene (*petB*) to explore the diversity of *Synechococcus* over time and with different water masses near Svalbard. Although not commonly used in diversity studies, much less so than 16S rRNA genes, the *petB* sequences enabled Paulsen et al. to find differences in *Synechococcus* populations between Svalbard samples and with lower latitude oceans. The data provide further insights into the success of *Synechococcus* in Arctic coastal waters.

DOM availability & transformation: It is well known that the Arctic Ocean has high concentrations of dissolved organic carbon (DOC) because of DOC carried in by large rivers. The riverine DOM is generally thought to be refractory to use by heterotrophic bacteria because it is dominated by lignin and other refractory polymers from terrestrial plants. Two observations reported in Paper 4 were unexpected. First, in contrast to other Arctic rivers, Paulsen et al. found that the DOC concentrations in the Greenland rivers they studied were lower than in Greenland coastal waters. This can be explained by the very low rates of terrestrial primary production in Greenland. However, even though concentrations were low, the DOM in the glacier meltwaters was more labile (higher percent was bioavailable) than was the case for DOM in coastal waters. Because of the labile DOM, total carbon use by heterotrophic bacteria was higher than primary production by phytoplankton. This work has implications for the fate of organic material released by the anticipated melting of glaciers on Greenland and elsewhere. As with Paper 3 on *Synechococcus*, Paulsen et al. used gene sequences, this time of the 16S rRNA gene, to explore in more detail DOM use by heterotrophic bacteria and relationships with primary production. The sequence data gave insights into possible transport and exchange of bacterial communities among the water masses they examined.

The land-to-ocean flux of organic carbon is increasing in polar regions. The characterization of the dissolved organic matter (DOM) and its relation with bacterial growth is another challenge undertaken in this thesis. The originality of this work has been to take into account different organic carbon sources and different water masses. The results show that since phytoplankton cannot sustain the bacterial carbon demand, bacteria exploit allochthonous carbon sources, and therefore the different water masses are characterized by specific bacterial populations. The last part of this section is particularly interesting since it shows that specialized fast growing bacteria are strongly associated with humic-DOM commonly considered as refractory. This explores still another aspect of the carbon cycle, this time the transformation of humic-like DOM in a Greenland fjord. Paulsen et al. used fluorescence characteristics of DOM (FDOM) to follow humic-like compounds, which are thought to be refractory to bacterial degradation, as well as protein (called "amino-FDOM" in the paper) and other DOM components with distinctive fluorescence characteristics. The paper reports a rich data set about basic physico-chemical and microbial oceanographic properties for these waters. That data set is worthy of discussing in a separate paper.

Even more novel are the experiments to explore the role of different microbes in the production and consumption of FDOM components. These experiments unexpectedly suggest that humic-like compounds are produced by protists grazing on bacteria. This is unexpected because these dissolved compounds are generally thought to come from soil and terrestrial sources. Another novel finding in this paper was the association of specific bacterial taxa, found by 16S rRNA gene sequences, associated with humic-like DOM degradation. This work may prove to be an important addition to our understanding of the role of different bacteria in DOM transformation and degradation.

Overall, what we particularly enjoyed with this work is that in each of the three supposedly 'well studied' topics, a new challenge was raised and met. Finally, we fully agree with Paulsen, that while the sequencing technologies and bioinformatic tools develop rapidly, the great challenge for contemporary biologists is to integrate and make use of sequencing data into biogeochemical models. Therefore, rates and stocks should be correctly measured. Notwithstanding, our methods of measuring production rates and even cell numbers of plankton organisms have a great margin for improvement. As Turner and Roff' said in a paper many years ago: 'Alexander wept because there were no more worlds to conquer. Plankton ecologists have nothing to cry about!'

Conclusion: It is clear that she has produced an important piece of experimental work - well documented, written in a logical order, original, and up-to-date. We particularly appreciated that for all parts of the study, all data were validated and all hypotheses explored, and new questions and hypothesis were always posed, with rationale never falling into useless speculation. The thesis is clear and easy to read, which is expected since all the chapters have been published or are ready for submission. We would like to congratulate Maria Lund Paulsen and her team of supervisors and collaborators for providing this work to the community of aquatic microbial ecologists. We are looking forward to the defense and the discussions around this excellent piece of work.

In conclusion, we find the thesis by Maria Lund Paulsen worthy to be publically defended at the University of Bergen.

16th of October 2017,

Urania Christaki (PR)

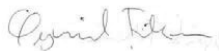
Øyvind Fiksen

David Kirchman

Université du Littoral

University of Bergen

University of Delaware







Winter–spring transition in the subarctic Atlantic: microbial response to deep mixing and pre-bloom production

Maria Lund Paulsen^{1,2,*}, Karen Riisgaard², T. Frede Thingstad¹, Mike St. John²,
Torkel Gissel Nielsen²

¹Marine Microbiology Research Group, Department of Biology, University of Bergen, Thormøhlensgate 53A/B, 5020 Bergen, Norway

²National Institute of Aquatic Resources, DTU-Aqua, Section for Ocean Ecology and Climate, Technical University of Denmark, Jægersborg Allé 1, 2920 Charlottenlund, Denmark

ABSTRACT: In temperate, subpolar and polar marine systems, the classical perception is that diatoms initiate the spring bloom and thereby mark the beginning of the productive season. Contrary to this view, we document an active microbial food web dominated by pico- and nanoplankton prior to the diatom bloom, a period with excess nutrients and deep convection of the water column. During repeated visits to stations in the deep Iceland and Norwegian basins and the shallow Shetland Shelf (26 March to 29 April 2012), we investigated the succession and dynamics of photo-synthetic and heterotrophic microorganisms. We observed that the early phytoplankton production was followed by a decrease in the carbon:nitrogen ratio of the dissolved organic matter in the deep mixed stations, an increase in heterotrophic prokaryote (bacteria) abundance and activity (indicated by the high nucleic acid:low nucleic acid bacteria ratio), and an increase in abundance and size of heterotrophic protists. The major chl *a* contribution in the early winter–spring transition was found in the fraction <10 µm, i.e. dominated by pico- and small nanophytoplankton. The relative abundance of picophytoplankton decreased towards the end of the cruise at all stations despite nutrient-replete conditions and increasing day length. This decrease is hypothesised to be the result of top-down control by the fast-growing population of heterotrophic protists. As a result, the subsequent succession and nutrient depletion can be left to larger phytoplankton resistant to small grazers. Further, we observed that large phytoplankton (chl *a* > 50 µm) were stimulated by deep mixing later in the period, while picophytoplankton were unaffected by mixing; both physical and biological reasons for this development are discussed herein.

KEY WORDS: Microbial food web · Winter–spring transition · Deep mixing · Picophytoplankton · Nanophytoplankton · Bacteria · Heterotrophic nanoflagellates · Microzooplankton · Subarctic Atlantic

INTRODUCTION

Much of our conceptual understanding of the marine pelagic food web originates from the pioneer work of Sverdrup (1953), Cushing (1959) and Steele (1974). This understanding was based on coarse-meshed samplers, e.g. continuous plankton recorder surveys and vertical net hauls, and used to describe

the seasonality of northern marine ecosystems and inspired generations of marine researchers. However, little attention was paid to the role of microbial communities, in part due to the difficulty in sampling this component of the food web. With the advent of suitable techniques, the microbial loop has been recognised to play a fundamental role in the flux of carbon and nutrients in marine ecosys-

*Corresponding author: maria.l.paulsen@uib.no

© The authors 2015. Open Access under Creative Commons by Attribution Licence. Use, distribution and reproduction are unrestricted. Authors and original publication must be credited.

tems (Pomeroy 1974, Sorokin 1977, Azam et al. 1983). Thus, the importance of the heterotrophic components of the microbial loop became recognised (Williams 1981); however, the role of photosynthetic picophytoplankton in northern ecosystems still received little attention. This was due to the fact that sampling efforts traditionally have been focused on the spring bloom period because the new production of larger-celled species in this period has a strong link to mesozooplankton and fish production (Sverdrup 1953, Steele 1974, Braarud & Nygaard 1978). During the spring bloom, the relative abundance of picophytoplankton is low (Li et al. 1993) when compared to oligotrophic subtropical waters (Agawin et al. 2000). The spring diatom bloom, however, is a short-term feature of the system, with smaller phytoplankton and their associated grazers dominating for the majority of the year. The microbial food web, including picophytoplankton, has received more attention in recent years in northern systems (Søndergaard et al. 1991, Joint et al. 1993, Sherr et al. 2003, Irigoien et al. 2005, Tremblay et al. 2009, Seuthe et al. 2011a,b).

In winter, the water column is characterized by high turbulent mixing, deep convection (Backhaus et al. 1999) and low irradiance. During this period, phytoplankton concentrations are dispersed (Li 1980), and the major mesozooplankton grazer, *Calanus finmarchicus*, is in diapause at depth (Hirche 1996). The onset of the bloom is affected by several physical factors, which have been thoroughly described, including a shoaling of deep convection (Taylor & Ferrari 2011), periods below the threshold of critical turbulence (Huisman 1999), eddy-driven stratification (Mahadevan et al. 2012) and irradiance (i.e. the critical depth model; Sverdrup 1953). Grazing by microzooplankton (MZP) has also been suggested to play a major role in the bloom development. Behrenfeld (2010) and Behrenfeld & Boss (2014) hypothesised that the increase in phytoplankton biomass in the North Atlantic during the winter–spring transition could be the result of a decoupling of the MZP grazers from their phytoplankton prey during mixed layer deepening (the dilution–recoupling hypothesis). There has been controversy as to the mechanisms controlling the onset of the bloom, resulting in a publication by Lindemann & St. John (2014) presenting a conceptual model of the interplay of these abiotic and biotic mechanisms. However, no attempt has been made to investigate the photosynthetic planktonic community composition and grazing dynamics in the subarctic Atlantic during deep convection.

Here, we shift the focus from the diatom spring bloom to the microbial community found during the winter–spring transition and evaluate the relative contributions of pico- and nanophytoplankton in the subarctic North Atlantic prior to the bloom. We investigate the succession of both photosynthetic and heterotrophic plankton components and evaluate a central hypothesis behind bloom formation in well-mixed waters, i.e. the decoupling of the heterotrophic protists from the phytoplankton community during deep mixing. In addition to the *in situ* observations presented here, an experimental approach was applied to study the microbial interactions in detail (e.g. estimation of growth and grazing rates); these are presented in K. Riisgaard et al. (unpubl.).

MATERIALS AND METHODS

Sampling site and hydrography

The study was conducted from 26 March to 29 April 2012 during a cruise aboard the RV 'Meteor' (cruise no. 87) coordinated by the University of Hamburg, Germany. The study focused on 3 stations located in the subarctic North Atlantic, representing different hydrographical regimes: 2 stations on the edge of the deep basins north and south of the Greenland–Scotland Ridge in the Norwegian Basin (1300 m) and Iceland Basin (1350 m), respectively, and 1 station on the shallow Shetland Shelf (160 m) (Fig. 1). Each station was revisited at 8 to 14 d intervals following a route circling the Faroe Islands. During each visit, vertical profiles of temperature, salinity and photosynthetically active radiation (PAR) were performed using a Sea-Bird CTD (SBE 9 plus) with an attached rosette of 10 l Niskin bottles.

Photic zone depth was defined as 0.1% of incident PAR measured at 5 m (Jerlov 1968). The depth of the mixed layer was identified as a decrease of 0.2°C from surface (10 m) temperatures (de Boyer Montégut et al. 2004), evaluated to be the most appropriate definition for high latitude regions where deep convection can occur.

Sampling depths were chosen based on water column structure and covered the full water column, with the highest resolution within the mixed layer. During each visit to the stations, 3 CTD profiles were taken within a time frame of 20 to 36 h to capture the temporal dynamics (i.e. data presented from each visit in the following discussion is an average of 3 profiles). Samples were collected to provide data on the abundance of microbial components, including

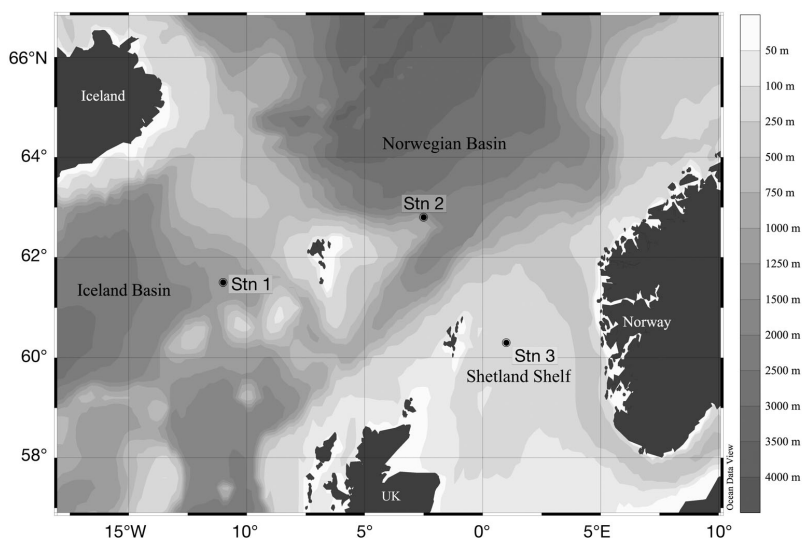


Fig. 1. Study area. Stn 1: 1350 m deep station in the Iceland Basin (61.5° N, 11° W); Stn 2: 1300 m deep station in the Norwegian Basin (62.8° N, 2.5° W); Stn 3: 160 m deep station on the Shetland Shelf (60.3° N, 1° E)

virus-like particles (hereafter referred to as virus), heterotrophic prokaryotes (Archaea and bacteria, hereafter referred to as bacteria), small (<10 μm) phytoplankton, unidentified heterotrophic nanoflagellates (HNF) and larger (>10 μm) ciliates and dinoflagellates (i.e. MZP) as well as chl *a*, nutrients and dissolved organic carbon and nitrogen (DOC and DON, respectively). The sampling of bacteria, viruses, small phytoplankton and total chl *a* was about twice as frequent as sampling of the more analytically time-consuming fractionated chl *a* and heterotrophic protists.

Nutrients, organic matter and chl *a*

Nitrate and nitrite (NO_3+NO_2), phosphate (PO_4) and silicic acid (H_4SiO_4) were measured on a Skalar Sanplus segmented-flow autoanalyser, following procedures outlined by Wood et al. (1967) for NO_3+NO_2 , Murphy & Riley (1962) for PO_4 and Koroleff (1983) for the determination of H_4SiO_4 .

Total organic carbon (TOC) in unfiltered seawater was analyzed by high-temperature combustion using a Shimadzu TOC- V_{CSH} . Standardization was achieved using potassium hydrogen phthalate. Calibration was performed using deep seawater and low carbon reference waters as provided by the Hansell consensus reference materials (CRM) program and performed every sixth analysis to assess the day-to-day and instrument-to-instrument variability. The precision of TOC analyses was $\sim 1 \mu\text{mol kg}^{-1}$, with a coef-

ficient of variation of 2 to 3%. Concentration of total nitrogen was determined simultaneously by high temperature combustion using a Shimadzu TNM1 attached to the Shimadzu TOC-V. Total organic nitrogen (TON) was calculated by subtracting total inorganic nitrogen (NO_3+NO_2) measured from parallel nutrient samples on board. As ammonium concentrations were negligible throughout the cruise, with a mean of $0.18 \mu\text{M} \pm 0.5$, $n = 400$, within the upper mixed layer (J. Jacob unpubl.), these were not included in the total inorganic nitrogen pool. Non-purgeable dissolved nitrogen compounds are combusted and converted to nitric oxide, which when mixed with ozone chemiluminesces for detection by a photomultiplier. Both measurements were quality controlled using CRMs distributed to the international community (Hansell 2005). The CRMs were analyzed at regular intervals during each analytical day (Hansell 2005). As the difference between TOC and DOC is minor in northern systems during non-bloom situations (Anderson 2002), we use the term DOC; for organic nitrogen, we use DON instead of TON.

Chl *a* concentrations were determined from 100 to 1000 ml samples and size fractionated on Whatman GF/F filters (0.7 μm pore size), 10 and 50 μm mesh; each fractionation treatment was triplicated. Filters were extracted in 5 ml of 96% ethanol for 12 to 24 h (Jespersen & Christoffersen 1987). Chl *a* concentrations were measured before and after addition of 1 drop of acid (1 M HCl) on a TD-700 Turner fluorometer, which was calibrated against a chl *a* standard.

Enumeration of bacteria, viruses and protists

Bacteria, viruses, small phytoplankton and HNF were enumerated using a FACSCalibur (Becton Dickinson) flow cytometer and analysed using CellQuest software.

Samples for phytoplankton and bacteria were fixed with glutaraldehyde (final conc. 0.5%) for 30 min in the dark at 4°C, while HNF were fixed with glutaraldehyde (final conc. 0.43%) for 2 h. Thereafter, all samples were flash frozen in liquid nitrogen and stored at -80°C until further analysis (within 4 mo).

Small phytoplankton were analysed directly after thawing for 5 min at a flow rate of 60 to 70 $\mu\text{l min}^{-1}$. Groups of picoeukaryotes, *Synechococcus* and small and large nanophytoplankton were discriminated on the basis of their side scatter (proportional to cell size) and red fluorescence (Fig. 2A) as in Larsen et al. (2004). Further, the mean red fluorescence per cell within each group was recorded.

For the enumeration of bacteria and viruses, samples were diluted (5- and 10-fold) with 0.2 μm filtered TE buffer (Tris 10 mM, EDTA 1 mM, pH 8), stained with a green fluorescent nucleic acid dye (SYBR Green I; Molecular Probes) and kept for 10 min at 80°C in a water bath to provide optimal staining of viruses (Marie et al. 1999). Samples were counted for 1 min at a flow rate of $\sim 30 \mu\text{l min}^{-1}$ and discriminated on the basis of their side scatter and green fluorescence (Fig. 2B). As reference, yellow-green fluorescent beads of 2 μm diameter (FluoSpheres® Molecular Probes carboxylate-modified microspheres) were added. Bacteria are often found to group into 2 distinct clusters of high and low green fluorescence (Sherr et al. 2006, Huete-Stauffer & Morán 2012). As division was clear in current samples (Fig. 2B), the total bacteria counts were divided into subgroups of low nucleic acid (LNA) and high nucleic acid (HNA).

Fig. 2. Biparametric flow cytometry plots with the applied grouping of the different microbial groups. (A) Populations of photosynthetic picoeukaryotes, *Synechococcus* sp. and 2 size groups of nanoflagellates distinguished on a plot of red fluorescence vs. orange fluorescence. (B) Heterotrophic bacteria and viruses as distinguished on a plot of green fluorescence vs. side scatter. The group of high nuclei acid (HNA) bacteria expresses higher fluorescence than the low nuclei acid (LNA) bacteria, yet another gate for total bacteria covered both HNA and LNA; 2 μm fluorescent reference beads appear in the right upper corner of the plot. (C) Heterotrophic nanoflagellates (HNF) are distinguished from nano-sized phototrophic protists on a plot of red fluorescence vs. green fluorescence. Bacteria and picophytoplankton are found at the bottom of the plot as well as 0.5 μm fluorescent beads (see further explanation in the text)

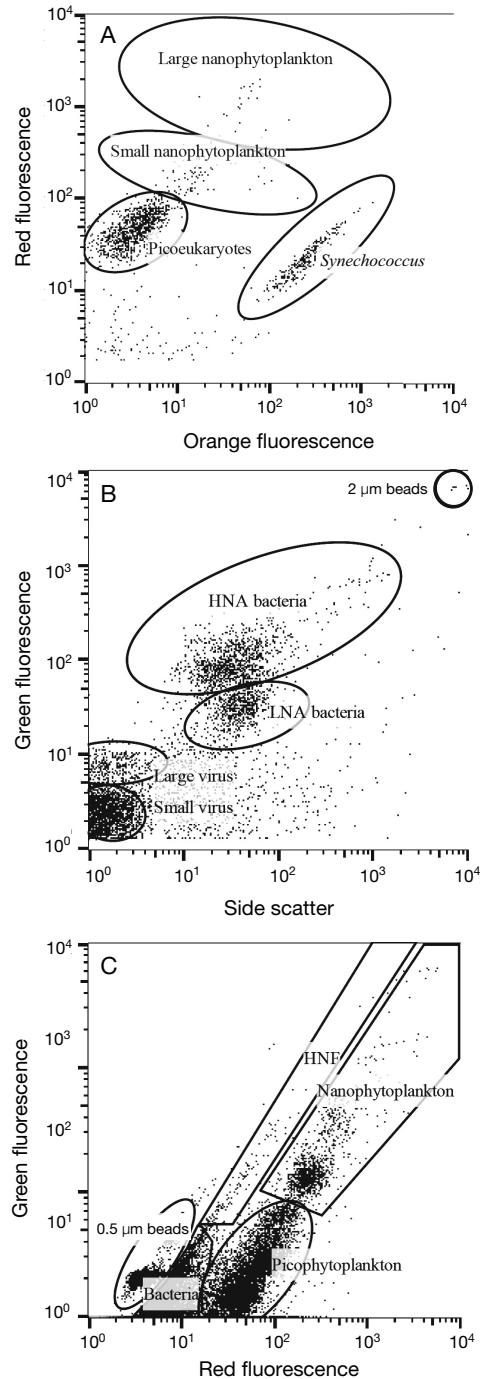


Table 1. Weighted arithmetic means of measured equivalent spherical diameter (ESD) within the size fractions chosen to represent small and large autotrophic nanoflagellates (ANF), heterotrophic nanoflagellates (HNF), picoeukaryotes and *Synechococcus* sp. as well as the carbon conversion factors used to convert estimates of cell abundance to biomass (pg C cell^{-1}). Dinoflagellates and ciliates are estimated from biovolumes (V) of each individual, and average ESD is therefore not presented. For smaller protist groups, average ESD was measured; for HNF, diameter was estimated by UV epifluorescence microscopy; for small phytoplankton, the weighted arithmetic mean of the diameter was calculated from the abundance within different size intervals using filtration (see further explanation in 'Size and biomass estimation of protists'). The biomass of bacteria is estimated using literature values. -: not measured

Group	Measured ESD (μm)	Carbon conversion ($\text{fg C } \mu\text{m}^{-3}$)	Conversion reference	Biomass (pg C cell^{-1})
Dinoflagellates	-	$\text{Log (pg C cell}^{-1}) = -0.353 + 0.864 \log (V)$	Menden-Deuer & Lessard (2000)	-
Aloricate ciliates	-	$\text{Log (pg C cell}^{-1}) = -0.639 + 0.984 \log (V)$	Putt & Stoecker (1989), modified by Menden-Deuer & Lessard (2000)	-
Loriccate ciliates	-	$\text{Log (pg C cell}^{-1}) = -0.168 + 0.841 \log (V)$	Verity & Langdon (1984), Menden-Deuer & Lessard (2000)	-
HNF	3.2 ± 0.3	220	Børsheim & Bratbak (1987)	3.80
Bacteria	-	-	Lee & Fuhrman (1987)	0.02
Large ANF	8 ± 0.7	220	Mullin et al. (1966)	58.98
Small ANF	4 ± 0.5	220	Mullin et al. (1966)	7.37
Picoeukaryotes	1.7 ± 0.4	220	Mullin et al. (1966)	0.57
<i>Synechococcus</i> sp.	1.1 ± 0.4	250	Kana & Glibert (1987)	0.17

Samples for HNF were stained with SYBR Green I for 2 to 4 h in the dark at 4°C, and 0.5 μm yellow-green fluorescent beads were added as reference. A 2 ml undiluted sample was analysed, and HNF were discriminated from phototrophic nanoflagellates in bivariate plots of the green fluorescence (from SYBR Green) vs. red fluorescence (from chl *a*) (Fig. 2C), following the method of Zubkov et al. (2007). The samples were measured at a lower flow rate (120 $\mu\text{l min}^{-1}$) than that used in Zubkov et al. (2007) (180 to 1000 $\mu\text{l min}^{-1}$); however, the lower flow rate was compensated by longer measuring time, i.e. comparable volumes were measured. With this method, we could not distinguish mixotrophic nanoflagellates.

For enumeration and sizing of larger protists, water samples of 500 ml were gently decanted from the Niskin bottle through a silicon tube into brown glass bottles and fixed in acidic Lugol's solution (final conc. 3%) and kept cool and dark until analysis. To concentrate the samples, 500 ml subsamples were allowed to settle for 48 h in tall cylinders (height: 34.5 cm, diameter: 5 cm) before the upper part of the sample was gently removed by decanting with a silicon tube, leaving 100 ml in the cylinder. All (or a minimum of 300) cells were counted using an inverted microscope (Nikon K18).

Size and biomass estimation of protists

Dinoflagellates and ciliates were identified morphologically and divided into size classes covering

10 μm ranges of equivalent spherical diameter (ESD) starting with 10 to 20 μm . ESD and cell volume are related by $\pi/6 \times \text{ESD}^3 = \text{cell volume}$. Cell volumes were calculated using appropriate geometric shapes without including the membranelles (tufted arrangements of cilia). The biovolumes were converted to carbon using the volume:carbon conversion factors given in Table 1. Qualitative observations of dominant microphytoplankton families and species were recorded in parallel.

The biomass of pico- and nanoflagellates was estimated based on literature conversion factors (Table 1). Size determinations of the various groups of phytoplankton (picoeukaryotes, *Synechococcus* sp. and small and large nanophytoplankton) were performed by filtering parallel samples through 0.8, 1, 2, 5 and 10 μm polycarbonate filters and counting the filtrate, thereby enumerating the percentage of each group within the given size interval, a method modified from Zubkov et al. (1998).

HNF size was estimated using epifluorescence microscopy. Samples (10 ml) were fixed with glutaraldehyde (final conc. 1%) for 1 h and stored at -80°C. The samples were filtered onto black polycarbonate filters (pore size 0.8 μm), stained with DAPI DNA-specific dye (Porter & Feig 1980) and analysed under a UV epifluorescence microscope (1000 \times). To ensure that the measured cells were heterotrophic, each cell was crosschecked for red fluorescence. A total of 170 HNF were measured (~30 HNF were measured from both surface and sub-surface samples at each station). As there was no sig-

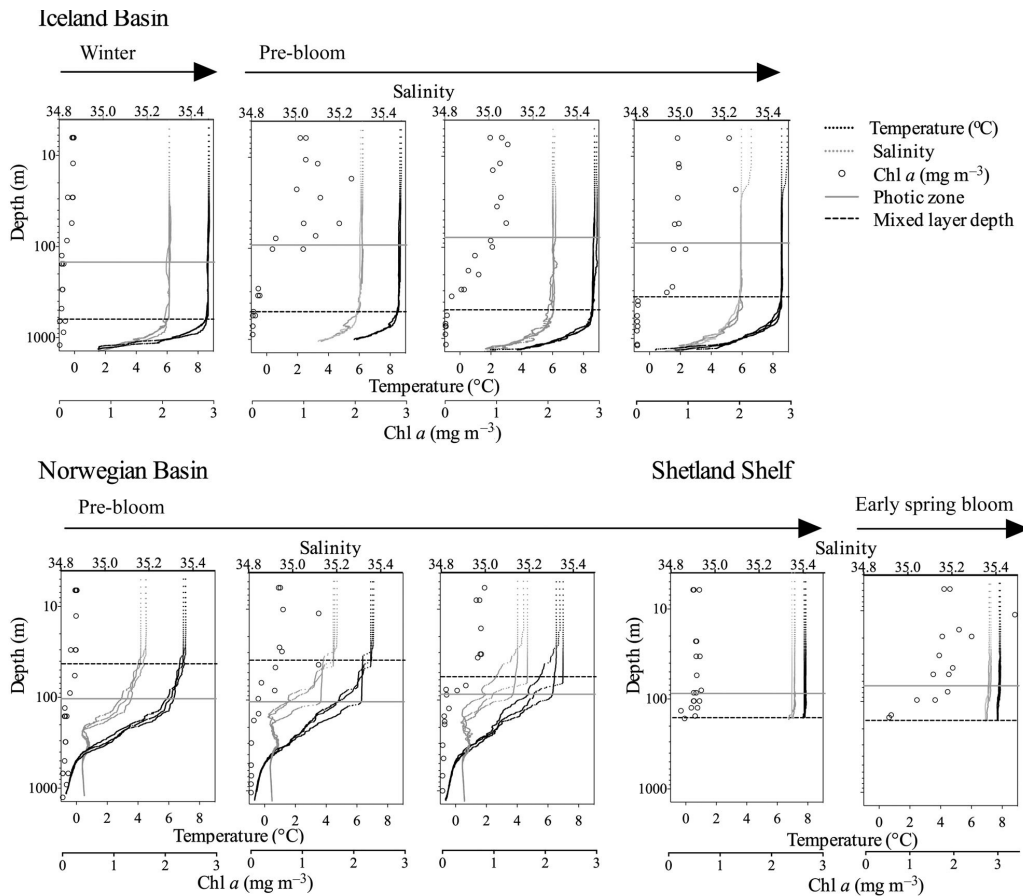


Fig. 3. Vertical profiles ($n = 3$) of salinity, temperature and total chl a (sampled from the chosen sampling depths). All profiles were taken within 20 to 36 h (first visit to the left). Horizontal arrows indicate the seasonal phase. Horizontal black dashed line indicates the mixed layer depth; gray line marks the photic zone

nificant difference between the size measures, a total mean was later used for biomass estimation. For both HNF and groups of small phytoplankton, the abundance within size intervals was converted to the weighted arithmetic averaged size and used for biomass estimation (Table 1).

Integrated values were calculated by trapezoid integration to the bottom, 600 m or the base of the mixed layer (see Figs. 4 & 7). When samples were not available from the exact mixed layer depth (MLD), a curve was fitted between the 2 neighbouring samples and the resulting curve equation used to estimate the value by the base of the mixed layer. The integrated biomass values (mg C m^{-2}) were converted to mg C m^{-3} by dividing by the depth of the mixed layer to enable comparison of the mean inte-

grated biomass within the mixed layer between stations. Data included in the paper are available from the data repository PANGAEA via Paulsen et al. (2014a,b) for abundance measurements of pico- and nanoplankton during RV 'Meteor' cruise no. 87.

RESULTS

Physical regime

Weather during the cruise was generally windy, causing mixing of the upper part of the water column in addition to the winter convection. The deep stations in the Iceland and Norwegian basins were mostly stormy, and on several occasions, winds

reached Beaufort force 10 with sustained periods of Beaufort 8 and wave heights of 3 to 5 m. The day length increased from 11 to 16 h during the cruise.

The deep Iceland Basin station (bottom = 1350 m) deep convection or remnants thereof was evident down to ~600 m but reduced gradually to ~350 m during the study period (MLD = 600 to 344 m) (Fig. 3). Based on the water mass definitions of Blindheim & Østerhus (2005) potential temperature (θ) and salinity, the Iceland Basin consisted mostly of Atlantic Water ($\theta = 5$ to 10.5°C , salinity = 35 to 35.05) reaching >1000 m depth, while Polar Overflow Water ($\theta < 0.5^\circ\text{C}$, salinity = 34.88 to 34.93) was observed near the bottom on a few occasions.

The deep Norwegian Basin (bottom = 1300 m) had a persistently shallower mixed layer around ~50 m (MLD = 37 to 56 m). Here, the Atlantic Water was constrained to the upper 100 m, while the major part of the water column (100 to 1300 m) consisted of cold Norwegian Sea Deep Water ($\theta < 0.5^\circ\text{C}$, salinity = 34.9), and there was a permanent density gradient between the 2 water masses. The shallow Shetland Shelf station was mixed to the bottom (MLD = bottom = 160 m), was characterized by a uniform water mass of Atlantic Water and remained similar between visits (Fig. 3). The dominating water masses at each of the 3 localities remained consistent throughout the period (the only intrusion of other water masses occurred in the Iceland Basin at 1200 to 1250 m).

Changes in chl *a*, nutrients and DOC:DON ratio

The integrated mean values of chl *a* (mg m^{-3}) within the mixed layer at the 3 stations all showed a gradual increase during the cruise (Table 2, Figs. 3 & 4). Because of the ongoing deep convection at the Iceland Basin and Shetland Shelf stations (from now on referred to as the deep mixed stations), a large fraction of chl *a* was detrained, i.e. mixed well below the photic zone (Fig. 3). The deep mixed stations showed the highest increase in chl *a*, in the Iceland Basin from <0.1 to 0.7 mg m^{-3} during a 30 d period and over the Shetland Shelf from 0.5 to 1.4 mg m^{-3} during a 14 d period. The increase in chl *a* at the deep mixed stations was mainly due to an increase in the >50 μm chl *a* fraction; however, the 10 to 50 μm fraction also increased in the Shetland Shelf (Fig. 4), which comprised up to 50% of the total chl *a* during the last visit. At the more stratified Norwegian Basin, chl *a* was retained within the photic zone (Fig. 3), yet here we observed the smallest increase in chl *a* within the mixed layer, from 0.4 to $0.6 \text{ mg chl a m}^{-3}$. The chl *a*

fraction <10 μm comprised a major part of total integrated chl *a*, ranging at all stations from $47 \pm 25\%$ at the Iceland Basin to $55 \pm 39\%$ on the Shetland Shelf and was especially dominant in the Norwegian Basin at $95 \pm 7\%$ on average during the study (Fig. 4).

Nutrient concentrations, i.e. $\text{NO}_3 + \text{NO}_2$, PO_4 and H_4SiO_4 , were high throughout the study and homogeneously distributed over the mixed layers (Table 2), with slightly elevated concentrations below the mixed layer (data not shown). Increases in the >50 μm chl *a* fraction were reflected in a slight decrease in H_4SiO_4 , from 4.7 to $4.2 \mu\text{M}$ at the Iceland Basin and from 2.8 to $1.7 \mu\text{M}$ at the Shetland Shelf, suggesting a net growth of diatoms at these locations. At the deep mixed stations, the carbon:nitrogen (C:N) ratio of the dissolved organic matter (DOM) decreased from 17 to 15 at the Iceland Basin and from 16 to 14 at the Shetland Shelf, i.e. became increasingly rich in nitrogen and closer to the Redfield ratio (C:N ratio of 6.63). There were no clear changes in DOC or DON at the more stratified Norwegian Basin (Table 2). When comparing our study period to the surface chl *a* during the full year of 2012, it is evident that spring bloom has not yet initiated at the deep basins (Daniels et al. 2015). We consider the initial visit to the Iceland Basin to represent winter conditions based on the extremely low chl *a* values (0.06 mg m^{-3}); the remaining sampling occasions are within the pre-bloom phase, while the last visits to the Shetland Shelf represent early bloom conditions, as substantial uptake of nutrients is evident, i.e. H_4SiO_4 no longer in excess (Egge & Aksnes 1992). The defined seasonal stages of the systems are indicated in Figs. 3, 4 & 7.

Succession of phytoplankton

The picophytoplankton community (<2 μm) was dominated by unidentified picoeukaryotes, while the prokaryotic component, *Synechococcus* sp., was considerably less abundant. However, the relative abundance of *Synechococcus* sp. increased during the study at all stations, from 700 to 1600, 2300 to 4700 and 300 to 600 cells ml^{-1} at the Iceland, Norwegian and Shetland stations, respectively (Fig. 5). The nanophytoplankton fraction (2 to 10 μm) was separated into 2 size groups of ESD: 2 to 5 and 6 to 10 μm (Fig. 3A). For conversion to biomass, the diameters of picoeukaryotes, *Synechococcus* sp. and small and large nanophytoplankton were estimated on 7 occasions (mean ESD \pm SD, $n = 7$) to be 1.7 ± 0.4 , 1.1 ± 0.4 , 4 ± 0.5 and $9 \pm 0.7 \mu\text{m}$, respectively.

Table 2. Water column characteristics during the study at Iceland Basin, Norwegian Basin and Shetland Shelf stations. Data are given as mean \pm SD and n within the mixed layer except chl *a*, for which the integrated mean within the mixed layer is presented (the mean of 3 integrated profiles from each visit). Ratio of the estimated pico- and nanophytoplankton biomass to the measured <10 μ m chl *a* fraction (C:chl *a*) is based on linear correlation. DOC concentration and DOC:DON, HNA:LNA bacteria, V:B, bacteria:HNF and picoeukaryotes:HNF ratios are also given. MLD: mixed layer depth; DOC: dissolved organic carbon; DON: dissolved organic nitrogen; HNA: high nucleic acid; LNA: low nucleic acid; V: virus; B: bacteria; HNF: heterotrophic nanoflagellates. --: data not available

Time (2012)	MLD (m)	Photic zone (m)	NO ₃ +NO ₂ , PO ₄ , H ₄ SiO ₄ (μ M)	Total chl <i>a</i> (mg m ⁻³)	Chl <i>a</i> >10 μ m (%)	Chl <i>a</i> >50 μ m (%)	C:chl <i>a</i>	DOC (μ M)	DOC: DON	HNA: LNA bacteria	V:B	V:B below mixed layer	Bacteria: HNF	Pico-eukaryotes: HNF
Iceland Basin														
26–28 Mar Winter	618	147	13, 0.8, 5	0.06 \pm <0.1 n = 3	13.1 \pm 5.2	4.7 \pm 2.8	47 \pm 10 (p < 0.005) r ² = 0.7	51.1 \pm 0.4 n = 20	17.2 \pm 0.9 n = 6	2.04 \pm 1.5 n = 16	8.2 \pm 3.1 n = 16	4.4 \pm 2.0 n = 6	8000 n = 16	72 n = 16
7–10 Apr Pre-bloom	493	92	12, 0.8, 5	0.4 \pm 0.1 n = 3	81.3 \pm 14.1	55.5 \pm 31.1	21 \pm 12 (p = 0.12) r ² = 0.35	52.4 \pm 2.2 n = 18	17.4 \pm 2.4 n = 19	2.3 \pm 1.9 n = 14	6.1 \pm 1.5 n = 16	6.3 \pm 1.9 n = 5	8250 n = 16	125 n = 16
18–21 Apr Pre-bloom	492	78	12, 0.8, 5	0.5 \pm 0.1 n = 3	53.7 \pm 14.6	45.1 \pm 19.8	21 \pm 6 (p = 0.01) r ² = 0.6	51.9 \pm 1.4 n = 17	14 \pm 1.9 n = 18	4.3 \pm 0.9 n = 16	2.9 \pm 0.6 n = 16	7.3 \pm 2.1 n = 6	1797 n = 16	17 n = 16
27–29 Apr Pre-bloom	344	90	12, 0.8, 4	0.7 \pm 0.2 n = 3	62.2 \pm 12.6	49.2 \pm 11.3	11 \pm 6 (p = 0.13) r ² = 0.25	51.9 \pm 0.6 n = 16	15.1 \pm 1.3 n = 16	3 \pm 0.6 n = 6	2.6 \pm 0.3 n = 12	4.7 \pm 0.9 n = 9	3280 n = 16	7.4 n = 16
Norwegian Basin														
30–31 Mar Pre-bloom	43	103	12, 0.8, 5	0.4 \pm 0 n = 3	2.9 \pm 1.4	0.2 \pm 0.7	43 \pm 9 (p < 0.005) r ² = 0.8	51.6 \pm 1.4 n = 7	15.6 \pm 2.6 n = 7	1.3 \pm 1.2 n = 6	4.4 \pm 3.4 n = 6	6 \pm 0.8 n = 14	6667 n = 7	281 n = 7
13–14 Apr Pre-bloom	37	105	13, 0.8, 5	0.5 \pm 0.1 n = 3	8.3 \pm 7.6	0.5 \pm 0.3	20 \pm 6 (p = 0.008) r ² = 0.6	51.8 \pm 0.8 n = 7	18.1 \pm 2.2 n = 7	3.3 \pm 1.4 n = 7	3.1 \pm 0.3 n = 6	5.1 \pm 1.04 n = 14	5517 n = 7	70 n = 7
22–25 Apr Pre-bloom	56	86	12, 0.8, 6	0.6 \pm 0.1 n = 3	5 \pm 2.3	1.0 \pm 0.2	39 \pm 8 (p < 0.005) r ² = 0.7	51.3 \pm 1.5 n = 18	14.9 \pm 1.5 n = 10	4.4 \pm 1.9 n = 7	2.5 \pm 0.4 n = 7	4.5 \pm 0.4 n = 13	3280 n = 7	32 n = 7
Shetland Shelf														
30–31 Mar Pre-bloom	160	87	9.5, 0.6, 2.8	0.5 \pm <0.1 n = 3	6.4 \pm 1.4	2.3 \pm 0.6	47 \pm 15 (p = 0.02) r ² = 0.5	52.5 \pm 2.3 n = 13	16.3 \pm 1.9 n = 13	1.4 \pm 0.2 n = 0.2	4.7 \pm 0.9 n = 13	–	4648 n = 10	21 n = 10
13–14 Apr Early bloom	160	67	8.5, 0.6, 1.7	1.4 \pm 0.2 n = 3	55.3 \pm 9.3	42.2 \pm 6.7	6 \pm 1.5 (p = 0.08) r ² = 0.8	54.3 \pm 0.8 n = 6	13.9 \pm 1.2 n = 6	2.4 \pm 0.2 n = 12	4.3 \pm 0.3 n = 14	–	3243 n = 9	5 n = 9

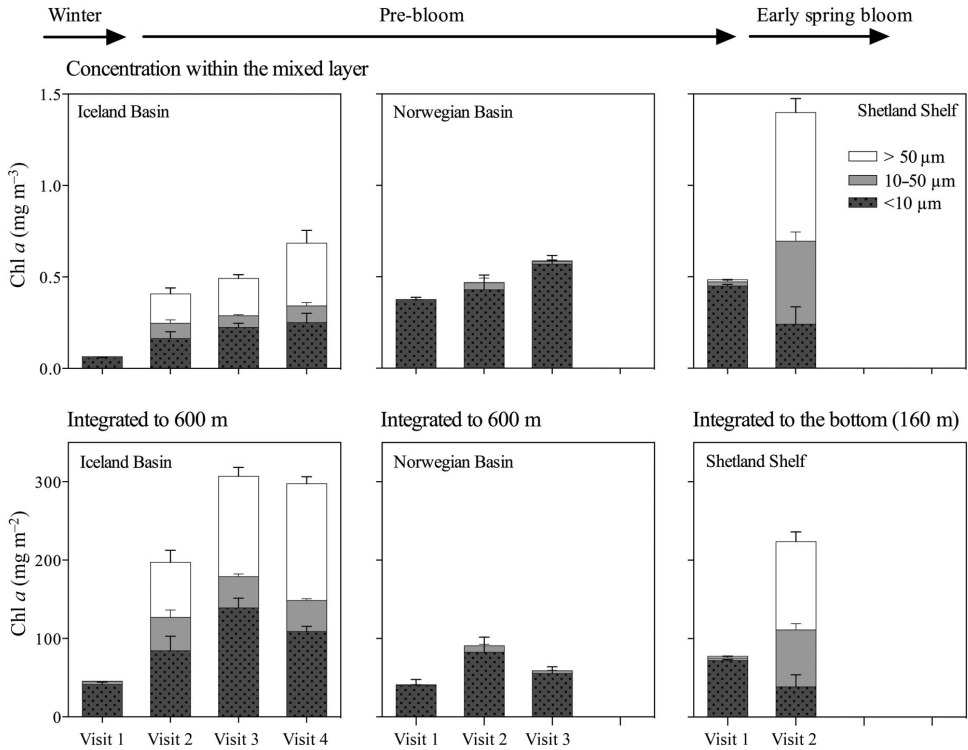


Fig. 4. Size-fractionated chl *a* at the 3 stations over time, shown as mean \pm SD ($n = 3$) of 3 sampled profiles at each visit. Horizontal arrows indicate the seasonal phase. In the upper panels, integrated biomass of chl *a* is divided by mixed layer depth to estimate mean concentration within the mixed layer ($\text{mg chl } a \text{ m}^{-3}$). The integrated biomass ($\text{mg chl } a \text{ m}^{-2}$) to 600 m at the deep stations and to the bottom (160 m) at Shetland Shelf is shown in the lower panels

The abundances of pico- and nanophytoplankton were obtained throughout the mixed layer at all stations (Fig. 5). Maximum abundance was obtained subsurface (below 5 m) at 24 of 27 stations and decreased exponentially below the mixed layer. The average red fluorescence (a measure of chl *a* content) per pico- and nanophytoplankton cell did not change with depth at the deep mixed stations but doubled at the base of the photic zone (± 50 m) at the more stratified Norwegian Basin (Fig. 6), suggesting that phytoplankton were able to adapt their chl *a* content to the decrease in irradiance with depth at the more stratified station but not at the mixed stations.

The integrated biomass of small phytoplankton was significantly correlated ($p < 0.05$) with the integrated chl *a* fraction $< 10 \mu\text{m}$. The averaged value of the slopes resulted in a chl *a*:carbon conversion factor of 29 ± 13 ($n = 7$) for the Iceland Basin and the Norwegian Basin combined. Poor correlations were

found for the Shetland Shelf, indicating contributions to the $< 10 \mu\text{m}$ chl *a* fraction elsewhere than from the enumerated pico- and nanophytoplankton (Table 2). We found that the $< 10 \mu\text{m}$ chl *a* fraction correlated significantly at all stations with the biomass of the pico- and nanophytoplankton converted from flow cytometer counts ($r^2 = 0.58$, $p < 0.0001$, $n = 9$, slope = 26.6).

The Norwegian Basin station had the highest cell number of pico- and nanophytoplankton within the mixed layer, about twice that of the Iceland Basin and triple that of the Shetland Shelf (Fig. 5). During the first visit to the Norwegian Basin, picoeukaryotes were highly abundant, reaching a maximum of $20 \times 10^3 \text{ cells ml}^{-1}$. Despite their small size, this fraction in this case comprised up to 64 % of total phytoplankton biomass (the total phytoplankton biomass is calculated from total chl *a* to total phytoplankton carbon by using the conversion factor of 29, described in the

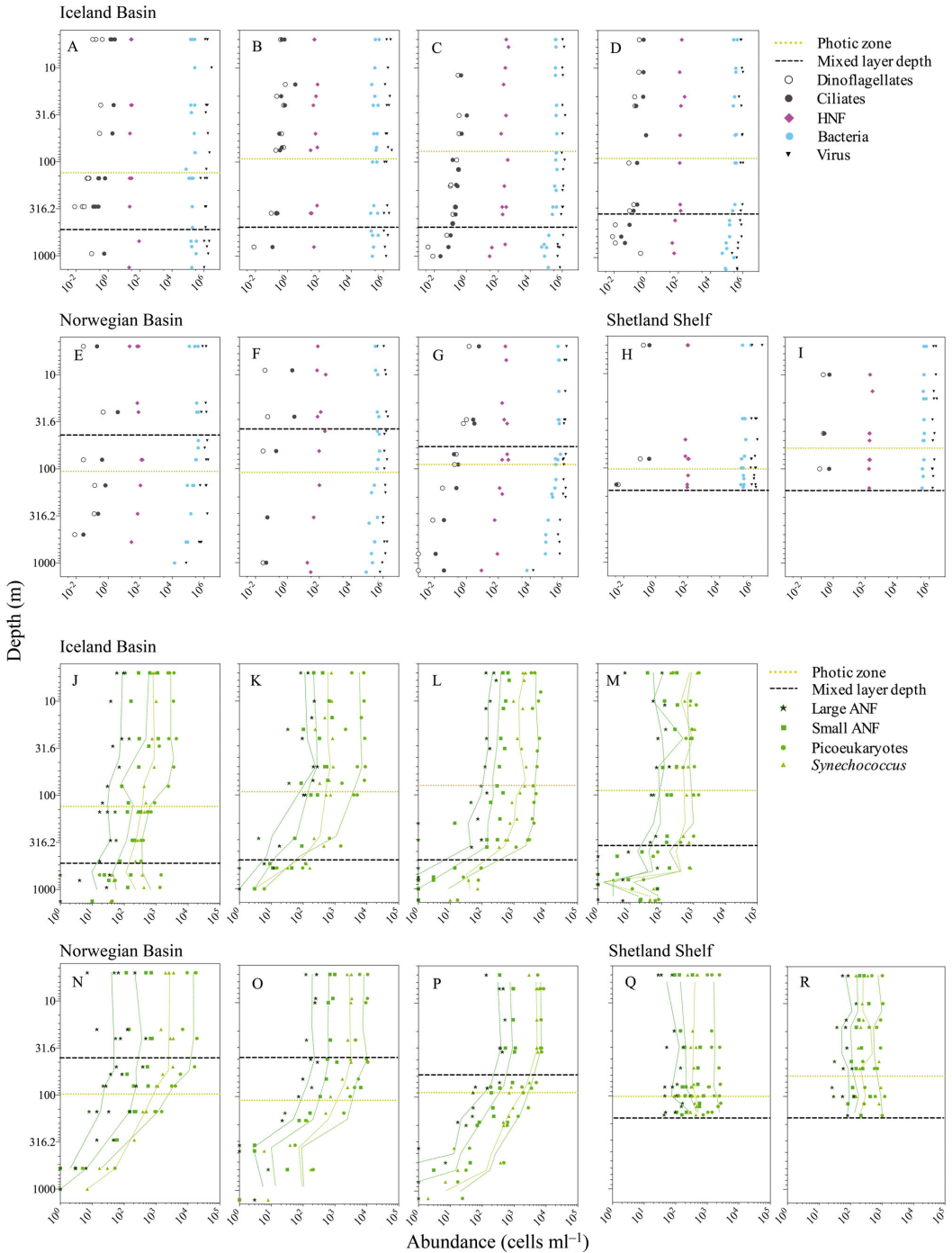


Fig. 5. Log-log scale vertical profiles showing the abundance of microorganisms throughout the study (first visit to the left). Triplicate vertical profiles were performed within 20 to 36 h at each visit to the stations. (A–I) Heterotrophic microorganisms: dinoflagellates, ciliates, heterotrophic nanoflagellates (HNF), bacteria and viruses. (J–R) Phototrophic microorganisms: small (>2 to 5 μm) and large (>5 to 10 μm) nanophytoplankton, picoeukaryotes and *Synechococcus* sp. Green and yellow vertical dashed lines (J–R) represent the mean abundance calculated within appropriate depth intervals. Horizontal black dashed lines indicate the depth of the mixed layer; horizontal yellow dashed line marks the photic zone

previous paragraph) (Fig. 7). During subsequent visits to the Norwegian Basin, the abundance of picoeukaryotes decreased gradually to average 6×10^3 cells ml^{-1} within the mixed layer, while small nanophytoplankton increased significantly (1-way ANOVA, $p < 0.05$) and became dominant in terms of biomass. Qualitative observations from Lugol's-fixed samples revealed that dominant nanophytoplankton by the end of the period were of the class Cryptophyceae, while diatoms were absent in the Norwegian Basin.

At the deep mixed stations, the increase in the >10 μm chl *a* fraction corresponded well to observations from Lugol's-fixed samples where we observed that larger phytoplankton became more dominant. At the second visit to the Iceland Basin station, we observed a high abundance of *Chaetoceros* spp. (up

to 200 cells ml^{-1}) and few *Leptocylindricus* spp., while *Pseudo-nitzschia* spp. became more dominant during the last 2 visits. At the Shetland Shelf station, the large phytoplankton community during the last visit was dominated by the diatoms *Thalassiosira* spp. and *Ditylum brightwellii*. See Daniels et al. 2015 for a more detailed description of the nano- and microphytoplankton community.

Succession of bacteria and virus ratios

In contrast to the photosynthetic plankton and the heterotrophic protists that were distributed evenly only within the mixed layer, bacteria were homogeneously distributed throughout the entire water column, except at the Norwegian Basin station, where a 100-fold decrease in bacterial abundance was evident below 1000 m (Fig. 5). Initially, in late March and early April, the bacterial abundance was low at all stations (2 to 3×10^5 cells ml^{-1}) but increased during the following 10 d at all stations to reach around 6 to 7×10^5 cells ml^{-1} .

The ratio of HNA:LNA bacteria increased significantly at all stations and was slightly lower below the mixed layer (Table 2, Fig. 8), i.e. fewer active bacteria. Bacteria were the most prominent heterotrophic biomass within the mixed layer (6 ± 3 mg C m^{-3} , $n = 27$), while viruses comprised the lowest biomass (0.1 ± 0.04 mg C m^{-3} , $n = 27$). The ratio of

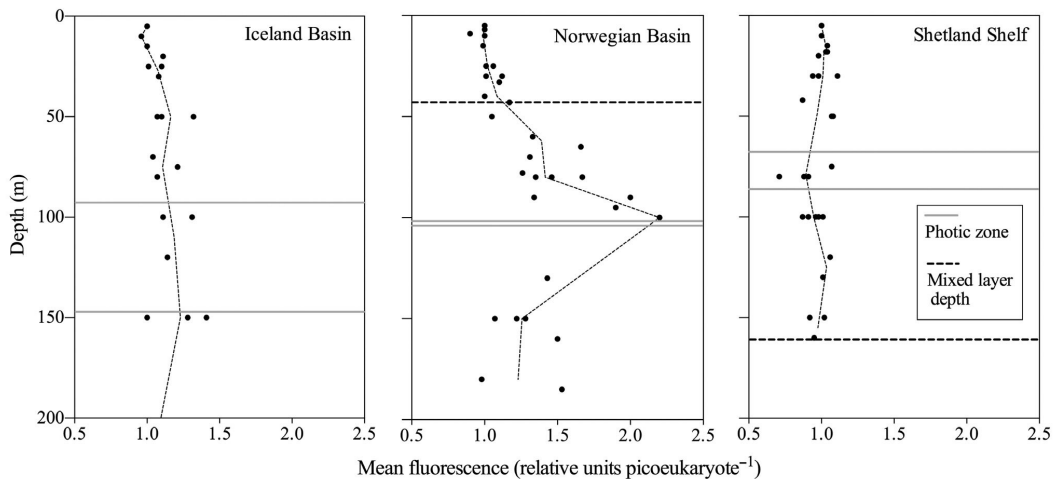


Fig. 6. Changes in mean fluorescence per picoeukaryote normalized by the 5 m value shown for the first 2 visits to each of the 3 stations in the upper 200 m. Horizontal dashed black line defines the mixed layer depth (no black dashed line in Iceland Basin as mixed layer is below 200 m; black dashed line in Shetland Shelf marks the bottom); solid horizontal gray lines mark

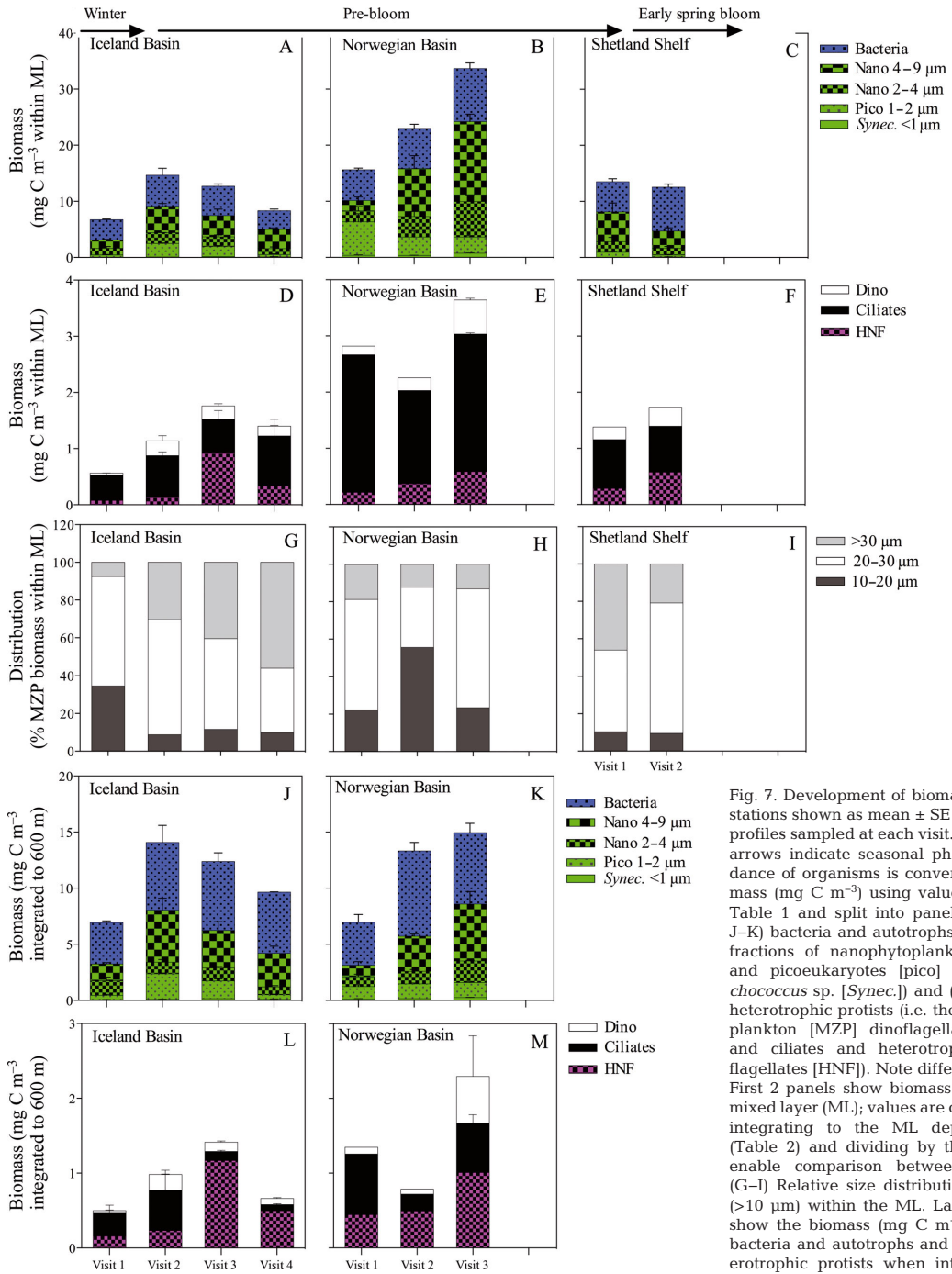


Fig. 7. Development of biomass at the 3 stations shown as mean ± SE (n = 3) of 3 profiles sampled at each visit. Horizontal arrows indicate seasonal phase. Abundance of organisms is converted to biomass (mg C m⁻³) using values given in Table 1 and split into panels of (A–C, J–K) bacteria and autotrophs (i.e. 2 size fractions of nanophytoplankton [nano] and picoeukaryotes [pico] and *Synechococcus* sp. [*Synech.*]) and (D–F, L–M) heterotrophic protists (i.e. the microzooplankton [MZP] dinoflagellates [dino] and ciliates and heterotrophic nanoflagellates [HNF]). Note different y-axis. First 2 panels show biomass within the mixed layer (ML); values are obtained by integrating to the ML depth (MLD) (Table 2) and dividing by the MLD to enable comparison between stations. (G–I) Relative size distribution of MZP (>10 μm) within the ML. Last 2 panels show the biomass (mg C m⁻³) of (J–K) bacteria and autotrophs and (L–M) heterotrophic protists when integrated to 600 m at the deep stations

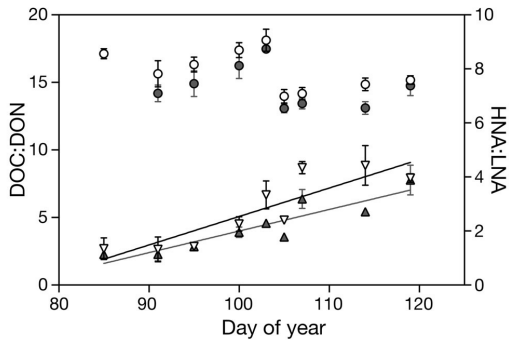


Fig. 8. Carbon:nitrogen ratios (dissolved organic carbon:dissolved organic nitrogen, DOC:DON) of dissolved organic matter within the mixed layer (○) and below the mixed layer (●) and high nucleic acid:low nucleic acid (HNA:LNA) bacteria ratios within the mixed layer (▽) and below the mixed layer (▲) from all 3 stations plotted over time (day of year) during the entire study. Values are given as mean \pm SE, $n = 6$ to 22, and represent the mean within and below the mixed layer (deep) or, for the Shetland Shelf, below 100 m. Linear regressions are given as straight lines for the HNA:LNA ratio within the mixed layer [$f(x) = -7.99 + 0.11x$, $r^2 = 0.83$, $p < 0.005$] and for the HNA:LNA ratio below the mixed layer [$f(x) = -5.99 + 0.08x$; $r^2 = 0.84$, $p < 0.005$]

viruses:bacteria (V:B) decreased at the Iceland Basin and Norwegian Basin stations during the pre-bloom period from 8.2 ± 3.1 and 4.4 ± 3.4 to 2.6 ± 0.3 and 2.5 ± 0.4 , respectively, within the upper mixed layer. Below the mixed layer, the V:B ratio was generally higher (Table 2).

HNF

The mean ESD of HNF was $3.2 \pm 0.3 \mu\text{m}$, $n = 170$, and did not change during the period. HNF were abundant below the mixed layer, but at depths below 1000 m, they were found in relatively low abundance ($23 \pm 4 \text{ cells ml}^{-1}$, $n = 4$) (Fig. 5). Within the upper mixed layer at the first visits to the Iceland Basin and Norwegian Basin stations, the abundance of HNF was low (25 and 48 cells ml^{-1} , respectively) but within 2 to 3 wk increased rapidly 4- to 5-fold. At the first visit to the Shetland Shelf station, the abundance was relatively higher ($97 \pm 14 \text{ cells ml}^{-1}$) and doubled over the next 10 d ($201 \pm 31 \text{ cells ml}^{-1}$). In terms of biomass, HNF averaged $\sim 3 \pm 1\%$ of their available prey (integrated biomass of bacteria, picoeukaryotes and *Synechococcus*) during the earliest visits to all stations, while later in the study the value increased to $\sim 7 \pm 3\%$ of their prey biomass.

MZP

MZP were found to be evenly distributed throughout the mixed layer at all 3 stations (Fig. 5). In the Norwegian and Iceland basins, the abundance of MZP decreased with depth below the mixed layer. At all stations, ciliates contributed on average 73 to 91% of the total MZP biomass, while dinoflagellates made up the remaining part of the biomass (Fig. 7). Integrated MZP biomass (mg C m^{-3}) within the mixed layer was lowest at the Iceland Basin, slightly higher at the Shetland Shelf station and by far highest at the Norwegian Basin (Fig. 7). At the Iceland Basin, MZP integrated biomass increased significantly from the first visit to the 3 later visits (1-way ANOVA, $p < 0.05$). A change in MZP biomass could not be tested for the Norwegian Basin and the Shetland Shelf stations due to lack of replicates, but those samples obtained suggest that there were no marked changes in MZP biomass. The MZP communities at all stations were generally composed of smaller (12 to $30 \mu\text{m}$) species (Fig. 7G–I). However, at the Iceland Basin station, the fraction of larger (ESD $> 30 \mu\text{m}$) species increased during the study, and during the last sampling day, 56% of the MZP biomass was composed of individuals with an ESD $> 30 \mu\text{m}$. The Norwegian Basin station was strongly dominated by small cells (ESD $< 30 \mu\text{m}$), contributing $> 80\%$ of the MZP biomass. Ciliates were dominated by oligotrichs at all stations, but mixotrophic cyclotrichs of the genus *Mesodinium* also contributed substantially to the ciliate biomass, especially at the 3 later visits to the Iceland Basin station. Naked gymnodiid species dominated the dinoflagellate biomass, whereas thecate species made a minimal contribution, $< 5\%$ of the total MZP biomass (Table 3).

DISCUSSION

Deep mixing enhances accumulation of large phytoplankton

Even during winter, when the sun stays well below the horizon, backscattered light can be detected below 6 m depth at levels high enough to enable photosynthesis (Eilertsen & Degerlund 2010). Backhaus et al. (2003) found presence of a winter stock of phytoplankton within the mixed layer of the Norwegian and Iceland basins and suggested this was enabled by phytoplankton occasionally re-entering the photic zone to harvest light as a result of deep convective mixing during winter. Based on the net increase in

Table 3. Biomass contribution (%) of major groups or species of microzooplankton (dinoflagellates and ciliates) at different visits to the 3 stations

	Iceland Basin				Norwegian Basin			Shetland Shelf	
	Visit: 1	2	3	4	1	2	3	1	2
Oligotrichs	87.4	53.5	57.3	62.7	85.9	79.4	83.3	75.6	39.4
<i>Mesodinium</i> spp.	3.7	23.8	18.0	14.8	4.7	8.2	5.7	4.6	33.0
Tintinnids	0.3	0.1	0.3	0.8	1.1	1.1	0.1	0.0	0.1
<i>Gyrodinium spirale</i>	1.0	4.6	5.0	4.5	0.7	1.6	0.5	0.0	1.7
Naked dinoflagellates	6.1	16.1	14.2	14.0	6.8	9.8	10.4	15.8	21.1
Thecate dinoflagellates	1.5	1.9	5.2	3.1	0.8	0.0	0.0	4.1	4.7

chl *a* concentrations, the mixed stations were the most productive, with chl *a* increasing up to 5-fold during the course of our study. In comparison, integrated chl *a* remained roughly the same in the Norwegian Basin, despite an increased day length and excess nutrients (Table 2, Fig. 4). In contrast to Backhaus et al. (2003), who only considered total chl *a* and counts of large phytoplankton, we also considered the community of small phytoplankton behind the chl *a* values.

As the pre-bloom develops, the relative contribution of small cells decreased at the mixed stations, while pico- and nanophytoplankton continued to dominate the phytoplankton biomass at the more stratified Norwegian Basin. This tendency suggests that convective mixing of the water column contributes to the maintenance of large cells such as diatoms in the water column, since the diatoms are otherwise subjected to high sinking losses. Similar selection has been observed in other turbulent systems (Kjørboe 1993). However, large diatoms can also express positive buoyancy under certain conditions, e.g. during light and nutrient saturation the large marine diatom *Ditylum brightwellii* expresses high buoyancy (Waite et al. 1992). Our observations support the fact that increasing light and nutrient-replete conditions could be favourable for large diatom species by further boosting their buoyancy. This is not the case at the Norwegian Basin, however, though light and nutrient conditions are similar, indicating that the convection is more likely an enhancer for diatoms during pre-bloom.

Contribution of picophytoplankton during pre-bloom

Our results demonstrate the quantitative importance of pico- and small nanophytoplankton in the subarctic Atlantic pre-bloom and suggest a new role of small phytoplankton production as an important

booster of the late winter microbial heterotrophic community prior to the diatom bloom. The <10 µm chl *a* fraction clearly dominated during the winter and pre-bloom. However, it is not straightforward to draw conclusions on fractionated chl *a*, as small phytoplankton are known to form aggregates (Barber 2007) (and thus may have contributed to the larger fractions of chl *a*) and underestimate the contribution of small phytoplankton. We further document that the more stratified water enables the small phytoplankton to increase their pigment content towards the base of the photic zone (Fig. 6); thereby, using chl *a* as a proxy would overestimate phytoplankton biomass at more stratified stations where phytoplankton are adapted to stable light conditions when compared to the mixed stations. The following discussion is strengthened by being based both on fractionated chl *a* and on the cell counts of small phytoplankton.

Picophytoplankton dominated in numbers throughout the cruise (Fig. 5J–R) but contributed moderately to the integrated phytoplankton biomasses (Fig. 7A–C). However, the fast turnover of picophytoplankton resulted in a larger contribution to phytoplankton production than their small biomass suggests (Agawin et al. 2000). The higher turnover of picophytoplankton was also documented during this study by fractionated primary production measurements, showing the contribution of <10 µm phytoplankton to primary production to be on average 2.7 ± 2.2 times higher than their <10 µm contribution to chl *a* biomass in the Iceland Basin. The same tendency was found at the Norwegian Basin; here, however, the contribution to both chl *a* biomass and the production of large phytoplankton >10 µm was negligible (5 to 10%) throughout the study (Daniels et al. 2015).

The success of picophytoplankton is often assumed to be due to their high affinity for nutrients (Agawin et al. 2000); however, the success of picoeukaryotes during the late winter in high-latitude systems may rather be explained by a high affinity for light com-

pared to larger phytoplankton due to the absence of a cell wall and since the small size of picophytoplankton enables an efficient packaging of photosynthetic pigments inside the cell (Raven 1998). This high affinity for light coupled with their low sinking rates (Kjørboe 1993) position picophytoplankton to respond earlier than other groups to the increase in irradiance in the early spring. This hypothesis is supported by culture experiments with the abundant picophytoplankton *Micromonas*, which were found to have a competitive advantage in both Arctic and subarctic regions due to their relatively high growth rate at low irradiance and low temperature conditions (Lovejoy et al. 2007).

The picophytoplankton community was dominated by picoeukaryote species, whereas the contribution by the prokaryotic compartment, *Synechococcus* sp., was minor. Numeric dominance of eukaryotic picophytoplankton relative to prokaryotes is characteristic for high-latitude waters (Tremblay et al. 2009). A picoeukaryote peak abundance of 20×10^3 cells ml⁻¹ was found in the Norwegian Basin, which is comparable to peak abundances reported prior to the bloom in Norwegian coastal waters (Sandaa & Larsen 2006, Bratbak et al. 2011). Tremblay et al. (2009) compared the abundance of picophytoplankton at 10 sites in northern systems during spring, summer and late summer. Our novel observations of picophytoplankton during the period of winter–spring transition are in general higher than those found later in the season.

It is open to dispute whether pico- and small nanophytoplankton are insignificant during the bloom period as found by Joint et al. (1993) or whether they may still comprise a substantial part of the bloom as found by Sherr et al. (2003). As also discussed in Daniels et al. (2015), it is likely that the development we observe during pre-bloom will result in different spring blooms; while the Norwegian Basin spring bloom may continue to be dominated by pico- and small nanophytoplankton, the deep mixed stations are likely to be dominated by diatoms. The composition of phytoplankton during blooms is crucial for zooplankton and the energy transfer to higher trophic levels.

Our initial observations in late March at the Iceland Basin indicate that there are surviving winter stocks of both large and small phytoplankton. The early succession suggests that picoeukaryotes have the greatest advantage earliest in the season with lowest light conditions. Nanophytoplankton remain unchanged in deep mixed waters, whereas the accumulation of large phytoplankton (diatoms) rapidly

increases in the deep convective waters of the Iceland Basin and Shetland Shelf (Fig. 4). In the more stratified Norwegian Basin, chl *a* remained in the <10 µm fraction, but within this fraction, there was a clear change from dominance of picophytoplankton to dominance of small nanophytoplankton (Fig. 7). The difference in development is likely caused by the difference in convective mixing, as discussed in the previous section. Moreover, difference in grazing control is likely to play a crucial role, as discussed in the next section.

Heterotrophic protist: top-down control on picophytoplankton?

The heterotrophic protists (HNF and MZP) followed the same homogeneous distribution within the mixed layer as the phytoplankton (Fig. 5); however, whereas MZP decreased exponentially below the mixed layer, HNF showed a more uniform distribution towards the bottom, resulting in a relatively higher biomass when integrated to 600 m (Fig. 7L,M). The highest biomass of heterotrophic protists was found in the more stratified Norwegian Basin, where ciliates dominated the biomass (Fig. 7E). Ciliates also dominated the biomass of heterotrophic protists at the 2 deep mixed stations. However, when considering the higher growth rates of HNF relative to MZP (Hansen et al. 1997), HNF's contribution to heterotrophic protist production may be higher than their biomass suggests. This is supported by incubation experiments conducted during the study with surface water from the Iceland Basin, which showed HNF to have significantly higher growth rates (0.48 ± 0.17 d⁻¹, *n* = 6) than MZP (0.15 ± 0.05 d⁻¹, *n* = 3) (K. Riisgaard et al. unpubl.).

The cell numbers of HNF we encountered were in general in the lower end of those observed globally (Sanders et al. 1992) but very similar to those found in Arctic marine systems during the period of winter–spring transition (Vaqué et al. 2008, Iversen & Seuthe 2011). Peak abundances of 300 cells ml⁻¹ were observed during our study period. Kuipers et al. (2003) document peak HNF numbers of up to 8000 cells ml⁻¹ in the Faroe–Shetland Channel (60 to 62°N) during summer. This suggests that the rapid increase in the abundance of HNF we observed might be sustained through the spring season, thus maintaining a high grazing pressure on bacteria and picophytoplankton. The average diameter of HNF found in this study, 3.2 ± 0.3 µm, agrees with the ≤ 3 µm obtained by Jürgens & Massana (2008) for 76 % of HNF across 4 different

marine systems. HNF with a diameter of 2 to 5 μm have been observed to ingest 1.5 to 2 μm picoeukaryotes and coccoid cyanobacteria (Sherr et al. 1997). It has long been assumed that HNF feed on pico-sized phytoplankton (Fenchel 1982, Azam et al. 1983), yet recent studies on the grazing potential of HNF focus on quantifying bacterivory and neglect the additional portion of carbon taken up via picophytoplankton (Tanaka et al. 1997, Iriarte et al. 2008). They are, however, major grazers of picophytoplankton (Christaki et al. 2001, Sherr & Sherr 2002, Bræk-Laitinen & Ojala 2011), and it remains for future studies to resolve the importance of HNF grazing. We here would suggest splitting the group into large and small HNF to test whether the size groups have different prey-size preferences as speculated by Sherr & Sherr (2002) and Vaqué et al. (2008). Both of these studies suggest that heterotrophic flagellates $<5 \mu\text{m}$ are the main grazers on bacteria, while flagellates $>5 \mu\text{m}$ select for picoeukaryotes. We observe that the decrease in picoeukaryote biomass mirrors the increase in HNF biomass within the mixed layer of the Norwegian Basin and Shetland Shelf (Fig. 7B,C,E,F), also implied by the gradual decreases in bacteria: HNF and picoeukaryote:HNF ratios during prebloom (Table 2). Still, it is impossible to resolve the top-down controls on pico-sized plankton from *in situ* abundances; however, quantifications of HNF grazing are documented through incubation experiments in K. Riisgaard et al. (unpubl.).

Effect of deep mixing on protist grazing

The biomass (mg C m^{-3}) of dinoflagellates and ciliates was low at all sampling stations compared to biomass obtained during spring and summer in the Norwegian Sea (Verity et al. 1993). However, when integrated over the depth of the mixed layer, MZP biomasses are comparable to spring integrated biomasses (300 to 500 mg C m^{-2}) within the mixed layer of the Norwegian Basin and the high Arctic Kongsfjorden (Verity et al. 1993, Seuthe et al. 2011a) and 2- to 3-fold higher than integrated values estimated during the winter–spring transition in the high Arctic Disko Bay (Levinsen et al. 2000). Thus, although MZP concentrations are relatively low, their integrated biomass is significant at all stations.

Ciliates dominated the MZP biomass, with a relative increase in naked and thecate dinoflagellates at the deep mixed Iceland Basin and Shetland Shelf as diatoms became more abundant. The positive relationship between dinoflagellates and diatoms sup-

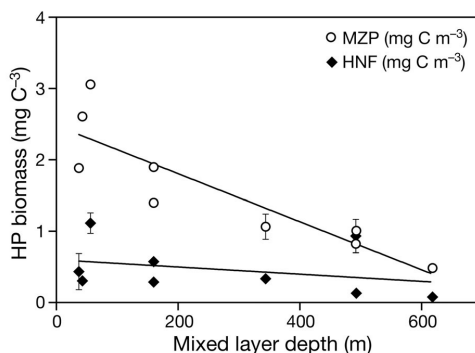


Fig. 9. Biomass of heterotrophic protists (HP) at the 3 stations during the study as a function of mixed layer depth (MLD). Heterotrophic nanoflagellates (HNF) and the sum of heterotrophic dinoflagellates and ciliates (MZP) are shown as average biomass within the MLD (mg C m^{-3}). Linear regression was significant for MZP [$f(x) = -0.0034x + 2.48$, $r^2 = 0.78$, $p < 0.05$] but not for HNF [$f(x) = -0.0005x + 0.6$, $r^2 = 0.10$, $p = 0.39$]

ports the hypothesis that heterotrophic dinoflagellates are important grazers of diatoms (Sherr & Sherr 2007). The Norwegian Basin was dominated (76 to 86%) by oligotrich ciliates throughout the study, which would also be expected with a phytoplankton community composed of mainly small cells. At all 3 stations, large ($>30 \mu\text{m}$) species became increasingly important at the Iceland Basin and mirrored the increase in large phytoplankton ($>50 \mu\text{m}$), while the smaller *Mesodinium* spp. became highly abundant at the Shetland Shelf.

Behrenfeld (2010) and Behrenfeld & Boss (2014) suggested that the higher net increase in phytoplankton biomass during events of deep convection is caused by a dilution of the grazing community. Although the grazers are possibly diluted, as indicated by the homogeneously vertical distribution of MZP throughout the mixed layer and a reduction in MZP biomass with increasing mixing depth (Fig. 9), a reduction in numbers of grazers will not necessarily benefit diatoms. Based on the composition of the heterotrophic protists, which were dominated by HNF and ciliates, we argue that a dilution of the grazing community would mainly benefit pico- and nanophytoplankton, whereas diatoms are largely unaffected, the latter because diatoms are unsuitable as prey for HNF and ciliates. Thus, the increase in the $>10 \mu\text{m}$ chl *a* fraction at the mixed stations is more likely to be explained by reduced sinking rates due to deep convection and increased irradiance as the day length increases rather than reduced grazing

pressure from heterotrophic protists being diluted. Alternatively, dilution may have reduced the grazing pressure from other grazers such as copepods (e.g. *Oithona* sp.), which could explain the net growth in large phytoplankton species at the mixed stations.

It must further be considered that the response of mixing is time dependent, i.e. organisms with high growth rates are less affected by dilution. The higher growth rates of HNF, compared to MZP, may be the reason that HNF seem unaffected by deep mixing, while MZP biomass decreases significantly with MLD (Fig. 9). Further, as MZP are also grazers of HNF, the HNF may benefit from the dilution of MZP during deep mixing. When HNF is favoured by deep mixing, the prey of HNF would equally not benefit from deep mixing. Here, we want to underline that the effect of deep mixing in regard to grazing on phytoplankton strongly depends on the size composition of the heterotrophic community.

Controls of bacteria

To our knowledge, there are no previous observations of bacterial abundance during the winter-spring transition in the subarctic North Atlantic. The abundances encountered initially in late March and early April (2 to 3×10^5 cells ml^{-1}) are an order of magnitude lower than those observed during the spring bloom in May (47° N, 20° W), where they have been documented to reach 2×10^6 cells ml^{-1} (Ducklow et al. 1993) but correspond to observations found during pre-bloom conditions elsewhere in the temperate and Arctic North Atlantic (Bratbak et al. 2011, Seuthe et al. 2011a). It is generally assumed that the growth of heterotrophic bacteria in the winter and pre-bloom phase is substrate limited and the increase in abundance is triggered by DOM excreted from the spring bloom production (Lancelot & Billen 1984, Teeling et al. 2012). Our observations, however, show that bacteria increase in abundance and activity (HNA:LNA ratio) already during pre-bloom. The fact that DOC does not accumulate in the surface layer, despite a net growth of phytoplankton (Fig. 4), infers that the DOC has been taken up by bacteria (Thingstad et al. 1997). Excretion from phytoplankton is generally a very labile carbon source. It has been suggested that smaller phytoplankton excrete relatively more, as the passive excretion is largely due to the passive diffusion of low molecular weight compounds over the cell membrane, which is proportional to the surface:volume ratio and therefore higher for small cells (Bjørnsen 1988), e.g. a study by

Malinsky-Rushansky & Legrand (1996) found that picoeukaryotes release 30% of their primary production, while larger nano-sized cells release only 4 to 5%. Therefore, a relatively high contribution to picophytoplankton may benefit bacteria. Our data suggest that bacteria in the deep basins initially were carbon limited, as they responded positively to the growing phytoplankton supply of labile DOC by increasing in numbers within the upper mixed layer between the first and second visits at all stations and expressing higher HNA:LNA ratios (Table 2). Control by bacterivorous grazers and nutrients were assumed to be less important due to low cell numbers of HNF grazers and since NO_3+NO_2 and PO_4 were found in excess.

The C:N ratio of DOM generally decreased during the study from 17.0 to 14.5 in the upper mixed layer and from 15.7 to 13.6 below the mixed layer (Fig. 8), possibly due to grazing and loss of carbon by respiration of the carbon-rich phytoplankton primary production. Labile DOM is characterized by low C:N ratios relative to refractory DOM (Carlson 2002), and therefore the decrease in C:N coincides (however does not correlate significantly, $p = 0.2$) with a significant increase in HNA:LNA bacteria ($r^2 = 0.83$, $p < 0.005$) ratios within the mixed layer as well as below the mixed layer ($r^2 = 0.84$, $p < 0.005$) (Fig. 8), indicating a more actively growing bacterial community (Sherr et al. 2006, Martínez-García et al. 2013). There was, however, an increase in the C:N ratio from the first to the second visit at the Norwegian Basin; this could be explained by a relatively high release of sugars (high C, low N) from picophytoplankton (Giroldo et al. 2005), which dominated at the time.

Decreasing V:B ratio

It is generally assumed that viruses are responsible for 10 to 50% of the bacterial mortality in surface waters and 50 to 100% in environments where grazing protists are low in numbers, e.g. the deep ocean (Fuhrman 1999). The higher the V:B ratio, the higher the expected bacterial mortality induced by strain-specific viruses. During this study, we found a significantly decreasing V:B ratio within the upper mixed layer at all stations (1-way ANOVA, $p < 0.0001$). This was due to an increase in bacteria, which was not mirrored as an increase in viruses. One explanation could be that the strains of bacteria which are the best competitors for the newly produced DOC became dominant over the strains that dominated during the substrate-limited winter, and thus the strain-

specific viruses have not yet evolved for the new strains of dominating bacteria, or that the abundance of bacteria was not sufficient to permit infection by a virus to influence the bacterial community (i.e. a Holling type III or IV reaction). This lag phase by viruses gives the bacterial competition specialists a head start in the pre-bloom phase. Eventually, viruses would be expected to increase in numbers and, according to the killing the winner hypothesis (Thingstad 2000), become a regulating factor for the bacteria community, and the V:B ratio would increase.

Bacteria in deep water benefit from deep mixing

Bacterial abundance in deep oceans is often observed to decline exponentially with depth (Nagata 2000). In contrast, we observed a vertical uniform distribution of bacteria to the bottom (1350 m) of the Iceland Basin, while bacteria decreased significantly towards the bottom at the equally deep Norwegian Basin station (Fig. 5A–G). The relatively high bacterial abundance and increasing HNA:LNA ratio in the deep water of the Iceland Basin is potentially a consequence of deep convective mixing, which has resulted in a homogeneous distribution of bacteria over the water column. This distribution extends below the observed mixed layer at all stations, suggesting that the depth of convective mixing has retreated prior to the program.

Conversely, the homogeneous distribution observed in the heterotrophic organisms is not evidenced in the photosynthetic community at the Iceland and Norwegian basins. The Shetland Shelf station, which was mixed to the bottom by convection during the study period, has a homogeneous distribution of all properties over the entire water column. These observations suggest that the conditions in the convective layer have the potential for a net positive, although low, growth rate as speculated by Backhaus et al. (2003) and Lindemann & St. John (2014). These authors have identified the role of phyto-convection (Backhaus et al. 2003) and below the threshold of critical turbulence resulting in surface blooms (Huisman 1999) in maintaining and fueling production in the convective mixed layer. The cell distributions we observed below the convective depth support the idea of Lindemann & St. John (2014) that cells are potentially detrained from the convective mixed layer, contributing to a pre-spring bloom flux of organic material to depth and here resulting in increased heterotrophic biomass. However, future research is clearly necessary to test this hypothesis.

Our interpretation of the data

This study highlights the importance of the small, fast-growing phytoplankton community as the base of the food web prior to the phytoplankton spring bloom and suggests that deep convection enhances not only phytoplankton accumulation within the mixed layer but also feeds a growing bacterial population below the deep mixed layer. The pre-bloom production feeds a growing community of heterotrophic bacteria and heterotrophic protists and alters the C:N ratio of DOM without depleting the nutrient reservoirs. The subsequent succession and nutrient depletion is caused by larger phytoplankton resistant to small grazers. Our data further suggest that deep mixing reduces grazing on and thus enhances the growth of $>10 \mu\text{m}$ phytoplankton but that the fast-growing HNF are able to keep a tight grazing control on picophytoplankton despite deep mixing. Experimental studies are needed to further assess the coupling between picophytoplankton and their small grazers.

Acknowledgements. The research leading to these results has received funding from the European Union Seventh Framework Programme project EURO-BASIN (ENV.2010.2.2.1-1) under grant agreement no. 264933, ERC grant Microbial Network Organization (MINOS 250254) and the US National Science Foundation (OCE-0752972). The Deep Convection cruise was funded by the Deutsche Forschungsgemeinschaft in a grant to M.S.J. We are very grateful to Dennis A. Hansell for supplying data on TOC and TN. We are also thankful to the crew of the RV 'Meteor' on the Deep Convection Cruise and especially to Françoise Morison and Chris Daniels for good teamwork and for language corrections. Big thanks to Mario Esposito for measuring nutrients during the cruise, and special thanks to Aud Larsen for steadfast flow cytometry assistance. For valuable discussions on an earlier version of the manuscript, we are grateful to Lena Seuthe, Marit Reigstad, Antonio Cuevas and Mathias Middelboe as well the constructive comments of reviewers who helped to improve this manuscript substantially.

LITERATURE CITED

- Agawin NSR, Duarte CM, Agustí S (2000) Nutrient and temperature control of the contribution of picoplankton to phytoplankton biomass and production. *Limnol Oceanogr* 45:591–600
- Anderson LG (2002) DOC in the Arctic Ocean. In: Hansell DA, Carlson CA (eds) Biogeochemistry of marine dissolved organic matter. Academic Press, San Diego, CA, p 665–684
- Azam F, Fenchel T, Field JG, Gray JS, Meyer-Reil LA, Thingstad F (1983) The ecological role of water-column microbes in the sea. *Mar Ecol Prog Ser* 10:257–263
- Backhaus JO, Wehde H, Hegseth EN, Kämpf J (1999) 'Phyto-convection': the role of oceanic convection in pri-

- mary production. *Mar Ecol Prog Ser* 189:77–92
- Backhaus JO, Hegseth EN, Wehde H, Irigoien X, Hatten K, Logemann K (2003) Convection and primary production in winter. *Mar Ecol Prog Ser* 251:1–14
- Barber RT (2007) Picoplankton do some heavy lifting. *Science* 315:777–778
- Behrenfeld MJ (2010) Abandoning Sverdrup's critical depth hypothesis on phytoplankton blooms. *Ecology* 91: 977–989
- Behrenfeld MJ, Boss ES (2014) Resurrecting the ecological underpinnings of ocean plankton blooms. *Annu Rev Mar Sci* 6:167–194
- Bjørnsen PK (1988) Phytoplankton exudation of organic matter: Why do healthy cells do it?. *Limnol Oceanogr* 33: 151–154
- Blindheim J, Østerhus S (2005) The Nordic seas, main oceanographic features. In: Drange H, Dokken T, Furevik T, Gerdes R, Berger W (eds) *The Nordic seas: an integrated perspective*. AGU Monograph 158, American Geophysical Union, Washington, DC, p 11–37
- Børsheim KY, Bratbak G (1987) Cell volume to cell carbon conversion factors for a bacterivorous *Monas* sp. enriched from seawater. *Mar Ecol Prog Ser* 36:171–175
- Braarud BY, Nygaard I (1978) Phytoplankton observations in offshore Norwegian coastal waters between 62°N and 69°N. *FiskDir Skr Ser Havunders* 16:489–505
- Bratbak G, Jacquet S, Larsen A, Petterson LH, Szahin AF, Thyrraug R (2011) The plankton community in Norwegian coastal waters—abundance, composition, spatial distribution and diel variation. *Cont Shelf Res* 31: 1500–1514
- Brek-Laitinen G, Ojala A (2011) Grazing of heterotrophic nanoflagellates on the eukaryotic picoautotroph *Choricystis* sp. *Aquat Microb Ecol* 62:49–59
- Carlson CA (2002) Production and removal processes. In: Hansell DA, Carlson CA (eds) *Biogeochemistry of marine dissolved organic matter*. Academic Press, San Diego, CA, p 91–152
- Christaki U, Giannakourou A, Wambeke FVANW, Grégori G (2001) Nanoflagellate predation on auto- and heterotrophic picoplankton in the oligotrophic Mediterranean Sea. *J Plankton Res* 23:1297–1310
- Cushing DH (1959) On the nature of production in the sea. *Fish Invest Lond Ser II* 22:1–40
- Daniels CJ, Poulton AJ, Esposito M, Paulsen ML, Bellerby R, St. John M, Martin AP (2015) Phytoplankton dynamics in contrasting early stage North Atlantic spring blooms: composition, succession, and potential drivers. *Biogeosciences* 12:2395–2409
- de Boyer Montégut C, Madec G, Fischer AS, Lazar A, Iudicone D (2004) Mixed layer depth over the global ocean: an examination of profile data and a profile-based climatology. *J Geophys Res* 109:C12003
- Dickson AG, Sabine CL, Christian JR (eds) (2007) Guide to best practices for ocean CO₂ measurements. PICES Special Publication 3. http://cdiac.ornl.gov/ftp/oceans/Handbook_2007/Guide_all_in_one.pdf
- Ducklow H, Kirchman D, Quinby H, Carlson C, Dam H (1993) Stock and dynamics of bacterioplankton carbon during the spring bloom in the eastern North Atlantic Ocean. *Deep-Sea Res II* 40:245–263
- EGge JK, Aksnes DL (1992) Silicate as regulating nutrient in phytoplankton competition. *Mar Ecol Prog Ser* 83: 281–289
- Eilertsen HC, Degerlund M (2010) Phytoplankton and light during the northern high-latitude winter. *J Plankton Res* 32:899–912
- Fenchel T (1982) Ecology of heterotrophic microflagellates. IV. Quantitative occurrence and importance as bacterial consumers. *Mar Ecol Prog Ser* 9:35–42
- Fuhrman JA (1999) Marine viruses and their biogeochemical and ecological effects. *Nature* 399:541–548
- Giroldo D, Augusto A, Vieira H (2005) Polymeric and free sugars released by three phytoplanktonic species from a freshwater tropical eutrophic reservoir. *J Plankton Res* 27:695–705
- Hansell DA (2005) Dissolved organic carbon reference material program. *EOS Trans. AGU* 86(35):318
- Hansen PJ, Bjørnsen PK, Hansen BW (1997) Zooplankton grazing and growth: scaling within the 2–2000 µm body size range. *Limnol Oceanogr* 42:687–704
- Hirche H (1996) Diapause in the marine copepod, *Calanus finmarchicus*—a review. *Ophelia* 44:129–143
- Huete-Stauffner TM, Morán XAG (2012) Dynamics of heterotrophic bacteria in temperate coastal waters: similar net growth but different controls in low and high nucleic acid cells. *Aquat Microb Ecol* 67:211–223
- Huisman J (1999) Critical depth and critical turbulence: two different mechanisms for the development of phytoplankton blooms. *Limnol Oceanogr* 44:1781–1787
- Iriarte A, Sarobe A, Orive E (2008) Seasonal variability in bacterial abundance, production and protistan bacterivory in the lower Urdaibai estuary, Bay of Biscay. *Aquat Microb Ecol* 52:273–282
- Irigoien X, Flynn KJ, Harris RP (2005) Phytoplankton blooms: a 'loophole' in microzooplankton grazing impact? *J Plankton Res* 27:313–321
- Iversen KR, Seuthe L (2011) Seasonal microbial processes in a high-latitude fjord (Kongsfjorden, Svalbard): I. Heterotrophic bacteria, picoplankton and nanoflagellates. *Polar Biol* 34:731–749
- Jerlov NG (1968) *Optical oceanography*. Elsevier, New York, NY
- Jespersen AM, Christoffersen K (1987) Measurement of chlorophyll-a from phytoplankton using ethanol as extraction solvent. *Arch Hydrobiol* 109:445–454
- Joint I, Pomroy A, Savidge G, Boyd P (1993) Size-fractionated primary productivity in the northeast Atlantic in May–July 1989. *Deep-Sea Res II* 40:423–440
- Jürgens K, Massana R (2008) Protistan grazing on marine bacterioplankton. In: Kirchman DL (ed) *Microbial ecology of the oceans*, 2nd edn. John Wiley & Sons, Hoboken, NJ, p 383–441
- Kana TM, Glibert PM (1987) Effect of irradiances up to 2000 µE m⁻² s⁻¹ on marine *Synechococcus* WH7803—I. Growth, pigmentation, and cell composition. *Deep-Sea Res* 34:479–495
- Kjørboe T (1993) Turbulence, phytoplankton cell size and the structure of pelagic food webs. *Adv Mar Biol* 29:2–61
- Koroleff F (1983) Determination of nutrients. In: Grasshoff K, Erhardt M, Kremling K (eds) *Methods of seawater analysis*. Verlag Chemie, Weinheim, p 125–187
- Kuipers B, Witte H, van Noort G, Gonzalez S (2003) Grazing loss-rates in pico- and nanoplankton in the Faroe-Shetland Channel and their different relations with prey density. *J Sea Res* 50:1–9
- Lancelot C, Billen G (1984) Activity of heterotrophic bacteria and its coupling to primary production during the spring phytoplankton bloom in the southern bight of the North Sea. *Limnol Oceanogr* 29:721–730

- Larsen A, Flaten GAF, Sandaa RA, Castberg T and others (2004) Spring phytoplankton bloom dynamics in Norwegian coastal waters: microbial community succession and diversity. *Limnol Oceanogr* 49:180–190
- Lee S, Fuhrman JA (1987) Relationships between biovolume and biomass of naturally derived marine bacterioplankton. *Appl Environ Microbiol* 53:1298–1303
- Levinsen H, Nielsen TG, Hansen BW (2000) Annual succession of marine pelagic protozoans in Disko Bay, West Greenland, with emphasis on winter dynamics. *Mar Ecol Prog Ser* 206:119–134
- Li WKW (1980) Temperature adaptation in phytoplankton: cellular and photosynthetic characteristics. In: Falkowski PG (ed) *Primary productivity in the sea*. Plenum Press, New York, NY, p 259–279
- Li WKW, Dickie PM, Harrison WG, Irwin BD (1993) Biomass and production of bacteria and phytoplankton during the spring bloom in the western North Atlantic Ocean. *Deep-Sea Res II* 40:307–327
- Lindemann C, St John MA (2014) A seasonal diary of phytoplankton in the North Atlantic. *Front Mar Sci* 37:1–6
- Lovejoy C, Vincent WF, Bonilla S, Roy S and others (2007) Distribution, phylogeny, and growth of cold-adapted picoprasinophytes in Arctic seas. *J Phycol* 43:78–89
- Mahadevan A, D'Asaro E, Lee C, Perry MJ (2012) Eddy-driven stratification initiates North Atlantic spring phytoplankton blooms. *Science* 337:54–58
- Malinsky-Rushansky NZ, Legrand C (1996) Excretion of dissolved organic carbon by phytoplankton of different sizes and subsequent bacterial uptake. *Mar Ecol Prog Ser* 132:249–255
- Marie D, Brussaard CPD, Thyrhaug R, Bratbak G, Vault D (1999) Enumeration of marine viruses in culture and natural samples by flow cytometry. *Appl Environ Microbiol* 65:45–52
- Martínez-García S, Fernández E, del Valle DA, Karl DM, Teira E (2013) Experimental assessment of marine bacterial respiration. *Aquat Microb Ecol* 70:189–205
- Menden-Deuer S, Lessard EJ (2000) Carbon to volume relationships for dinoflagellates, diatoms, and other protist plankton. *Limnol Oceanogr* 45:569–579
- Mullin MM, Sloan PR, Eppley RW (1966) Relationship between carbon content, cell volume, and area in phytoplankton. *Limnol Oceanogr* 11:307–311
- Murphy J, Riley JP (1962) A modified single solution method for the determination of phosphate in natural waters. *Anal Chim Acta* 27:31–36
- Nagata T (2000) Production mechanisms of dissolved organic matter. In: Kirchman DL (ed) *Microbiology of the oceans*. Wiley-Liss, New York, NY, p 121–152
- Paulsen ML, Riisgaard K, Nielsen TG (2014a) Abundance of bacteria and virus during the Meteor cruise M87/1. PANGAEA, doi:10.1594/PANGAEA.839415
- Paulsen ML, Riisgaard K, Nielsen TG (2014b) Abundance of pico- and nanophytoplankton during the Meteor cruise M87/1. PANGAEA, doi:10.1594/PANGAEA.839416
- Pomeroy LR (1974) The ocean's food web, a changing paradigm. *Bioscience* 24:499–504
- Porter KG, Feig YS (1980) The use of DAPI for identifying and counting aquatic microflora. *Limnol Oceanogr* 25:943–948
- Putt M, Stoecker DK (1989) An experimentally determined carbon:volume ratio for marine 'oligotrichous' ciliates from estuarine and coastal waters. *Limnol Oceanogr* 34:1097–1103
- Raven JA (1998) Small is beautiful: the picophytoplankton. *Funct Ecol* 12:503–513
- Sandaa RA, Larsen A (2006) Seasonal variations in virus-host populations in Norwegian coastal waters: focusing on the cyanophage community infecting marine *Synechococcus* spp. *Appl Environ Microbiol* 72:4610–4618
- Sanders RW, Caron DA, Berninger UG (1992) Relationships between bacteria and heterotrophic nanoplankton in marine and fresh waters: an inter-ecosystem comparison. *Mar Ecol Prog Ser* 86:1–14
- Seuthe L, Iversen KR, Narcy F (2011a) Microbial processes in a high-latitude fjord (Kongsfjorden, Svalbard): II. Ciliates and dinoflagellates. *Polar Biol* 34:751–766
- Seuthe L, Töpper B, Reigstad M, Thyrhaug R, Vaquer-Sunyer R (2011b) Microbial communities and processes in ice-covered Arctic waters of the northwestern Fram Strait (75 to 80°N) during the vernal pre-bloom phase. *Aquat Microb Ecol* 64:253–266
- Sherr EB, Sherr BF (2002) Significance of predation by protists in aquatic microbial food webs. *Antonie van Leeuwenhoek* 81:293–308
- Sherr EB, Sherr BF, Wheeler PA, Thompson K (2003) Temporal and spatial variation in stocks of autotrophic and heterotrophic microbes in the upper water column of the central Arctic Ocean. *Deep-Sea Res I* 50:557–571
- Sherr EB, Sherr BF (2007) Heterotrophic dinoflagellates: a significant component of microzooplankton biomass and major grazers of diatoms in the sea. *Mar Ecol Prog Ser* 352:187–197
- Sherr EB, Sherr BF, Fessenden L (1997) Heterotrophic protists in the central Arctic Ocean. *Deep-Sea Res II* 44:1665–1682
- Sherr EB, Sherr BF, Longnecker K (2006) Distribution of bacterial abundance and cell-specific nucleic acid content in the northeast Pacific Ocean. *Deep-Sea Res I* 53:713–725
- Søndergaard M, Jensen LM, Årtebjerg G (1991) Picoalgae in Danish coastal waters during summer stratification. *Mar Ecol Prog Ser* 79:139–149
- Sorokin YI (1977) The heterotrophic phase of plankton succession in the Japan Sea. *Mar Biol* 41:107–117
- Steele JH (1974) *The structure of marine ecosystems*. Harvard University Press, Cambridge, MA
- Sverdrup H (1953) On conditions for the vernal blooming of phytoplankton. *J Cons Int Explor Mer* 18:287–295
- Tanaka T, Fujita N, Taniguchi A (1997) Predator-prey eddy in heterotrophic nanoflagellate-bacteria relationships in a coastal marine environment: a new scheme for predator-prey associations. *Aquat Microb Ecol* 13:249–256
- Taylor JR, Ferrari R (2011) Shutdown of turbulent convection as a new criterion for the onset of spring phytoplankton blooms. *Limnol Oceanogr* 56:2293–2307
- Teeling H, Fuchs BM, Becher D, Klockow C and others (2012) Substrate-controlled succession of marine bacterioplankton populations induced by a phytoplankton bloom. *Science* 336:608–611
- Thingstad TF (2000) Elements of a theory for the mechanisms controlling abundance, diversity, and biogeochemical role of lytic bacterial viruses in aquatic systems. *Limnol Oceanogr* 45:1320–1328
- Thingstad TF, Hagström Å, Rassoulzadegan F (1997) Accumulation of degradable DOC in surface waters: Is it caused by a malfunctioning microbial loop? *Limnol Oceanogr* 42:398–404
- Tremblay G, Belzile C, Gosselin M, Poulin M, Roy S, Tremblay JE (2009) Late summer phytoplankton distribution

- along a 3500 km transect in Canadian Arctic waters: strong numerical dominance by picoeukaryotes. *Aquat Microb Ecol* 54:55–70
- ▶ Vaqué D, Guadayol O, Peters F, Felipe J and others (2008) Seasonal changes in planktonic bacterivory rates under the ice-covered coastal Arctic Ocean. *Limnol Oceanogr* 53:2427–2438
 - ▶ Verity PG, Langdon C (1984) Relationships between lorica volume, carbon, nitrogen, and ATP content of tintinnids in Narragansett Bay. *J Plankton Res* 6:859–868
 - ▶ Verity PG, Stoecker DK, Sieracki ME, Nelson JR (1993) Grazing, growth and mortality of microzooplankton during the 1989 North Atlantic spring bloom at 47°N, 18°W. *Deep-Sea Res I* 40:1793–1814
 - ▶ Waite AM, Thompson PA, Harrison PJ (1992) Does energy control the sinking rates of marine diatoms? *Limnol Oceanogr* 37:468–477
 - ▶ Williams PJLB (1981) Incorporation of microheterotrophic processes into the classical paradigm of the planktonic food web. *Kieler Meeresforsch Sondh* 5:1–28
 - ▶ Wood ED, Armstrong FAJ, Rich FA (1967) Determination of nitrate in seawater by cadmium-copper reduction to nitrate. *J Mar Biol Assoc UK* 47:23–31
 - ▶ Zubkov MV, Sleigh M, Tarran GA, Burkill P, Leakey RJ (1998) Picoplanktonic community structure on an Atlantic transect from 50°N to 50°S. *Deep-Sea Res I* 45: 1339–1355
 - ▶ Zubkov MV, Burkill PH, Topping JN (2007) Flow cytometric enumeration of DNA-stained oceanic planktonic protists. *J Plankton Res* 29:79–86

Editorial responsibility: Urania Christaki, Wimereux, France

*Submitted: January 13, 2015; Accepted: July 25, 2015
Proofs received from author(s): September 7, 2015*



III



Synechococcus in the Atlantic Gateway to the Arctic Ocean

Maria L. Paulsen^{1*}, Hugo Doré², Laurence Garczarek², Lena Seuthe³, Oliver Müller¹, Ruth-Anne Sandaa¹, Gunnar Bratbak¹ and Aud Larsen⁴

¹ Department of Biology, University of Bergen, Bergen, Norway, ² Centre National de la Recherche Scientifique, UMR 7144, Station Biologique, Sorbonne Universités, UPMC Université Paris 06, Roscoff, France, ³ Department of Arctic and Marine Biology, Faculty of Biosciences, Fisheries and Economics, UiT-The Arctic University of Norway, Tromsø, Norway, ⁴ Hjort Centre for Marine Ecosystem Dynamics, Uni Research Environment, Bergen, Norway

OPEN ACCESS

Edited by:

Connie Lovejoy,
Laval University, Canada

Reviewed by:

David J. Scanlan,
University of Warwick, UK
William Li,
Fisheries and Oceans Canada,
Canada

*Correspondence:

Maria L. Paulsen
maria.l.paulsen@uib.no

Specialty section:

This article was submitted to
Aquatic Microbiology,
a section of the journal
Frontiers in Marine Science

Received: 28 June 2016

Accepted: 21 September 2016

Published: 05 October 2016

Citation:

Paulsen ML, Doré H, Garczarek L,
Seuthe L, Müller O, Sandaa R-A,
Bratbak G and Larsen A (2016)
*Synechococcus in the Atlantic
Gateway to the Arctic Ocean.*
Front. Mar. Sci. 3:191.
doi: 10.3389/fmars.2016.00191

Increasing temperatures, with pronounced effects at high latitudes, have raised questions about potential changes in species composition, as well as possible increased importance of small-celled phytoplankton in marine systems. In this study, we mapped out one of the smallest and globally most widespread primary producers, the picocyanobacterium *Synechococcus*, within the Atlantic inflow to the Arctic Ocean. In contrast to the general understanding that *Synechococcus* is almost absent in polar oceans due to low temperatures, we encountered high abundances (up to 21,000 cells mL⁻¹) at 79°N, and documented their presence as far north as 82.5°N. Covering an annual cycle in 2014, we found that during autumn and winter, *Synechococcus* was often more abundant than picoeukaryotes, which usually dominate the picophytoplankton communities in the Arctic. *Synechococcus* community composition shifted from a quite high genetic diversity during the spring bloom to a clear dominance of two specific operational taxonomic units (OTUs) in autumn and winter. We observed abundances higher than 1000 cells mL⁻¹ in water colder than 2°C at seven distinct stations and size-fractionation experiments demonstrated a net growth of *Synechococcus* at 2°C in the absence of nano-sized grazers at certain periods of the year. Phylogenetic analysis of *petB* sequences demonstrated that these high latitude *Synechococcus* group within the previously described cold-adapted clades I and IV, but also contributed to unveil novel genetic diversity, especially within clade I.

Keywords: picocyanobacteria, picoeukaryotes, temperature adaptation, *petB* sequences, flow cytometry, high latitude ecosystems, Svalbard, West Spitsbergen Current

INTRODUCTION

The widely abundant picocyanobacterium *Synechococcus* is estimated to be responsible for about 17% of ocean net primary productivity and thus to have a high impact on ocean ecosystems and biogeochemical cycles (Flombaum et al., 2013). *Synechococcus* is normally not considered to be bloom-forming even though they can appear in abundances as high as 1.2–3.7 × 10⁶ cells mL⁻¹ in the Costa Rica dome (Saito et al., 2005). Using 37,699 discrete global *Synechococcus* observations between 69°S and 81°N and quantitative niche models, Flombaum et al. (2013) demonstrated temperature to be the main environmental parameter explaining the global distribution of *Synechococcus*. Accordingly, the regional range of temperature was found to be a relatively good predictor for the seasonal change in *Synechococcus* abundance (Tsai et al., 2013). Although the

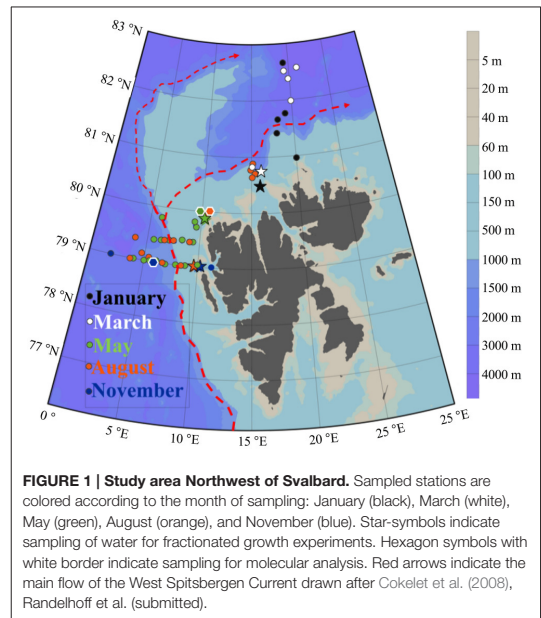
marine *Synechococcus* that have been studied in culture so far have a temperature optimum ranging from 20 to 33°C depending on the clade (Pittera et al., 2014), the highest annual average *in situ* cell abundances were found at temperatures around 10°C in the Indian and western Pacific Oceans, with averages of 34,000 and 40,000 cells mL⁻¹, respectively (Flombaum et al., 2013).

There has been observations of *Synechococcus* at low temperatures e.g., <4°C in low numbers (<100 cells mL⁻¹; Waterbury et al., 1986) and <2°C (Shapiro and Haugen, 1988; Gradinger and Lenz, 1995), but they are still often considered to be nearly absent from the polar ocean (Pedrós-Alió et al., 2015) in contrast to cold adapted eukaryotic picophytoplankton that occur in high abundances both in Arctic (Sherr et al., 2003; Lovejoy et al., 2007; Tremblay et al., 2009; Zhang et al., 2015) and in Antarctic waters (Doolittle et al., 2008). Only a few studies have actually documented *Synechococcus* north of 70° and none have so far described the genetic diversity of these northern populations or tested their temperature optimum.

During four expeditions Gradinger and Lenz (1995) observed maximal abundances of 5500 *Synechococcus* cells mL⁻¹ in the Atlantic inflow to the Arctic Ocean west of Svalbard at 78°N, while they did not find any *Synechococcus* cells in surface samples of polar water (defined as water having Temp < 0°C; Salinity < 34). Further south, following a transect from 70.5 to 74°N, Not et al. (2005) recorded a maximum abundance of 25,000 cells mL⁻¹ in the Norwegian and Barents Seas in August 2002. In the western Canadian Arctic, Cottrell and Kirchman (2012) found abundances of 40–80 cells mL⁻¹ in coastal waters of the Chukchi Sea and the Beaufort Sea at 71.5°N, both during summer and winter cruises. Nelson et al. (2014) concluded in their overview that the *Synechococcus* distribution in this region is controlled mainly by inflow of the relatively warm Pacific water, but argue that water temperature alone cannot be used to define environments in which *Synechococcus* may reside as they do persist at water temperatures near the freezing point (−1.8°C) (Nelson et al., 2014).

Synechococcus is often found in Arctic lakes and rivers, and freshwater runoff may thus also represent a source of *Synechococcus* cells to the Arctic Ocean (Vincent et al., 2000). Using 16S rRNA analysis, Waleron et al. (2007) revealed that picocyanobacteria present in the Canadian Beaufort Sea originate from the Mackenzie River and other nearby inflows. High abundances of *Synechococcus* (30,000 cells mL⁻¹) were also found in the Laptev Sea, but were restricted to brackish waters near the Lena River delta, while further away from the delta, abundances decreased with increasing salinity to a total absence at salinities >20 (Moreira-Turcq and Martin, 1998). All these studies support Waterbury et al. (1986) claiming that only few brackish species tolerate wide salinity ranges and that many strains are obligate marine. Assuming that Atlantic *Synechococcus* have a low tolerance to salinity changes, the question remains whether the low salinity in the Arctic surface waters constrains their distribution in the polar ocean.

The Atlantic inflow is the main conveyor, not only of water and heat, but also of more southern species into the Arctic Ocean. *Synechococcus* has accordingly been suggested as a bio-indicator for the advection of Atlantic waters into the Arctic Ocean



(Murphy and Haugen, 1985; Gradinger and Lenz, 1995). The main transport follows the West Spitsbergen Current (WSC) which is an extension of the Norwegian Atlantic Current splitting up into two branches around 79–80°N (Figure 1). The WSC is about 100 km wide and is confined over the continental slope along the Norwegian coast. It has an average speed of 10 cm s⁻¹ (Cokelet et al., 2008) but can reach a speed of up to 24–35 cm s⁻¹ (Boyd and D’Asaro, 1994; Fahrback et al., 2001). The inflow follows a strong annual cycle with maximum volume transport during winter (20 Sv in February) and minimum during summer (5 Sv in August, Fahrback et al., 2001) (N.B. the unit sverdrup (Sv) is equal to 1 million m³ s⁻¹). Strong variations in the strength of the Atlantic inflow combined with varying sea ice extension make it challenging to assess the spread of Atlantic organisms in this area. Little is known about how *Synechococcus* populations, originating from the Norwegian coast or further south, are affected as they are transported into the Arctic Ocean or whether some *Synechococcus* lineages are favored under the transition to more Arctic conditions.

Temperature is one of the main drivers of *Synechococcus* biogeography. Among the five globally dominating *Synechococcus* lineages (clades I, II, III, IV, and CRD1), clades I and IV dominate at high latitudes in cold and coastal waters, while clades II and III are mostly found in warm, (sub)tropical areas (Zwirgmaier et al., 2008; Farrant et al., 2016; Sohm et al., 2016). Populations adapted to distinct thermal niches were also identified within the CRD1 clade, including one co-occurring with clade I and IV in cold, mixed waters of the Pacific Ocean (Farrant et al., 2016).

Increasing ocean temperature in high latitude systems has drawn attention towards the growth of invasive organisms with higher temperature optima and subsequent ecosystem changes. In marine systems, small phytoplankton are expected to become relatively more abundant with warming (Morán et al., 2010; Tremblay et al., 2012) and it has been speculated that the warming of the Arctic Ocean could lead to a shift from picoeukaryotes to picocyanobacteria, with implications for food quality (Vincent, 2010). Flombaum et al. (2013) projected up to a 50% increase in *Synechococcus* at 60°N by the end of the twenty first century. Their models were however not able to make projections for higher latitude systems because observations in these areas are scarce. The aim of the present study is therefore to examine the distribution of *Synechococcus* in relation to environmental parameters and other microbial plankton groups within the Atlantic gateway to the Arctic. The genetic diversity of *Synechococcus* populations was also unveiled using a high resolution genetic marker, the *petB* gene (encoding the cytochrome *b₆* subunit), in order to trace the geographical origin and seasonal changes of these populations.

MATERIALS AND METHODS

Locality and Sampling

This study covers the eastern part of the Fram Strait, where Atlantic water (AW) is transported northward by the West Spitsbergen Current (WSC). Data were collected during five cruises in 2014: January (06.01–15.01), March (05.03–10.03), May (15.05–02.06), August (07.08–18.08), and November (03.11–10.11). Transects were made across the core of AW inflow at 79 and 79.4°N during May, August and November. Further north (80.5 to 82.6°N) we investigated the WSC southern branch into the Arctic Ocean in January, March and August (Figure 1). The choice of sampling area and stations was largely determined by the extension of the sea ice (Figure 3). Vertical profiles of temperature, salinity and fluorescence were recorded on each sampling occasion using a SBE 911plus system. Water masses were defined based on the criteria presented in Table 1. Discrete water samples for analyses of nutrients ($\text{NO}_2^- + \text{NO}_3^-$, NH_4^+ , PO_4^{3-} , H_4SiO_4) and enumeration of phytoplankton, viruses, bacteria, and heterotrophic nanoflagellates (HNF) were collected from 11 depths (1, 5, 10, 20, 30, 50, 100, 200, 500, 750, and 1000 m) using 10 L Niskin bottles. During the summer cruises we collected additional samples from the Deep Chlorophyll Maximum (DCM) (when different from any of the standard depths). The shallow shelf stations were sampled to near bottom and with higher sampling resolution in the surface.

Flow Cytometry

Abundances of pico- and nano-sized phytoplankton, viruses, bacteria and HNF were determined on an Attune[®] Acoustic Focusing Flow Cytometer (Applied Biosystems by Life technologies) with a syringe-based fluidic system and a 20 mW 488 nm (blue) laser. Samples were fixed with glutaraldehyde

TABLE 1 | Criteria determining the water masses.

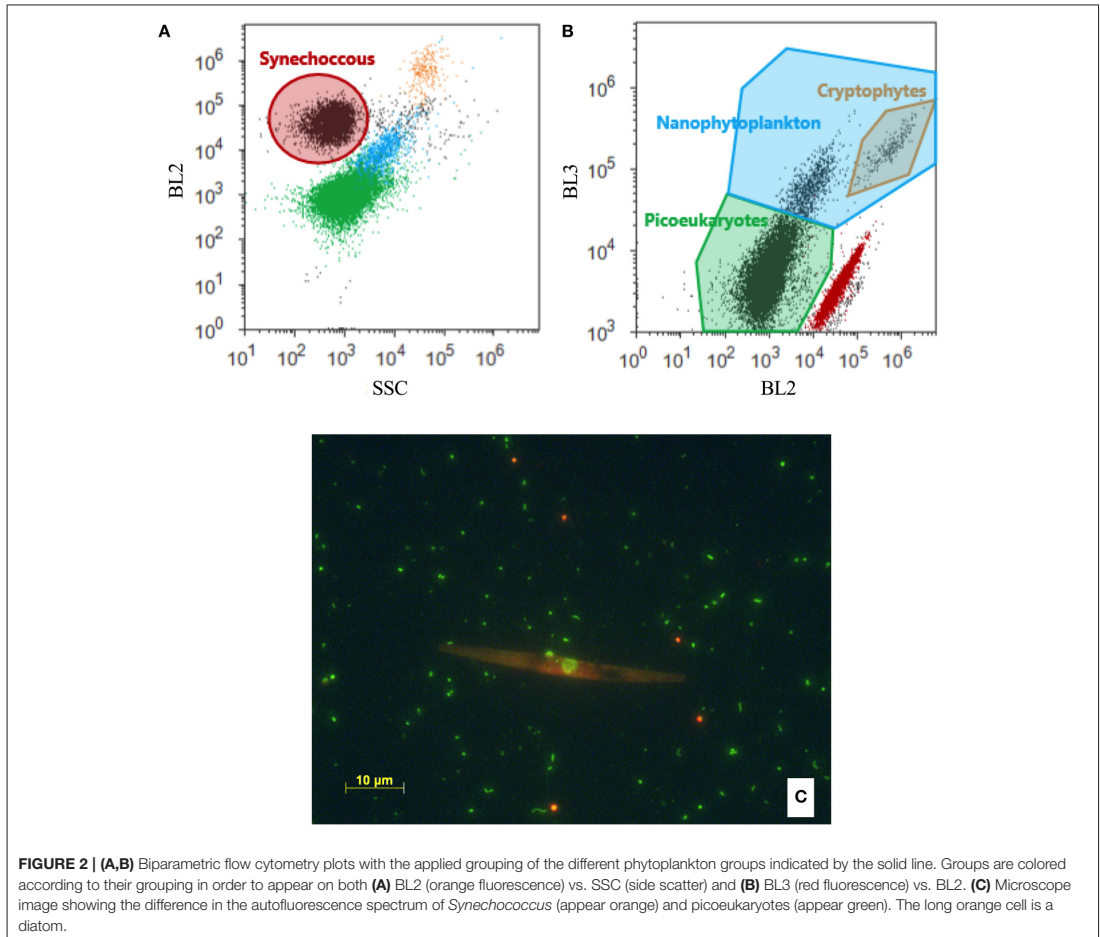
Water masses	Temperature (°C)/or density (kg m^{-3})	Salinity
Atlantic water (AW)	>2°C	>34.9
cold Atlantic water (cAW)	0<T<2°C	>34.9
Intermediate water (IW)	<0°C	>34.9
Arctic water (ArW)	>27.7 kg m^{-3}	<34.9
Surface water (SW)	<27.7 kg m^{-3}	<34.9
Polar water (PW)	<0°C	<34.7

For further explanation see Cokelet et al. (2008). PW overlaps with SW and ArW.

(0.5% final conc.) at 4°C for a minimum of 2 h, flash frozen in liquid nitrogen and stored at –80°C until analysis, except in November, when phytoplankton was enumerated using fresh samples. For analysis of HNF the samples were stained with SYBR Green I (Molecular Probes, Eugene, Oregon, USA) for 2 h in the dark and a minimum of 1 mL was measured at a flow rate of 500 $\mu\text{l min}^{-1}$ following the protocol of Zubkov et al. (2007). The HNF population was discriminated from nano-sized phytoplankton based on green vs. red fluorescence and from large bacteria on a plot of side scatter vs. green fluorescence following the recommendations of Christaki et al. (2011). Pico- and nano-sized phytoplankton were counted directly after thawing and the various groups discriminated based on their side scatter signals (SSC) vs. orange fluorescence (Figure 2A; Marie et al., 1997; Larsen et al., 2001) as well as their red vs. orange fluorescence (Figure 2B). *Synechococcus* was identified in plots of orange fluorescence vs. side scatter signals (Figure 2A). For samples with low abundance of phytoplankton (March and January) a volume of 1.5 mL was counted, while 0.5 mL was sufficient for May, August and November-samples. Regular blank measurements using Milli-Q[®] water were made to ensure that there was no carry over of cells between samples and that electronic noise did not disturb the counts. Due to the inherent uncertainty connected to enumeration of cells when concentrations are low, we only included samples with > 20 cells mL^{-1} when relating counts to other environmental parameters (Figure 5). Samples for which 0–20 cells were detected (i.e., mainly those deeper than 500 m) are included in our total data set (Table S1, Figure S2).

Microscopy

The presence of *Synechococcus* was also confirmed by fluorescence microscopy (Figure 2C). Samples were fixed and stored as for flow cytometry. The samples were thawed, filtered onto Anodisc filters (Whatman, pore size 0.2 μm) and stained with SYBR Green I (Molecular Probes Inc., Eugene, Oregon) according to Patel et al. (2007). The samples were viewed and photographed at 400X using a Zeiss Axio Imager Z1 microscope with AxioCam MRm BW-camera, extended focus, epifluorescence illumination (HXP Illuminator) and Zeiss filter sets 09 and 43 for SYBR Green and chlorophyll fluorescence, respectively.



Size-Fractionated Growth Experiments

Water fractionation experiments were used to examine interaction between different size groups of microorganisms and to estimate growth rates of the different microbial components (Simek and Chrzanowski, 1992; Jürgens et al., 2000; Christaki et al., 2001; Sato et al., 2007). Experiments were performed once every cruise using water collected from 20 m (in August and May this depth was near DCM) at stations on the shelf (marked on **Figure 1**). The water was gently screened through 3, 5, 10, and 90 μm mesh size filters by reverse filtration in order to successively exclude grazers of different sizes and thus create communities with increasing “top-predators” sizes. Water from each filtration treatment was gently transferred into triplicate 3.9 L transparent polycarbonate bottles (Nalgene[®]) by staggered filling using silicone tubing. The incubation experiments ran for 5 to 10 days but we show data only from

the initial 5 days of incubation in order to better represent dynamics of the initial communities. Incubation water was sampled daily for enumeration of microorganisms and every second day for nutrients. Prior to setup, all bottles, carboys and silicon tubs were acid washed and then rinsed with Milli-Q[®] water. During the summer cruises (May and August) the experimental bottles were incubated on deck in plexiglass tanks with seawater flow-through (continuously pumped from 7 m depth), keeping the temperature close to *in situ* (May: $1.7 \pm 1.6^\circ\text{C}$ and August: $1 \pm 0.8^\circ\text{C}$). A nylon net was wrapped around each bottle to reduce the PAR to about 30% of the surface irradiation. In the winter months (January, March, November), incubations were kept in a cooling room at a constant temperature of 2°C and in darkness, except in March were an *in situ* light cycle was set (16 h darkness and 8 h at $5 \mu\text{mol photons m}^{-2} \text{ s}^{-1}$). The fractionation experiments

provided net growth rates of *Synechococcus* and HNF by fitting exponential functions to the change in the abundance of cells every 24 h during the first 5 days of the experiments (Figure S1).

DNA Extraction, PCR Cloning and Phylogenetic Analysis

Environmental samples for molecular analysis were collected by filtering water onto 0.22 μm pore size Millipore® Sterivex filters. The filters were immediately flash frozen in liquid nitrogen and stored at -80°C until extraction. DNA and RNA were extracted simultaneously using the AllPrep DNA/RNA Mini Kit (Qiagen, Hilden, Germany) according to manufacturer's instructions with some optimisation for extraction from Sterivex filters as follows. The filters were thawed on ice and 1 mL extraction buffer (990 μL RLT buffer; containing guanidine isothiocyanate + 10 μL β -mercaptoethanol) was added before incubating for 4 min on a Vortex adapter at medium speed. The resulting lysates were recovered using a 10 mL syringe and used for nucleic acids extraction. DNA samples harvested from Arctic surface water collected in May (80°N , 10.7°E at 1 m depth, 10 L water filtered), August (80°N , 10.8°E at 1 m, 7.5 L filtered) and November (79°N , 6°E , 20 m, 20 L filtered) were selected to amplify the *Synechococcus petB* marker gene (stations marked on Figure 1 and profiles of picophytoplankton are included in Figure S2). Polymerase chain reaction (PCR) were performed using the *petB* primers and set-up recommended by Mazard et al. (2012) using 30–40 amplification cycles (iCycler, Bio-Rad, CA, USA). Positive PCR products were purified using the Zymo DNA Clean and Concentrator™.5 kit (Zymo research, CA, USA) and subsequently cloned with the StrataClone™ PCR Cloning Kit (Agilent Technologies, CA, USA) following the manufacturer's instructions. A total of 96 clones from each of the three samples were picked (total 288 clones) and sequenced by LCG Genomic GmbH (Berlin, Germany) using Sanger sequencing. A total of 229 *petB* sequences were obtained and deposited in the GenBank database (accession no. KX345947–KX346174). These sequences are in the following referred to as “MicroPolar sequences.”

The 229 MicroPolar sequences include 174 unique full-length sequences. Together with 721 *petB* sequences from a non-redundant reference database (representing most of the genetic diversity so far identified within *Prochlorococcus* and *Synechococcus* genera; Farrant et al., 2016), the MicroPolar sequences were used to define operational taxonomical units (OTUs) at 97% identity using Mothur v1.34.4 (Table S2). Since all MicroPolar sequences clustered with clades I and IV reference sequences, a subset of the *petB* database, comprising only the 117 reference sequences of these clades, as well as the 174 unique MicroPolar *petB* sequences was used for a subsequent analysis. Phylogenetic reconstructions were based on multiple alignments of *petB* nucleotide sequences generated using MAFFT v7.164b with default parameters (Katoh and Standley, 2014). A maximum likelihood tree was inferred using PHYML v3.0, (Guindon and Gascuel, 2003) with the HKY + G substitution model, as determined using jModeltest v2.1.4 (Darrriba et al., 2012) and estimation of the gamma distribution parameter of the

substitution rates among sites and of the proportion of invariable sites. The tree was drawn using iTOL (Letunic and Bork, 2007). The 229 sequences retrieved from MicroPolar were recruited using BLASTN (v2.2.28+) against the full *petB* database: reads with more than 90% of their sequence aligned and with more than 80% sequence identity to their BLASTN best-hit were taxonomically assigned to their best-hit and subsequently used to build per-sequence read counts tables. Counts were then aggregated by OTUs and relative abundance was computed for each MicroPolar station.

Nutrients

Unfiltered seawater was filled directly from the Niskin bottles into 30 mL acid washed HDPE bottles and stored at -20°C . Nitrite and nitrate ($\text{NO}_2^- + \text{NO}_3^-$), phosphate (PO_4^{3-}) and silicic acid (H_4SiO_4) were measured on a Smartchem200 (by AMS Alliance) autoanalyser following procedures as outlined in Wood et al. (1967) for $\text{NO}_3^- + \text{NO}_2^-$, Murphy and Riley (1962) for PO_4^{3-} and Koroleff (1983) for the determination of H_4SiO_4 . The determination of NO_3^- was done by reduction to NO_2^- on a built-in cadmium column, which was loaded prior to every sample run. Seven-point standard curves were made prior to every run. Two internal standards and one blank were inserted for every 8 samples and these were used to correct for any drift in the measurements. Concentration of NH_4^+ was determined directly in fresh samples using ortho-phthalaldehyde according to Holmes et al. (1999).

RESULTS

Synechococcus cells were detected by flow cytometry in all samples within the upper 100 m of the water column during all seasons (Figure 3 and Figure S2). The identity of *Synechococcus* was confirmed by epifluorescence microscopy (Figure 2C) and by sequencing of the *petB* gene (Figure 7). The closely related genus *Prochlorococcus* was never detected.

Synechococcus Distribution

The highest sampling frequency was obtained in May and August, when the sampling sites were restricted to latitudes below 80°N (May) and 81°N (August) by sea ice (Figure 3), while the most northern samples were acquired in January and March at around 82.5°N . *Synechococcus* was present in abundances higher than 50 cells mL^{-1} in 337 samples both within the Atlantic water, Arctic water, Surface water and Polar water (water mass definitions are shown in Table 1). Within the cold surface water ($<2^{\circ}\text{C}$, upper 50 m), 60% of the samples contained *Synechococcus* with abundances ranging from 50 to 4300 cells mL^{-1} . *Synechococcus* was not detected in the cold Atlantic water or intermediate water masses, which comprise water collected deeper than 500 m (see temperature-salinity plots in Figure 3).

In January, the average abundance in the upper 100 m was 51 cells mL^{-1} , with highest abundance found at 100 m depth (maximum 106 cells mL^{-1}) and generally low numbers in the surface (Figures 3F, 4A). The lowest average abundance of

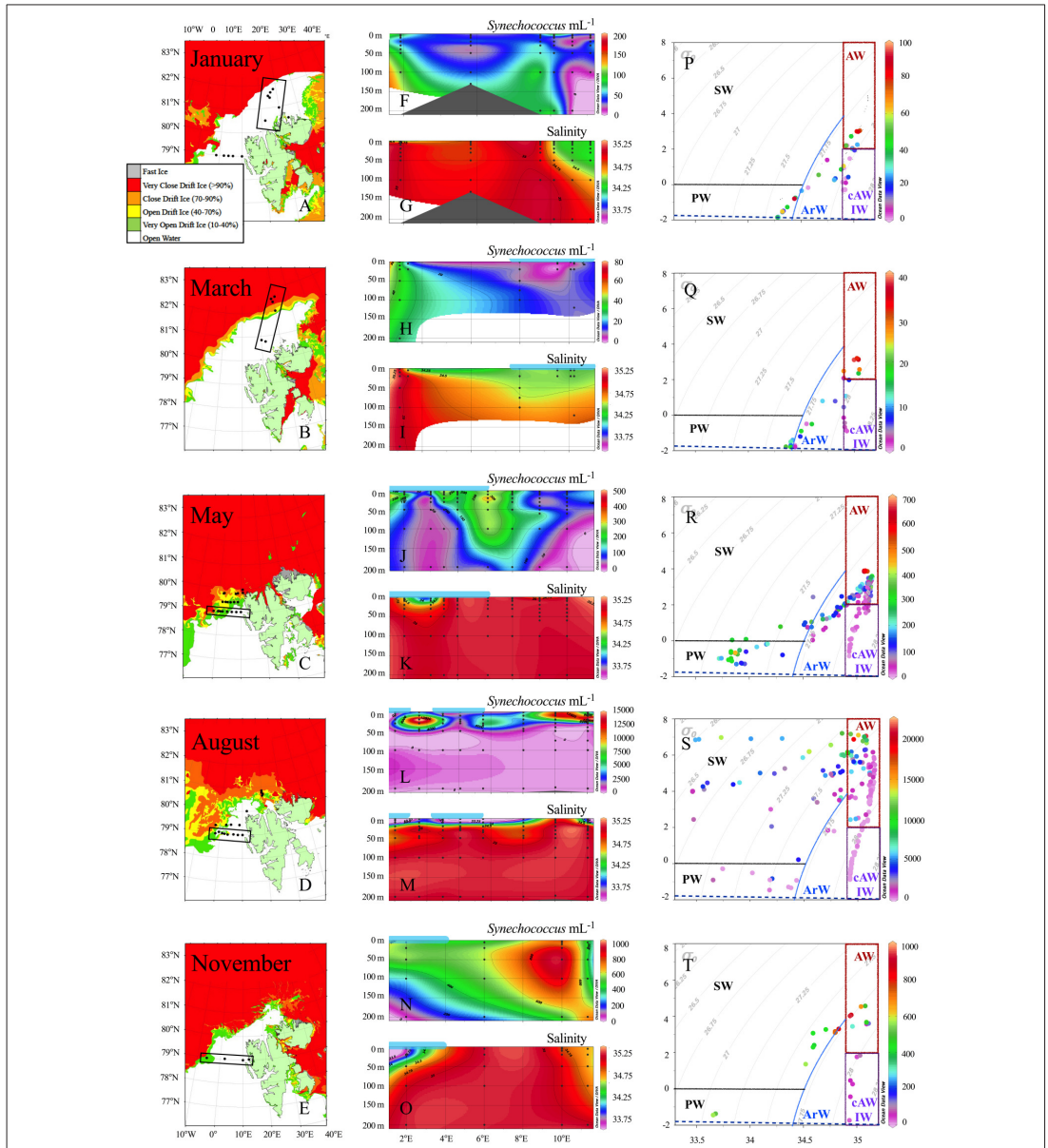


FIGURE 3 | (Left panel) Ice-maps provided from the Norwegian Meteorological Institute (istjenesten@met.no) from following dates; January 10, March 7, May 23, August 12, and November 7, 2014. Transects shown in the middle panel as contour plots are marked with black boxes. **(Middle panel)** Contour plots showing the abundance (cells mL^{-1}) of *Synechococcus* and salinity of the upper 200 m from 4 cruises. January transect stretches from North-South between 15 and 20°E, while the remaining transects expands West-East (2–11°E) following the 79°N latitude isoline (see transect marked in boxes left of plots). The horizontal light blue lines above the plots roughly mark the cover of open drift ice. Note different scales for *Synechococcus* abundance. **(Right panel)** Potential temperature and salinity (TS) diagram for each month. Data included for all depths 1–1000 m. *Synechococcus* abundance is given on the z-axis by color gradient (N.B. different scales). Potential density (σ_t , kg/m^3) isolines overlaid with gray and the surface freezing line is show in dashed blue. Following water masses (**Table 1**) are marked: Atlantic water (AW), cold Atlantic water or Intermediate water (cAW or IW), which consist mainly of deep water samples (>500 m), Arctic water (ArW), surface water (SW) and Polar water (PW).

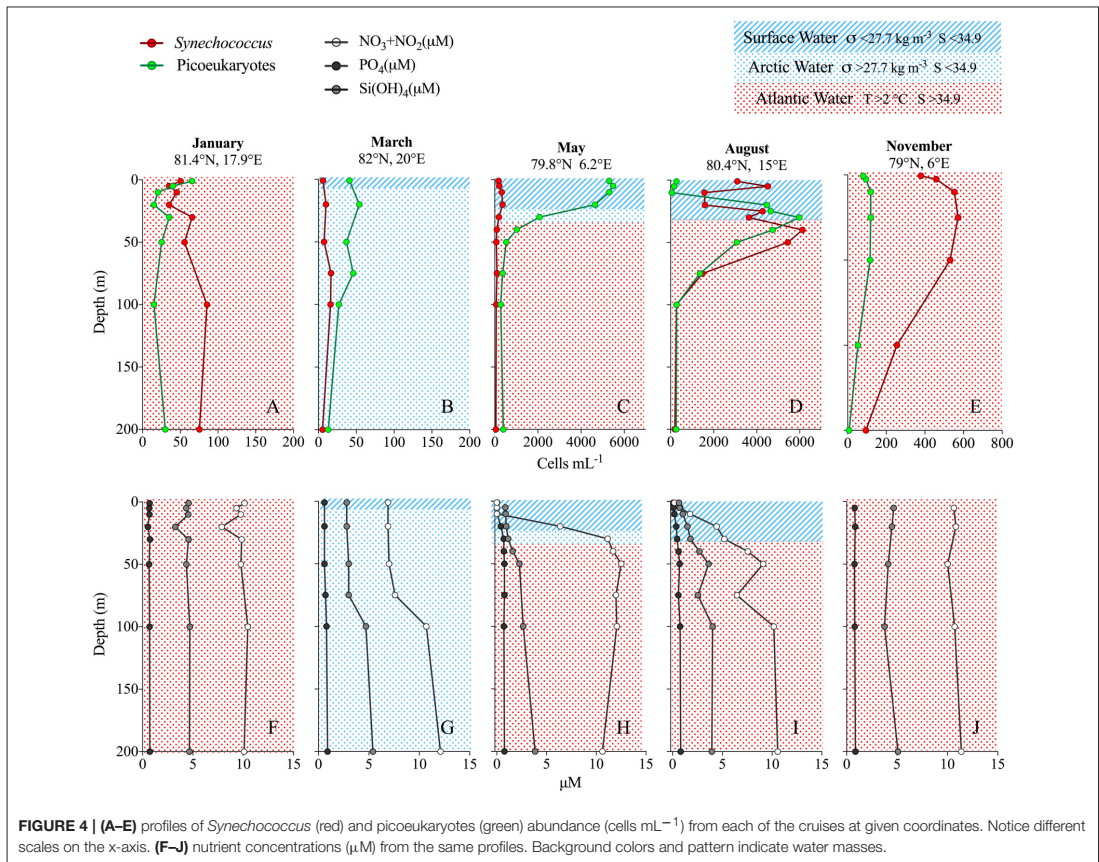
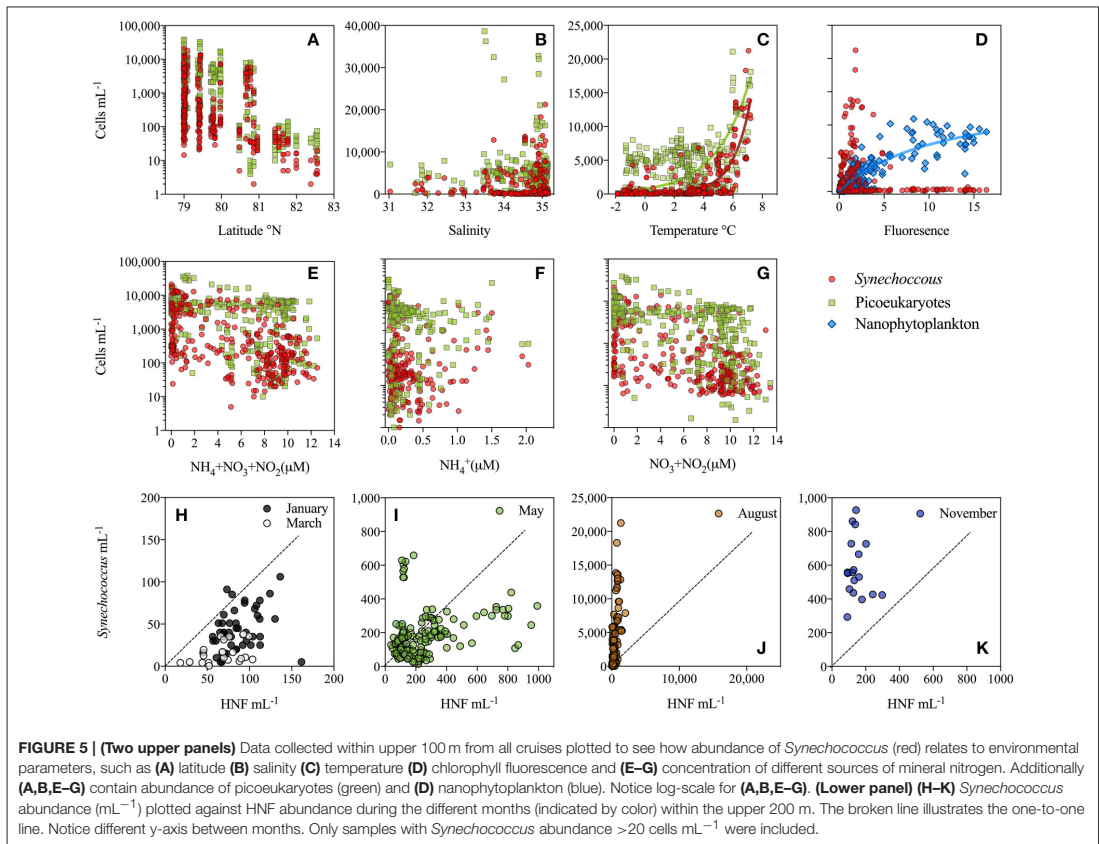


FIGURE 4 | (A–E) profiles of *Synechococcus* (red) and picoeukaryotes (green) abundance (cells mL⁻¹) from each of the cruises at given coordinates. Notice different scales on the x-axis. **(F–J)** nutrient concentrations (μM) from the same profiles. Background colors and pattern indicate water masses.

Synechococcus was found in March with 13 cells mL⁻¹ and a maximum abundance that did not exceed 40 cells mL⁻¹ (Figures 3H, 4B). In May the maximum abundance was around 1300 cells mL⁻¹ and the average \pm SD was 181 ± 147 cells mL⁻¹ ($n = 150$; Figures 3J, 4C). The highest *Synechococcus* abundances were detected in August with a maximum of 21,300 cells mL⁻¹. When averaged for the upper 50 m at most southern stations (79–79.4°N), abundances were 5700 ± 4200 cells mL⁻¹ ($n = 61$) (Figure 3L) over the whole transect, while abundances at the stations north of 80°N averaged to about 3000 ± 2000 cells mL⁻¹ ($n = 27$). In November *Synechococcus* cells were evenly distributed down to 200 m (Figure 4E), with a maximum of 1000 cells mL⁻¹ and an average abundance of 600 ± 250 cells mL⁻¹ ($n = 18$) within the upper 200 m. The vertical distribution of *Synechococcus* varied from mainly surface peaks in May (upper 20 m) to maximum abundance at depths greater than 50 m in August and November, to a more vertically uniform distribution in January and March with maxima in abundance at around 100 m depth (Figures 4A–E and Figure S2).

Biotic and Abiotic Environment

The association between phytoplankton abundances and environmental parameters showed that the abundance of both *Synechococcus* and picoeukaryotes decreased with increasing latitude, but that picoeukaryotes were relatively more abundant at the northernmost stations (Figure 5A). No clear relationship was found for salinity (ranging from 31 to 35 in this study), although the highest *Synechococcus* abundances were found at salinities >34.5, while picoeukaryotes had their peak abundance at lower salinities of 33.5–34 (Figure 5B). Further, we found picoeukaryotes to be strongly dominant over *Synechococcus* in 14 out of 17 samples with lowest salinity (31–33), all sampled in August. The abundance of *Synechococcus* ranged from 250 to 4000 cells mL⁻¹ in these low salinity samples (Figure 3S). The presence of sea ice had no clear effect on the vertical distribution of picophytoplankton but at the ice-covered stations, a subsurface maximum of *Synechococcus* was most prominent. On the other hand, picoeukaryotes tended to peak near surface in ice-covered stations in March and May, while in August the highest surface



maximum of picoeukaryotes was found within the freshwater lens at stations without ice-cover (Figure S2).

The highest water temperatures were measured in August followed by those measured in January. The lowest surface temperatures were recorded in the ice-influenced surface waters in March and May. Temperature was the only parameter that displayed a strong relationship with *Synechococcus* abundance resulting in an exponential fit ($r^2 = 0.66$, $p < 0.005$, $n = 346$; Figure 5C), while picoeukaryotes did not show a similar strong relationship ($r^2 = 0.31$, $p < 0.005$, $n = 372$; Figure 5C). *Synechococcus* was more dominant at stations with low chlorophyll *a* (i.e., chl *a* fluorescence) compared to larger nanophytoplankton, which correlated positively to chl *a* (Figure 5D).

Nutrients were evenly distributed over the upper 200 m in the winter months (January to November), although a slightly lower concentration was observed in March within the upper 100 m (Figures 4F,G,I). In May and August all nutrients were depleted in the upper 10–20 m, with NO_3^- reaching the lowest values (Figures 4H,I). NH_4^+ reached

the highest values around $2 \mu\text{M}$ in August at depths below 20 m. At high N concentrations ($>2 \mu\text{M}$; Figure 5E) *Synechococcus* were generally less abundant than picoeukaryotes, while under low N conditions they were equally numerous. When looking at the N sources separately it appears that at $\text{NH}_4^+ > 0.5 \mu\text{M}$, *Synechococcus* increased at higher NH_4^+ levels, whereas they decreased with increasing $\text{NO}_3^- + \text{NO}_2^-$ (Figures 5F,G).

The abundance of HNF increased during the summer months, from less than 200 cells mL^{-1} in the winter months up to 1000 and 1500 HNF mL^{-1} in May and August, respectively (Figures 5H–K). *Synechococcus* and HNF abundances generally showed a positive relationship within the upper 100 m. In January and March, *Synechococcus* and HNF cell numbers were within the same order of magnitude, but with slightly more HNF than *Synechococcus* (i.e., below the dotted line; Figure 5H). In May highest *Synechococcus* abundances were found at the lowest HNF abundance and vice versa (Figure 5I). In August, *Synechococcus* was generally 10 times more abundant than HNF, a trend also observed in November, although less pronounced (Figures 5J,K).

Growth and Microbial Interactions

Net-growth rates of *Synechococcus* and HNF were estimated from four different size fractions (<3, <5, <10, and <90 μm) from each of the five cruises and summarized in **Figure 6** (for abundances during incubation see **Figure S1**). *Synechococcus* showed positive net growth in 9 out of 20 experiments mainly in January and March. Positive growth rates ranged from 0.01 to 0.13 d^{-1} . HNF showed positive growth in 14 out of 20 experiments, displaying a maximum growth rate of 0.45 d^{-1} when water was filtered through a $5 \mu\text{m}$ mesh (Treat < $5 \mu\text{m}$) in January, otherwise the highest HNF growth rates were measured in May ranging from 0.13 to 0.3 d^{-1} . In January, November, and August HNF growth was reduced to zero after filtering in the Treat < $90 \mu\text{m}$ and in March HNF showed negative growth in all treatments. *Synechococcus* showed positive growth in January, March in all size-fractions and in the Treat < $90 \mu\text{m}$ in May, which became strongly dominated by *Phaeocystis* sp. and where both HNF, picoeukaryotes and heterotrophic bacteria increased in abundance simultaneously. *Synechococcus* had the strongest negative growth in August and in the Treat < $3 \mu\text{m}$ in May (**Figure 6**). In summary, we measured a positive growth of *Synechococcus* and negative growth of HNF in March, but in general negative *Synechococcus* and positive HNF growth in May, August, and November. Only in January and in the May < $90 \mu\text{m}$ treatment, both *Synechococcus* and HNF displayed positive net growth. Corresponding to the seasonal changes in abundance (**Figures 5H–K**) the prey:HNF ratio (prey being the sum of all picoplankton; *Synechococcus* + picoeukaryotes + heterotrophic bacteria) of the initial community was highest in May i.e., most prey per HNF grazer and lowest in August, when HNF were more abundant. Generally, the maximum growth rates of *Synechococcus* were found when prey:HNF was at its highest (**Figure S1**).

Synechococcus Diversity

The gene *petB*, which has proved to display a high taxonomic resolution for picocyanobacteria (Mazard et al., 2012), was used as phylogenetic marker for *Synechococcus* genetic diversity. Only *petB* sequences related to clade I and IV were retrieved from our dataset (MicroPolar). Based on a *petB* reference database (including 117 sequences from clade I and IV, described in Farrant et al., 2016), enriched with the 174 unique *petB* sequences retrieved from MicroPolar samples, 41 OTUs were defined at 97% ID within clade I and IV (**Figure 7**). The *petB* sequences obtained in the present study correspond more specifically to sub-clades Ib and IVb, with a clear dominance of subclade Ib. Although none of these 41 OTUs form a new subclade, 17 OTUs were composed of only MicroPolar sequences and were not represented in the previous reference database (colored branches, **Figure 7**). In May sub-clade Ib was the only one present, whereas subclade IVb appeared in August and increased in relative abundance in November, indicating seasonal changes in the community composition. Seasonality was also found within subclade Ib. The majority of sequences obtained in August and November belonged to two specific OTUs (Arctic732-2b_Ib_IA and Arctic732-35b_Ib_IA), which mostly gather reference sequences from the Barents Sea (“Arctic,”

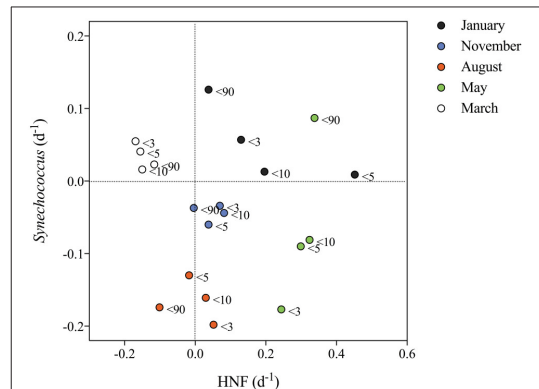
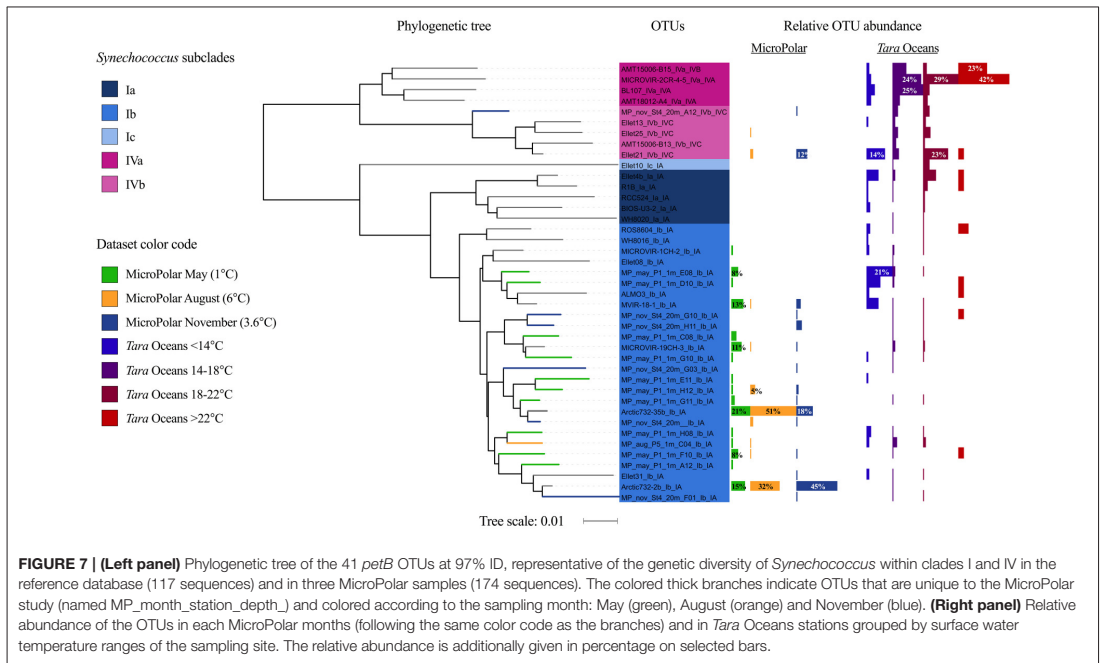


FIGURE 6 | Net growth rates (d^{-1}) of *Synechococcus* plotted against HNF net-growth. Net growth rates are obtained from the fractionation experiments from each cruise where an exponential growth curve was fitted to the change in abundance of the respective cells during a 5-day period (**Figure S1**). The color indicates the month and the legend at each point indicates the size-fraction treatment from which the values were obtained.

72.5°N , 19.57°W) and the North Atlantic Ocean (The Extended Ellett Line; “EEL” $57\text{--}63^\circ\text{N}$). In contrast, sequences retrieved from samples harvested in May were more evenly distributed over all other OTUs defined within subclade Ib that mainly gather sequences from The Atlantic Meridional Transect (“AMT,” <http://www.amt-uk.org/>) and the North Sea (“MICROVIR” cruise $50\text{--}60^\circ\text{N}$).

In order to assess whether the genetic populations sampled in MicroPolar cruises could be related to other cold-water populations, we also recruited Illumina reads from 62 surface water metagenomes collected during the Tara Oceans cross-ocean ecosystem study using the same *petB* database (Karsenti et al., 2011; Farrant et al., 2016) (<https://doi.pangaea.de/10.1594/PANGAEA.840718>, note that the Tara Oceans samples analyzed here do not include recent Arctic samples from the latest Tara Ocean cruise as they are not yet published). These data showed that the two most abundant MicroPolar OTUs in subclade Ib (Arctic732-2b_Ib_IA and Arctic732-35b_Ib_IA) had a low relative abundance in Tara Oceans stations. Other OTUs identified in MicroPolar samples were also poorly represented in the Tara Oceans dataset, with the notable exception of two subclade Ib OTUs, “MP_may_P1_1m_E08_Ib_1” and “MP_may_P1_1m_D10_Ib_IA” (formed only of MicroPolar sequences), that were dominant in Tara Oceans coldest stations ($<14^\circ\text{C}$), and of the subclade IVb OTU “Ellet21_IVb_IVC” present in the Tara Oceans dataset at all temperatures and especially at cold ($<14^\circ\text{C}$) and intermediate ($18\text{--}22^\circ\text{C}$) temperatures. Other MicroPolar OTUs were detected at a similarly low level in all temperature ranges of Tara Oceans stations.



DISCUSSION

Arctic Adaptation; *Synechococcus* vs. *Micromonas*

For the first time we here documented a high abundance of *Synechococcus* in the Atlantic gateway to the Arctic Ocean north of 79°N. *Synechococcus* is generally not thought to be part of the picophytoplankton community in Arctic water masses (e.g., Pedrós-Alió et al., 2015), which has repeatedly been found to be dominated by picoeukaryotes, such as *Micromonas* spp. (Not et al., 2005). Li et al. (2013) do document their existence in the Canadian Basin of the Arctic proper although as a very small fraction (2%) of the total picophytoplankton community at the only one station higher north than 70°. Arctic *Micromonas* spp. differ from *Micromonas* genotypes identified elsewhere in the World Ocean (Lovejoy et al., 2007), with these Arctic types being adapted to low temperatures. Similarly, by combining our observations with data from the *Tara* Ocean we confirmed the latitudinal shift previously described within the *Synechococcus* genus between the warm-adapted clades II and III and the cold-adapted clades I and IV (Zwirgmaier et al., 2008; Mazard et al., 2012; Farrant et al., 2016). Interestingly, clade IV was clearly dominating in Atlantic waters from the *Tara* Oceans dataset and its relative contribution seemed to increase with temperature in August and November in MicroPolar samples, while clade I appeared to dominate in colder Arctic waters. Thus, although this would need to be confirmed by physiological characterization of representative strains, it suggests that clade I could be adapted to

colder waters than clade IV. Overall, it seems that temperature is the main driver of *Synechococcus* abundance and diversity in this area.

In laboratory experiments using isolates from tropical sites, *Synechococcus* has been found not to grow at temperatures below 10°C (Mackey et al., 2013), even though they have been observed in nature at temperatures as cold as 2°C (Shapiro and Haugen, 1988), and 0°C (Gradinger and Lenz, 1995). Our deck incubation experiments showed that northern *Synechococcus* populations can actually grow at 2°C, although with a quite low growth rate (maximum of 0.13 d⁻¹), suggesting a physiological adaptation of Arctic populations to low temperatures that further supports the existence of *Synechococcus* thermotypes (Pittera et al., 2014). This hypothesis is strengthened by our findings that many MicroPolar sequences formed new OTUs, unveiling an important novel genetic diversity (especially within clade I), which seems to be specific to this geographic area (17 OTUs out of the 41 OTU identified within clades I and IV). Furthermore, sequences obtained from August and November are mainly found in two OTUs within subclade Ib, gathering reference sequences retrieved only at high latitude from the Barents Sea (72°N) and the North Atlantic Ocean (57°N), but hardly detected in the *Tara* Oceans dataset. Altogether, these results point toward the existence of *Synechococcus* populations endemic to these Arctic or subarctic areas.

The peak-values of *Synechococcus* were clearly associated with the Atlantic inflow (salinity > 34.9) and abundances decreased exponentially with decreasing temperature and were

most often low in ice-associated water. This, along with the tendency of decreasing concentrations with decreasing salinity, is in accordance with the suggestion of *Synechococcus* being an indicator of saline Atlantic water transported into the Arctic (Murphy and Haugen, 1985; Gradinger and Lenz, 1995) as well as the low tolerance to wide salinity ranges of obligate marine *Synechococcus* (Waterbury et al., 1986). It should also be noted that although *Synechococcus* peak abundances were found in the relatively warm, saline Atlantic water, equally high abundances were observed in discrete samples from non-Atlantic water masses throughout the year (Figure 3), indicating the potential of *Synechococcus* to adapt to cold, low saline water, as also suggested by Nelson et al. (2014) for Canadian Arctic *Synechococcus*. The observed maximum abundance of picoeukaryotes, on the other hand, was found at a salinity of 33.5 and they were in general less affected by low salinities than *Synechococcus*. The dominance of picoeukaryotes over *Synechococcus* in the Arctic region may thus be connected to their capacity to stand a wide range of salinities in addition to an adaptation to low temperature. As only a few of our samples had a low salinity (17 surface samples in August have salinity <33), more efforts are needed to confirm this trend. In the Canada Basin of the Arctic Ocean proper *Synechococcus* abundance of 60 cell mL⁻¹ was found at salinities substantially lower than 33 (Li et al., 2013).

The extreme changes in light conditions in polar environments may also have been a driver for the diversification of the *Synechococcus* populations. However, in contrast to *Prochlorococcus*, obvious light partitioning is usually not observed for *Synechococcus* (Scanlan et al., 2009) since only one study reported a vertical partitioning of some *Synechococcus* genotypes so far (Gutiérrez-Rodríguez et al., 2014). In our incubations *Synechococcus* surprisingly showed a net growth in January and March when light was absent or low, respectively, while picoeukaryotes did not grow (data not shown) (Figure 6). The ability of *Synechococcus* to grow under very low light conditions is presumably related to their capacity to consume dissolved organic matter (Palenik et al., 2003; Cottrell and Kirchman, 2009). Yelton et al. (2016) indeed found that the genetic potential for mixotrophy in picocyanobacteria (through osmotrophy) is globally distributed. Although this still needs to be confirmed by laboratory experiments, it is possible that *Synechococcus* OTUs detected in November, when there is no light, belong to mixotrophic populations that are adapted to slow growth in the dark. Picoeukaryotes may use another mixotrophic strategy, i.e., bacterial grazing, to sustain growth during dark months (Sanders and Gast, 2012). Our observations that *Synechococcus* can be more abundant than picoeukaryotes in the Arctic in autumn and winter (Figure 4) are consistent with previous results [Gradinger and Lenz, 1995; unpublished results from Adventfjorden, Svalbard (I. Kessel Nordgård, personal communication)] and may suggest that cyanobacterial osmotrophy is a more efficient strategy than picoeukaryotic phagotrophy to survive in the dark.

Grazing on *Synechococcus*

The highest *Synechococcus* abundances were observed when NO₃⁻ concentrations were low. Hence, there is no reason to believe that they were resource controlled. The tendency of

increased growth when potential grazers were removed, rather points at a top-down control. The all-year-round presence of heterotrophic flagellates (HNF), considered to be their main predators (Sanders et al., 1992; Christaki et al., 2001; Kuipers et al., 2003; Zwirgmaier et al., 2009) indeed allows for grazer control of the *Synechococcus* populations. Still, grazing losses of *Synechococcus* are challenging to estimate as potential grazers can include various nano—but also microzooplankton and the specific loss also depends on the presence of other prey types (i.e., bacteria and picoeukaryotes; Pernthaler, 2005). This is illustrated by the different outcomes of successively removing various grazer fractions, which in March, August and November did not result in different growth patterns, but in January and May led to higher growth rates of *Synechococcus* when organisms larger than 90 μm were removed (Figure S1). Thus, this may reflect a trophic cascade where the microzooplankton graze on HNF and thereby release picoplankton from grazing pressure in the <90 μm fraction. In March, August and November, however, there was little effect of size fractionation, which indicates that small HNF (<3 μm) were the main grazers of picoplankton and that these were not grazer-controlled themselves. Exactly “who” were the most important *Synechococcus* grazers is not possible to deduce from the presented data, and probably varies over the season. In addition, infection by viruses probably also functions as a top down regulator of these *Synechococcus* populations (Sandaa and Larsen, 2006), however virus counts remained relatively constant in all five experiments (data not shown). Still, we did find the highest net growth rates for *Synechococcus* when the HNF abundance was lowest (January and March) as well as the highest *Synechococcus* *in situ* abundance in water with low HNF concentration (and vice versa), which is in accordance with the view that HNF control their abundance and distribution at large. The picoeukaryote abundance did not follow the same patterns (data not shown), suggesting that they may have different predators. The fact that autotrophs, such as *Synechococcus* and picoeukaryotes, persist during winter in very low abundances further suggests that low encounter rates between predator and prey in the highly diluted wintry environment release the picophytoplankton from grazing pressure and allows survival despite adverse growth conditions (Kjørboe, 2008). The experiments also illustrate that *Synechococcus* in both January, March and August have the highest growth rates in the fractions where the total prey:HNF ratio is highest, indicating that *Synechococcus* might escape the grazers when other potential prey organisms are relatively abundant.

Synechococcus As an Active Player in the Arctic and Future Implications

It may be questioned whether the observed occurrence of *Synechococcus* was simply a result of advection and passive transport via the Atlantic water inflow. Since the highest measured abundances were found within the core of the Atlantic water, this probably represents the major source. The seasonal maximum *Synechococcus* abundance, which was observed in August, does however coincide in time with the seasonal *Synechococcus* bloom further south along the Norwegian coast. Given the average transportation time is at its minimum in summer (Fahrbach et al., 2001), it seems unlikely that the

encountered seasonal change in *Synechococcus* community we observed was a mere product of advection of Atlantic water. Moreover, the spatial and temporal distribution of clades and OTUs as well as the observed growth at low temperatures when released from grazing pressure, rather suggests that at least some of the observed *Synechococcus* populations are adapted to Arctic conditions and are indigenous to these waters.

Due to their small size ($1.1 \pm 0.4 \mu\text{m}$ diameter in the subarctic Atlantic; Paulsen et al., 2015), *Synechococcus* cells are largely grazed by HNF and microzooplankton (Christaki et al., 1999, 2005). This implies that their biomass production will be largely recycled in the microbial food web and thus be of minor contribution to higher trophic levels in the grazing food web. Even at the highest abundances observed in this study, *Synechococcus* only constitutes a minor part of the Arctic epipelagic carbon and energy pool (e.g., 21,000 cells mL^{-1} is equal to $2.3 \mu\text{g C L}^{-1}$, assuming a diameter of $1.1 \mu\text{m}$ and $250 \text{ fg C } \mu\text{m}^{-3}$; Kana and Glibert, 1987) relative to the total phytoplankton biomass of $42 \mu\text{g C L}^{-1}$ (assuming a carbon to chl *a* conversion of 30). A warmer Arctic ocean that may favor *Synechococcus* at the expense of larger phytoplankton species (Flombaum et al., 2013) implies that more energy and carbon could be retained within the microbial food web, further reducing the contribution of Arctic primary production to the top of the food chain.

AUTHOR CONTRIBUTIONS

MP led the collection and analysis of data, and the writing of the paper. All other authors contributed to writing the paper and in addition AL, OM, RS, and LS helped collecting data and performing experiments. LG, HD, OM, and GB helped analyse the data and prepare figures.

FUNDING

The work was conducted by the projects MicroPolar (RCN 225956) and CarbonBridge (RCN 226415), both funded by the Norwegian Research Council. HD and LG were supported by the French "Agence Nationale de la Recherche" Program SAMOSA (ANR-13-ADAP-0010).

REFERENCES

- Boyd, T. J., and D'Asaro, E. A. (1994). Cooling of the West Spitsbergen Current: wintertime observations west of Svalbard. *J. Geophys. Res.* 99, 22597–22618. doi: 10.1029/94JC01824
- Christaki, U., Courties, C., Massana, R., Catala, P., Lebaron, P., Gasol, J. M., et al. (2011). Optimized routine flow cytometric enumeration of heterotrophic flagellates using SYBR Green I. *Limnol. Oceanogr. Methods* 9, 329–339. doi: 10.4319/lom.2011.9.329
- Christaki, U., Giannakourou, A., Wambeke, F. V., and Grégori, G. (2001). Nanoflagellate predation on auto- and heterotrophic picoplankton in the oligotrophic Mediterranean Sea. *J. Plankton Res.* 23, 1297–1310. doi: 10.1093/plankt/23.11.1297
- Christaki, U., Jacquet, S., Dolan, J. R., Vault, D., and Rassoulzadegan, F. (1999). Growth and grazing on *Prochlorococcus* and *Synechococcus* by two marine ciliates. *Limnol. Oceanogr.* 44, 52–61. doi: 10.4319/lo.1999.44.1.0052

ACKNOWLEDGMENTS

We thank the helpful crew of RV Helmer Hanssen and RV Lance and to the MicroPolar and CarbonBridge teams for always being helpful during sample collection. A special thank you to Jean-Éric Tremblay for providing ammonium measurements and to Sophie Radeke for steadfast assistance at the flow cytometer and to Hilde M. K. Stabell for making the clone library. We also thank Daniel Vault for fruitful discussions.

SUPPLEMENTARY MATERIAL

The Supplementary Material for this article can be found online at: <http://journal.frontiersin.org/article/10.3389/fmars.2016.00191>

Figure S1 | The abundance (cells mL^{-1}) of *Synechococcus* (red) and HNF (blue) plotted on the left y-axis during the first 5 days of fractionation experiments performed during the 5 cruises. The fractions $<90 \mu\text{m}$ (A-E), $<10 \mu\text{m}$ (F-J), $<5 \mu\text{m}$ (K-O) and $<3 \mu\text{m}$ (Q-U) are represented on each row. Exponential functions were fitted (lines) to the abundance providing the net growth rates (μ) given in the upper left corner for *Synechococcus* (red) and HNF (blue). The total prey (sum of *Synechococcus*, picoeukaryotes and heterotrophic bacteria) to HNF ratio is plotted for each triplicate on the right y-axis (open black circles), the black line connects the daily average prey:HNF ratio.

Figure S2 | The abundance (cells mL^{-1}) of *Synechococcus* (red) and picoeukaryotes (green) for all months within the upper 500 m, except for March where profiles are shown down to 1000 and 3000 m. Horizontal light blue lines mark the stations that were influenced by sea ice. Note the different x-axis for different months. Coordinates are given for each station above each graph.

Table S1 | Environmental from the cruises containing: dates (mm/dd/yy), latitude and longitude of stations (decimal degrees), depth (m), flow cytometer counts of *Synechococcus*, picoeukaryotes, nanophytoplankton, heterotrophic bacteria, and nanoflagellates (cells mL^{-1}), the growth rates *Synechococcus* and HNF (d^{-1}) from the $<90 \mu\text{m}$ incubation, salinity, temperature and potential temperature ($^{\circ}\text{C}$), CTD-fluorescence (RUF), total chl *a* and the chl *a* fraction $>10 \mu\text{m}$ ($\mu\text{g L}^{-1}$), and nutrients (NH_4^+ , NO_3^- , NO_2^- , PO_4^+ , Si(OH)_4 (μM)). N.B. nutrients from January, May and August are not included here but will be available in Randelhoff et al. submitted.

Table S2 | Sequence ID of the members of each Operational Taxonomical Unit (OTU) defined for *petB* at 97% nucleotide sequence identity.

- Christaki, U., Vázquez-Domínguez, E., Courties, C., and Lebaron, P. (2005). Grazing impact of different heterotrophic nanoflagellates on eukaryotic (*Ostreococcus tauri*) and prokaryotic picoautotrophs (*Prochlorococcus* and *Synechococcus*). *Environ. Microbiol.* 7, 1200–1210. doi: 10.1111/j.1462-2920.2005.00800.x
- Cokelet, E. D., Tervalon, N., and Bellingham, J. G. (2008). Hydrography of the West Spitsbergen Current, Svalbard Branch: autumn 2001. *J. Geophys. Res. Ocean.* 113, 1–17. doi: 10.1029/2007JC004150
- Cottrell, M., and Kirchman, D. (2012). Virus genes in Arctic marine bacteria identified by metagenomic analysis. *Aquat. Microb. Ecol.* 66, 107–116. doi: 10.3354/ame01569
- Cottrell, M. T., and Kirchman, D. L. (2009). Photoheterotrophic microbes in the arctic ocean in summer and winter. *Appl. Environ. Microbiol.* 75, 4958–4966. doi: 10.1128/AEM.00117-09
- Darriba, D., Taboada, G. L., Doallo, R., and Posada, D. (2012). jModelTest 2: more models, new heuristics and parallel computing. *Nat. Methods* 9, 772–772. doi: 10.1038/nmeth.2109

- Doolittle, D. F., Li, W. K. W., and Wood, A. M. (2008). Wintertime abundance of picoplankton in the Atlantic sector of the Southern Ocean by. *Nov. Hedwigia* 133, 147–160.
- Fahrbach, E., Meincke, J., Østerhus, S., Rohardt, G., Schauer, U., Tverberg, V., et al. (2001). Direct measurements of volume transports through Fram Strait. *Polar Res.* 20, 217–224. doi: 10.1111/j.1751-8369.2001.tb00059.x
- Farrant, G. K., Doré, H., Cornejo-Castillo, F. M., Partensky, F., Ratin, M., Ostrowski, M., et al. (2016). Delineating ecologically significant taxonomic units from global patterns of marine picocyanobacteria. *Proc. Natl. Acad. Sci. U.S.A.* 113, E3365–E3374. doi: 10.1073/pnas.1524865113
- Flombaum, P., Gallegos, J. L., Gordillo, R. A., Rincón, J., Zabala, L. L., Jiao, N., et al. (2013). Present and future global distributions of the marine Cyanobacteria *Prochlorococcus* and *Synechococcus*. *Proc. Natl. Acad. Sci. U.S.A.* 110, 9824–9829. doi: 10.1073/pnas.1307701110
- Gradinger, R., and Lenz, J. (1995). Seasonal occurrence of picocyanobacteria in the Greenland Sea and central Arctic Ocean. *Polar Biol.* 15, 447–452. doi: 10.1007/BF00239722
- Guindon, S., and Gascuel, O. (2003). A simple, fast, and accurate algorithm to estimate large phylogenies by maximum likelihood. *Syst. Biol.* 52, 696–704. doi: 10.1080/10635150390235520
- Gutiérrez-Rodríguez, A., Slack, G., Daniels, E. F., Selph, K. E., Palenik, B., and Landry, M. R. (2014). Fine spatial structure of genetically distinct picocyanobacterial populations across environmental gradients in the Costa Rica Dome. *Limnol. Oceanogr.* 59, 705–723. doi: 10.4319/lo.2014.59.3.0705
- Holmes, R. M., Aminot, A., Kerouel, R., Hooker, B. A., and Peterson, B. J. (1999). A simple and precise method for measuring ammonium in marine and freshwater ecosystems. *Can. J. Fish. Aquat. Sci.* 56, 1801–1808. doi: 10.1139/f99-128
- Jürgens, K., Gasol, J. M., and Vagué, D. (2000). Bacteria-flagellate coupling in microcosm experiments in the Central Atlantic Ocean. *J. Exp. Mar. Biol. Ecol.* 245, 127–147. doi: 10.1016/S0022-0981(99)00156-2
- Kana, T. M., and Gilbert, P. M. (1987). Effect of irradiances up to 2000 $\mu\text{E m}^{-2}\text{s}^{-1}$ on marine *Synechococcus* WH7803-I. Growth, pigmentation, and cell composition. *Deep Sea Res.* 34, 479–495. doi: 10.1016/0198-0149(87)90001-X
- Karsenti, E., Acinas, S. G., Bork, P., Bowler, C., de Vargas, C., Raes, J., et al. (2011). A holistic approach to marine eco-systems biology. *PLoS Biol.* 9:e1001177. doi: 10.1371/journal.pbio.1001177
- Kato, K., and Standley, D. M. (2014). MAFFT: iterative refinement and additional methods. *Methods Mol. Biol.* 1079, 131–146. doi: 10.1007/978-1-62703-646-7_8
- Kjørboe, T. (2008). “Zooplankton feeding rates and bioenergetics,” in *A Mechanistic Approach to Plankton Ecology* (Oxfordshire: Princeton University Press), 224.
- Koroleff, F. (1983). “Determination of nutrients,” in *Methods of Seawater Analysis*, eds K. Grasshoff, M. Erhardt, and K. Kremling (Weinheim: Verlag Chemie), 125–187.
- Kuipers, B., Witte, H., van Noort, G., and Gonzalez, S. (2003). Grazing loss-rates in pico- and nanoplankton in the Faroe-Shetland Channel and their different relations with prey density. *J. Sea Res.* 50, 1–9. doi: 10.1016/S1385-1101(03)00043-1
- Larsen, A., Castberg, T., Sandaa, R. A., Brussaard, C. P. D., Egge, J., Heldal, M., et al. (2001). Population dynamics and diversity of phytoplankton, bacteria and viruses in a seawater enclosure. *Mar. Ecol. Prog. Ser.* 221, 47–57. doi: 10.3354/meps221047
- Letunic, I., and Bork, P. (2007). Interactive Tree Of Life (iTOL): an online tool for phylogenetic tree display and annotation. *Bioinformatics* 23, 127–128. doi: 10.1093/bioinformatics/btl529
- Li, W. K. W., Carmack, E. C., McLaughlin, F. A., Nelson, R. J., and Williams, W. J. (2013). Space-for-time substitution in predicting the state of picoplankton and nanoplankton in a changing Arctic Ocean. *J. Geophys. Res. Ocean* 118, 5750–5759. doi: 10.1002/jgrc.20417
- Lovejoy, C., Vincent, W. F., Bonilla, S., Roy, S., Martineau, M.-J., Terrado, R., et al. (2007). Distribution, phylogeny, and growth of cold-adapted picoprasinophytes in Arctic seas. *J. Phycol.* 43, 78–89. doi: 10.1111/j.1529-8817.2006.00310.x
- Mackey, K. R. M., Paytan, A., Caldeira, K., Grossman, A. R., Moran, D., McIlvin, M., et al. (2013). Effect of temperature on photosynthesis and growth in marine *Synechococcus* spp. *Plant Physiol.* 163, 815–829. doi: 10.1104/pp.113.221937
- Marie, D., Partensky, F., Jacquet, S., and Vault, D. (1997). Enumeration and cell cycle analysis of natural populations of marine picoplankton by flow cytometry using the nucleic acid stain SYBR Green I. *Appl. Environ. Microbiol.* 63, 186–93.
- Mazard, S., Ostrowski, M., Partensky, F., and Scanlan, D. J. (2012). Multi-locus sequence analysis, taxonomic resolution and biogeography of marine *Synechococcus*. *Environ. Microbiol.* 14, 372–386. doi: 10.1111/j.1462-2920.2011.02514.x
- Morán, X. A. G., López-Urrutia, A., Calvo-Díaz, A., and Li, W. K. W. (2010). Increasing importance of small phytoplankton in a warmer ocean. *Glob. Change Biol.* 16, 1137–1144. doi: 10.1111/j.1365-2486.2009.01960.x
- Moreira-Turcq, P. F., and Martin, J. M. (1998). Characterisation of fine particles by flow cytometry in estuarine and coastal Arctic waters. *J. Sea Res.* 39, 217–226. doi: 10.1016/S1385-1101(97)00053-1
- Murphy, J., and Riley, J. P. (1962). A modified single solution method for the determination of phosphate in natural waters. *Anal. Chim. Acta* 26, 31–36. doi: 10.1016/S0003-2670(00)88444-5
- Murphy, L. S., and Haugen, E. M. (1985). The distribution and abundance of phototrophic ultraplankton in the North Atlantic. *Limnol. Oceanogr.* 30, 47–58. doi: 10.4319/lo.1985.30.1.0047
- Nelson, R. J., Ashjian, C. J., Bluhm, B. A., Conlan, K. E., Gradinger, R. R., Grebmeier, J. M., et al. (2014). “Biodiversity and biogeography of the lower trophic taxa of the Pacific Arctic Region: sensitivities to climate change,” in *The Pacific Arctic Region: Ecosystem Status and Trends in a Rapidly Changing Environment*, eds J. M. Grebmeier and W. Maslowski (Dordrecht, NL: Springer Science+Business Media Dordrecht 2014), 269–336.
- Not, F., Teissier, P. G., Massana, R., Latasa, M., Marie, D., Colson, C., et al. (2005). Late summer community composition and abundance of photosynthetic picoeukaryotes in Norwegian and Barents Seas. *Limnol. Oceanogr.* 50, 1677–1686. doi: 10.4319/lo.2005.50.5.1677
- Palenik, B., Brahmsha, B., Larimer, F. W., Land, M., Hauser, L., Chain, P., et al. (2003). The genome of a motile marine *Synechococcus*. *Nature* 424, 1035–1037. doi: 10.1038/nature01883.1
- Patel, A., Noble, R. T., Steele, J. A., Schwalbach, M. S., Hewson, I., and Fuhrman, J. A. (2007). Virus and prokaryote enumeration from planktonic aquatic environments by epifluorescence microscopy with SYBR Green I. *Nat. Protoc.* 2, 269–276. doi: 10.1038/nprot.2007.6
- Paulsen, M. L., Riisgaard, K., Thingstad, T. F., and St. John, M. (2015). Winter–spring transition in the subarctic Atlantic: microbial response to deep mixing and pre-bloom production. *Aquat. Microb. Ecol.* 76, 49–69. doi: 10.3354/ame01767
- Pedros-Álió, C., Potvin, M., and Lovejoy, C. (2015). Diversity of planktonic microorganisms in the Arctic Ocean. *Prog. Oceanogr.* 139, 233–243. doi: 10.1016/j.pocean.2015.07.009
- Perenthaler, J. (2005). Predation on prokaryotes in the water column and its ecological implications. *Nat. Rev. Microbiol.* 3, 537–546. doi: 10.1038/nrmicro1180
- Pittera, J., Humily, F., Thorel, M., Grulois, D., Garczarek, L., and Six, C. (2014). Connecting thermal physiology and latitudinal niche partitioning in marine *Synechococcus*. *ISME J.* 8, 1221–1236. doi: 10.1038/ismej.2013.228
- Saito, M. A., Rocap, G., and Moffett, J. W. (2005). Production of cobalt binding ligands in a *Synechococcus* feature at the Costa Rica upwelling dome. *Limnol. Oceanogr.* 50, 279–290. doi: 10.4319/lo.2005.50.1.0279
- Sandaa, R.-A., and Larsen, A. (2006). Seasonal variations in virus-host populations in Norwegian coastal waters: focusing on the cyanophage community infecting marine *Synechococcus* spp. *Appl. Environ. Microbiol.* 72, 4610–4618. doi: 10.1128/AEM.00168-06
- Sanders, R. W., Caron, D. A., and Berninger, U.-G. (1992). Relationships between bacteria and heterotrophic nanoplankton in marine and fresh waters: an inter-ecosystem comparison. *Mar. Ecol. Prog. Ser.* 86, 1–14.
- Sanders, R. W., and Gast, R. J. (2012). Bacterivory by phototrophic picoplankton and nanoplankton in Arctic waters. *FEMS Microbiol. Ecol.* 82, 242–253. doi: 10.1111/j.1574-6941.2011.01253.x
- Sato, M., Yoshikawa, T., Takeda, S., and Furuya, K. (2007). Application of the size-fractionation method to simultaneous estimation of clearance rates by heterotrophic flagellates and ciliates of pico- and nanophytoplankton. *J. Exp. Mar. Biol. Ecol.* 349, 334–343. doi: 10.1016/j.jembe.2007.05.027
- Scanlan, D. J., Ostrowski, M., Mazard, S., Dufresne, A., Garczarek, L., Hess, W. R., et al. (2009). Ecological genomics of marine picocyanobacteria. *Microbiol. Mol. Biol. Rev.* 73, 249–299. doi: 10.1128/MMBR.00035-08
- Shapiro, L. P., and Haugen, E. M. (1988). Seasonal distribution and temperature tolerance of *Synechococcus* in Boothbay Harbor, Maine. *Estuar. Coast. Shelf Sci.* 26, 517–525.

- Sherr, E. B., Sherr, B. F., Wheeler, P. A., and Thompson, K. (2003). Temporal and spatial variation in stocks of autotrophic and heterotrophic microbes in the upper water column of the central Arctic Ocean. *Deep Sea Res. I* 50, 557–571. doi: 10.1016/S0967-0637(03)00031-1
- Simek, K., and Chrzanowski, T. (1992). Direct and indirect evidence of size-selective grazing on pelagic bacteria by fresh-water nanoflagellates. *Appl. Environ. Microbiol.* 58, 3715–3720.
- Sohm, J. A., Ahlgren, N. A., Thomson, Z. J., Williams, C., Moffett, J. W., Saito, M. A., et al. (2016). Co-occurring *Synechococcus* ecotypes occupy four major oceanic regimes defined by temperature, macronutrients and iron. *ISME J.* 10, 333–345. doi: 10.1038/ismej.2015.115
- Tremblay, G., Belzile, C., Gosselin, M., Poulin, M., Roy, S., and Tremblay, J. (2009). Late summer phytoplankton distribution along a 3500 km transect in Canadian Arctic waters: strong numerical dominance by picoeukaryotes. *Aquat. Microb. Ecol.* 54, 55–70. doi: 10.3354/ame01257
- Tremblay, J.-É., Robert, D., Varela, D. E., Lovejoy, C., Darnis, G., Nelson, R. J., et al. (2012). Current state and trends in Canadian Arctic marine ecosystems: I. Primary production. *Clim. Change* 115, 161–178. doi: 10.1007/s10584-012-0496-3
- Tsai, A. Y., Gong, G. C., Sanders, R. W., and Chiang, K. P. (2013). Relationship of *Synechococcus* abundance to seasonal ocean temperature ranges. *Terr. Atmos. Ocean. Sci.* 24, 925–932. doi: 10.3319/TAO.2013.06.17.01(Oc)
- Vincent, W. F. (2010). Microbial ecosystem responses to rapid climate change in the Arctic. *ISME J.* 4, 1087–1090. doi: 10.1038/ismej.2010.108
- Vincent, W. F., Bowman, J. P., Rankin, L. M., and Mcmeekin, T. A. (2000). “Microbial biosystems,” in *New Frontiers Proceedings of the 8th International Symposium on Microbial Ecology*, eds C. R. Bell, M. Brylinsky, and P. Johnson-Green (Halifax, NS: Atlantic Canada Society for Microbial Ecology).
- Waleron, M., Waleron, K., Vincent, W. F., and Wilmotte, A. (2007). Allochthonous inputs of riverine picocyanobacteria to coastal waters in the Arctic Ocean. *FEMS Microbiol. Ecol.* 59, 356–365. doi: 10.1111/j.1574-6941.2006.00236.x
- Waterbury, J. B., Watson, S. W., Valois, F. W., and Franks, D. G. (1986). “Biological and ecological characterisation of the marine unicellular cyanobacterium *Synechococcus*,” in *Photosynthetic Picoplankton*, eds T. Platt and W. K. W. Li (Ottawa, ON: Canadian Bulletin of Fisheries and Aquatic Sciences), 71–120.
- Wood, E. D., Armstrong, F. A. J., and Rich, F. A. (1967). Determination of nitrate in seawater by cadmium-copper reduction to nitrate. *J. Biol. Assoc. UK.* 47, 23–31.
- Yelton, A. P., Acinas, S. G., Sunagawa, S., Bork, P., Pedrós-Alió, C., and Chisholm, S. W. (2016). Global genetic capacity for mixotrophy in marine picocyanobacteria. *ISME J.* doi: 10.1038/ismej.2016.64. [Epub ahead of print].
- Zhang, F., He, J., Lin, L., and Jin, H. (2015). Dominance of picophytoplankton in the newly open surface water of the central Arctic Ocean. *Polar Biol.* 38, 1081–1089. doi: 10.1007/s00300-015-1662-7
- Zubkov, M. V., Burkill, P. H., and Topping, J. N. (2007). Flow cytometric enumeration of DNA-stained oceanic planktonic protists. *J. Plankton Res.* 29, 79–86. doi: 10.1093/plankt/fbl059
- Zwirgmaier, K., Jardillier, L., Ostrowski, M., Mazard, S., Garczarek, L., Vaulot, D., et al. (2008). Global phylogeography of marine *Synechococcus* and *Prochlorococcus* reveals a distinct partitioning of lineages among oceanic biomes. *Environ. Microbiol.* 10, 147–161. doi: 10.1111/j.14622920.2007.01440.x
- Zwirgmaier, K., Spence, E., Zubkov, M. V., Scanlan, D. J., and Mann, N. H. (2009). Differential grazing of two heterotrophic nanoflagellates on marine *Synechococcus* strains. *Environ. Microbiol.* 11, 1767–1776. doi: 10.1111/j.1462-2920.2009.01902.x

Conflict of Interest Statement: The authors declare that the research was conducted in the absence of any commercial or financial relationships that could be construed as a potential conflict of interest.

Copyright © 2016 Paulsen, Doré, Garczarek, Seuthe, Müller, Sandaa, Bratbak and Larsen. This is an open-access article distributed under the terms of the Creative Commons Attribution License (CC BY). The use, distribution or reproduction in other forums is permitted, provided the original author(s) or licensor are credited and that the original publication in this journal is cited, in accordance with accepted academic practice. No use, distribution or reproduction is permitted which does not comply with these terms.



IV



Carbon Bioavailability in a High Arctic Fjord Influenced by Glacial Meltwater, NE Greenland

Maria L. Paulsen^{1*}, Sophia E. B. Nielsen^{2,3}, Oliver Müller¹, Eva F. Møller^{4,5}, Colin A. Stedmon², Thomas Juul-Pedersen⁶, Stiig Markager⁴, Mikael K. Sejr⁵, Antonio Delgado Huertas⁷, Aud Larsen⁸ and Mathias Middelboe³

¹ Department of Biology, University of Bergen, Bergen, Norway, ² National Institute for Aquatic Resources, Technical University of Denmark, Charlottenlund, Denmark, ³ Marine Biological Section, University of Copenhagen, Helsingør, Denmark, ⁴ Department of Bioscience, Aarhus University, Roskilde, Denmark, ⁵ Arctic Research Centre, Aarhus University, Aarhus, Denmark, ⁶ Climate Research Centre, Greenland Institute of Natural Resources, Nuuk, Greenland, ⁷ Instituto Andaluz de Ciencias de la Tierra (CSIC-UGR), Armilla, Granada, Spain, ⁸ Uni Research Environment, Bergen, Norway

OPEN ACCESS

Edited by:

Ingrid Obermosterer,
FR3724 Observatoire Océanologique
de Banyuls sur Mer (OOB), France

Reviewed by:

Emma Jane Rochelle-Newall,
Institut de Recherche Pour le
Développement, France
Xosé Anxelu G. Morán,
King Abdullah University of Science
and Technology, Saudi Arabia

*Correspondence:

Maria L. Paulsen
maria.l.paulsen@uib.no

Specialty section:

This article was submitted to
Aquatic Microbiology,
a section of the journal
Frontiers in Marine Science

Received: 18 October 2016

Accepted: 19 May 2017

Published: 08 June 2017

Citation:

Paulsen ML, Nielsen SEB, Müller O,
Møller EF, Stedmon CA,
Juul-Pedersen T, Markager S,
Sejr MK, Delgado Huertas A,
Larsen A and Middelboe M (2017)
Carbon Bioavailability in a High Arctic
Fjord Influenced by Glacial Meltwater,
NE Greenland. *Front. Mar. Sci.* 4:176.
doi: 10.3389/fmars.2017.00176

The land-to-ocean flux of organic carbon is increasing in glacierized regions in response to increasing temperatures in the Arctic (Hood et al., 2015). In order to understand the response of the coastal ecosystem metabolism to the organic carbon input it is essential to determine the bioavailability of the different carbon sources in the system. We quantified the bacterial turnover of organic carbon in a high Arctic fjord system (Young Sound, NE Greenland) during the ice-free period (July–October 2014) and assessed the quality and quantity of the 3 major organic carbon sources; (1) local phytoplankton production (2) runoff from land-terminating glaciers and a lowland river and (3) inflow from the ocean shelf. We found that despite relatively low concentrations of DOC in the rivers, the bioavailability of the river–DOC was significantly higher than in the fjord, and characterized by high cell-specific bacterial production and low C:N ratios. In contrast, the DOC source entering via inflow of coastal shelf waters had high DOC concentrations with high C:N and low specific bacterial production. The phytoplankton production in the fjord could not sustain the bacterial carbon demand, but was still the major source of organic carbon for bacterial growth. We assessed the bacterial community composition and found that communities were specific for the different water types i.e., the bacterial community of the coastal inflow water could be traced mainly in the subsurface water, while the glacial river community strongly dominated the surface water in the fjord.

Keywords: bacterial carbon demand, bacterial diversity, dissolved organic matter, runoff, glacial meltwater, high arctic ecosystems, young sound

INTRODUCTION

Carbon consumption and mineralization by pelagic heterotrophic bacteria play a key role in marine ecosystems. Increasing temperatures, with pronounced effects at high latitudes, have raised questions about how reduced ice-cover and increased runoff can affect the ecosystem metabolism i.e., the balance between respiration and primary production. Bacterial carbon turnover was traditionally suggested to be limited by low temperature in high latitude systems, and consequently

play only a minor role in turning over primary production (Pomeroy and Deibel, 1986; Pomeroy et al., 1991). Several high latitude studies during the past decade have however reported bacterial production rates similar to those reported in low-latitude non-oligotrophic systems (Borsheim, 2000; Rysgaard and Nielsen, 2006; Sejr et al., 2007). Two seasonal studies found annual ranges in bacterial production of 5–42 mg C m⁻² d⁻¹ in Kobbefjord (64°N) (Middelboe et al., 2012) and 90–165 mg C m⁻² d⁻¹ in Kongsfjorden, Svalbard (78°N) (Iversen and Seuthe, 2011), with maximum values during spring, coinciding with the spring phytoplankton bloom.

Estimates of bacterial carbon cycling is often based on measurements of net bacterial production, however variability in the factors used to convert radioisotope (e.g., ¹⁴C-leucine or ³H-thymidine) incorporation to carbon production affects the growth estimates and potentially complicates comparison of studies. Measurements of the bacterial respiration (BR) are required in order to estimate the bacterial carbon demand (BCD) and growth efficiency (BGE). Such measurements in Arctic systems are few and the BGE reported are highly variable, but all in the low end of those reported in other aquatic systems (del Giorgio and Cole, 1998). It has been hypothesized that low temperatures limit substrate uptake and consequently argued that Arctic bacteria need relatively higher concentrations of carbon to grow at low temperatures (Pomeroy and Wiebe, 2001). Other studies have demonstrated an inverse relationship between BGE and temperature (Rivkin and Legendre, 2001; Apple et al., 2006) leading to speculations that the low efficiency found in the Arctic may instead be a result of poor quality carbon sources (Middelboe et al., 2012). While the concentration of organic matter alone does not reflect the carbon quality (Kirchman et al., 2005), the elemental ratios of the dissolved organic matter (DOM) i.e., the C:N ratio has provided insight on the DOM bioavailability (del Giorgio and Cole, 1998; Pradeep Ram et al., 2003; Kragh and Søndergaard, 2004).

The activity of bacteria is tightly coupled to DOM bioavailability (Amon and Benner, 1996; Kragh and Søndergaard, 2004). Bioavailable dissolved organic carbon (BDOC) has been estimated to constitute on average <1% of the oceanic DOC pool, however elevated in the surface waters (Hansell, 2013). Studies in the Greenland Sea, Fram Strait, and Kobbefjord have shown that BDOC constitutes 13–36% of total DOC in surface water (Middelboe and Lundsgaard, 2003; Middelboe et al., 2012; Jørgensen et al., 2014). Glacial meltwater from both Alaskan (Hood et al., 2009) and Alpine glaciers (Singer et al., 2012) contained highly bioavailable (>60%) DOC. As the Greenland Ice Sheet is melting at record speed (Nghiem et al., 2012) and the melt is projected to continue increasing (Keegan et al., 2014) it poses the question whether coastal bacterial carbon turnover will increase and drive the fjord systems toward more heterotrophic conditions in the future.

The bioavailability of different DOM types is influenced by a number of factors including composition of substrate, availability of mineral nutrients and the bacterial communities and their enzymatic capabilities (Middelboe and Lundsgaard, 2003; Kritzberg et al., 2010; Traving et al., 2016). Only few studies have tried to directly connect specific bacterial groups to

different types of DOM (Kirchman et al., 2007; Baña et al., 2013; Osterholz et al., 2016). Meltwater from glaciers has been found to significantly modify the structure of microbial communities in the connected fjord (Gutiérrez et al., 2015). Consequently, increased runoff associated with warming climate will not only affect the transport of organic matter, it may also change the dynamics of coastal bacterial communities toward a higher influence of riverine bacteria and thus potentially changes in BGE and DOM degradation of the coastal bacterial community (Fortunato et al., 2013). Exploring links between the bacterial community composition and the various DOM sources, are therefore highly relevant in Arctic environments. Young Sound receives most of its runoff from the Greenland Ice Sheet via land terminating glaciers (Citterio et al., 2017), resulting in a clear gradient of allochthonous sources of both organic matter and silt throughout the fjord (Murray et al., 2015). The organic carbon sources in the fjord comprise two allochthonous carbon sources 1) meltwater from land-terminating glaciers and a lowland river and 2) coastal water that contains traces of DOM from the Arctic Ocean (Amon and Budéus, 2003).

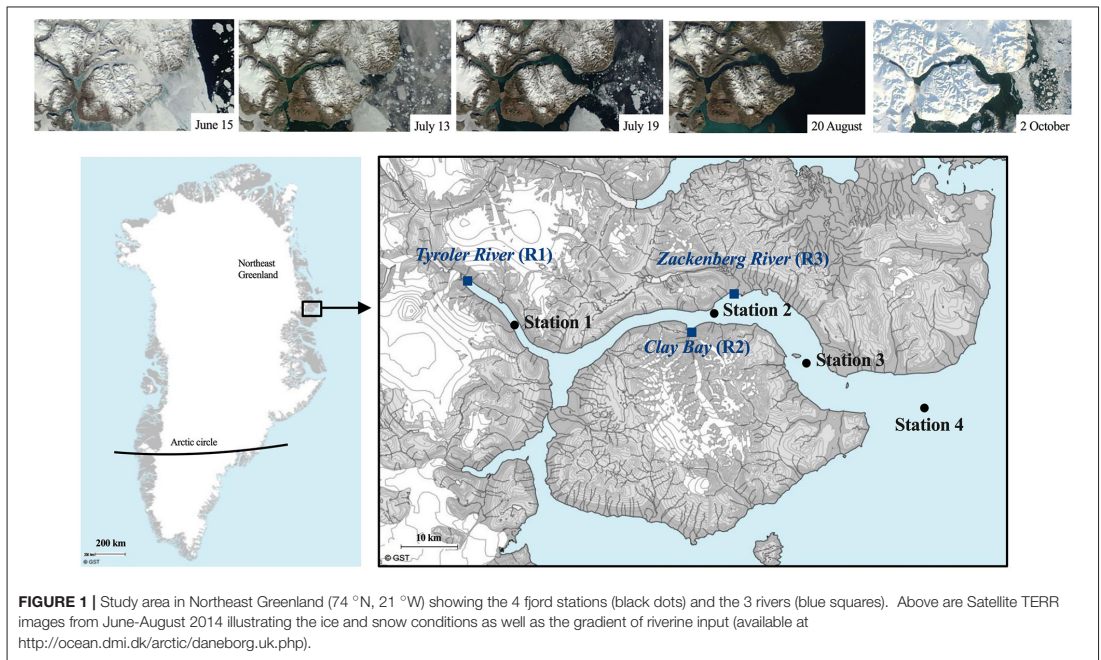
Based on previous findings we hypothesize that the glacial runoff in Young Sound contains highly bioavailable DOM compared to the local production and inflowing coastal water. In order to understand the response in ecosystem metabolism we evaluate the importance of each of the 3 carbon sources as substrate for bacterial carbon degradation and examine associations between the bacterial DOM degradation and the genetic diversity.

MATERIALS AND METHODS

Study Site and Sampling

The study was conducted in the high arctic fjord Young Sound, NE Greenland (74.2–74.3°N, 19.7–21.9°W). A sill of 45 m depth separates the deeper parts of the fjord from the coastal shelf waters, which are influenced by the East Greenland Current (for more info see Rysgaard et al., 2003). Sampling was conducted at four stations located along a length section from the inner fjord (St. 1) to the shelf waters on the outer side of the sill (St. 4) (Figure 1). The stations 1, 2, 3, and 4 are located according to stations monitored yearly by the Greenland Ecosystem Monitoring (GEM) MarinBasis Zackenberg programme in which they are named Tyro 05, YS 3.18, Standard St. and GH 05, respectively. The fjord stations were each sampled approximately every 10th during the early ice-free period (July 15–August 7) and the late summer period before new ice formation (September 4–October 4) (Figure S1).

The first sampling was conducted prior to the sea-ice break-up through a hole in the ice at St. 3, when only the central part of the fjord was still ice covered (see satellite photos Figure 1). The ice broke up in the central part on July 15 and the fjord rendered ice-free within 24 h. The remaining sampling was carried out from the research vessel *Aage V. Jensen* using mini rosette with 12 × 1.7 L Niskin bottles from 6 standard depths (1, 10, 20, 30, 40, and 100 m) and 1–2 additional depths at the deep chlorophyll maximum (DCM) when this did not overlap with one of the standard depths. The DCM was determined



prior to every sampling using a Satlantic Free-falling Optical Profiler (Murray et al., 2015). A Seabird SBE 19+ CTD profiler was deployed at every sampling occasion and recorded vertical profiles of temperature ($^{\circ}\text{C}$), salinity (ratio; no units), chlorophyll fluorescence (flu_{chl} , relative; no units), turbidity (FTU), and photosynthetically active radiation (PAR , $\mu\text{mol m}^{-2} \text{s}^{-1}$) at every sampling occasion. The light attenuation was estimated from the CTD-profiles using a two-phase Weibull function as described in Murray (2015).

Glaciers cover ca. 33% of the drainage area of the fjord and land-terminating glaciers contribute 50–80% of the annual terrestrial runoff with highest contribution in the inner fjord (Bendtsen et al., 2014; Citterio et al., 2017). Three of the major rivers discharging into the fjord were sampled as long as sufficient water was flowing (last sampling was on September 10). The meltwater in the Tyroler river (R1) and Clay Bay river (R2) flows from glaciers through rocky sediment basins with close to zero vegetation for a distance of ca. 0.5 and 2 km, respectively, before they reach the fjord. A model study estimate the residence time of river water in the fjord to be about 2 weeks in July and up to a month in August (Bendtsen et al., 2014).

R1 receives water directly from the Greenland Ice Sheet and has the largest catchment area (Bendtsen et al., 2014), while R2 receives meltwater from smaller local glaciers (Figure 1). The largest river, R3 (Zackenbergl river) has the second largest catchment area and is connected to 2 lakes. It flows through lowland permafrost soils covered with vegetation types like dwarf shrub heath (*Salix arctica*) and grasses (e.g., *Arctagrostis latifolia*),

however the riverbed is rocky and without vegetation (Elberling et al., 2008). River water was collected just below surface in 5 L plastic bottles. A 10-year time series of temperature and the organic and inorganic particulate biomass and the dissolved organic carbon (DOC) recorded from the Zackenbergl river by the GeoBasis programme by Greenland Ecosystem Monitoring are included in Figure S3.

A total of 25 profiles were sampled at the fjord stations and the rivers were sampled each 3 times. Based on the salinity and temperature (Figure 2) five water types were defined (Table 1). Bacterial abundance, production and chemical parameters (nutrients, DOC, DON, and chl *a*) were measured in total 174 times each. A total of 42 samples were collected in the rivers and at 1 m and DCM for “extra” analysis of carbon bioavailability, particle associated bacterial production and community composition analysis. These “focus samples” are marked with large symbols in Figure 2. Environmental data associated with these 42 focus samples are given in Table S1. Note no focus samples were collected from the water mass defined as Shelf water.

Chlorophyll *a* and Primary Production

Concentrations of chlorophyll *a* (chl *a*) were determined according to Jespersen and Christoffersen (1987). Triplicates of 250 mL water was filtered onto GF/F, 2 and 10 μm polycarbonate filters and chl *a* was extracted in 5 mL 96% ethanol for 12–24 h and analyzed on a Turner Design Fluorometer calibrated against a chl *a* standard. The measurements were done in

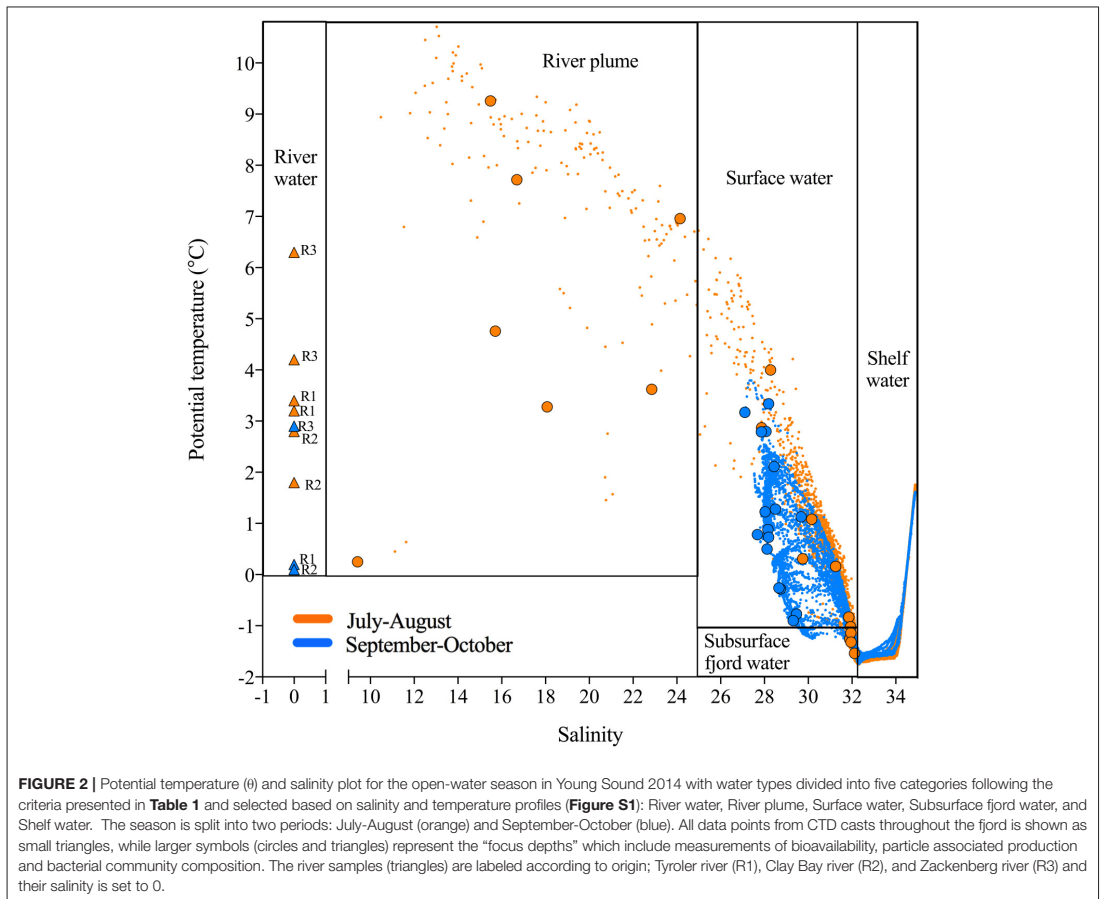


TABLE 1 | Thermohaline properties describing the classification of water types.

Water types	Salinity	Potential temperature (°C)
Shelf water	>32.5	
Subsurface fjord water	<32.5	< -1°C
Surface water	25–32.5	> -1°C
River plume	<25	
River water	<1	

triplicates. Primary production (PP) was measured as ^{14}C -uptake (Nielsen, 1952) according to Markager et al. (1999) and measured for 3 size fractions; dissolved (<0.7 μm), small phytoplankton (0.7–10 μm) and larger phytoplankton (>10 μm). Samples were collected at 1 m depth and at one or two additional depth with a notable DCM (26 samples in total). The areal primary production was calculated according to Lyngsgaard et al. (2014). The daily area production was estimated by integrating over 24 h and with

depth. The light intensity at each depth was calculated from the light attenuation and the surface light measured at the nearby Zackenberg research station as part of the GEM Programme.

Flow Cytometry

The abundance of bacteria was determined on an Attune[®] Acoustic Focusing Flow Cytometer (Applied Biosystems by Life technologies) with a syringe-based fluidic system and a 20 mW 488 nm (blue) laser. Samples were fixed with glutaraldehyde (0.5% final conc.) and kept dark at 4°C until analysis within 12 h. Samples were stained with SYBR Green I (Molecular Probes, Eugene, Oregon, USA) for min 0.5 h at low flow rate of 25 $\mu\text{L min}^{-1}$ following the protocol of Marie et al. (1999). It should be noted that the bacterial abundance in the rivers was not easily counted by flow cytometry as the inorganic particle signal was high and obscured the counts of free-living bacteria. To reduce the problem the samples were diluted x10 with TE-buffer.

Nutrients

Unfiltered seawater was filled directly from the Niskin bottles into 30 mL acid washed HDPE bottles and stored at -20°C . Nitrite and nitrate ($\text{NO}_2^- + \text{NO}_3^-$), phosphate (PO_4^{3-}) and silicic acid (H_4SiO_4) were measured on a Smartchem200 (by AMS Alliance) autoanalyser following procedures as outlined in Wood et al. (1967) for $\text{NO}_3^- + \text{NO}_2^-$, Murphy and Riley (1962) for PO_4^{3-} and Koroleff (1983) for the determination of H_4SiO_4 . Concentration of NH_4^+ was determined directly in fresh samples using ortho-phthalaldehyde according to Holmes et al. (1999).

Organic Matter Concentration

DOC and DON samples for determining the initial concentration of DOC were collected in 60 mL acid washed HDPE (high-density polyethylene) bottles and stored frozen (-20°C) until analysis. DOC is here considered to equal total organic carbon (TOC) according to (Anderson, 2002). DOC concentrations were determined by high temperature combustion (720°C) using a Shimadzu TOC-V CPH-TN carbon and nitrogen analyser calibrated using a standard series of acetanilide and the accuracy of the instrument was evaluated using seawater reference material provided by the Hansell CRM (consensus reference material) program. DON was calculated by subtraction of inorganic nitrogen. For particulate organic carbon and nitrogen (POC and PON) a total of 85 samples were collected. 15 L samples from the rivers and 30 L samples from the fjord (collected at 1 m, DCM and 100 m) were filtered onto 47 mm pre-combusted GFF filters using a peristaltic pump. The filters were placed in a desiccator containing concentrated 37% HCl for 12–14 h to remove inorganic carbon. POC and PON was measured using a Carlo Elba NC1500 (Milan, Italy) CHN elemental analyser following the method of Hedges and Stern (1984).

Bacterial Production

Bacterial production was estimated from incorporation of ^3H -thymidine (Riemann et al., 1982). From each water sample, four replicates of 10 mL unfiltered seawater samples were transferred to 20 mL plastic vials. One replicate was immediately amended with 500 μL of 100% trichloroacetic acid (TCA) and served as control. Samples were incubated with 10 nM ^3H -thymidine (final concentration) for 3–5 h at *in situ* temperature and stopped by addition of 500 μL 100% TCA. Samples were filtered onto 0.2 μm cellulose-nitrate filters, which were subsequently washed 10 times with ice-cold 5% TCA. Filters were transferred to 6-mL plastic vials and stored at -20°C until analysis. In the laboratory 5 mL of scintillation liquid was added and the radioactivity was counted on a Perkin Elmer Liquid Scintillation Analyzer Tri-Carb 2800TR. The measured thymidine incorporation was converted to cell production assuming 2.0×10^{18} cells produced per mole ^3H thymidine incorporated (Fuhrman and Azam, 1980). Bacterial population growth rate (GR) was calculated as cell production ($\text{cells mL}^{-1} \text{d}^{-1}$) divided by the cell abundance (cells mL^{-1}). Cell production was converted to bacterial carbon production (BP) assuming 2.0×10^{-14} g C cell^{-1} (Lee and Fuhrman, 1987). For the calculation of area-integrated bacterial carbon consumption, the bacterial production was depth-integrated across the upper 100 m, and divided by the BGE measured in July

(see below). Additionally, at the “focus depths” and in the rivers the particulate bacterial production was measured as the fraction associated with particles larger than 3 μm and calculated as the total BP subtracted the $<3 \mu\text{m}$ fraction.

Bacterial Respiration and Growth Efficiency (BGE)

Bacterial respiration (BR) was measured as oxygen consumption for ~ 48 h at constant temperature in water from 1 m and DCM in triplicate 12 mL gas tight Exetainers equipped with an optical sensor. Water was pre-filtered through a 3 μm - polycarbonate filter to reduce bias from eukaryotic cell respiration and grazing. A sample with 20 μL HgCl served as control. Oxygen was measured every 5 min for >24 h using a 4-channel Fiber-Optic Oxygen Meter (FireSting, Pyroscience) using the program Pyro Oxygen Logger Software version 2.37 (PyroScience). Respiration rates were calculated as the decrease in oxygen concentration (μM) over the incubation time after subtracting control values. Conversion from oxygen consumption to carbon respiration was done assuming a respiratory quotient (RQ) of 0.82 (Søndergaard and Middelboe, 1995). BGE was calculated from measurements of net bacterial production (NBP) and bacterial respiration (BR) in the 3 μm -filtered samples as: $\text{BGE} (\%) = \text{BP} / (\text{BP} + \text{BR}) \times 100$. BGE was measured at all four stations at 1 m depth and DCM, and from the three rivers, however only BR measurements that fulfilled the three following criteria were used: (1) constant incubation temperature ($\pm 0.1^{\circ}\text{C}$) for > 24 h, (2) low abundance ($< 5,000 \text{ cells mL}^{-1}$) of small phytoplankton ($< 3 \mu\text{m}$) (as we saw indications of possible respiration contamination from these), and finally (3) the measured respiration rate should not exceed the total respiration rate of the system (measured by T. Dalsgaard unpublished).

Long Term BDOC Experiments

The quantity of DOC available for bacterial degradation (BDOC) was measured in long term (126–148 d) oxygen consumption experiments. A total of 36 incubations were established from the focus depths and rivers (Table S1). 2 L were 0.22 μm filtered (Millipore® Sterivex) into acid washed HDPE bottles (the filters were later used for extraction of nucleic acids). Note we thus did not measure the bioavailability of the particulate organic matter. The bacterial inoculum was prepared by GF/F filtering 100 mL into 2×50 mL falcon tubes. The 0.22 μm -filtered water and bacterial inoculum was stored cold (2°C) until experimental set-up. The oxygen consumption experiment was set up with five replicate 65 mL Winkler glass bottles equipped with an optical oxygen sensor for each sample and incubated in dark at 8°C for 148 days (samples collected in July and August) or 126 days (samples collected September and October). Prior to incubation NO_3^- and PO_4^{3-} (final conc. 5 μM and 1 μM , respectively) were added along with the bacterial inoculum (10% vol.) to ensure that N or P was not limiting C-degradation during incubation. Consequently, these measurements do not reflect *in situ* conditions neither the bacterial communities at the time of sampling, but are rather quantitative measure of the bioavailable DOC pool. All Winkler bottles contained a magnet to ensure mixing, and were incubated

in a water bath in order to minimize oxygen contamination. In addition, parallel bottles containing 100 and 0% air saturated seawater were measured to correct oxygen measurements for deviations in the 100% control. As control incubations, triplicates of sample water were incubated without bacterial inoculum as well as a sample with 20 μL HgCl. The change in % air saturation over time was monitored every 7–14 days using a Fibox 3 fiber optic patch oxygen sensor (Presense) calibrated with 100% and 0% air saturation using the program OxyView-PST3-V6.02. As for the BGE measurements the change in oxygen concentration over time was converted to carbon consumption assuming an RQ of 0.82 (Søndergaard and Middelboe, 1995). DOC concentration was measured initially and by the end of the incubation.

Nucleic Acids Extraction, Amplification, and Amplicon Sequencing

All environmental samples for molecular analysis were collected by filtering water onto 0.22 μm pore size Millipore® Sterivex filters (the filtrate was used for bioavailability measurements described above). Note that samples were not prefiltered i.e., also the particle associated bacteria are included in this analysis. The filters were immediately frozen and stored at -80°C until nucleic acid extraction. DNA and RNA were extracted simultaneously using the AllPrep DNA/RNA Mini Kit (Qiagen, Hilden, Germany) according to manufacturer's instructions with modifications for extraction from Sterivex filters as in Paulsen et al. (2016). RNA was subsequently treated with the DNA-free DNA Removal kit (Invitrogen, CA, USA) and reverse transcribed using the SuperScript III First-Strand Synthesis System for RT-PCR (Invitrogen). Amplification of cDNA and DNA was performed using a two-step nested PCR approach with primers 519F (CAGCMGCCGCGGTAA; Øvreås et al. (1997) and 806R (GGACTACHVGGGTWTCTAAT; Caporaso et al. (2011) targeting the bacterial (and Archaeal) 16S rRNA gene V4 hypervariable region. For the first PCR step triplicate samples were amplified in reaction volumes of 20 μL including 10 ng DNA or cDNA, 10 μL HotStarTaq Master Mix (Qiagen), 500 nM of each primer and nuclease free water. PCR cycles consisted of an initial denaturation of 15 min at 95°C , followed by 25 cycles of 95°C for 20 s, 55°C for 30 s and 72°C for 30 s and a final extension step of 72°C for 7 min. Triplicate PCR products were pooled, purified using the DNA Clean & Concentrator-5 kit (Zymo Research Corporation, CA, USA) and quantified using the Qubit 3.0 Fluorometer. For the second PCR step, 10 ng of pooled PCR product was used in a reaction mixture containing 25 μL HotStarTaq Master Mix, 500 nM of each nested primer with a unique eight-nucleotide barcode (total of 96 combinations) and nuclease-free water to bring the mixture to the total volume of 50 μL . Thermal cycles had an initial denaturation for 15 min at 95°C , followed by 15 cycles at 95°C for 20 s, 62°C for 30 s, 72°C for 30 s, and a final extension step of 72°C for 7 min. PCR products were purified using Agencourt AMPure XP Beads (Beckman Coulter Inc., CA, USA) and prepared for sequencing by pooling the amplicons in equimolar amounts.

The quality and concentration of the amplicon pool were assessed by agarose gel electrophoresis and by using a Qubit 3.0 Fluorometer, before sending to the Norwegian Sequencing Centre (Oslo, Norway) for High-Throughput Sequencing on a MiSeq platform (Illumina, CA, USA) using the MiSeq Reagent Kit v2 (Illumina). Sequencing data is available at "The European Bioinformatics Institute" under study accession number PRJEB16067 (<http://www.ebi.ac.uk>).

16S rRNA Gene Sequence Analysis

Paired-end sequences were processed using different bioinformatic tools incorporated on a qiime-processing platform (Caporaso et al., 2010). FASTQ files were quality end-trimmed at a phred quality score ≥ 24 using Trimmomatic (Bolger et al., 2014) and merged using PANDAseq (Masella et al., 2012), while all reads < 200 bp were removed. Prokaryotic OTUs were selected at a sequence similarity threshold of 97% using a de novo uclust (Edgar, 2010) OTU clustering method with default parameters and taxonomy assigned using the Silva 111 reference database (Quast et al., 2013). OTUs with a taxonomic identification were assembled to an OTU table providing abundances for each sample excluding singletons and rarefied to the number of sequences of the smallest samples (5,000 sequences). A total of 4,096,371 sequences were retrieved from the Illumina sequencing of the 16S rRNA gene V4 hypervariable region from total RNA across 52 samples. After removal of singletons, unassigned OTUs and chloroplast reads, sequences were rarefied to 5,000 reads per sample, with a total of 15,922 unique OTUs at 97% sequence identity. Multivariate statistical analysis was performed on basis of the rarefied OTU matrix to explain variations in the data and test for multivariate environmental correlation with the prokaryotic community structure. Bray-Curtis resemblance, ANOSIM, principal component analysis and redundancy analysis were calculated using primer-e version 6 (Plymouth, UK) and Canoco 5 (Ter Braak and Šmilauer, 2012).

Source Tracker Analysis

To illustrate the spread of bacterial communities in the fjord the SourceTracker 0.9.5 software (Knights et al., 2011) was applied in QIIME. It is designed to track the relative contribution of predefined microbial sources in sink samples using a Bayesian approach, as done in Storesund et al., in review. The relative abundance of 16S rRNA genes of all focus samples was used as input data. The OTU table, comprising all OTUs with a taxonomic identification (excluding singletons and chloroplast reads) was rarefied to 1,000 sequences and filtered to only include OTUs that were abundant in more than 3 samples. The rivers (R1, R2 and R3) and as a proxy for inflowing coastal water St. 4 DCM samples were used as "source populations." All remaining stations during the sampling period from July until October were defined as the "sink samples." The result is given as % likely origin from the 4 defined sources. The remaining are categorized as "unknown source". The result were visualized as fjord transects with weighted-average extrapolation between points using Ocean Data View (Schlitzer, 2016).

RESULTS

Hydrography

During the first period (July–August) the fjord was stratified by a strong halocline at 5–6 m depth with low salinity (<20) in the surface and more saline bottom water (>30). The stratification was strongest in the inner fjord and the salinity of the surface water increased eastwards toward the shelf (Figure S1). The later period (September–October) was in general colder (surface water <2°C) and frequent storms mixed the upper layer, which deepened to 30 m at the two inner stations and down to 50 and 80 m at St. 3 and 4, respectively (Figure S1). Five water types were defined for this study based on the thermohaline properties (Table 1 and Figure 2). This was done to facilitate the interpretation of the results as the dominant carbon sources can be expected to differ across these water types. The “Shelf water” represented the mixing of waters from the East Greenland Current ($T \sim 1.5^\circ\text{C}$, $S < 34$) with warmer and more saline Atlantic water ($S > 34.4$). “Surface water” is influenced by runoff and the seasonal surface heating, while “Subsurface fjord” water represents the shelf water that has entered the fjord passing over the sill and gradually being mixed with the “Surface water.” We defined the “River plume waters” to be the fjord surface waters that were under direct influence of the river discharge. The change between the two periods is apparent in the T-S plot (Figure 2). The runoff was strongest in July and during the last river sampling on September 10 the flow from the glacial rivers (R1 and R2) had almost terminated, while Zackenberg river (R3) was still flowing until end-September. The inner stations were strongly affected by the river silt, with a high turbidity of surface water and the photic zone was therefore initially shallow at St. 1 and 2 (<5 and 10 m, respectively), however later in September it deepened to 25–35 m as turbidity decreased. The opposite trend was observed at the outermost station where the photic depth decreased from 35 to 10 m from July to October, due to the decreasing irradiation.

Bacterial Abundance and Chlorophyll *a*

While the central fjord was still ice-covered (Figure 1), the inner part was ice-free and a reduction in nutrients measured below the ice at St. 3; $\text{NO}_2^- + \text{NO}_3^-$, PO_4^{3-} , SiO_4 , in the surface (0.01, 0.33, 1 μM) compared to 100 m values (3.2, 0.7, 6.4 μM) indicated that a phytoplankton spring bloom had already initiated in the inner fjord prior to current sampling program. Chl *a* was highest (up to 3.1 $\mu\text{g L}^{-1}$) in the outer region of the fjord in July and August with a deep maximum at 20–40 m (Figure 3D), while in the late period chl *a* was highest in the inner fjord (Figure 3A). The average bacterial abundance (BA) in the surface water was $3.2 \pm 1.0 \times 10^5 \text{ mL}^{-1}$ and generally peaked at 0–20 m in the first period, with a maximum abundance in the outer fjord. BA was significantly higher in the upper 20 m for 19 out of 25 profiles, thus the BA maxima were decoupled from the chl *a*, especially in the first period where the chl *a* max was deep (20–40 m) (Figure 3). Overall only a weak significant linear correlation was found between BA and chl *a* ($r^2 = 0.03$, $p = 0.03$, $n = 164$). At the innermost station BA did not correlate with chl *a* at any time, but there was a positive correlation between BA and turbidity

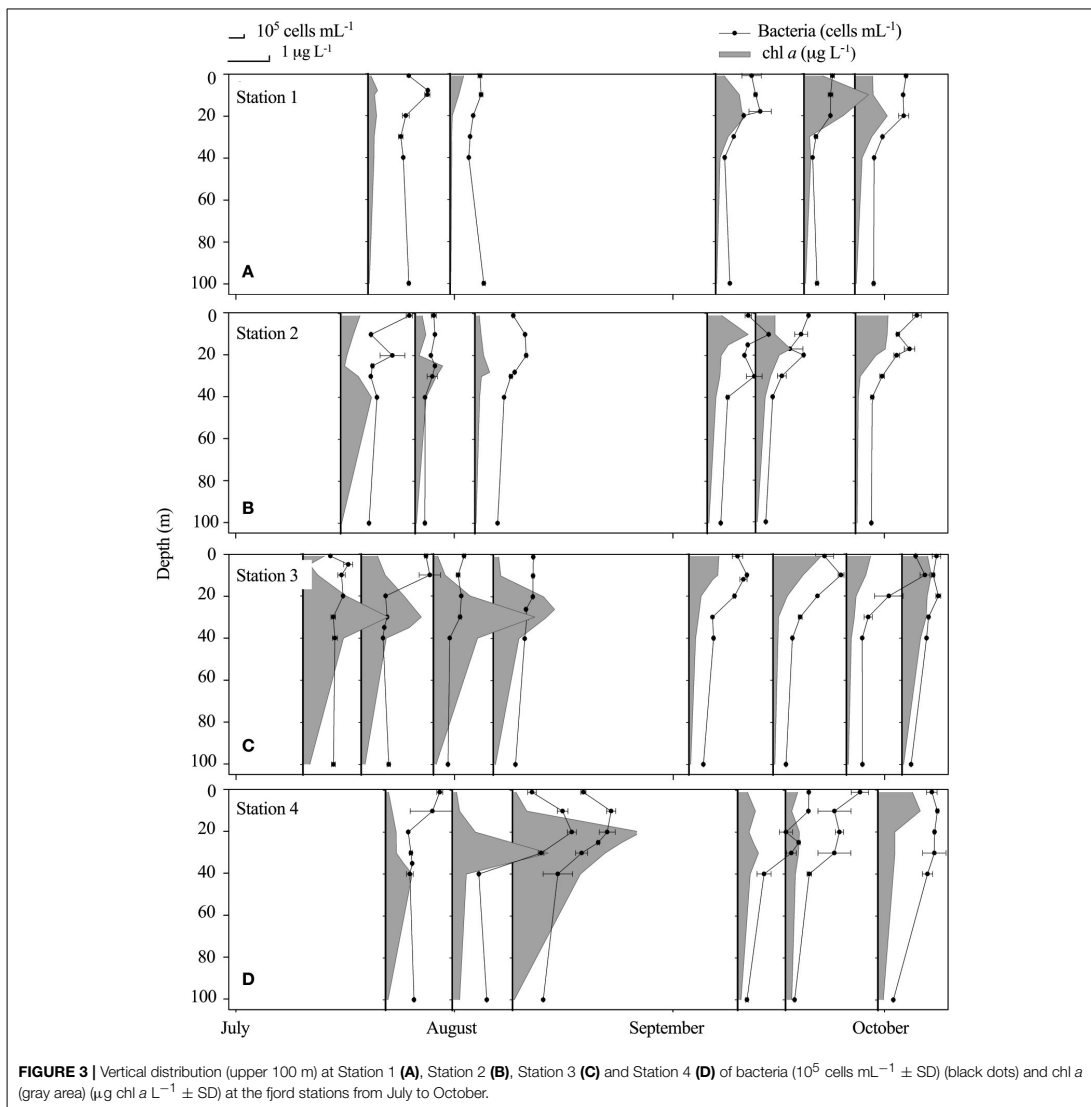
($r^2 = 0.757$, $p < 0.01$, $n = 31$). At the outermost station chl *a* correlated with BA during the study ($r^2 = 0.44$, $p < 0.01$). At the two mid-fjord stations (2 and 3), correlation between BA and chl *a* was found only after the runoff had ceased (St. 2: $r^2 = 0.83$, $p < 0.01$ and St. 3: $r^2 = 0.64$, $p < 0.01$). BA in the rivers was significantly lower than in the fjord surface waters (Table 3). Abundances ranged from a minimum of 1.3×10^5 in the glacial rivers (R1 and R2) to $6.4 \times 10^5 \text{ cells mL}^{-1}$ in R3 (Table 2). Note that only the free-living bacteria were enumerated.

Bacterial Production and Particle Association

Bacterial production (BP) was highest in the beginning of the sampling period (17–21 July) with a maximum of $2 \mu\text{g C L}^{-1} \text{ d}^{-1}$ in the river plume water (St.1 + 2, 1 m) (Table 2, Figures 4A,B). The third highest measure of BP ($1.7 \mu\text{g C L}^{-1} \text{ d}^{-1}$) was found in the fresh water layer just below the ice sampled on July 11. BP was lowest within the Shelf water at St. 4 where it remained below $0.09 \mu\text{g C L}^{-1} \text{ d}^{-1}$ throughout the entire study period, despite BA being relatively high. BP in the rivers was on average $0.39 \pm 0.07 \mu\text{g C L}^{-1} \text{ d}^{-1}$ and $0.32 \pm 0.06 \mu\text{g C L}^{-1} \text{ d}^{-1}$ in the first and the second period, respectively, and thus generally higher than those measured in the fjord despite low BA (Table 3). We found a larger fraction of BP in the R3 to be free-living (Table 2), which is possibly due to the presence of lakes acting as sedimentation basins. The contribution of particle-associated (>3 μm) bacterial production was considerable in both the fjord and rivers. In 17 out of 25 cases particle association was higher in the DCM sample than in the associated 1 m sample, however there was no significant difference between the %particle associations at the two depths (Figure 4).

Bacterial Carbon Demand and Primary Production

Only two of the BR measurements fulfilled all criteria for solid measurements of oxygen consumption throughout the incubation. These gave growth efficiency values of 7.3 ± 1.0 and $6.4 \pm 2.0\%$, during incubation at the *in situ* temperature of -1.1°C (St. 3, July) and at 3°C (St. 4), respectively. The average BGE of 6.9% was applied for determination of bacterial carbon demand (BCD) to allow comparison with the total amount of carbon fixed by planktonic primary production (PP). When integrated over the photic zone the estimated BCD:PP was on average 1.7 ± 1.2 across the sampling period, suggesting that bacterial carbon demand could not be sustained by the local phytoplankton production. There were no clear spatial or temporal trends in the BCD:PP ratio (Figure 5), and estimates were similar when integrated to 100 m. PP was highest initially and could support a high BCD at St. 1 and 3, while bacteria were not sustained by fresh PP initially at St. 2 and 4 in this period. Toward the end of the open water period different patterns developed as bacteria in the inner fjord could be sustained by fresh PP, while BCD was decoupled (up to 5 times higher) from PP at the outermost station (Figure 5). The dissolved fraction (<0.7 μm) of PP was in general high in the fjord and contributed 39–52% in the first period and less, 27–36%, in the late period.



The largest fraction contributed most at the outer station (max 32%) and in the last period it was never higher than 13%, whereas the fraction 0.7–10 μm became dominant in the late period (Figure 5).

Organic Matter Concentrations and C:N Ratios

DOC concentrations showed little systematic vertical variability except for the surface samples at 1 m, which had significantly lower concentrations in 19 out of 25 profiles (Figure S2). On

average, the DOC concentration decreased from the outer part to the inner fjord from $130 \pm 16 \mu\text{M}$ at St. 4 to $106 \pm 30 \mu\text{M}$ at St. 1 (Figure 6). From the first to the second sampling period where the mixed layer deepened, the DOC concentration at 1 m increased, while at the DCM there was a slight decrease. The DOC concentration was highest in the deep water types characterized as Subsurface fjord water ($101 \pm 20 \mu\text{M}$, $n = 49$) and slightly lower in the Surface water ($97 \pm 27 \mu\text{M}$, $n = 97$). The River water had significantly lower DOC ($40 \pm 13 \mu\text{M}$, $n = 24$), and thus the River plume water was diluted to an averaged concentration of

TABLE 2 | River properties presented as average \pm SD (n varies from 3 to 6) for each of the two time periods.

Average \pm SD	First period (July-August)			Second period (September)		
	Tyroler river (R1)	Clay bay (R2)	Zackenber river (R3)	Tyroler river (R1)	Clay bay (R2)	Zackenber river (R3)
Temperature ($^{\circ}$ C)	3.4 \pm 0.1	2.3 \pm 0.5	5.3 \pm 1	0.1	0.2	2.9
NO ₂ ⁻ +NO ₃ ⁻ (μ M)	1.7 \pm 0.7	1.4 \pm 0.7	0.5 \pm 0.3	1.7 \pm 0.2	0.06 \pm 0.03	1.5 \pm 0.15
PO ₄ ³⁻ (μ M)	0.4 \pm 0.2	0.5 \pm 0.1	0.08 \pm 0.04	0.2 \pm 0.01	0.2 \pm 0.04	0.6 \pm 0.1
H ₄ SiO ₄ (μ M)	5.8 \pm 1.8	12.4 \pm 1.9	9.8 \pm 3.8	33.3 \pm 1.9	40.2 \pm 4.1	16.4 \pm 0.4
BA (cells mL ⁻¹) x10 ⁵	1.8 \pm 1.0	1.3 \pm 0.03	2.7 \pm 0.15	NA	NA	6.4 \pm 0.1
%Alphaproteobact.	10	4 \pm 1	4 \pm 1	4 \pm 2	1	10 \pm 5
%Betaproteobact.	14	7 \pm 1	24 \pm 7	47 \pm 0.4	5	7 \pm 2
%Gammaproteobact.	44	50 \pm 35	49 \pm 5	21 \pm 1	87	34 \pm 6
%Cyanobact.	1.1	2.3	0.7	0.2	0.7	1.8
DOC (μ M)	47 \pm 13	34 \pm 16	46 \pm 6	36 \pm 10	36 \pm 5	27 \pm 2
DOC:DON	10 \pm 2	7.5 \pm 2	8.5 \pm 1	10 \pm 4	6 \pm 1.5	6 \pm 1.8
POC (μ g C L ⁻¹)	44	32.9 \pm 5.9	75.8 \pm 64	28.1	71.2	52.4
POC:PON	7.2	4.8 \pm 0.5	4.9 \pm 1.3	4.8	6.5	6.3
BP (μ g C L ⁻¹ d ⁻¹)	0.25 \pm 0.06	0.13 \pm 0.03	0.5 \pm 0.2	0.06 \pm 0.02	1.1 \pm 0.29	0.17 \pm 0.02
BG (d ⁻¹)	0.65 \pm 0.5	0.13	1.94 \pm 0.2	NA	NA	0.013 \pm 0.00
%Particulate BP	74.5 \pm 20%	72.5 \pm 15%	64.6 \pm 13%	93%	94%	13%
%BDOC	39 \pm 2%	39 \pm 8%	29 \pm 8%	9%	45%	37%

Where there is no SD, only one sample was available.

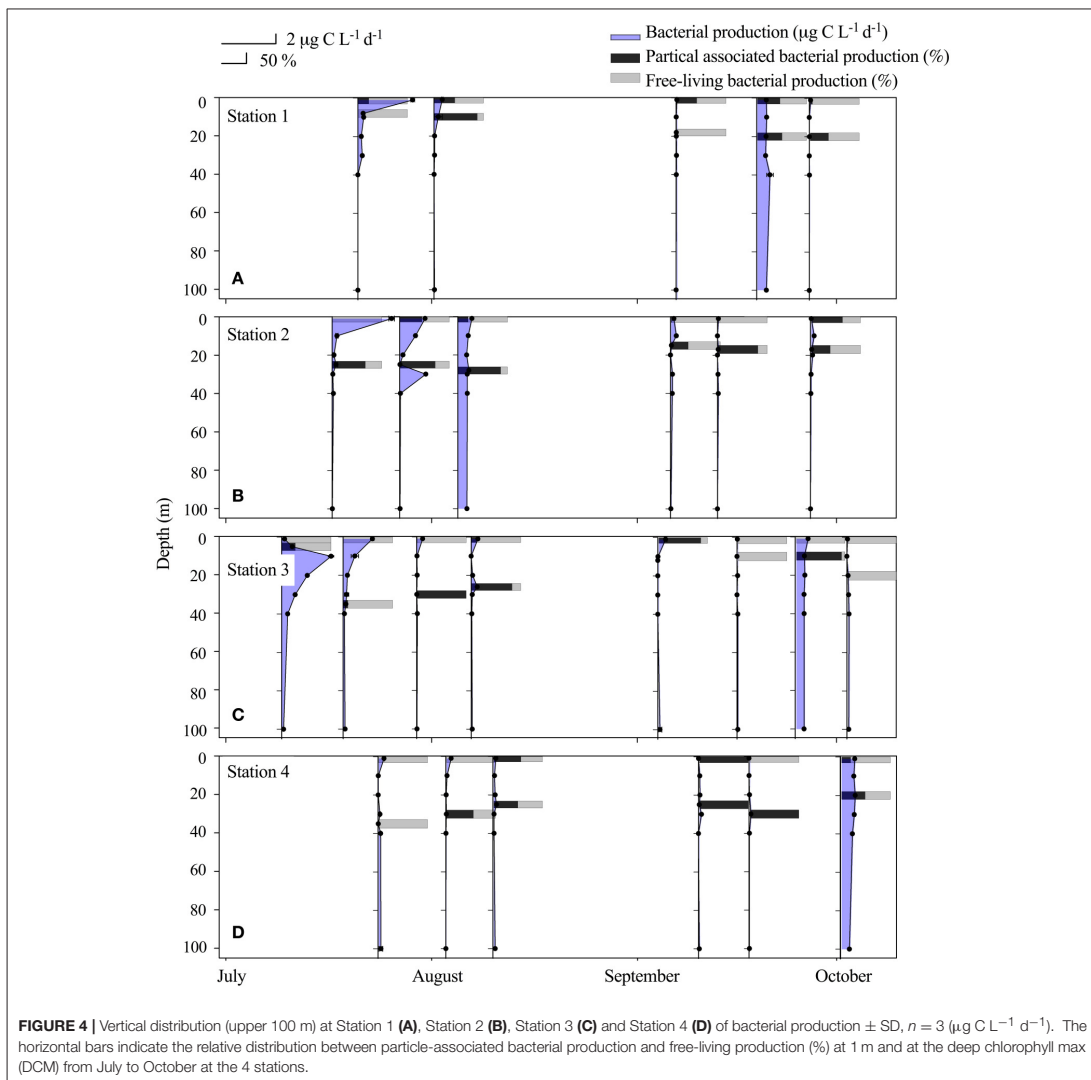
TABLE 3 | Water type characteristics and properties shown as average \pm SD of the 5 water types for each of the two periods.

Average \pm SD	First period (July-August)					Second period (September-October)			
	River water	River plume water	Surface water	Subsurface fjord water	Shelf water	River water	Surface water	Subsurface fjord water	Shelf water
Temperature ($^{\circ}$ C)	3.7 \pm 1.4	6.1 \pm 2	0.3 \pm 1.2	-1.4 \pm 0.2	-1.6 \pm 0.01	1.2 \pm 1.3	0.2 \pm 1.1	-1.5 \pm 0.2	-1.6 \pm 0.01
Salinity	NA	19.3 \pm 3.4	30.9 \pm 1.1	32.1 \pm 0.1	33.6 \pm 0.1	NA	29.2 \pm 1.4	32.2 \pm 0.2	33.5 \pm 0.04
NO ₂ ⁻ +NO ₃ ⁻ (μ M)	1.2 \pm 0.74	0.08 \pm 0.09	0.36 \pm 0.42	1.9 \pm 1.4	6.4 \pm 1.1	1 \pm 0.7	0.4 \pm 0.7	3.2 \pm 1.2	5.6 \pm 0.2
PO ₄ ³⁻ (μ M)	0.29 \pm 0.2	0.24 \pm 0.1	0.48 \pm 0.3	0.61 \pm 0.3	1.18 \pm 0.5	0.35 \pm 0.2	0.38 \pm 0.1	0.64 \pm 0.1	0.62 \pm 0.2
H ₄ SiO ₄ (μ M)	9.52 \pm 3.8	6.12 \pm 2.4	2.12 \pm 1.7	3.91 \pm 1.8	6.66 \pm 0.4	29.57 \pm 10.9	3.77 \pm 0.7	6.36 \pm 1.5	6.5 \pm 0.1
Chl <i>a</i> (μ g L ⁻¹)	NA	0.2 \pm 0.15	0.28 \pm 0.3	0.7 \pm 0.79	0.09 \pm 0.06	NA	0.5 \pm 0.3	0.2 \pm 0.1	0.3 \pm 0.03
BA (cells mL ⁻¹) x10 ⁵	0.6 \pm 0.9	2.8 \pm 1.5	3.3 \pm 1.8	2.3 \pm 1.4	2.1 \pm 0.2	0.6 \pm 0.004	2.8 \pm 1.1	1.1 \pm 0.3	6.4 \pm 1
%Alphaproteobact.	5 \pm 3	12 \pm 8	14 \pm 9	6 \pm 3	NA	6 \pm 5	18 \pm 6	NA	NA
%Betaproteobact.	15 \pm 9	28 \pm 27	21 \pm 23	1 \pm 1	NA	23 \pm 22	10 \pm 14	NA	NA
%Gammaproteobact.	49 \pm 18	55 \pm 23	54 \pm 18	80 \pm 8	NA	40 \pm 28	55 \pm 18	NA	NA
%Cyanobact.	1.2	2.6	2.1	0	0	1	2.7 \pm 1.7	0	0
DOC (μ M)	42 \pm 14	67 \pm 13	107 \pm 24	105 \pm 20	89 \pm 15	33 \pm 7	93 \pm 24	90 \pm 17	93 \pm 3
DOC:DON	8.6 \pm 1.8	11 \pm 1.9	12.3 \pm 2.1	13 \pm 2.4	12.5 \pm 0.5	6 \pm 4	14 \pm 4	18 \pm 6	29 \pm 3
POC (μ g C L ⁻¹)	56.2 \pm 50	23.5 \pm 7.3	24.3 \pm 9	26.6 \pm 10.6	25 \pm 13	53.4 \pm 16.7	22.9 \pm 5.5	19.3 \pm 5.9	11.8 \pm 4.6
POC:PON	4.9 \pm 3.5	5.6 \pm 0.5	5.5 \pm 0.5	6.5 \pm 0.9	7.2 \pm 0.3	6.0 \pm 0.7	7.9 \pm 1.1	8.7 \pm 2.2	7.4 \pm 3.1
BP (μ g C L ⁻¹ d ⁻¹)	0.39 \pm 0.07	0.92 \pm 0.69	0.13 \pm 0.13	0.14 \pm 0.15	0.06 \pm 0.04	0.32 \pm 0.06	0.06 \pm 0.06	0.02 \pm 0.02	0.02 \pm 0.01
BG (d ⁻¹)	0.92 \pm 0.63	0.17 \pm 0.12	0.03 \pm 0.04	0.02 \pm 0.06	0.01 \pm 0.01	0.013 \pm 0.00	0.01 \pm 0.02	0.01 \pm 0.01	0.02 \pm 0.01
%Particulate BP	70 \pm 17	20 \pm 18	42 \pm 36	59 \pm 26	NA	67 \pm 38	24 \pm 30	NA	NA
%BDOC	35.6 \pm 8.2	11 \pm 3.4	7.9 \pm 3.5	5.3 \pm 1.8	NA	30 \pm 15	18 \pm 7	NA	NA

Note Shelf water was only found at 100 m depth. Where there is no SD, only one sample was available.

67 \pm 13 μ M, n = 7. DOC:DON was also lowest in the River water (8 \pm 2) and the River plume water (11 \pm 2), while the Shelf water had a significantly higher C:N ratio (21 \pm 8) (Table 3).

Maximum POC concentration was found in the rivers with up to 14 μ M, while in the fjord a maximum of 4 μ M POC was found at the DCM. In the fjord the particulate fraction (%) of the total organic matter was in general minor (avg. 2.3 \pm 1, max = 5%),



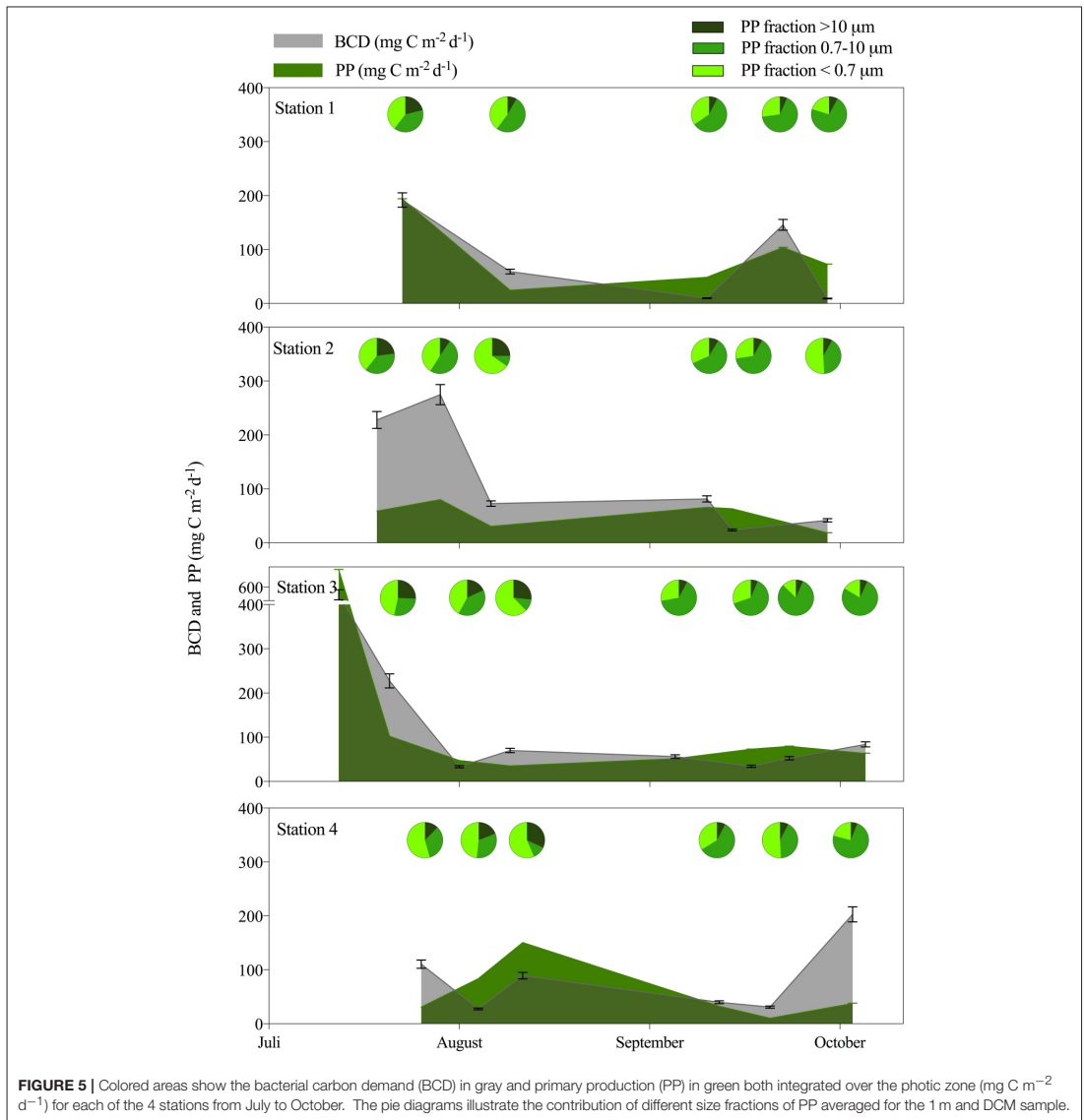
while in the rivers the contribution of POC was significant (avg. 13 ± 8 , max = 35%) (Tables 2, 3). This gave a significant negative relationship between salinity and POC ($r^2 = 0.3$, $p < 0.001$, $n = 86$). POC did not correlate with chl *a*, turbidity or to particulate bacterial production. The C:N ratio of the particulate matter was significantly lower in the rivers than in the fjord ($p = 0.047$, *F*-test). In the fjord, the C:N ratio increased from the first period to the end of the open water season ($p = 0.0023$, *F*-test), whereas no trend was observed in the rivers.

Inorganic nitrogen ($\text{NO}_2^- + \text{NO}_3^-$) was the limiting inorganic nutrient for primary production and was reduced to $0.4 \mu\text{M}$ in the surface water during the entire period, while the background

level in the Shelf water was ca. $6 \mu\text{M}$ (Table 3, Figure S2). Ammonium (NH_4^+) was only measured at St. 3 and ranged between 0.05 and $0.4 \mu\text{M}$, with a maximum at 40 m (below DCM).

Bioavailability of DOM

Despite the increase in average DOC concentration from St. 1 to 4, there was a slight decrease in the concentration of BDOC from 19 ± 10 to $11 \pm 8 \mu\text{M}$ from St. 1 and 4, respectively (when values were averaged for 1 m and DCM over the entire period). The fraction of BDOC relative to total DOC (%BDOC) thus decreased from the inner to the outer part of the fjord (Figure 6).

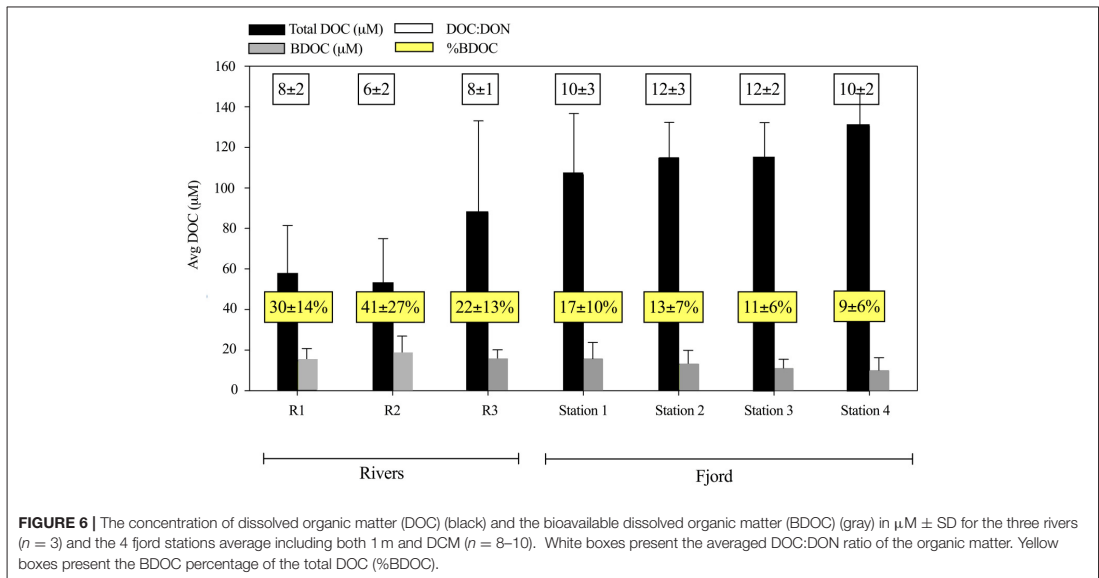


BDOC concentrations in the rivers were relatively high (avg. $18 \pm 8 \mu\text{M}$), resulting in significantly higher %BDOC in the rivers than in the fjord ($p < 0.005$, t -test) (Figure 6, Table 3). Averaging %BDOC within each water type revealed a decrease as river water was mixed with the fjord water, i.e., River water \rightarrow River plume \rightarrow Surface water \rightarrow Subsurface water (Table 3). There was a significant negative correlation between the relative abundance of C to N (DOC:DON) and %BDOC ($r^2 = 0.17$, $p = 0.08$, $n = 42$). C:N ratios were generally higher in the last

period and the highest C:N of 29 ± 3 was found in the Shelf water.

Bacterial Community Composition

In general, Proteobacteria were the most abundant bacteria phylum in both fjord and river samples ($\sim 86\%$ of the bacterial phylum). Differences in community composition were observed at class level, with fjord DCM samples containing more Alphaproteobacteria than the rivers and the Subsurface



water being strongly dominated by Gammaproteobacteria (80%), opposed to surface samples and rivers samples with a higher share of Betaproteobacteria (Table 3). Cyanobacteria were present in all rivers and constituted up to $2.7 \pm 1.7\%$ of the microbial community in the innermost stations. Alpha diversity (described by the Shannon index) ranged from 4.9 to 9 (Table S2) indicating a greater diversity in the rivers and lowest in fjord samples from July and August (Figure 7). A redundancy analysis (including spatial and temporal parameters) was performed to identify factors that significantly affect bacterial community composition. This explained 47.2% of the total variation in the OTU data, with “water type” (19.5%; river (13%), $p = 0.002$) and time of sampling expressed as “month” (10.8%; September (8.5%), $p = 0.002$) being the most significant variables. As “station” generally explained <5% this variable was not included. Samples from all three rivers with overall higher species richness clustered together. The majority of the September fjord samples clustered tightly together, independent of their respective water types and differences between surface and DCM were minimal. Samples from July and August however clustered according to sample depth (i.e., surface or DCM) (Figure 7). Explanatory variables (water type, month and station) explain in total less than 50% of the variation in diversity for the entire data set.

To elucidate changes in community composition throughout the fjord the complexity of the dataset was reduced by constraining a phylogenetic analysis to only include the most abundant bacterial taxa (relative abundance >1%). Further the temporal factor was reduced by restricting the analysis to cover a 10-day period in early August (Figure 8). The heat map shows that all three rivers were very different from the fjord community, and that each river had unique taxa as the most abundant

(blue = high, red = low relative abundance). While bacteria found in R1 (with the closest connection to the Greenland Ice Sheet) all could be found in the two other rivers, the R3 (that runs through vegetation-covered catchment area) included some unique families e.g., *Granulosicoccaceae*, *Alcaligenaceae*, and an unknown family from the order vadinha64 (the latter presented as “uncultured_bacterium” from the class Opitutae in Figure 8). In early August the majority of the most abundant river taxa were absent in the fjord samples, with the exception of R1 that shared a great number of its most abundant taxa with the nearby Station 1 surface sample which had more unique taxa than any other station (Figures 1, 8). Stations 2, 3, and 4 showed a higher number of shared taxa indicating a gradient from the inner to the outer fjord. The opposite was observed for the deeper DCM samples, which showed a gradual decrease of certain taxa from the outer St. 4 toward the innermost St. 1.

The SourceTracker analysis (including the full dataset at OTU level) showed clear contribution of especially the R1 community to the surface fjord stations with maxima of 75, 63, and 66% similarity at St. 1, 3, and 4, respectively in July-August and ca. 40% in September (Figure 9). The coastal community (source set as St. 4 DCM) entering the outer part of the fjord dominated strongly in the deeper fjord samples throughout the entire study (Figure 9 and Table S1). However, the coastal communities also dominated at the surface waters of St. 2 in the first period, where R1 only contributed 15%. As the R1 community was also present in R2 and R3, overall river contribution is incorporated in the R1 plot (Figures 9A,B). The community unique to R2 and R3 only contributed to minor degree (7–15%) to the fjord surface community.

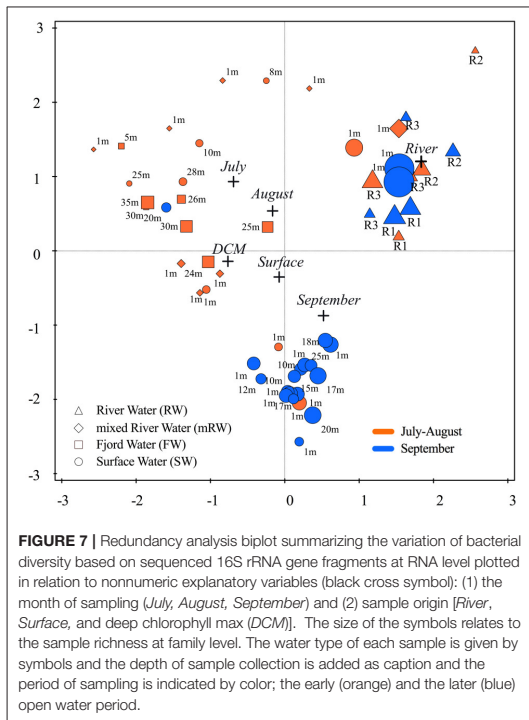


FIGURE 7 | Redundancy analysis biplot summarizing the variation of bacterial diversity based on sequenced 16S rRNA gene fragments at RNA level plotted in relation to nonnumeric explanatory variables (black cross symbol): (1) the month of sampling (July, August, September) and (2) sample origin [River, Surface, and deep chlorophyll max (DCM)]. The size of the symbols relates to the sample richness at family level. The water type of each sample is given by symbols and the depth of sample collection is added as caption and the period of sampling is indicated by color; the early (orange) and the later (blue) open water period.

In order to investigate the influence of environmental parameters exerted on the bacterial community structure, we performed canonical correspondence analysis (CCA) between numerical factors, such as bacterial production, chl *a* fluorescence, temperature, salinity, DOC, and %BDOC, (Figure S2). Due to the complexity of the dataset no strong correlations were found with this analysis. However, when single taxa were correlated to specific environmental parameters we found that especially genera from the class Gammaproteobacteria showed correlations with specific DOM characteristics e.g., a strong positive correlation was found between the genus *Glaciecola* (order: Alteromonadales) and bacterial production ($r^2 = 0.5283$; $p < 0.0001$) with a maximum relative abundance of 25% when BP was highest. Another unknown genus from the order Alteromonadales showed a positive correlation with %BDOC ($r^2 = 0.2720$; $p < 0.0075$).

DISCUSSION

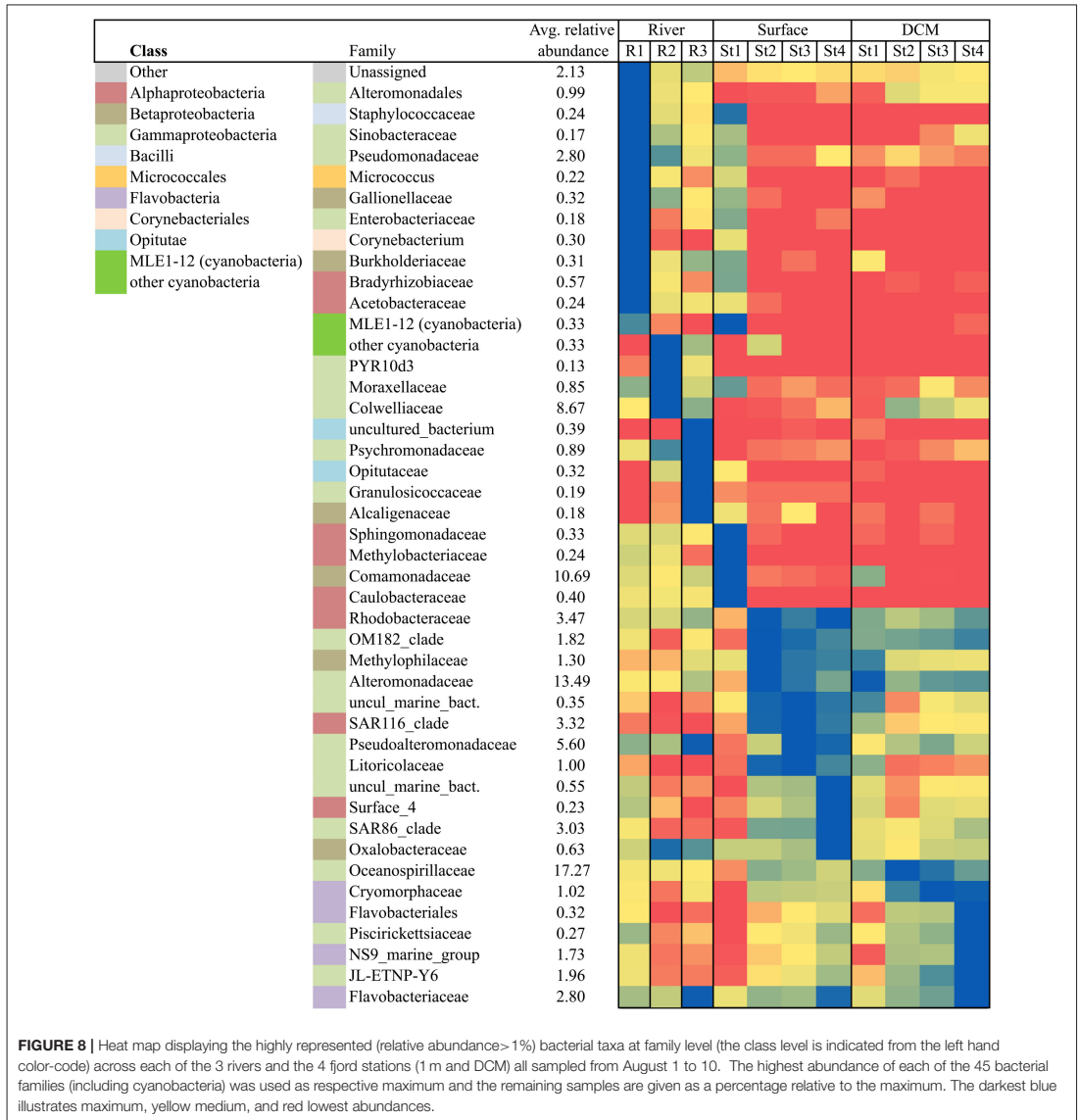
Bioavailability of Allochthonous DOM Sources

River input in marine systems are often a source of high DOM concentrations and therefore DOM often correlate negatively to salinity (Cauwet, 2002). The Young Sound system however deviates from this trend due to two factors. Firstly the freshwater

input in fjord has low DOC concentrations due to the dominance of glacial meltwater and limited catchment vegetation. Secondly, we hypothesize that the coastal shelf waters entering the fjord are characterized by high levels of terrestrial organic matter that originates predominantly from Siberian rivers (we did however not sample sufficiently deep at St. 4 to capture the pure Polar water). These rivers discharge into the Arctic Ocean (Amon and Budéus, 2003) and the terrestrial DOC is retained in the surface waters exiting the Arctic Ocean via the Fram Strait as part of the East Greenland Current (Granskog et al., 2012). A large fraction of the terrestrially derived DOM transported by the major rivers Ob and Yenisei is found to be refractory (Meon and Amon, 2004), which explain the low bacterial activity and low DOC bioavailability we found in the Shelf water despite high concentrations. These conditions therefore result in a positive correlation between DOC and salinity ($r = 0.51$, $p < 0.001$, $df = 175$) in Young Sound.

In addition to the quantitative difference, the qualitative C:N ratio of the two allochthonous DOM sources differ. The ratio between bioavailable DOC and inorganic nitrogen exceeded the Redfield ratio (C:N:P = 106:16:1) by thousand fold, whereas the BDOC:PO₄³⁻ ratio was 45 ± 30 . This emphasizes the importance of DON as the main source of nitrogen for bacteria. The low C:N ratios in the river water resemble those reported from Alaskan glacial rivers, where the relatively high source of DON is explained by microbial production of protein-rich DOM in the subglacial environment (Hood and Scott, 2008). The concentration of bioavailable DOM in the rivers entering Young Sound was slightly lower than values obtained in Alaskan glacier outflow (Hood et al., 2009), but very similar to other studies from the Greenland ice sheet meltwater (Lawson et al., 2014). In contrast to the river DOC, the allochthonous DOC entering the fjord from the open ocean had high C:N ratios, similar to Arctic surface water (Benner et al., 2005). Together, our results demonstrate that open ocean DOC is less labile than the DOC produced in the fjord and that supplied from the rivers.

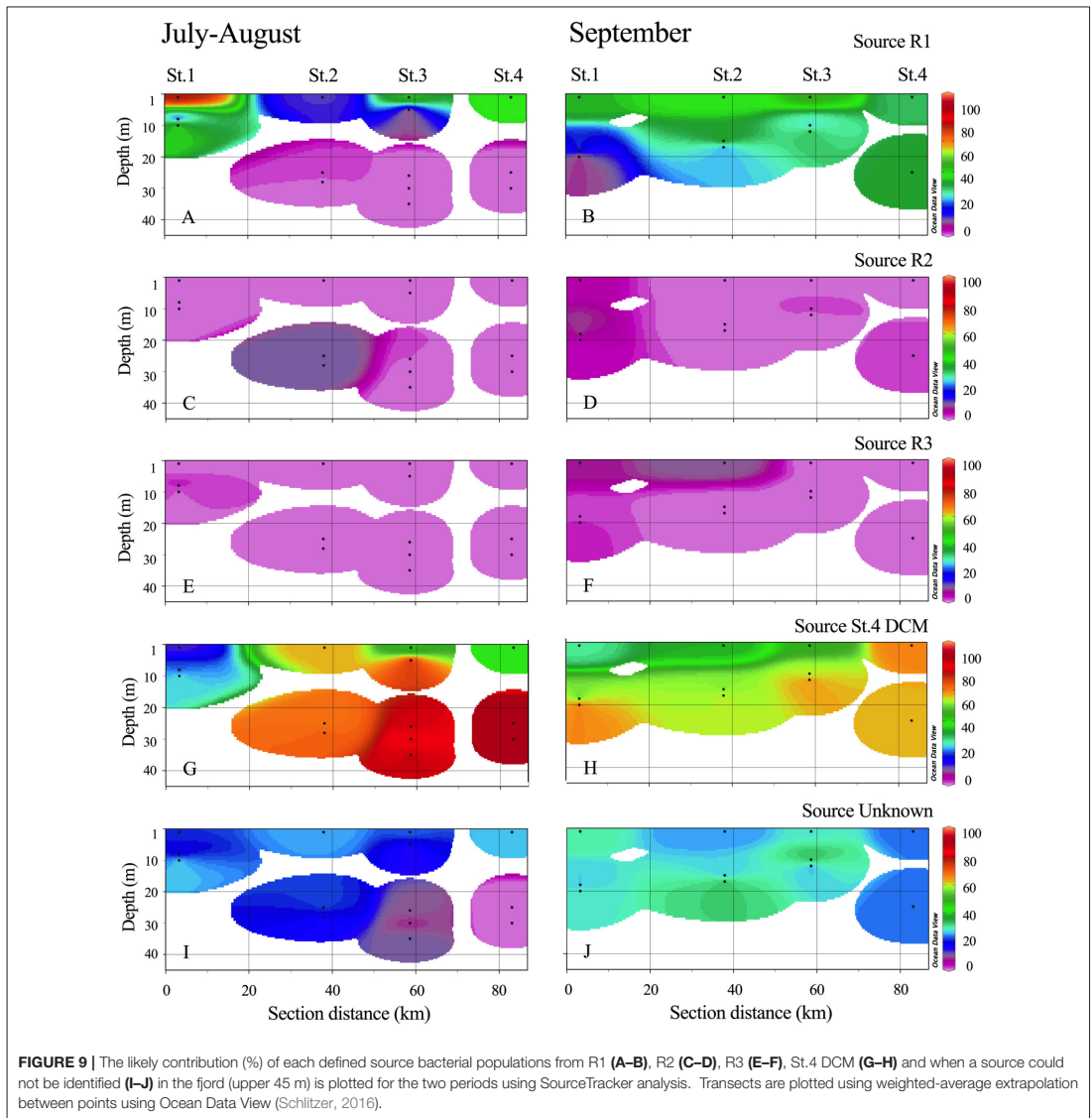
As expected the load of particulate organic carbon was relatively high in the rivers (Hood et al., 2015). However a high POC-signal was not traceable in the surface water of the inner fjord stations as was the case e.g., for the silt particles (measured as turbidity) and silicate. This indicates that the POC has been lost from water column either by sedimentation, dissolution or bacterial degradation. Bioavailability of POC was not determined, and BDOC values thus potentially represent an underestimation of labile organic carbon concentration. However, since POC on average accounted for $2.3 \pm 1.0\%$ and $13 \pm 8\%$ of total DOC in the fjord and rivers, respectively, the contribution of bioavailable POC to total bioavailable carbon is probably relatively small. The spatial gradient in %BDOC along the fjord transect suggests a gradual consumption of the labile DOC entering the fjord via the rivers. Consumption of riverine DOC in the fjord is supported by the high BP in the river and river plume water (Table 3) and the negative correlation of BP to salinity. The differences in DOM concentration and composition has been suggested as a driver for diversification of bacterial communities (Crump and Hobbie, 2005; Blanchet et al., 2016; Roiha et al., 2016). Our study



suggests that the labile character of the river-DOM may have a role stimulating and shaping the activity and structure of bacterial communities in the fjord, by favoring fast growing bacteria. In samples where the community structure was analyzed, high BP was negatively correlated to salinity ($r^2 = 0.2743$; $p < 0.0103$). Further, high bacterial production was associated with growth of specific taxa, such as a positive correlation between BP and the relative abundance of the genus *Glaciicola*.

Bacterial Community Composition

In general, our results suggest that the bacterial community is largely structured by the different water sources to the fjord and changes along the salinity gradient, as also found in other coastal environments (del Giorgio and Bouvier, 2002; Crump and Hobbie, 2005; Gutiérrez et al., 2015). Especially in the early period large differences were observed between 1 m and DCM bacterial communities, which were explained by the



strong stratification at 5–7 m in this period (Figure S1). This resulted in lower species richness during stratification in July and August (Figure 8), possibly because bacterial communities exhibit environmental niche partitioning when the water masses remain separated in this period (Morris et al., 2005; Delong et al., 2006; Chow et al., 2013; Salter et al., 2014). As river runoff decreased and mixing events increased (September) the resemblance between communities at 1 m and DCM naturally increased. One specific strong storm that lasted for several days

(21–26 September) may explain the high similarity of 1 m surface samples from St. 1 and 2 to the river samples (Figure 8), as samples were collected immediately after the storm where the disturbance apparently caused transport of terrestrial bacteria to the fjord (Crump and Hobbie, 2005).

In temperate and Polar Regions Flavobacteria often dominate during phytoplankton bloom (Wilson et al., 2017). We also found this group to dominate when chl *a* concentrations were high (i.e., DCM samples at St. 4), while they contributed only marginally

(<0.1%) to the total bacterial community in the remaining fjord and particularly little in the rivers (Figure 8). Cyanobacteria were relatively abundant in the glacial runoff and can be considered as freshwater tracer, since marine cyanobacteria are usually not found in these Arctic regions (Paulsen et al., 2016). The bacterial communities in the rivers were highly specific to each of them (Figure 8), which we suggest is due to their difference in origin and catchment area; close connection (0.5 km) to the Greenland Ice Sheet (R1), longer distance (2 km) from smaller local glacier (R2), and the lowland vegetation rich river with lake connection (R3). This is in agreement with a recent study from West Greenland that similarly show distinct communities in rivers and a proglacial lake over a 2 km distance (Hauptmann et al., 2016), and find less terrestrial species in river samples with a more direct connection to glaciers.

In the present study R1 has the closest connection to the glacier and all the bacterial families found in R1 were also found in the two other rivers. The SourceTracker analysis (Figure 9) revealed that the R1 community had the far most influence on the surface water, despite not being the largest river. The species unique to R3 hardly contributed to the fjord community, despite being the largest river in terms of volume. This suggests that there is a higher potential for the glacial bacterial community to persist in the fjord than terrestrial communities. Gutiérrez et al. (2015) also found persistence of specific bacterial communities in the surface water of a glacier influenced fjord in Patagonia, and suggested that the glacial meltwater community in the surface was maintained by the competitive advantage of tolerating the cold fresh conditions. Given the averaged doubling time of bacteria in the surface water of Young Sound of 11 ± 7 days (fastest doubling time of 0.9 days) and a transport time of 14–30 days from innermost to the mouth of the fjord, the persistence of the specific communities may be a result of fast transport within the surface water and limited mixing. The differentiation between surface and subsurface communities was lost when the thermal stratification broke down in present study and in Gutiérrez et al. (2015).

Annual Estimations of Carbon Production and Turnover in Young Sound

Due to the strong stratification, high turbidity and input of allochthonous carbon sources, relatively heterotrophic conditions were expected to prevail in the fjord system as concluded in Nielsen et al. (2007). The seasonal and spatial resolution of bacterial carbon demand and primary production allowed a rough, but more robust than previous estimates of the annual carbon budget in Young Sound (Rysgaard and Nielsen, 2006; Nielsen et al., 2007), as previous studies cover a shorter period of the productive season and use a literature BGE of 33%. However, the present study did not cover the early productive season during ice cover in June. As an attempt to account for that we extrapolate the carbon uptake and primary production during the ice-covered productive period using the values obtained on July 11 at St. 3 during ice-cover and by assuming a productive period of 125 days. Based on these assumptions, the annual bacterial production amounted to $1.3 \text{ g C m}^{-2} \text{ year}^{-1}$, corresponding to a carbon demand of $18 \text{ g C m}^{-2} \text{ year}^{-1}$ in the upper 100 m. This BP value is ~ 3 times lower than a previous

estimate of net annual bacterial production in Young Sound of $4.2 \text{ g C m}^{-2} \text{ year}^{-1}$, based on measurements conducted during ice-cover at St. 3 (Rysgaard and Nielsen, 2006), emphasizing that the conditions at St. 3 in June are not representative for the late open water period (August–October) or for the entire Fjord system.

The assessment of bacterial carbon demand rely greatly on estimates of BGE, which is known to depend on a number of factors including DOC composition and lability, bacterial community and temperature, thus it is important to emphasize that BGE is likely to vary across time and space in Young Sound. The BGE we found (6.9%) is low, but still in line with other Arctic studies ranging from $2.2 \pm 2.1\%$ in the Chucki Sea (Cota et al., 1996), $6.3 \pm 3\%$ in the Fram Strait (Kritzberg et al., 2010), $19.1 \pm 9.5\%$ in the rivers Ob, Yenisei and the adjacent Kara Sea (Meon and Amon, 2004) and $9.5 \pm 8.7\%$ in Kobbefjord, Greenland (Middelboe et al., 2012).

The bacterial carbon demand on average exceeded primary production during the study period (Figure 5) and indicated that only about 30% of the PP is dissolved and thus potentially available for bacterial uptake. Further, protist and copepod grazing of phytoplankton consumed a substantial fraction of the particulate PP (Middelboe et al. submitted; Arendt et al., 2016). Even though some of the particulate primary production are eventually degraded by pelagic bacteria as detrital matter, our results strongly indicated that primary production could not sustain bacterial carbon demand in the fjord within the productive 125 days and much less on an annual basis. Consequently, the allochthonous DOM sources contributes significantly to the bacterial carbon turnover in Young Sound.

The current study presents an overview of the organic carbon sources and their turnover in the high Arctic Young Sound. Further it highlights that the meltwater associated bacterial community from the glacial rivers persists and is actively transforming the river-DOM within the freshwater lens. The calculations of annual carbon production and turnover are obviously associated with large uncertainties regarding extrapolations across time and space and use of factors for converting thymidine incorporation to carbon production and net bacterial production to carbon demand. However, by applying a high temporal and spatial resolution of sampling and on-site estimation of BGE, this study provides a relatively solid estimation of the annual carbon budget in a high Arctic Fjord compared to previous studies. The fjord is net heterotrophic and in future scenarios with increasing temperatures the relative contribution of riverine DOC is expected to increase, driving the system toward more heterotrophic conditions. However, more measurements of bacterial growth efficiency and factors controlling this are required to provide more solid budget estimates of bacterial carbon consumption on an ecosystem scale.

AUTHOR CONTRIBUTIONS

MP and SN led the collection and analysis of data and the writing of the paper with equal contribution. MM led the planning of the study, and contributed with sample collection, data analysis and contributing greatly to the writing of the paper. OM led the collection, laboratory work and analysis of the molecular data.

SM led the planning and calculations of primary production. AD led the collection and measurements of POC and PON. All other authors contributed to writing the paper. In addition EM, AL, TJ, and MS helped collecting data and CS helped analysing the organic matter samples.

FUNDING

This study was funded by research grants from the Danish Ministry of the Environment (DANCEA), the project MicroPolar (RCN 225956) funded by the Norwegian Research Council, Carlsberg Foundation and the Arctic Research Centre at Aarhus University. CS was funded by the Danish Research Council for Independent Research (DFR 1323–00336). The Arctic Science Partnership and the Greenland Ecosystem Monitoring program facilitated this work.

ACKNOWLEDGMENTS

Big thanks to Egon Frandsen, Kunuk Lennert, and Ivali Lennert for organization, expertise in the area and technical assistance in the field and to Johan the polar fox for entertainment. We are

grateful to be able to include data from the Greenland Ecosystem Monitoring Programme were provided by the Department of Bioscience, Aarhus University, Denmark in collaboration with Department of Geosciences and Natural Resource Management, Copenhagen University, Denmark.

SUPPLEMENTARY MATERIAL

The Supplementary Material for this article can be found online at: <http://journal.frontiersin.org/article/10.3389/fmars.2017.00176/full#supplementary-material>

Figure S1 | Profiles of salinity, temperature (°C), DOC (μM), DOC:DON and the concentration of nutrients $\text{NO}_2^- + \text{NO}_3^-$ and Si (μM) at the 4 stations in the periods from July–August (red colors) and September–October (blue colors).

Figure S2 | Canonical correspondence analysis (CCA) for sequencing data of 16S rRNA gene fragments at RNA level (most abundant OTUs >1%). Arrows indicate selected environmental variables: bacterial production, dissolved organic carbon (DOC), percent bioavailable dissolved organic carbon (%BDOC), fluorescence, temperature and salinity. The OTUs selected for further analysis are labeled with their genus classification.

Figure S3 | Time-series measurements from Zackenberg River of temperature (°C), Sediment (mg L^{-1}), LOI (mg L^{-1}) (LOI is organic matter determined by Loss On Ignition when heated at $105^\circ\text{C} \approx$ particulate organic matter), DOC (μM). Data is collected by Greenland Ecosystem Monitoring, the GEOBASIS Programme.

REFERENCES

- Amon, R. M. W., and Benner, R. (1996). Bacterial utilization of different size classes of dissolved organic matter. *Limnol. Oceanogr.* 41, 41–51. doi: 10.4319/lo.1996.41.1.0041
- Amon, R. M. W., and Budéus, G. (2003). Dissolved organic carbon distribution and origin in the Nordic Seas: exchanges with the Arctic Ocean and the North Atlantic. *J. Geophys. Res.* 108, 1–17. doi: 10.1029/2002JC001594
- Anderson, L.G. (2002). "DOC in the Arctic Ocean," in *Biogeochemistry of Marine Dissolved Organic Matter*, eds D. A. Hansell and C. A. Carlson (Academic Press Inc.), 665–683.
- Apple, J. K., del Giorgio, P. A., and Kemp, W. M. (2006). Temperature regulation of bacterial production, respiration, and growth efficiency in a temperate salt-marsh estuary. *Aquat. Microb. Ecol.* 43, 243–254. doi: 10.3354/ame.043243
- Arendt, K. E., Agersted, M. D., Sejr, M. K., and Juul-pedersen, T. (2016). Glacial meltwater influences on plankton community structure and the importance of top-down control (of primary production) in a NE Greenland fjord. *Estuar. Coast. Shelf Sci.* 183, 123–135. doi: 10.1016/j.ecss.2016.08.026
- Bañá, Z., Ayo, B., Marrasé, C., Gasol, J. M., and Iriberry, J. (2013). Changes in bacterial metabolism as a response to DOM modification during protozoan grazing in coastal Cantabrian and Mediterranean waters. *Environ. Microbiol.* 16, 498–511. doi: 10.1111/1462-2920.12274
- Bendtsen, J., Mortensen, J., and Rysgaard, S. (2014). Seasonal surface layer dynamics and sensitivity to runoff in a high Arctic fjord (Young Sound/Tyrolerfjord, 74°N). *J. Geophys. Res. Ocean.* 119, 6461–6478. doi: 10.1002/2014JC010077
- Benner, R., Louchouart, P., and Amon, R. M. W. (2005). Terrigenous dissolved organic matter in the Arctic Ocean and its transport to surface and deep waters of the North Atlantic. *Global Biogeochem. Cycles* 19, 1–11. doi: 10.1029/2004GB002398
- Blanchet, M., Pringault, O., Panagiotopoulos, C., Lefe, D., Fernandez, C., Aparicio, F. L., et al. (2016). When riverine dissolved organic matter (DOM) meets labile DOM in coastal waters: changes in bacterial community activity and composition. *Aquat. Sci.* 79, 27–43. doi: 10.1007/s00027-016-0477-0
- Bolger, A. M., Lohse, M., and Usadel, B. (2014). Trimmomatic: a flexible trimmer for Illumina sequence data. *Bioinformatics* 30, 2114–2120. doi: 10.1093/bioinformatics/btu170
- Borsheim, K. Y. (2000). Bacterial production rates and concentrations of organic carbon at the end of the growing season in the Greenland Sea. *Aquat. Microb. Ecol.* 21, 115–123. doi: 10.3354/ame021115
- Caporaso, J. G., Kuczynski, J., Stombaugh, J., Bittinger, K., Bushman, F. D., Costello, E. K., et al. (2010). QIIME allows analysis of high-throughput community sequencing data. *Nat. Methods* 7, 335–336. doi: 10.1038/nmeth.f.303
- Caporaso, J. G., Lauber, C., Walters, W. A., Berg-Lyons, D., Lozupone, C. A., Turnbaugh, P. J., et al. (2011). Global patterns of 16S rRNA diversity at a depth of millions of sequences per sample. *Proc. Natl. Acad. Sci. U.S.A.* 108, 4516–4522. doi: 10.1073/pnas.1000080107
- Cauwet, G. (2002). "DOM in the coastal zone," in *Biogeochemistry of Marine Dissolved Organic Matter*, eds D. A. Hansell and C. A. Carlson (San Diego, CA: Academic Press), 579–609.
- Chow, C. T., Sachdeva, R., Cram, J. A., Steele, J. A., Needham, D. M., Patel, A., et al. (2013). Temporal variability and coherence of euphotic zone bacterial communities over a decade in the Southern California Bight. *ISME J.* 7, 2259–2273. doi: 10.1038/ismej.2013.122
- Citterio, M., Sejr, M. K., Langen, P. L., Mottram, R. H., Abermann, J., Larsen, S. H., et al. (2017). Towards quantifying the glacial runoff signal in the freshwater input to Tyrolerfjord – Young Sound, NE Greenland. *Ambio* 46, 146–159. doi: 10.1007/s13280-016-0876-4
- Cota, G. F., Pomeroy, L. R., Harrison, W. G., Jones, E. P., Peters, F., Sheldon Jr, W. M., et al. (1996). Nutrients, primary production and microbial heterotrophy in the southeastern Chukchi Sea: Arctic summer nutrient depletion and heterotrophy. *Mar. Ecol. Prog. Ser.* 135, 247–258. doi: 10.3354/meps.135247
- Crump, B. C., and Hobbie, J. E. (2005). Synchrony and seasonality in bacterioplankton communities of two temperate rivers. *Limnol. Oceanogr.* 50, 1718–1729. doi: 10.4319/lo.2005.50.6.1718
- del Giorgio, P. A., and Bouvier, T. C. (2002). Linking the physiological and phylogenetic successions in free-living bacterial communities along an estuarine salinity gradient. *Limnol. Oceanogr.* 47, 471–486. doi: 10.4319/lo.2002.47.2.0471

- del Giorgio, P. A., and Cole, J. J. (1998). Bacterial growth efficiency in natural aquatic systems. *Annu. Rev. Ecol. Syst.* 29, 503–541. doi: 10.1146/annurev.ecolsys.29.1.503
- Delong, E. F., Preston, C. M., Mincer, T., Rich, V., Hallam, S. J., Frigaard, N., et al. (2006). Community genomics among stratified microbial assemblages in the ocean's interior. *Science* 311, 496503. doi: 10.1126/science.1120250
- Edgar, R. C. (2010). Search and clustering orders of magnitude faster than BLAST. *Bioinformatics* 26, 2460–2461. doi: 10.1093/bioinformatics/btq461
- Elberling, B., Tamstorf, M. P., Michelsen, A., Arndal, M. F., Sigsgaard, C., Illeris, L., et al. (2008). Soil and plant community characteristics and dynamics at Zackenberg. *Adv. Ecol. Res.* 40, 223–248. doi: 10.1016/S0065-2504(07)00010-4
- Fortunato, C. S., Eiler, A., Herfort, L., Needoba, J. A., Peterson, T. D., and Crump, B. C. (2013). Determining indicator taxa across spatial and seasonal gradients in the Columbia River coastal margin. *ISME J.* 7, 1899–1911. doi: 10.1038/ismej.2013.79
- Fuhrman, J. A., and Azam, F. (1980). Bacterioplankton secondary production estimates for coastal waters of British Columbia, Antarctica, and California. *Appl. Environ. Microbiol.* 39, 1085–1095.
- Granskog, M. A., Stedmon, C. A., Dodd, P. A., Amon, R. M. W., Pavlov, A. K., De Steur, L., et al. (2012). Characteristics of colored dissolved organic matter (CDOM) in the Arctic outflow in the Fram Strait: assessing the changes and fate of terrigenous CDOM in the Arctic Ocean. *J. Geophys. Res.* 117, 1–13. doi: 10.1029/2012JC008075
- Gutiérrez, M. H., Galand, P. E., Moffat, C., and Pantoja, S. (2015). Melting glacier impacts community structure of Bacteria, Archaea and fungi in a Chilean Patagonia fjord. *Environ. Microbiol.* 17, 3882–3897. doi: 10.1111/1462-2920.12872
- Hansell, D. A. (2013). Recalibrating dissolved organic carbon fractions. *Ann. Rev. Mar. Sci.* 5, 421–445. doi: 10.1146/annurev-marine-120710-100757
- Hauptmann, A. L., Markussen, T. N., Stibal, M., and Olsen, N. S. (2016). Upstream freshwater and terrestrial sources are differentially reflected in the bacterial community structure along a small arctic river and its estuary. *Front. Microbiol.* 7:1474. doi: 10.3389/fmicb.2016.01474
- Hedges, J. I., and Stern, J. H. (1984). Carbon and nitrogen determinations of carbonate-containing solids. *Limnol. Oceanogr.* 29, 657–663. doi: 10.4319/lo.1984.29.3.0657
- Holmes, R. M., Aminot, A., Kérouel, R., Hooker, B. A., and Peterson, B. J. (1999). A simple and precise method for measuring ammonium in marine and freshwater ecosystems. *Can. J. Fish. Aquat. Sci.* 56, 1801–1808. doi: 10.1139/f99-128
- Hood, E., Battin, T. J., Fellman, J., Neel, S. O., and Spencer, R. G. M. (2015). Storage and release of organic carbon from glaciers and ice sheets. *Nat. Geosci.* 8, 91–96. doi: 10.1038/ngeo2331
- Hood, E., Fellman, J., Spencer, R. G. M., Hernes, P. J., Edwards, R., Amore, D. D., et al. (2009). Glaciers as a source of ancient and labile organic matter to the marine environment. *Nature* 462, 1044–1047. doi: 10.1038/nature08580
- Hood, E., and Scott, D. (2008). Riverine organic matter and nutrients in southeast Alaska affected by glacial coverage. *Nat. Geosci.* 583–587. doi: 10.1038/ngeo280
- Iversen, K. R., and Seuthe, L. (2011). Seasonal microbial processes in a high-latitude fjord (Kongsfjorden, Svalbard): I. Heterotrophic bacteria, picoplankton and nanoflagellates. *Polar Biol.* 34, 731–749. doi: 10.1007/s00300-010-0929-2
- Jespersen, A. M., and Christoffersen, K. (1987). Measurement of chlorophyll-a from phytoplankton using ethanol as extraction solvent. *Arch. Hydrobiol.* 109, 445–454.
- Jørgensen, L., Stedmon, C. A., Granskog, M. A., and Middelboe, M. (2014). Tracing the long-term microbial production of recalcitrant fluorescent dissolved organic matter. *Geophys. Res. Lett.* 41, 2481–2488. doi: 10.1002/2014GL059428
- Keegan, K. M., Albert, M. R., McConnell, J. R., and Baker, I. (2014). Climate change and forest fires synergistically drive widespread melt events of the Greenland ice sheet. *Proc. Natl. Acad. Sci. U.S.A.* 111, 7964–7967. doi: 10.1073/pnas.1405397111
- Kirchman, D. L., Elifantz, H., Dittel, A. I., Malmstrom, R. R., and Cottrell, M. T. (2007). Standing stocks and activity of Archaea and Bacteria in the western Arctic Ocean. *Limnol. Oceanogr.* 52, 495–507. doi: 10.4319/lo.2007.52.2.0495
- Kirchman, D. L., Malmstrom, R. R., and Cottrell, M. T. (2005). Control of bacterial growth by temperature and organic matter in the Western Arctic. *Deep Sea Res. Part II Top. Stud. Oceanogr.* 52, 3386–3395. doi: 10.1016/j.dsr2.2005.09.005
- Knights, D., Kuczynski, J., Charlson, E. S., Zaneveld, J., Mozer, M. C., Collman, R. G., et al. (2011). Bayesian community-wide culture-independent microbial source tracking. *Nat. Methods* 8, 761–763. doi: 10.1038/nmeth.1650
- Koroleff, F. (1983). “Determination of nutrients,” in *Methods of Seawater Analysis*, eds K. Grasshoff, M. Erhardt and K. Kremling (Weinheim: Verlag Chemie), 125–187.
- Kragh, T., and Sondergaard, M. (2004). Production and bioavailability of autochthonous dissolved organic carbon: effects of mesozooplankton. *Aquat. Microb. Ecol.* 36, 61–72. doi: 10.3354/ame036061
- Kritzbeg, E. S., Duarte, C. M., and Wassmann, P. (2010). Changes in Arctic marine bacterial carbon metabolism in response to increasing temperature. *Polar Biol.* 33, 1673–1682. doi: 10.1007/s00300-010-0799-7
- Lawson, E. C., Wadhwa, J. L., Tranter, M., Stibal, M., Lis, G. P., Butler, C. E. H., et al. (2014). Greenland ice sheet exports labile organic carbon to the Arctic oceans. *Biogeosciences* 11, 4015–4028. doi: 10.5194/bg-11-4015-2014
- Lee, S., and Fuhrman, J. A. (1987). Relationships between biovolume and biomass of naturally derived marine bacterioplankton. *Appl. Environ. Microbiol.* 53, 1298–1303.
- Øvreås, L., Forney, L., and Daae, F. L. (1997). Distribution of bacterioplankton in meromictic lake saelenvannet, as determined by denaturing gradient gel electrophoresis of PCR-amplified gene fragments coding for 16S rRNA. *Appl. Environ. Microbiol.* 63, 3367–3373.
- Lyngsgaard, M. M., Markager, S., and Richardson, K. (2014). Changes in the vertical distribution of primary production in response to land-based nitrogen loading. *Limnol. Oceanogr.* 59, 1679–1690. doi: 10.4319/lo.2014.59.5.1679
- Marie, D., Brussaard, C. P. D., Thyraug, R., Bratbak, G., and Vault, D. (1999). Enumeration of marine viruses in culture and natural samples by flow cytometry. *Appl. Environ. Microbiol.* 65, 45–52.
- Markager, S., Vincent, W. F., and Tang, E. P. Y. (1999). Carbon fixation by phytoplankton in high Arctic lakes: Implications of low temperature for photosynthesis. *Limnol. Oceanogr.* 44, 597–607. doi: 10.4319/lo.1999.44.3.0597
- Masella, A. P., Bartram, A. K., Truszkowski, J. M., Brown, D. G., and Neufeld, J. D. (2012). PANDAseq: PAired-eND assembler for illumina sequences. *BMC Bioinformatics* 13:1. doi: 10.1186/1471-2105-13-31
- Meon, B., and Amon, R. M. W. (2004). Heterotrophic bacterial activity and fluxes of dissolved free amino acids and glucose in the Arctic rivers Ob, Yenisei and the adjacent Kara Sea. *Aquat. Microb. Ecol.* 37, 121–135. doi: 10.3354/ame037121
- Middelboe, M., Glud, R. N., and Sejr, M. K. (2012). Bacterial carbon cycling in a subarctic fjord: a seasonal study on microbial activity, growth efficiency, and virus-induced mortality in Kobbefjord, Greenland. *Limnol. Oceanogr.* 57, 1732–1742. doi: 10.4319/lo.2012.57.6.1732
- Middelboe, M., and Lundsgaard, C. (2003). Microbial activity in the Greenland sea: role of DOC lability, mineral nutrients and temperature. *Aquat. Microb. Ecol.* 32, 151–163. doi: 10.3354/ame032151
- Morris, R. M., Vergin, K. L., Rappe, M. S., Carlson, C. A., and Giovannoni, S. J. (2005). Temporal and spatial response of bacterioplankton lineages to annual convective overturn at the Bermuda Atlantic Time-series Study site. *Limnol. Oceanogr.* 50, 1687–1696. doi: 10.4319/lo.2005.50.5.1687
- Murphy, J., and Riley, J. P. (1962). A modified single solution method for the determination of phosphate in natural waters. *Anal. Chim. Acta.* 26, 31–36. doi: 10.1016/S0003-2670(00)88444-5
- Murray, C. (2015). *Light Attenuation in Natural Waters*. Ph. D. thesis. Department of Earth Sciences, Aarhus University, Riso National Laboratory.
- Murray, C., Markager, S., Stedmon, C. A., Juul-Pedersen, T., Sejr, M. K., and Bruhn, A. (2015). The influence of glacial melt water on bio-optical properties in two contrasting Greenlandic fjords. *Estuar. Coast. Shelf Sci.* 163, 72–83. doi: 10.1016/j.ecss.2015.05.041
- Nghiem, S. V., Hall, D. K., Mote, T. L., Tedesco, M., Albert, M. R., Keegan, K., et al. (2012). The extreme melt across the Greenland ice sheet in 2012. *Geophys. Res. Lett.* 39, 6–11. doi: 10.1029/2012GL053611
- Nielsen, S. E. (1952). The use of radio-active carbon (14C) for measuring organic production in the sea. *ICES J. Mar. Sci.* 18, 117–140. doi: 10.1093/icesjms/18.2.117
- Nielsen, T. G., Ottsen, L. D., and Hansen, B. W. (2007). Structure and function of the pelagic ecosystem in young sound, NE Greenland. *Carbon Cycl. Arct. Mar. Ecosyst. Case Study Young Sound* 58, 88–107. doi: 10.3354/meps179013

- Osterholz, H., Singer, G., Wemheuer, B., Daniel, R., Simon, M., Niggemann, J., et al. (2016). Deciphering associations between dissolved organic molecules and bacterial communities in a pelagic marine system. *ISME J.* 10, 1–14. doi: 10.1038/ismej.2015.231
- Paulsen, M. L., Doré, H., Garczarek, L., Seuthe, L., Müller, O., Sandaa, R., et al. (2016). Synechococcus in the Atlantic Gateway to the Arctic Ocean. *Front. Mar. Sci.* 3:191. doi: 10.3389/fmars.2016.00191
- Pomeroy, L. R., and Deibel, D. (1986). Temperature regulation of bacterial activity during the spring bloom in Newfoundland coastal waters. *Science* 233, 359–361. doi: 10.1126/science.233.4761.359
- Pomeroy, L. R., and Wiebe, W. J. (2001). Temperature and substrates as interactive limiting factors for marine heterotrophic bacteria. *Aquat. Microb. Ecol.* 23, 187–204. doi: 10.3354/ame023187
- Pomeroy, L. R., Wiebe, W. J., Deibel, D., Thompson, R. J., Rowe, G. T., and Pakulski, J. D. (1991). Bacterial responses to temperature and substrate concentration during the Newfoundland spring bloom. *Mar. Ecol. Prog. Ser.* 75, 143–159. doi: 10.3354/meps075143
- Pradeep Ram, A. S., Nair, S., and Chandramohan, D. (2003). Bacterial growth efficiency in the tropical estuarine and coastal waters of Goa, Southwest Coast of India. *Microb. Ecol.* 45, 88–96. doi: 10.1007/s00248-002-3005-9
- Quast, C., Pruesse, E., Yilmaz, P., Gerken, J., Schweer, T., Glo, F. O., et al. (2013). The SILVA ribosomal RNA gene database project: improved data processing and web-based tools. *Nucleic Acid Res.* 41, 590–596. doi: 10.1093/nar/gks1219
- Riemann, B., Fuhrman, J., and Azam, F. (1982). Bacterial secondary production in freshwater measured by super(3)H-thymidine incorporation method. *Microb. Ecol.* 8, 101–114. doi: 10.1007/BF02010444
- Rivkin, R. B., and Legendre, L. (2001). Biogenic carbon cycling in the upper ocean: effects of microbial respiration. *Science* 291, 2398–2400. doi: 10.1126/science.291.5512.2398
- Roiha, T., Peura, S., Cusson, M., and Rautio, M. (2016). Allochthonous carbon is a major regulator to bacterial growth and community composition in subarctic freshwaters. *Sci. Rep.* 6:34456. doi: 10.1038/srep34456
- Rysgaard, S., and Nielsen, T. G. (2006). Carbon cycling in a high-arctic marine ecosystem – young Sound, NE Greenland. *Prog. Oceanogr.* 71, 426–445. doi: 10.1016/j.pocean.2006.09.004
- Rysgaard, S., Vang, T., Stjernholm, M., Rasmussen, B., Windelin, A., and Kiilsholm, S. (2003). Physical conditions, carbon transport, and climate change impacts in a Northeast Greenland Fjord. *Arct. Antarct. Alp. Res.* 35, 301–312. doi: 10.1657/1523-0430(2003)035[0301:PCCTAC]2.0.CO;2
- Salter, I., Galand, P. E., Fagervold, S. K., Lebaron, P., Obernosterer, I., Oliver, M. J., et al. (2014). Seasonal dynamics of active SAR11 ecotypes in the oligotrophic Northwest Mediterranean Sea. *ISME J.* 9, 347–360. doi: 10.1038/ismej.2014.129
- Schlitzer, R. (2016). *Ocean Data View*. Available online at: <http://odv.awi.de>
- Sejr, M. K., Nielsen, T. G., Rysgaard, S., Risgaard-Petersen, N., Sturluson, M., and Blicher, M. E. (2007). Fate of pelagic organic carbon and importance of pelagic-benthic coupling in a shallow cove in Disko Bay, West Greenland. *Mar. Ecol. Prog. Ser.* 341, 75–88. doi: 10.3354/meps341075
- Singer, G. A., Fasching, C., Wilhelm, L., Niggemann, J., Steier, P., Dittmar, T., et al. (2012). Biogeochemically diverse organic matter in Alpine glaciers and its downstream fate. *Nat. Geosci.* 5, 710–714. doi: 10.1038/ngeo1581
- Sondergaard, M., and Middelboe, M. (1995). A cross-system analysis of labile dissolved organic carbon. *Mar. Ecol. Prog. Ser.* 118, 283–294. doi: 10.3354/meps118283
- Ter Braak, C. J. F., and Šmilauer, P. (2012). *Canoco Reference Manual and User's Guide: Software for Ordination, Version 5.0* (Ithaca, NY: Microcomputer Power), 496.
- Traving, S. J., Bentzon-tilia, M., Knudsen-leerbeck, H., and Mantikci, M. (2016). Coupling bacterioplankton populations and environment to community function in coastal temperate waters coupling bacterioplankton populations and environment to community function in coastal temperate waters. *Front. Microbiol.* 7:1533. doi: 10.3389/fmicb.2016.01533
- Wilson, B., Müller, O., Nordmann, E.-L., Seuthe, L., Bratbak, G., and Øvreås, L. (2017). Changes in marine prokaryote composition with season and depth over an arctic polar year. *Front. Mar. Sci.* 4:95. doi: 10.3389/fmars.2017.00095
- Wood, E. D., Armstrong, F. A. J., and Rich, F. A. (1967). Determination of nitrate in seawater by cadmium-copper reduction to nitrate. *J. Biol. Assoc. UK.* 47, 23–31. doi: 10.1017/S00253154003352X

Conflict of Interest Statement: The authors declare that the research was conducted in the absence of any commercial or financial relationships that could be construed as a potential conflict of interest.

Copyright © 2017 Paulsen, Nielsen, Müller, Møller, Stedmon, Juul-Pedersen, Markager, Sejr, Delgado Huertas, Larsen and Middelboe. This is an open-access article distributed under the terms of the Creative Commons Attribution License (CC BY). The use, distribution or reproduction in other forums is permitted, provided the original author(s) or licensor are credited and that the original publication in this journal is cited, in accordance with accepted academic practice. No use, distribution or reproduction is permitted which does not comply with these terms.

